Levels of Schwann cell c-Jun control nerve development and response to injury

SHALINE VANESSA FAZAL

Thesis submitted for the degree of Doctor of Philosophy
University College London
March 2017

Abstract

Peripheral nerves have a remarkable ability to regenerate following nerve injury, unlike their counterparts in the central nervous system. This phenomenal ability of nerves to regenerate in the peripheral nervous system is due to cross communication between different cell populations, a focal group being the glial cells known as Schwann cells.

The transcription factor c-Jun is highly expressed in distal stump Schwann cells following injury. It is this c-Jun expression in Schwann cells following peripheral nerve injury that is crucial for the cellular reprogramming of mature Schwann cells (Remak and Myelin Schwann cells) into repair Bungner Schwann cells. Repair Bungner Schwann cells are important for providing the necessary maintenance and trophic support to regenerating axons. Mice that lack c-Jun in their Schwann cells and therefore fail to express it after injury have impaired regeneration.

With this idea in mind, it was of interest to see what happens when c-Jun is overexpressed in Schwann cells. Thus, a new transgenic mouse was bred to conditionally overexpress c-Jun in Schwann cells only. c-Jun protein levels were elevated 5 fold and 7 fold in heterozygous and homozygous mice respectively, in developing Schwann cells. The elevation of c-Jun specifically in Schwann cell nuclei in c-Jun overexpressing mice (heterozygous and homozygous), allowed *in vivo* examination of the effects of a graded increase in c-Jun expression on Schwann cells in uninjured and injured nerves.

Evidence presented below suggests that Schwann cells can tolerate moderately elevated levels of c-Jun expression from birth (5 fold) without it being detrimental to nerve development. These observations demonstrate that heterozygous c-Jun overexpressing mice which show a substantial elevation in c-Jun protein level (which is localized to Schwann cell nuclei) compared to wildtype (WT), although there is an initial delay in myelination at postnatal day (P) 7, in adult life they achieve normal Schwann cell and nerve architecture, with the exception of modestly reduced myelin thickness. However in contrast to the heterozygotes, higher levels of c-Jun in Schwann cells from birth in homozygous mice results in severe myelin inhibition,

which manifests itself very early on at P1. In the homozygous mice the strongly increased c-Jun expression in Schwann cells resulted in defects that included an obvious delay in myelination, thinner myelin sheaths (in those Schwann cells that eventually myelinated axons), increased Schwann cell proliferation and an increase in nerve area. These homozygous overexpressing mutant nerves were also examined for the presence of tumours or cellular arrangements that precede tumour formation, but no evidence was found to support this.

To elucidate the potential significance of c-Jun elevation in Schwann cells after injury specifically in the proximal stump (where axons are still in contact with the neuronal cell body), the proximal stump of WT mice was compared with that of Schwann cells and axons in the proximal stump of a well-established Schwann cell c-Jun conditional knockout mouse (cKO).

Proximal stump Schwann cell c-Jun was expressed very rapidly and the profile of Schwann cells was highly elevated as early as 1 hour following sciatic nerve transection, with this elevation being maintained up to 48 hours after nerve injury and further away from the injury site.

The lack of Schwann cell c-Jun in the proximal stump did not affect the expression of some well known regeneration associated genes (RAGs), including c-Jun, ATF3, p-STAT3 Ser727 and Tyr705, yet had a modest effect on the elevation of GAP43, after injury in L4 DRG neurons. Schwann cell c-Jun in Schwann cells of the proximal stump has a small effect on axonal outgrowth following a conditioning lesion, shown *in vivo*. Neuronal cultures from L4 DRGs derived from WT and cKO mice (with sciatic nerve injuries), grown on myelin inhibitory substrate *in vitro*, suggest that Schwann cell c-Jun is not affecting neuronal outgrowth.

Impact Statement

The remarkable ability of peripheral nerves to regenerate following nerve injury remains an area of high importance and interest. Central nervous system nerves, unlike their peripheral counterparts do not have the intrinsic ability to regenerate. Schwann cells, the glial supporting cells of these nerves, play a crucial role in enabling the regeneration of axons to occur after injury. Despite this, in humans injured peripheral nerves often fail to regenerate properly.
Research in the field has shown that the important transcription factor c-Jun, is a crucial regulator of the Schwann cell injury response.

The findings outlined in this thesis focus on the role of levels of Schwann cell c-Jun in development, adulthood and after nerve injury. With this in mind, the research questions addressed and the results presented in this work aim to widen the knowledge and insight into the potential of peripheral nerves to regenerate, by exploiting mouse models that conditionally overexpress and conditionally knockout c-Jun specifically in Schwann cells.

In terms of academic and clinical research, the possibility of identifying factors that will promote more successful regeneration of injured mouse nerves opens up avenues for improved treatments of peripheral nerve injury in humans. Further insight into mechanisms that influence successful peripheral nerve regeneration can also assist in understanding why nerves of the central nervous system do not react in the same way. This will ultimately be important in the translational studies from laboratories into a clinical setting.

The work presented here is not only important in an academic and potentially medical setting, but also of value for non-academic platforms such as undergraduate and postgraduate teaching programmes, where this information will broaden the current knowledge and insight into Schwann cell biology and peripheral nerve regeneration.

Declaration

I, Shaline Vanessa Fazal, confirm that the work presented in this thesis is my own. Where information has been derived from other sources, I confirm that this has been indicated in the thesis.

Signed

Date

Acknowledgements

This thesis is dedicated to the memory of my grandfather (baba), Sefou Mamodaly, who until the end never stopped seeking knowledge.

I would like to thank my supervisors Professor Kristjan Jessen and Professor Rhona Mirsky immensely for allowing me to be a part of their lab, where I have been given the opportunity to progress from my BSc into my PhD. I thank them for their guidance, support, teaching and invaluable advice along the way. Without them I would not have been able to undertake this PhD. I would also like to thank my second supervisor Professor Patrick Anderson and my graduate tutor Professor Steve Hunt for their helpful comments.

To my parents Nadjma and Azim without whom this journey would not have begun all those years ago when I moved to the UK. In particular, I would like to thank them both for spending all those arduous hours reading over my thesis with a fine-tooth and comb. To my "maman" for her constant nurturing and want for me to aim for the stars. Those 11+ days seem much easier in hindsight! To my "daddy" for teaching me that it's not what you deserve, but what you can negotiate. Those matchsticks days saw me through a lot! Most importantly, I am grateful for their unconditional support in whatever I do and always being there for me.
To my uncle "kaka" Salim, who may seem behind the scenes, but is very much at the forefront of my journey. Most importantly, I would like to thank him for his printer! I also thank my immediate family for their help, especially for all those late night train pickups.

A special mention to my aunty Zeenat Bhullar who gave me the confidence not to live in the shadow of others. She showed a genuine interest in what I was doing and I wish she could have been here to see the finished product.

I thank all past (Daniel Wilton, Elodie Chabrol, Susanne Quintes, Lucy Carty, Billy Jenkins, Nicolo Musner and Cristina Benito Sastre) and present (Laura Wagstaff and José Gomez-Sanchez) lab members who have come and gone along the way for their

kindness, support and help- Laura thanks for all the Haribo! In particular, I would like to extend a special thanks to both Cristina and José for their patience and advice but most importantly their unconditional support throughout. Cristina has been there with me from the start and has shared this journey in all its glory. José has highlighted the joys of teamwork and I owe him a lot for making me a better scientist. I particularly acknowledge his input into this thesis in Figures 3.12, 4.3, 4.4 and 4.5.

Finally I would like to say thanks to Jasbir Basi for being a great support and being part of the rollercoaster ride, providing the needed distractions along the way. To Joseph Darragh and Sophie Williams who have been there through all the ups and downs. Marc Astick, Kristina Tubby and Lewis Brayshaw, thanks for all the laughs and banter which made 206 such a great environment to be in; no wonder I am still here! In particular, thank you to the best Life Coach, Lewis, whose energy and enthusiasm knows no bounds. I couldn't have done it without all the support from my friends and family, to whom I am eternally grateful.

Table of Contents

List of Figures

1. Introduction

1.1 Schwann cells: the glial cells of peripheral nerves

The peripheral nervous system is made up of a network of neurons and glia that work synchronously with each other to ensure there is proper transmission of information from sensory organs to the central nervous system (CNS), as well as from the CNS to various muscles and effectors that are located throughout the body. The complex relationship between neurons and glia is crucial in determining the proper functioning and development of nerves.

Theodor Schwann first described Schwann cells over 200 years ago. Schwann cells deriving from neural crest cells are the principal glia of peripheral nerves. They wrap around axons, and classically can form a 1:1 relationship with large calibre axons (>1.5μm in diameter) resulting in Myelin Schwann cells, or ones that associate with several axons, known as non-myelin Schwann cells (Remak Schwann cells) (Jessen and Mirsky, 1997; Dong et al., 1999; Armati, 2007; Griffin and Thompson, 2008). It is important to note that the term "non-myelin Schwann cell" encompasses several subtypes including Remak Schwann cells, terminal Schwann cells and satellite Schwann cells, however more commonly this term refers to Remak Schwann cells. Remak Schwann cells are found in spinal nerves and nerve roots, and small diameter axons get enveloped in invaginations of the Remak Schwann cell membrane (Berthold et al., 2005; Jessen and Mirsky, 2005; Armati, 2007). Myelin Schwann cells are better characterised and studied than Remak Schwann cells due to the extensive research on myelination in development and commonly in demyelinating diseases, where disruption of Myelin Schwann cells is the defining feature (Bunge, 1993; Garbay et al., 2000; Jessen and Mirsky, 2002; Corfas et al., 2004; Sherman and Brophy, 2005; Jessen et al., 2015a; Monk et al., 2015). The myelin sheaths formed are essential for the rapid transmission of action potentials along axons, a process known as saltatory conduction (Huxley and Stämpfli, 1949; Rasminsky et al., 1978; Salzer et al., 2008).

The interdependence and communication between the Schwann cell and neuron determines the functioning of the peripheral nervous system (Armati, 2007). Nerve cells and Schwann cells essentially form a symbiotic relationship where each cell type is dependent on the other for normal development, maintenance and function. Signals

from axons control the initiation of myelination and the maintenance of the complex Schwann cell organisation, yet it is the Schwann cell that regulates axonal diameter and the clustering of ion channels around the Nodes of Ranvier, to name a few of its functions (Hsieh et al., 1994; Poliak and Peles, 2003; Michailov et al, 2004).
It is important to note however, that work has demonstrated that multipotent Schwann cell precursors which are present in peripheral nerves at E14-17, can also give rise to endoneurial fibroblasts, parasympathetic neurons, melanocytes and tooth pulp cells through multi-lineage differentiation (Morrison et al., 1999; Bixby et al., 2002; Joseph et al., 2004; Jessen et al. 2015).

1.2 Schwann cell development

Mature Myelin and Remak Schwann cells are generated from the neural crest through two intermediary cell types: (i) the Schwann cell precursor and (ii) the immature Schwann cell. The transition step from neural crest cell to Schwann cell precursor takes places between embryonic day (E) 12-13 in the mouse (E14-15 in the rat). The next stage in this lineage is the formation of immature Schwann cells from Schwann cell precursors, which takes place between E13-15 in the mouse (E15-17 in the rat). Immature Schwann cells persist until the perinatal period (Jessen et al., 1994; Dong et al., 1995; Dong et al., 1999; Jessen and Mirsky, 2005). The final transition step in the Schwann cell lineage is, on one hand, the formation of mature Myelin Schwann cells that occurs via a step involving a pro-myelin Schwann cell, and on the other hand, the formation of Remak Schwann cells (Salzer et al., 1980; Bunge et al., 1982; Mirsky and Jessen, 1996; Dong et al., 1999; Jessen and Mirsky, 2015; Monk et al., 2015). These transition steps are summarised in the diagram below (Figure 1.1).

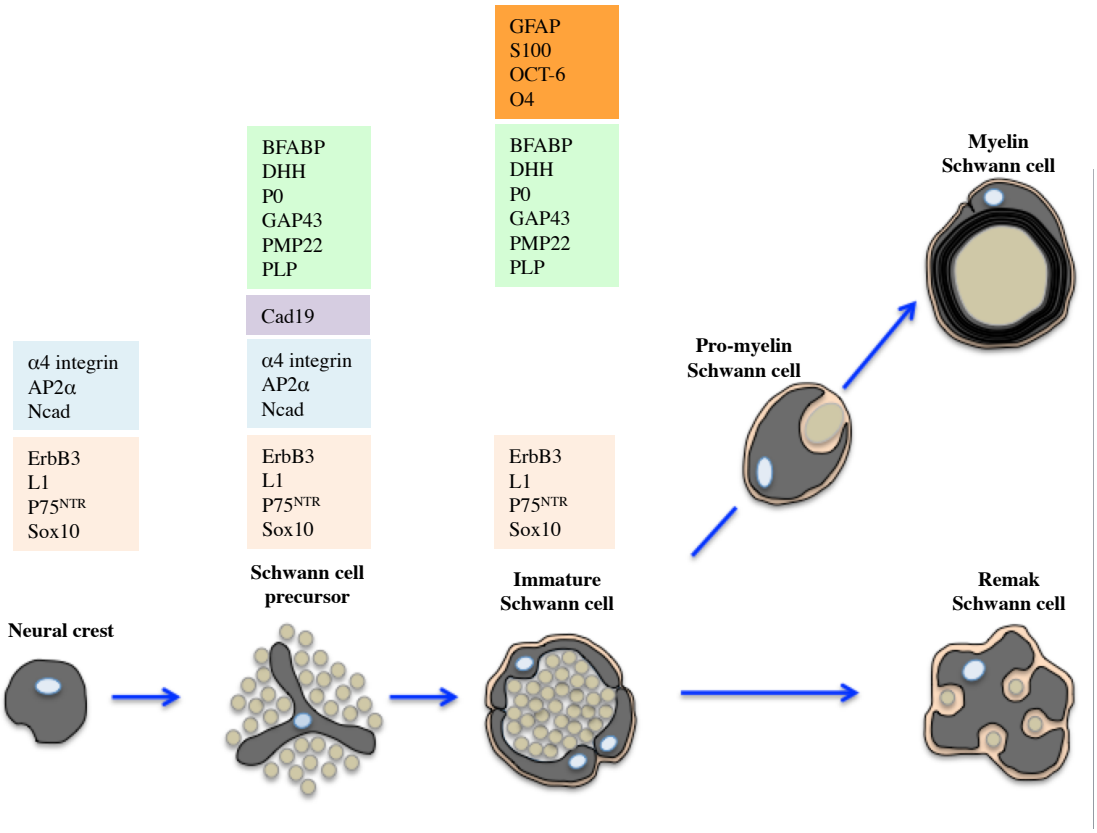

Figure 1.1 | Schwann cell lineage
A schematic representation of the main transition stages that take place within the Schwann cell lineage and the different molecular markers expressed by different types of Schwann cells.
Adapted from Jessen and Mirsky, 2005.

1.2.1 Schwann cell precursors

Growing nerves initially consist of outgrowing axons with closely associated Schwann cell precursors, essential for proper development of both the nerve and maturation of Schwann cells into later developmental stages (Jessen and Mirsky 2005). At this early stage, the nerve lacks blood vessels, and fibrous connective tissue within and around the nerve is rare. Blood vessels invade and the nerve begins to develop its connective tissue layer, which coincides with the time immature Schwann cells are formed (Ziskind-Conhaim, 1988; Jessen and Mirsky 2005; Jessen and Mirsky, 2008; Wanner et al., 2006; Jessen et al., 2015a; Monk et al., 2015).

Schwann cell precursors, like neural crest cells, are proliferative and migratory. They are found closely associated along the length of axons during peripheral nerve development and require axonal signals for survival (Jessen and Mirsky, 1991; Dong et al., 1995; Mirsky et al., 2002; Mirsky et al., 2007). This constant axon-glial cross-talk is crucial for the maintenance and survival of the lineage (Levi et al., 1995; Morrissey et al., 1995; Wolpowitz et al., 2000; Jessen and Mirsky, 2002; Gomez-Sanchez et al., 2009).

The molecular mechanisms that determine the changes that have to occur for transition of neural crest cells into Schwann cell precursors are still not completely understood and this therefore remains an active area of research in the field, though some key players have been identified. Among them, the transcription factor Sox10 (SRY-related HMG-box10), is expressed very early in neural crest cells. Its expression is maintained in peripheral nerve glia, including Schwann cell precursors, Schwann cells and in melanocytes, while this expression is later down-regulated in both neurons and other neural crest cell derivatives (Kuhlbrodt et al. 1998; Woodhoo and Sommer 2008).

Another important determining factor in the early stage of Schwann cell precursor formation is the trophic factor Neuregulin 1 (NRG1), which favours glial specification by suppressing neuronal differentiation (Shah et al., 1994; Mei and Xiong, 2008). Exposure of Schwann cell precursor cultures *in vitro* to NRG1 supports the survival

of Schwann cell precursors and results in the generation of Schwann cells within a similar time frame to that seen when Schwann cells appear in peripheral nerves *in vivo*. This is indicative of the fact that NRG1 is important in the survival of the precursors and the progression of the Schwann cell lineage (Jessen et al.1994; Dong et al., 1995).

NRG1 binding to ErbB2/3 (receptor tyrosine kinases) on Schwann cell precursors activates important downstream signaling cascades. This binding of NRG1 to ErbB2/3 receptors is also crucial for Schwann cell precursor proliferation and migration (Shah et al., 1994; Taveggia et al., 2005; Aquino et al., 2006; Newbern and Birchmeier, 2010; Monk et al., 2015).

Using the sympathetic nervous system as an example, in mice in which NRG signaling is deficient (knocking out NRG1, ErbB2 or ErbB3), neural crest cells fail to migrate past the dorsal aorta to the point where sympathetic ganglia are formed (Britsch et al., 1998).

In mice deficient in NRG1 or NRG1 Type III, or in erbB2 or ErbB3 receptors almost no Schwann cell precursors are present in developing peripheral nerves although the satellite cells of the DRG do develop (Meyer and Birchemeier, 1994; Meyer and Birchmeier, 1995; Syroid et al., 1996; Meyer et al., 1997; Morris et al., 1999; Newbern and Birchmeier, 2010). Thus NRG signalling, particularly NRG1 types I and III with the receptors ErbB2 and ErbB3, is required to maintain the migratory ability of neural crest cells, but more importantly to maintain the survival and progression of Schwann cell precursors. NRG signaling also has important roles to play in myelination.

More recent research in the field has also highlighted the importance of histone deacetylases 1 and 2 (HDAC1/2) in the development of the lineage. Among other functions they induce the expression of the paired box family transcription factor Pax3. Pax3 is important for Schwann cell differentiation and proliferation (Kioussi et al. 1995; Blanchard et al. 1996; Doddrell et al., 2012) and also induces the expression of important Schwann cell lineage genes such as myelin protein zero (Mpz) (Jacob et al., 2014; Monk et al., 2015).

1.2.2 Immature Schwann cells

Several days following specification, Schwann cell precursors develop further to form immature Schwann cells. As mentioned earlier, at this transition point between Schwann cell precursors and immature Schwann cells, which occurs between E13-15 in the mouse, immature Schwann cells gradually acquire the ability to support their own survival by an autocrine signaling system through the release of a cocktail of survival factors, without being reliant on axonal signals in the way that Schwann cell precursors are. At this point in the lineage, the cytoarchitecture of the nerve transforms and immature Schwann cells surround smaller bundles of axons and start to deposit a basal laminae around them, which adds to the defining features that make them different from Schwann cell precursors (Jessen and Mirsky, 2005; Monk et al., 2015).

Up to the point of the generation of immature Schwann cells, the composition of peripheral nerves consists of axons and Schwann cells. As immature Schwann cells develop, they signal to surrounding mesenchymal cells to differentiate into arterial and perineurial cells, which ultimately populate and surround mature nerves (Parmantier et al. 1999; Mukouyama et al. 2005; Monk et al., 2015). The mechanisms that determine the transition of Schwann cell precursors into immature Schwann cells are still poorly understood.

An important regulator of this process however, is Notch1. Schwann cells are derived from Schwann cell precursors through continual proliferation, which reaches a peak at the immature Schwann cell stage (Stewart et al., 1993; Yu et al., 2005; Woodhoo and Sommer, 2008). Inactivation of Notch1 specifically in Schwann cells results in lower Schwann cell precursor proliferation, and delayed immature Schwann cell formation (Woodhoo et al., 2009; Jessen et al., 2015). It is important to note that Notch1 has also been implicated in other aspects of Schwann cell biology such as controlling the responses of mature Schwann cells to nerve injury (Woodhoo et al., 2009). Endothelin and AP2 act to delay this transition (Brennan et al., 2000; Stewart et al., 2001).

Another defining function of immature Schwann cells is their role in isolating

individual large diameter axons to be ensheathed by a single Schwann cell. Immature Schwann cells extend radial lamellipodia into the axon bundles and via this process separate out large diameter axons (Webster and Favilla, 1984). This is known as radial sorting.

1.2.3 Radial Sorting

Immature Schwann cells take distinct pathways determined by many factors, to form mature Remak or Myelin Schwann cells. Immature Schwann cells accomplish two important steps: (1) radial sorting (separation of axons, most of which are destined to be myelinated) and (2) cell differentiation (signalling to perineurial cells) (Monk et al., 2015). The process of radial sorting is discussed below.

As immature Schwann cells form in the nerve, axons are separated into smaller bundles surrounded by a "family" of 3-8 immature Schwann cells that deposit a basal lamina. The work of Henry D Webster and others in 1973 showed that these "families" surrounded mixed calibre axons. Immature Schwann cells further segregate these axon bundles by extending lamellipodia processes between individual large diameter axons, isolating them towards the periphery of the bundle. Schwann cells surrounding a single axon divide and separate from the bundle so that these axons can form a 1:1 relationship with Schwann cells that will individually surround it. These axons then have the possibility to become myelinated axons (Webster et al., 1973; Jessen and Mirsky, 2005; Feltri et al., 2016).
As Schwann cells in families continue to proliferate, with progressive axonal segregation, the axonal bundles become smaller as more and more large caliber ones are segregated away. Axon bundles made up of small diameter axons are left behind, and will develop into Remak bundles (one Remak Schwann cell associated with several axons) (Feltri et al., 2016).

Radial sorting is a multi-faceted process that requires a fine balance between many different aspects including the deposition of extracellular matrix (ECM) components and their organisation within the basal lamina, Schwann cell-axon interactions and the correct amount of Schwann cell proliferation and differentiation, to name a few

(Jessen and Mirsky, 2005; Porrello et al., 2014; Feltri et al., 2016). The appropriate control of the number of Schwann cells and their proliferation is crucial for coordinating the proper segregation of axons. In order for pro-myelinating Schwann cells to be formed, that will ultimately result in Myelin or Remak Schwann cells, there needs to be a timely withdrawal of immature Schwann cells from the cell cycle (Monk et al., 2015; Feltri et al., 2016).

These important morphogenetic changes ultimately lead to the mature nerve architecture which consists of 1:1 myelinated fibres with Schwann cells and Remak bundles (several small calibre axons ensheathed by one Schwann cell), all surrounded by extracellular matrix consisting prominently of collagen fibres and blood vessels (Monk et al., 2015). The process of radial sorting is summarised in a simplified diagram shown below (Figure 1.2).

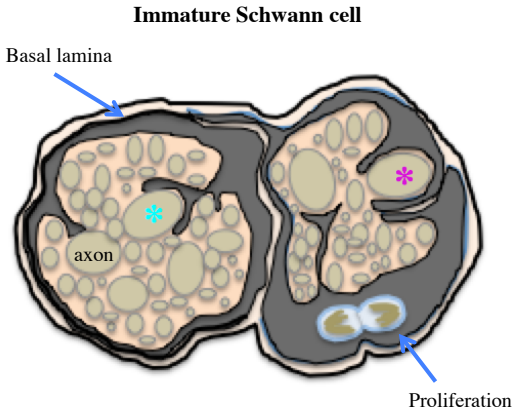

Figure 1.2 | Radial sorting
A schematic representation showing radial sorting. Radial sorting is performed by immature Schwann cells and can be divided in stages. The basal lamina is deposited and the formation Schwann cell "families" begins. Schwann cell processes are inserted into axonal bundles. Large calibre axons are recognised as shown by the turquoise asterisk above and are radially sorted and segregated to the periphery as shown by the purple asterisk above.
Adapted from Feltri et al., 2016.

1.2.4 Pro-myelin Schwann cell

Radial sorting is the final step that determines the transition of a pro-myelin Schwann cell, into a mature Myelin Schwann cell (Pereira et al., 2012). It was well established in the beginning of 1970s that large caliber axons, greater than a certain diameter became myelinated (Friede, 1972), yet the way in which this process was regulated only became apparent by the mid 1970s through cross-anastomosis experiments. When myelinated axons were cross-anastomosed into a non-myelinating environment, the axons that were initially non-myelinated, became myelinated, confirming earlier suggestions that it was signals from the axons that determined when myelination by Schwann cells would ensue (Weinberg and Spencer 1975; Aguayo et al. 1976; Monk et al., 2015). Many factors are involved in the process of myelination among the most important of which are NRG1 (specifically type III), Oct-6, Krox20 and Sox10 (Bermingham et al., 1996; Jaegle et al., 2003; Michailov et al., 2004; Parkinson et al., 2004; Svaren and Meijer, 2008; Mei and Xiong, 2008; Monk et al., 2015).

As already discussed, the long lasting embryonic period of gliogenesis originating from neural crest cells, beginning with the formation of Schwann cell precursors, followed by immature Schwann cells (Jessen and Mirsky, 1991; Jessen et al., 1994), is controlled by many signals that determine the progression of this development. The subsequent postnatal formation of mature Schwann cells (Remak and Myelin Schwann cells) from immature Schwann cells is determined by the cessation of proliferation and resistance to cell death (Jessen and Mirsky, 2005; Armati, 2007). This nerve maturation process can be defined as a balance between signals that act as promoters of myelination such as Krox20 and Oct-6, or those that act as brakes on the system such as c-Jun or Sox2 (Topilko et al., 1994; Bermingham et al., 1996; Jaegle et al., 1996; Jaegle and Meijer, 1998; Le et al., 2005; Parkinson et al., 2008).

1.2.5 Myelin Schwann cells

As mentioned above, Schwann cells that form a 1:1 relationship with a single large calibre axon are called Myelin Schwann cells. The process of ensheathing these single large diameter axons begins when the leading edge of the Myelin Schwann cell's inner-mesaxon starts to extend and wrap in a spiral manner around the axon. The synthesis of this membrane and the continual spiral wrapping around the axon is what generates the complex myelin structure (Bunge et al., 1989). Schwann cell myelination is determined by strict transcriptional control of opposing signals, viz positive and negative regulators of myelination. As previously mentioned, such positive transcriptional regulators of myelination include Sox10 and Oct-6, where they are able to work together to induce the expression of a crucial positive regulator of myelination, Krox20 (Jagalur et al., 2011; Pereira et al., 2012).

1.2.6 Regulation of myelination

Krox20 has been shown to be a regulator of Schwann cell myelination. Krox20 is able to not only activate myelin genes, but also inhibit negative regulators of myelination, such as c-Jun and Notch, and maintain the myelination phenotype (Topilko et al., 1994; Topilko and Meijer, 2001; Parkinson et al., 2004; Ghislain and Charnay, 2006; LeBlanc et al., 2006; Svaren and Meijer, 2008; Mirsky et al., 2008; Woodhoo et al., 2009; Pereira et al., 2012). Krox20 inactivation in Schwann cells resulted in arrest at the pro-myelinating stage and when inactivated in adult Schwann cells, resulted in severe demyelination, indicating that Krox20 is important both for the onset of myelination and for the maintenance of the myelinating phenotype (Topilko et al., 1994; Nagarajan et al., 2001; Decker et al., 2006).

Oct-6 expression is important in timing the onset of myelination. Schwann cells of peripheral nerves express the POU domain transcription factor Oct-6 from E16 onwards (Monuki et al., 1990; Jaegle et al., 1996). During postnatal development, the expression of Oct-6 mRNA is present in both Myelin and Remak Schwann cells. Oct-6 expression is gradually down-regulated and then diminishes, up to the point where in Schwann cells of adult nerves, Oct-6 expression is infrequent. Schwann cells

lacking Oct-6 showed a transient delay in myelination (Jaegle et al., 1996). The work of Ghislain and others in 2002 identified a transcriptional enhancer known as the myelinating Schwann cell element (MSE), which regulates Krox20 and is under the control of Oct-6 (Ghislain et al., 2002; Ghislain and Charnay, 2006). The use of cell culture experiments and transgenics demonstrated that during the transition from pro-myelin Schwann cell to Myelin Schwann cell, Krox20 expression is directly controlled by Oct-6 and another POU domain transcription factor Brn-2 binding to the transcriptional enhancer of Krox20. From this work, it also became apparent that Sox10 along with the POU transcription factors Oct-6 and Brn-2 are needed for Krox20 expression (Ghislain and Charnay, 2006).

As stated above, myelin is important for saltatory conduction and therefore successful transmission of impulses. The identification of the axonal signals that induce the formation of the myelin sheaths was originally thought to either be based on a critical axonal size that triggers myelination, or alternatively specific biochemical signals stemming from the axon itself determining ensheathment (Salzer, 1995; Salzer, 2012). It later became apparent that these two hypotheses were not mutually exclusive. Therefore, the thickness of myelin sheaths around axons is tightly regulated and linked to the axon diameter. NRG1 is the most well studied determinant of myelin sheath thickness. NRG1 exists in many isoforms, however it is the expression of the membrane bound type III specifically, found on the axonal membrane, which is important for myelination (Birchmeier and Nave, 2008). The first indication that NRG1 type III was important in determining myelination of axons was through the inactivation of its receptor (ErbB2 expressed by Schwann cells), where hypomyelination of peripheral nerves was noted (Garratt et al., 2000). Conversely, overexpression of NRG1 type III led to hypermyelination (Michailov et al., 2004). Another indication that myelination of axons is dependent on NRG1 type III was from experiments where overexpression on NRG1 type III in sympathetic neurons (which are normally unmyelinated) became myelinated (Taveggia et al., 2005), indicating that the axonal NRG1 type III signal is what dictates the amount of myelin that needs to be produced to wrap around axons (Garratt et al., 2000; Birchmeier and Nave, 2008; Raphael and Talbot, 2011; Salzer, 2012).

Multiple negative regulators of myelination have been identified including Sox2,

Notch1 and more importantly in the context of the work presented below, c-Jun (Le et al., 2005, Parkinson et al., 2008; Woodhoo et al., 2009).

c-Jun is strongly expressed in immature Schwann cells, prior to the beginning of myelination, as shown *in vivo* (Parkinson et al., 2008) and in cultured Schwann cells, as well as following nerve injury in the distal nerve stump (De Felipe and Hunt, 1994; Stewart, 1995; Shy et al., 1996; Parkinson et al., 2004; Arthur-Farraj et al., 2012). c-Jun levels present in myelinating Schwann cells are low, while Krox20 levels in these cells are high (Parkinson et al., 2001; Parkinson et al., 2004; Parkinson et al., 2008).

Notch signaling is down-regulated at the onset of myelination by Krox20, similar to c-Jun. In Krox20 knockout mutant nerves, a downstream component of the Notch pathway, NICD, remains highly expressed and this enforced expression *in vivo*, reduces myelination (Jessen and Mirsky, 2008; Woodhoo et al., 2009).
The evidence above indicates that Krox20 works antagonistically to both Notch and c-Jun, as well as the fact that Notch and c-Jun negatively regulate the myelin differentiation program of immature Schwann cells, by acting as myelination brakes (Jessen and Mirsky, 2008; Parkinson et al., 2008; Woodhoo et al., 2009).

New evidence has shown that the zinc-finger E-box-binding homeobox 2 (Zeb2) transcription factor is important in antagonising inhibitory effectors such as Notch and Sox2, but not c-Jun, therefore making Zeb2 a crucial timer for controlling Schwann cell differentiation both at the onset of myelination during development, and in remyelination following nerve injury (Wu et al., 2016; Quintes et al., 2016).

1.2.7 Remak Schwann cells

Many nerve fibres of the peripheral nervous system can be non-myelinated, including C fibre nociceptors, post-ganglionic sympathetic and parasympathetic fibres and motor nerve terminals found at the neuromuscular junctions (Monk et al., 2015).
Remak Schwann cells, as briefly described above, enclose several small diameter axons, forming a Remak bundle. Remak Schwann cells vastly outnumber Myelin Schwann cells present in peripheral nerves, which reflects the presence of large numbers of non-myelinated axons compared to myelinated ones (Dyck et al., 1972; Griffin and Thompson, 2008). Morphological studies have shown that in peripheral nerves Remak Schwann cells are shorter in length than Myelin Schwann cells (Aguayo et al. 1972; Monk et al., 2015).

1.2.8 Repair Bungner Schwann cells

A recent addition to the Schwann cell lineage is the repair Bungner Schwann cell. Nerve injury triggers both Myelin and Remak Schwann cells to convert into a cell type that is specific and specialised in promoting nerve repair. It was previously thought that Myelin and Remak Schwann cells reverted to a cell type reminiscent of their original immature Schwann cell counterparts following nerve injury (Jessen and Mirsky, 2008). However, more recent evidence has in fact confirmed that the cell type produced following nerve injury, is a distinct cell which is unlike the immature Schwann cell, both in terms of its molecular profile and morphology (Arthur-Farraj et al., 2012; Jessen and Mirsky, 2016). The process through which this unique repair Bungner Schwann cell is formed is through a combination of both de-differentiation and activation, as following nerve injury Schwann cells not only down-regulate their characteristic myelin gene expression (sign of de-differentiation), but also activate a repair program (sign of activation) (Jessen et al., 2015a; Jessen and Mirsky, 2016). The transcription factor c-Jun is a key regulator of this process following nerve injury.

The development of Schwann cells from embryonic stages, into adulthood and after injury are summarised in Figure 1.3 shown below.

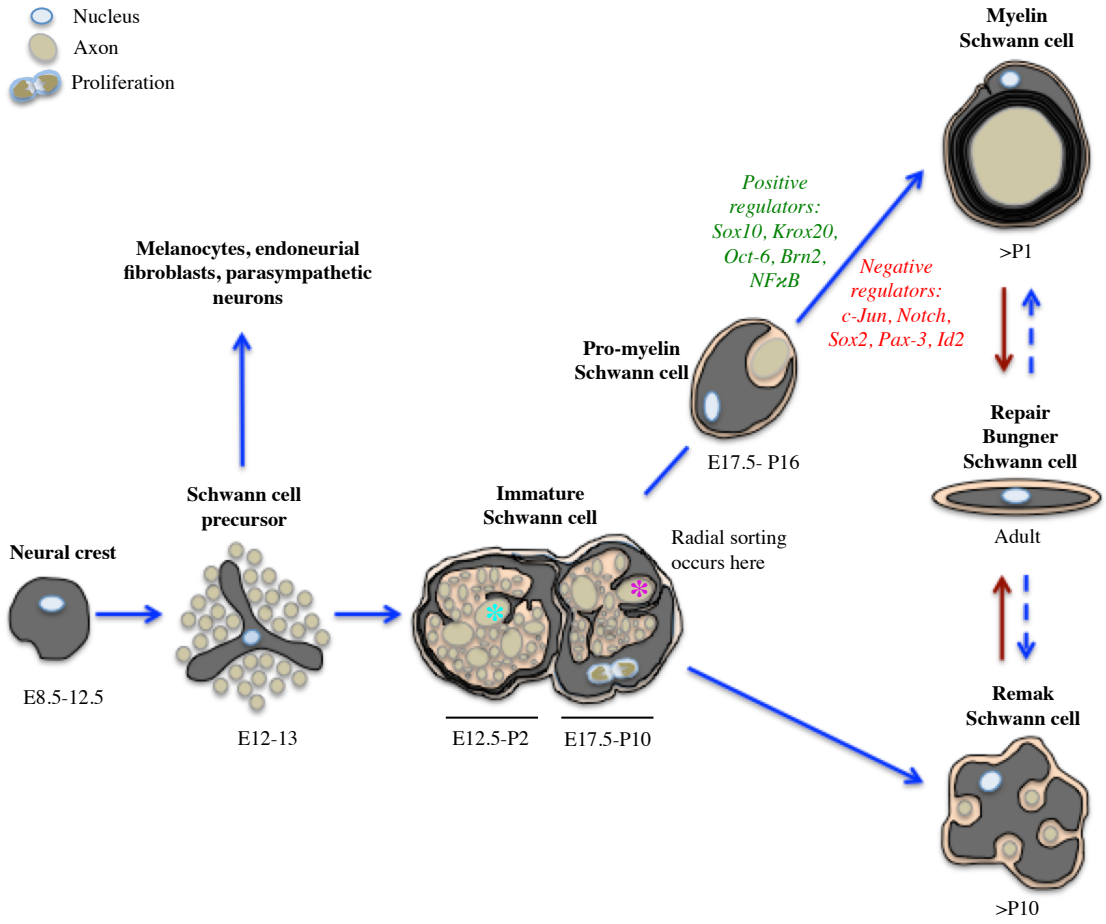

Figure 1.3 | Summary of Schwann cell development
A schematic representation of the transitional steps that occur during Schwann cell development. Neural crest cells give rise to Schwann cell precursors. Schwann cell precursors give rise to immature Schwann cells, as well as other cell types including melanocytes and endoneurial fibroblasts. Radial sorting is performed by immature Schwann cells and can be divided in stages. Firstly, the basal lamina is deposited and the formation of Schwann cell and axon "families" begins. Schwann cell processes are inserted into axonal bundles (shown above E12.5-P2). Large calibre axons are recognised as shown by the turquoise asterisk above. Large axons are then radially segregated to the periphery as shown by the purple asterisk above between E17.5-P10. The final stage is the establishment of 1:1 relationship between an axon and a pro-myelin Schwann cell), which can then become a mature Myelin Schwann cell depending on the timely activation of positive and negative regulators of myelination (shown above). Immature Schwann cells form Remak Schwann cells when Schwann cells are in contact with small caliber axons, that they eventually surround. Following nerve injury, both Myelin and Remak Schwann cells form a new and unique repair Bungner Schwann cell which is essential for successful nerve regeneration. Blue solid lines indicate transition steps along the Schwann cell lineage, dark red arrows indicate the Schwann cell injury response and the blue dotted lines indicate the re-formation of Myelin and Remak Schwann cells following nerve injury.
Adapted from Feltri et al., 2016 and Jessen and Mirsky, 2016.

1.3 Nerve injury

Axons of peripheral nerves have the remarkable ability to successfully regenerate and re-innervate their targets to result in functional recovery (though it may be poor, especially in humans). As previously discussed, this ability of peripheral nerves to regenerate is reliant on the plasticity of the Schwann cells of the distal stump that can be reprogrammed into a new, distinct and functional cell known as the repair Büngner Schwann cell. This repair Bungner Schwann cell is essential for successful nerve regeneration, as well as the cellular events that take place soon after nerve injury (Rotshenker, 2011; Arthur-Farraj et al., 2012; Jessen et al., 2015; Jessen and Mirsky 2016).

Sciatic nerve crush models are a common way of studying nerve regeneration. In this model axons are severed but the basal lamina of Schwann cells is not interrupted, to allow for a permissive environment for optimal regeneration (Sunderland, 1951; Fowler et al., 2015). In contrast, after nerve transection basal lamina tubes are severed and become discontinuous at the point of transection. Peripheral nerves are reliant on the fine details of their structures and the communication between axons and Schwann cells for correct function.

Upon nerve injury, peripheral nerve structures and the cross-talk between Schwann cells and axons are disrupted, which brings about Wallerian degeneration, particularly to the distal stump of the nerve, where axons are separated from the neuronal cell body (Waller, 1850; Kaplan et al., 2009). Axons of the distal stump do not breakdown immediately; there is a delay of 24-48 hours in rodents (and several days in humans) (Lubinska, 1977; Chaudry and Cornblath 1992). Upon nerve transection both ends (proximal and distal) retract and outgrowths occur from both proximal and distal ends, yet the reaction of the proximal stump is slower than that of the distal stump (Thomas, 1966; Thomas and Jones, 1967). These proximal and distal reactions to nerve injury are important for successful nerve repair.

The distal stump disintegrates due to Wallerian degeneration, which is a multi-faceted process (Rotshenker, 2011), whereas the proximal stump acts to transmit injury signals from the site of injury retrogradely to the neuronal cell body, to make it switch from a transmission mode to one of growth (Abe and Cavalli, 2008).

1.3.1 Wallerian degeneration and events that follow

Wallerian degeneration describes the events that take place distally to the injury site in a peripheral nerve injury.

Following nerve injury, the disconnection of the nerve trunk from its "trophic" centre (neuronal cell body) is what Augustus Waller described as being the cause of axons degenerating during Wallerian degeneration (Gutmann and Holubar, 1950). Work carried out using mice and rats has provided better insight into blebbing, and swelling of the axolemma (axon membrane), and "granular disintegration" (subsequent breakdown of cytoskeletal elements), all of which are characteristic features of Wallerian degeneration (George et al., 1995). The more recent use of the Wallerian degeneration (Wld^S) mouse model has helped to understand and clarify the process of Wallerian degeneration in greater detail. Axons in Wld^S mouse nerves, are shown to collapse more slowly than those of wild-type (WT) mice, and the axonal granular disintegration of the cytoskeleton is delayed (Coleman et al., 1998).

The process driving successful nerve repair after injury is a complex one. It is not only the axonal response that is important, but also other changes that take place within the distal stump after nerve injury. These include: increase in blood-tissue barrier permeability, Schwann cell demyelination, cellular reprogramming of Schwann cells to become a repair cell phenotype (Arthur-Farraj et al., 2012; Jessen et al., 2015; Jessen and Mirsky, 2016), the recruitment and influx of macrophages (Rotshenker, 2011; Benowitz and Popovich, 2011), and finally the removal of myelin and axonal debris (Gaudet et al., 2011). Wallerian degeneration is the key process that accounts for the hospitable environment created in and around axons and which allows them to regenerate following nerve injury (Dubovy, 2011).

Following nerve injury Schwann cells play a key role in myelin breakdown, macrophage recruitment, the formation of regeneration tracts (bands of Büngner) and the expression of proteins which promote axon outgrowth; thereby providing trophic support and creating a favourable environment for regenerating axons (Gaudet et al., 2011; Arthur-Farraj et al., 2012; Gomez-Sanchez et al., 2015). The Schwann cell response to nerve injury is very rapid (as early as 48 hours) and is evident even before

any visible axonal degeneration has occurred. Within 48 hours after nerve injury the Schwann cell stops producing myelin proteins and begins to up-regulate the expression of genes that are involved in potentiating and promoting neuronal survival and axonal outgrowth, including neurotrophic factors, adhesion proteins, inflammatory cytokines and extracellular matrix components (Arthur-Farraj et al., 2012). Schwann cells of the distal stump, within a short space of time, release pro-inflammatory cytokines including tumour necrosis factor-α (TNF-α), interleukin (IL)-1α and IL-1β as well as IL-6, Leukaemia Inhibitory Factor (LIF) and Macrophage Chemoattractant Protein1 (MCP-1), in response to peripheral nerve injury. These factors are important because they are required for immune cell chemotaxis including recruitment of macrophages to the injury site (Tofaris et al., 2002; Rotshenker, 2011). Although it is commonly thought that the release of pro-inflammatory factors are detrimental, the release of certain pro-inflammatory cytokines and chemokines (such as LIF and MCP-1) have been shown to be important for successful peripheral nerve regeneration (Tofaris et al., 2002; Painter et al., 2014).

The ability of Schwann cells to recruit macrophages to the site of injury appears to have an importance in other aspects of peripheral nerve repair including new blood vessel formation (Cattin et al., 2015), as complete ablation of myeloid cells reduces axon outgrowth and prevents functional recovery (Barrette et al., 2008).

Macrophages are a major cell type found in sciatic nerves with important functions in allowing for successful nerve regeneration following injury. Resident macrophages account for 2-9% of the cell populations present in peripheral nerves. These resident macrophages are thought to originate from circulating monocytes (Mueller et al., 2003). Nerve injury triggers an inflammatory response, involving the recruitment of macrophages to the injured nerve. Macrophages are known as the secondary responders to injury after Schwann cells (primary responders), where they assist in the break down of myelin and its clearance through phagocytosis (Gaudet et al., 2011). Recent evidence has highlighted that in the absence of macrophages in the nerve, regeneration is severely compromised (Barrette et al., 2008; Cattin et al., 2015). Macrophages are already present as early as 4 hours at the injury site and steadily increase in numbers up to 2 days. The presence of macrophages along the distal stump peaks between 7 and 21 days post injury, depending on the type of injury and the

macrophage marker used. As the nerve regenerates these macrophages diminish in number (Perry et al., 1987; Stoll et al., 1989; Perry and Brown, 1992; Dailey et al., 1998).
Therefore, following nerve injury, Schwann cells and macrophages work in conjunction with each other.

Schwann cells then begin to proliferate (Gaudet et al., 2011), forming bands of Büngner within their basal lamina tubes. Schwann cell proliferation and their alignment to form these bands of Büngner, along with the removal of myelin debris (which acts as a barrier to re-growing axons in the distal nerve) is a process now known as myelinophagy. These events are important for providing the growth supportive environment to allow axons to regenerate (Gomez-Sanchez et al., 2015).

As already mentioned, the ability of the Schwann cells to carry out these different functions is due to their highly plastic nature. In response to nerve injury, Schwann cells distal to the lesion site undergo a process of cellular reprogramming (down-regulating myelin genes and in addition express new genes related to its function as a repair cell) (Jessen et al., 2015; Jessen and Mirsky, 2016) but also adopt a unique phenotype to produce repair Bungner Schwann cells (Arthur-Farraj et al., 2012).

The end of Wallerian degeneration is marked by re-myelination, where axons have re-grown and Schwann cells have been able to myelinate them. By this point in nerve regeneration following peripheral nerve injury, newly regenerated axons will have reached their targets, and functional recovery is regained (Gaudet et al., 2011; Fricker et al., 2011).

1.4 The proximal stump

The proximal stump is of great interest as the Schwann cells remain in close contact with the axons throughout the regenerative process, unlike in the distal stump, where Schwann cell-axonal contact is lost. Studies into the proximal stump resulting from nerve transection originate from studies dating back to the 1920s and earlier. Following nerve transection, outgrowths are seen from the transected nerves at both ends, and Schwann cells multiply in both proximal and distal stumps during the immediate days following nerve transection (Young et al., 1940; Thomas and Jones, 1967). Axons of the proximal stump quickly seal their ends to prevent loss of axoplasm (Waller, 1850).

Within 1-2 days of the nerve transection, axons of the proximal stump begin to develop swellings often referred to as boutons, which have been suggested to influence nerve regeneration through the release of regeneration promoting molecules such as calcitonin gene related protein (CGRP) and nitric oxide (Li et al., 2004). The axonal sprouts originating from the proximal stump are important as it is these that advance across the "nerve bridge" (consisting mainly of fibroblasts and Schwann cells) which is formed between the proximal and distal stumps following nerve transection. This sprouting is thought to originate from either the first or second node of Ranvier (Friede and Bischhausen, 1980). The rate at which axonal sprouts advance is much slower than compared to axonal sprouts in a nerve crush, where the endoneurial tubes are intact and Schwann cells line these structures to form the guiding regeneration tracks: the Bands of Büngner (Zochodne, 2008).

More recent work shows that the changes that occur within the proximal stump axons and their neuronal cell bodies vary based on the location of the injury. The closer the nerve transection is to the neuronal cell body, the more chance of neuronal apoptosis. Breakdown of proximal stump axons is limited to the point up to the first Node of Ranvier (Tetzlaff and Bisby, 1989, Zochodne, 2003), unlike in the distal stump where axons are broken down in their entirety (Stoll et al., 1999; Rotshenker et al., 2011; Gomez-Sanchez et al., 2015).

Within hours of nerve transection, the axonal cytoskeleton is re-arranged and microtubules are re-organised to form microtubule based traps for anterogradely

transported vesicles that are important for forming the growth cone complex (Erez et al., 2007).

The anterograde response is not the only important response that takes place. The influx of calcium ions (Ca^{2+}) into the severed axons determines calcium-dependent axonal degeneration, which begins to take place immediately after nerve injury (Mandolesi et al., 2004). Recent evidence has highlighted that the retrograde calcium signalling that takes place following nerve injury transection, can cause the export of histone deacetylase 5 (HDAC5) in the neuronal nucleus, which is able to remodel the chromatin and in this way prime the neuron for an injury response through epigenetic changes (Cho et al. 2013).

This limited breakdown of the axons in the proximal stump is expected because they are still connected to the cell bodies after transection. This enables a switch to a growth mode from a neuro-transmitting mode, unlike the distal stump, which is no longer connected to the cell body and breaks down. The importance of Schwann cells within the proximal stump is investigated in this thesis (Chapter 5).

1.5 c-Jun and nerve regeneration

The timely down-regulation of c-Jun expression in Schwann cells during development is a determinant of the progression of immature Schwann cells into mature myelinating Schwann cells (Monuki et al., 1989; Shy et al., 1996; Parkinson et al., 2004; Jessen and Mirsky, 2005). The activation of JNK/c-Jun pathway is involved in regulating proliferation in many cell types (Leppa and Bohmann, 1999; Shaulin and Karin, 2001; Parkinson et al., 2008). In Schwann cells the JNK/c-Jun pathway is important in apoptosis induced by TGF-β and in regulating Schwann cell proliferation in cultured cells (Parkinson et al., 2001; Parkinson et al., 2004). Nevertheless, c-Jun can also be activated by other cell signalling pathways such as ERK and P38 pathways (Monje et al., 2005; Yang et al., 2012).

The process of cellular reprogramming that Schwann cells in the distal stump undergo after nerve injury, relies on the ubiquitin-proteasome system (Lee et al., 2009) and is driven by re-expression of the transcription factor c-Jun, which forms part of the AP-1 early response transcription factor complex (Parkinson et al., 2008; Arthur-Farraj et al., 2012; Jessen et al., 2015; Jessen and Mirsky, 2016). In order to form transcriptionally active complexes, c-Jun has to homo or hetero-dimerise with itself or another member of the AP-1 transcription factor family (Deng and Karin, 1992; May et al., 1998).

c-Jun is an immediate early gene and its expression in Schwann cells is seen very rapidly after nerve injury. As mentioned earlier, recent work shows that c-Jun is a global regulator of the Schwann cell injury response, and is important in the cellular reprogramming process of Schwann cells (an important step in response to nerve injury) in achieving successful nerve repair. This is highlighted by the fact that in mice where c-Jun is ablated specifically from Schwann cells, there is impaired and delayed axon outgrowth, neuronal death and minimal functional recovery (Arthur-Farraj et al., 2012).

It is currently unknown which family member(s) of the AP-1 transcription factors may be the binding partners for c-Jun in repair Bungner Schwann cells, however recent evidence would suggest they may include Fosl2 and ATF3 (Arthur-Farraj et al.,

2017, in preparation and personal communication).

It is now accepted that c-Jun within Schwann cells governs major aspects of the injury response. This includes determining the expression of trophic factors and adhesion molecules, myelin clearance, and its importance in the cellular reprogramming process, which governs the formation of bands of Büngner. However, it appears that c-Jun is less important in controlling the expression of Schwann cell cytokines, which are important for macrophage invasion after injury (Arthur-Farraj et al., 2012; Napoli et al., 2012; Martini et al., 2013; Jessen et al., 2015; Jessen and Mirsky, 2016).

1.6 Neuronal regeneration associated gene (RAG) expression following nerve injury

As previously mentioned, a phenomenon that is commonly seen when peripheral nerves are transected is their ability to regenerate, whereas this is not often the case within the CNS. The regenerative ability of the PNS is due to both the activity of non-neuronal cells distal to the lesion site, as well as specific changes that take place within the neuronal cell body. These changes result in a change in the neuronal phenotype of the cell soma from a state of "transmission" of specific signals, to a "regenerative" mode, essential for outgrowth (Navarro et al., 2007).
Successful nerve repair within the PNS is reliant on the ability of the dorsal root ganglia (DRG) of sensory neurons and motor neurons that project from the CNS to the PNS, to become activated and switch from a signalling state to one of growth in response to nerve injury. Compared with the minimal neurite outgrowth seen after CNS injury, the ability of PNS neurons to be activated after nerve injury represents a significant difference, resulting in successful nerve regeneration. Even if CNS axons are provided with a favourable substrate such as a PNS graft, outgrowth is comparatively poor compared with that seen when similar grafts are attached to PNS nerves (David and Aguayo, 1981).

Peripheral nerve axotomy also triggers morphological changes within the neuronal cell body, known as chromatolysis, which includes the dispersal of the Nissl substance, the movement of the nucleus to the periphery of the cell, the swelling of the cell body, and the retraction of the synaptic terminals at the neuromuscular junction (Fawcett and Keynes, 1990).

Neuronal activation is thought to be caused by signals originating from the injury site. Studies carried out in the late 1990s in the mollusc Aplysia californica provided evidence for the existence of multiple injury signals (Ambron and Walters, 1996).
Not much is known about the mechanism which initiates the increase in retrograde signals, but as mentioned earlier, injured Schwann cells release cytokines and growth factors including LIF, IL-6, IL-1α, IL-1β, TNF-α and MCP-1 (Banner et al., 1994; Bolin et al., 1995; Kurek et al., 1996; Tofaris et al., 2002; Rotshenker, 2011; Arthur-

Farraj et al., 2012), which are capable of activating MAPKs and the JAK-STAT pathway.

Additionally, in IL-6 knockout mice, GAP43 (a known RAG) is not up-regulated in DRG neurons following peripheral nerve injury (Cafferty et al., 2004), showing that the release of cytokines and chemokines is important in successful initiation of retrograde axonal injury signals and their transport to the neuronal cell bodies.

Retrograde axonal injury signals are the important link between the site of injury and the neuronal cell body response, because if there is a delay or ablation of certain axonal injury signals, then the neuronal cell body response will not be able to up-regulate specific RAGs and therefore change from a "transmission" mode to a "growth" mode (Abe and Cavalli, 2008).

Neuronal activation (in terms of its growth activation), involves significant changes in the gene transcription profile of the neuron. Many RAGs including members of the immediate-early gene families c-Jun and JunD (Leah et al., 1991; Jenkins and Hunt, 1991; Abe and Cavalli, 2008), as well as constitutive transcription factors such as CREB, STAT3, SOX11, ATF3 and SMAD1 (Schwaiger et al., 2000; Tanabe et al., 2003; Abe and Cavalli, 2008; Fagoe et al., 2015) are up-regulated in response to neuronal activation, while other genes such as SMAD2 and ATF2 (Martin-Villalba et al., 1998) are down-regulated.

To re-enforce the importance of RAG up-regulation, it has been shown that forced up-regulation of RAGs even in CNS neurons is sufficient to promote some axon outgrowth (Kobayashi et al., 1997). A more recent large-scale gene screen analysis of the intrinsic axonal growth programme of peripheral nerves following injury was carried out highlighting how complex the gene network of RAGs is, however, Jun was shown to be a central component (Chandran et al., 2016).

c-Jun acts as a key regulator of neuronal plasticity and is required for the initiation of additional transcriptional changes that not only play a role in successful axonal regeneration (Raivich et al., 2004), but also in the Schwann cell. Some of the genes up-regulated by c-Jun in neurons include CD44, galanin and integrin $\alpha 7\beta 1$ which have themselves been implicated in regeneration (Holmes et al., 2000; Patodia and Raivich).

As mentioned earlier, similarly to c-Jun, ATF3 and p-STAT3 are also up-regulated in

DRG neurons after peripheral nerve injury (Herdegen et al., 1997; Tsujino et al., 2000; Cafferty et al., 2004; Raivich et al., 2004; Seijffers et al., 2007; Tedeschi, 2012). Treatment with the JAK2 inhibitor AG490 blocks STAT3 phosphorylation and impairs axon outgrowth (Qiu et al 2005). A mouse model that shows the role of p-STAT3 in retrograde axonal injury signalling is the Dual Leucine Zipper kinase (DLK) knockout model, which demonstrates that if the retrograde transport of p-STAT3 to the neuronal cell body is disrupted, and its up-regulation is prevented within the soma, impaired axon outgrowth and regeneration results (Shin et al., 2012). Overexpression of ATF3 in neurons both in vivo and in vitro increases neurite outgrowth (Seijffers et al., 2006; Seijffers et al., 2007). Growth-associated protein (GAP43) also acts to promote regeneration, since its over-expression induces nerve sprouting in mouse nervous systems (Aigner et al., 1995).

Neuronal activation following nerve injury is summarised in the diagram shown in Figure 1.4.

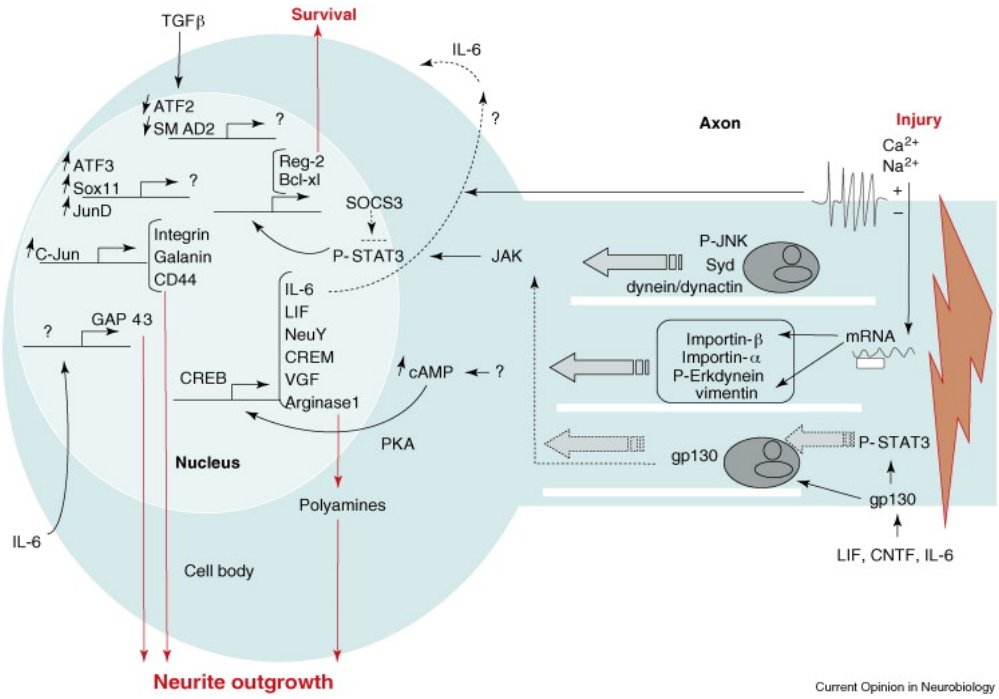

Figure 1.4 | Neuronal expression of RAGs following nerve injury
A diagram to show the main events that take place following nerve injury in the neuronal cell body. Following nerve injury, multiple signaling events in the axon are triggered, including membrane depolarization, JNK activation, mRNA translation, and cytokine-mediated STAT3 activation, which in turn activates the neuronal cell body. When these signaling molecules reach the cell body, they mediate the expression of a number of transcription factors that regulate the expression of genes involved in neurite outgrowth.
This diagram is taken from Abe and Cavalli, 2008

1.7 Conditioning lesion paradigm

The difference between the ability of peripheral and central nerves to regenerate was first described by Ramon y Cajal, who demonstrated that peripheral nerves could not regenerate through a central nerve graft tissue following injury (Cajal, 1928). It was later shown that CNS nerves that were transplanted to grow through peripheral nerves were able to, in contrast to their behaviour in the native CNS environment (David & Aguayo 1981; Richardson et al., 1980; Richardson and Verge, 1986). These experiments demonstrated that peripheral nerves provide the necessary growth permissive conditions to allow central nerves to have limited regeneration.

As mentioned above, nerve injury causes the neuronal cell body to respond by activating a growth programme that supports regeneration (Abe and Cavalli, 2008; Huebner and Strittmatter, 2009). DRG sensory neurons are unique in that they possess a single branched axon that extends into the periphery, and the spinal column. These two branches elicit different responses. Experiments showed that when the peripheral branch of DRG neurons is injured first, followed by a lesion in the central branch of DRG neurons, these central neurons are able to project axons into the CNS (McQuarrie, 1985; Neumann and Woolf, 1999; Chong et al., 1999; Hoffman, 2010). The idea of having a 'conditioning' lesion, is a way of exaggerating the neuronal cell body response to injury, and is a commonly used paradigm, particularly in the central nervous system where limited axonal regeneration is seen.

1.7.1 Myelin as an inhibitory substrate

As mentioned earlier, trauma to the brain and spinal cord can produce irreparable damage It is thought that part of this failure of CNS neurons to regenerate is due to the inhibitory environment created by myelin (Buchser et al., 2012).

Although myelin is considered an inhibitory substrate, work by Davies et al., 1997 showed that DRG neurons were able to grow across the corpus callosum along the myelin rich substrate, yet a similar experiment carried out using CNS neurons failed to exhibit this outcome. For this reason and other evidence, it is widely accepted that PNS neurons have an intrinsic ability to grow on otherwise inhibitory substrates (Shen et al., 1998; Buchser et al., 2012; McKerracher and Rosen, 2015)

1.8 Aims

Although c-Jun in Schwann cells is dispensible for normal Schwann cell development, it performs vital functions in controlling nerve regeneration following nerve injury (Arthur-Farraj et al., 2012). This thesis aims to investigate whether increasing c-Jun in Schwann cells to levels above those normally seen in developing or regenerating nerves would have beneficial or deleterious effects. It also aims to address the importance of Schwann cell c-Jun in the neuronal cell body response following nerve injury. This was approached in the following way:

1. To characterise the development of postnatal and adult nerves in transgenic mice that overexpress Schwann cell c-Jun (Chapter 3)
2. To determine whether c-Jun overexpression in Schwann cells accelerates nerve regeneration following nerve injury (Chapter 4)
3. To establish the significance of c-Jun expression in the proximal stump following nerve injury (Chapter 5)
4. To elucidate whether Schwann cell c-Jun can affect the ability of DRG neurons to respond to nerve injury (Chapter 6)

2. Materials and Methods

2.1 List of abbreviations

ADS-	Antibody Diluting Solution
APS-	Ammonium Persulfate
AraC-	Cytosine Arabinoside
ATF3-	Activating Transcription Factor 3
BDMA-	N-benzyldimethylamine
BSA-	Bovine Serum Albumin
dbcAMP-	dibutyryl Cyclic Adenosine Monophosphate
DDSA-	Dodecenyl Succinic Anhydride
DM-	Defined Medium
DMSO-	Dimethyl Sulphoxide
DMEM-	Dulbecco's Modified Eagle's Medium
DS-	Donkey serum
FBS-	Foetal Bovine serum
GAP43-	Growth Associated Protein 43
GS-	Goat serum
HS-	Horse serum
MNA-	Methyl Nadic Anhydride
NRG1-	Neuregulin 1
PB-	Phosphate Buffer
PBS-	Phosphate Buffered Saline
PLL-	Poly-L-lysine
RPMI-	Roswell Park Memorial Institute medium
Sox10-	SRY-Box 10
STAT3-	Signal Transducer and Activator of Transcription 3
TEMED-	Tetramethylethylenediamine
TBS-	Tris-Buffered Saline

2.2 List of materials and reagents

2.2.1 List of recipes

Alkaline lysis reagent- pH 12 (HOTShot)

(make up to 50ml with dH_2O without adjusting pH)

Reagent	*Amount*
25mM NaOH	50mg
0.2mM disodium EDTA	3.72mg

Neutralising reagent- pH 5

(make up to 50ml with Tris-HCl in dH_2O without adjusting pH)

Reagent	*Amount*
40mM Tris-HCl	315.2mg

10X PBS

(make up to 1L with dH_2O)

Reagent	*Amount*
NaCl	80g
Na_2HPO_4	11.5g
KCl	2g
KH_2PO_4 (anhydrous)	2g

5X Laemmli buffer

(use at a final concentration of 1X)

Reagent	*Amount*
1M Tris pH 6.8	1.25ml
20% SDS	5ml
glycerol	2.5ml
β-mercaptoethanol	1ml
dH_2O	0.25ml

RIPA buffer

(final volume of 20.2ml)

Reagent	*Amount*
1M Tris-HCl pH 8	5ml
5M NaCl	10ml
20% Triton-X-100	5ml
5mM EDTA	200 µl

10X Running buffer

(adjust pH to 8.3, make up to 1L with dH_2O, and use at a final concentration of 1X)

Reagent	*Amount*
Tris Base	30g
Glycine	144g
SDS	10g

10X TBS

(adjust pH to 7.4, make up to 1L with dH_2O, and use at a final concentration of 1X)

Reagent	*Amount*
Tris HCl (500mM)	78.6g
NaCl (150mM)	87.6g

8% Resolving gel

(based on making 1 gel)

Reagent	*Amount*
40% acrylamide	2.5ml
1.5M Tris pH8.8	3.2ml
10% SDS	125µl
dH_2O	6.8ml
TEMED	10µl
APS	100µl

10% Resolving gel

(based on making 1 gel)

Reagent	*Amount*
40% acrylamide	3.2ml
1.5M Tris pH8.8	3.2ml
10% SDS	125µl
dH_2O	6.1ml
TEMED	10µl
APS	100µl

Stacking gel

(based on making 1 gel)

Reagent	*Amount*
40% acrylamide	625µl
0.5M Tris pH6.8	1.25ml
10% SDS	50µl
dH_2O	3.1ml
TEMED	7.5µl
APS	37.5µl

Transfer buffer

(adjust pH to 8.3, make up to 1L with dH_2O)

Reagent	*Amount*
48mM Tris Base	5.82g
39mM Glycine	2.93g
10% SDS	3.75ml
100% methanol	200ml

Resin

Reagent	*Amount*
Agar	12g
DDSA	8g
MNA	5g
BDMA*	16 drops

*Use a 1.5ml Pasteur pipette, this is counted dropwise

Defined Medium

Reagent	*Amount*	*Concentration*
Ham's/F12	48.3ml	50%
DMEM	48.3ml	50%
BSA	1ml	0.035%
Putrescine	1ml	16 μg/ml
Transferrin	1ml	100 μg/ml
T4 (L-Thyroxine)	100μl	400 ng/ml
Progesterone	100μl	60 ng/ml
Insulin (High)	100μl	10^{-6}M
Dexamethasone	77μl	38 ng/ml
T3 (L-Thyronine)	10μl	10.1 ng/ml
Selenium	10μl	160 ng/ml

Calcium and magnesium free medium

(store at 4°C)

Reagent	*Amount*
Water	80ml
10X Krebs Solution	10ml
50% amino acid solution	2ml
7.5% $NaHCO_3$	2.5ml
Phenol red solution	0.5ml
50% glucose	0.4ml

10X Krebs solution

(make up to 200ml with dH_2O)

Reagent	*Amount*
NaCl	14g
KCl	0.7g
KH_2PO_4	0.3mg/ml

Enzyme cocktail

(made up in calcium and magnesium free medium)

Reagent	*Amount*
Collagenase	3mg/ml
Hyaluronidase	1.2mg/ml
Trypsin Inhibitor	0.3mg/ml

2.2.2 List of antibodies

2.2.2.1 Immunofluorescence primary antibodies

Name of Antibody	*Host species*	*Dilution*	*Diluent*	*Company*
Anti-Sox10	Goat	1:100	10%HS/0.2%Triton-X-100/PBS	R and D Sytems
Anti-NF200	Chicken	1:10000	0.1%BSA/PBS	Abcam
F480	Rat	1:100	10%HS/0.2%Triton-X-100/PBS	R and D Systems
Anti-L1 (supernatant) (324 Hybridoma)	Rat	1:10	10%HS/0.2%Triton-X-100/PBS	Jessen/Mirsky Lab
Anti-c-Jun	Rabbit	1:800 1:3200	10%HS/0.2%Triton-X-100/PBS 0.1%BSA/PBS	New England Biolabs
Anti-Krox20	Rabbit	1:100	10%HS/0.2%Triton-X-100/PBS	Millipore
Anti-Ki67	Rabbit	1:100	10%HS/0.2%Triton-X-100/PBS	Abcam
Anti-Tuj1	Rabbit	1:500	0.2%Triton-X-100/ADS	Covance
Anti-ATF3	Rabbit	1:500	0.1%BSA/PBS	Santa Cruz
Anti-p-STAT3 tyr705	Rabbit	1:500	0.1%BSA/PBS	New England Biolabs
Anti-p-STAT3 ser727	Rabbit	1:50	0.1%BSA/PBS	New England Biolabs
Anti-GAP43	Rabbit	1:1000	0.1%BSA/PBS	Millipore
Anti-CGRP	Rabbit	1:10000	0.1%BSA/PBS	2BScientific
Anti-Galanin	Rabbit	1:10000	0.1%BSA/PBS	2BScientific

2.2.2.2 Immunofluorescence secondary/ biotinylated antibodies

Name of Antibody	*Host species*	*Dilution*	*Diluent*	*Company*
Anti chicken (IgG) alexafluor 488	Goat	1:1000	10%HS/0.2%Triton-X-100/PBS 0.1%BSA/PBS	Molecular probes
Anti chicken (IgG) cy3	Donkey	1:500	10%HS/0.2%Triton-X-100/PBS 0.1%BSA/PBS	Jackson Immunoresearch
Anti goat (IgG) alexafluor 488	Donkey	1:1000	10%HS/0.2%Triton-X-100/PBS	Molecular probes
Anti rabbit (IgG) alexafluor 488	Goat	1:1000	10%HS/0.2%Triton-X-100/PBS 0.1%BSA/PBS	Molecular probes
Anti rabbit (IgG) cy3	Donkey	1:500	10%HS/0.2%Triton-X-100/PBS 0.1%BSA/PBS	Jackson Immunoresearch
Anti rat (IgG) alexafluor 488	Goat	1:1000	10%HS/0.2%Triton-X-100/PBS	Molecular probes
Anti rat cy3 (IgG)	Donkey	1:500	10%HS/0.2%Triton-X-100/PBS	Jackson Immunoresearch
Anti rabbit (IgG), biotinylated species	Donkey	1:600	10%HS/0.2%Triton-X-100/PBS	Amersham
Streptavidin-cy3	*Streptomyces avidinii*	1:500	10%HS/0.2%Triton-X-100/PBS	Jackson Immunoresearch
DAPI	n/a	1:100000	Different per protocol used	Thermofisher Scientifc

2.2.2.3 Western blot primary antibodies

Name of Antibody	*Host species*	*Dilution*	*Diluent*	*Company*
Anti- GAPDH	Rabbit	1:5000	5% milk TBS-T	Sigma
Anti-Calnexin	Mouse	1:1000	5% milk TBS-T	Enzo Life Sciences
Anti-c-Jun	Rabbit	1:1000	5% milk TBS-T	New England Biolabs
Anti-Krox20	Rabbit	1:500	5% milk TBS-T	Millipore
Anti-Mpz	Chicken	1:2000	5% milk TBS-T	Aves Labs
Anti-Cyclin D1	Rabbit	1:100	5% milk TBS-T	Santa Cruz
Anti-ATF3	Rabbit	1:500	5% milk TBS-T	Santa Cruz
Anti-p-STAT3 tyr705	Rabbit	1:1000	5% BSA TBS-T	New England Biolabs
Anti-p-STAT3 ser727	Rabbit	1:1000	5% BSA TBS-T	New England Biolabs
Anti-STAT3	Mouse	1:1000	5% BSA TBS-T	New England Biolabs
Anti-GAP43	Rabbit	1:1000	5% BSA TBS-T	Millipore

2.2.2.4 Western blot secondary antibodies

Antibody	*Host species*	*Dilution*	*Diluent*	*Company*
Anti-rabbit (IgG) HRP	Rabbit	1:2000	5% milk TBS-T	Promega
Anti-mouse (IgG) HRP	Mouse	1:2000	5% milk TBS-T	Promega
Anti-chicken (IgG) HRP	Chicken	1:2000	5% milk TBS-T	Promega

2.2.3 Transgenic mice

All mice used were 6-10 weeks old and on a C57BL/6 background. Mice were housed in UCL Biological Services Unit (BSU). All mouse work was carried out in accordance with Home Office guidelines and mice 6-10 weeks old (unless otherwise specified) were culled using schedule 1.

P_0Cre transgenic mice (P_0Cre)

The P_0Cre mice used in the following experiments were kindly gifted by Dr L. Wrabetz and Dr L. Fletri (Italy). The mice express mP_0TOT(Cre) transgene (P_0Cre), driven by the Mpz (P_0) promoter (Feltri et al., 1999). The Cre-mediated recombination specifically in Schwann cells takes place between embryo day (E) 13.5 and E14.5 in the mouse and is activated by the P_0Cre transgene. P_0Cre activity is most strongly detected only in peripheral nerves, however there is minimal activity seen in the occipital lobe of the cerebral cortex, Purkinje cell layer of the cerebellum and in the heart (Feltri et al., 1999; Feltri, 2002; D'Antonio et al., 2006; Parkinson et al., 2008; Woodhoo et al., 2009; Yu et al., 2009).

c-Jun overexpressing mice (OE)

The mice overexpressing c-Jun (OE) were kindly gifted by the lab of Klaus Rajewsky (Max Delbruck Center, Berlin). These mice carry a lox-P flanked STOP cassette in front of a CMV early enhancer/chicken β actin (CAG) promoter driven c-Jun cDNA, inserted into the ROSA26 locus (c-Jun^{OE}). These mice, c-Jun$^{OE/OE}$ were crossed with P_0-Cre$^+$ mice (Jackson Laboratories) to generate the P_0-Cre$^+$/c-Jun$^{OE/+}$ mice referred to as OE/+. These mice were subsequently back-crossed with c-Jun$^{OE/OE}$ mice to generate P_0-Cre$^+$/c-Jun$^{OE/OE}$ mice referred to as OE/OE. P_0-Cre$^-$ littermates were used as controls and are referred to as wildtype (WT) in subsequent chapters.
This is summarised in Figure 2.1 shown below.

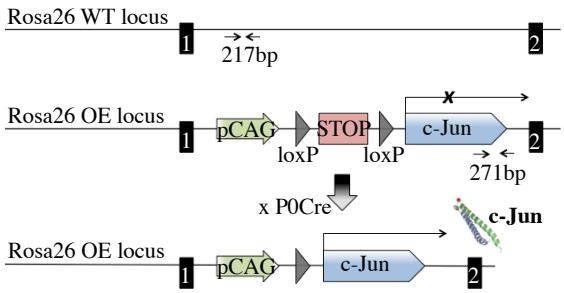

Figure 2.1 | Summary diagram showing the construct of c-Jun overexpressing mice
The mice overexpressing c-Jun overexpressing (OE) carry a lox-P flanked STOP cassette in front of a CAG promoter driven c-Jun cDNA, inserted into the ROSA26 locus. These mice, c-Jun$^{OE/OE}$ were, crossed with P0-Cre$^+$ mice to generate the P0-Cre$^+$/c-Jun$^{OE/+}$ mice referred to as OE/+. These mice were subsequently back-crossed with c-Jun$^{OE/OE}$ to generate P0-Cre$^+$/c-Jun$^{OE/OE}$ mice referred to as OE/OE.
Diagram courtesy of JA Gomez-Sanchez.

Schwann cell c-Jun conditional knockout mice (cKO)

The c-Jun floxed mice (c-Jun$^{fl/fl}$) were kindly gifted by Dr A. Behrens (London). To generate Schwann cell c-Jun conditional knockout mice (cKO), the c-Jun$^{fl/fl}$ mice were crossed with P_0-Cre mice. The resulting P_0Cre$^+$/c-Jun$^{fl/wt}$ mice were back-crossed to c-Jun$^{fl/fl}$ animals producing P_0Cre$^+$/c-Jun$^{fl/fl}$ (cKO) mice and P_0Cre$^-$/Jun$^{fl/fl}$ control litter-mates (WT). Polymerase Chain Reaction (PCR) gel analysis was carried out to ensure that the mice used were P_0Cre$^+$/c-Jun$^{fl/fl}$.

2.2.4 Genotyping

2.2.4.1 List of primers

Primers listed below were used to genotype transgenic mice using PCR gel analysis.

P_0cre Forward: 5'-GCTGGCCCAAATGTTGCTGG-3'
P_0cre Reverse: 5'-CCACCACCTCTCCATTGCAC-3'

Rosa26 Forward: 5'-GGAGTGTTGCAATACCTTTCTGGGAGTTC-3'
Rosa26 Reverse: 5'-TGTCCCTCCAATTTTACACCTGTTCAATTC-3'

c-Jun^{OE} Forward: 5'-TGGCACAGCTTAAGCAGAAA-3'
c-Jun^{OE} Reverse: 5'-GCAATATGGTGGAAAATAAC-3'

c-Jun$^{f/f}$ Forward: 5'-CCGCTAGCACTCACGTTGGTAGGC-3'
c-Junf^{f} Reverse: 5'-CTCATACCAGTTCGCACAGGCGGC-3'

2.2.4.2 PCR mastermix recipes and list of conditions

To determine whether or not mice were OE/+ or OE/OE, a combination of P_0cre and Rosa26WT PCRs were carried out. To check for the presence of the c-Jun^{OE}, the c-Jun^{OE} PCR was run in parallel.

P_0cre			
Sample	Volume (ml)	PCR conditions	
Buffer 5X	5	4 minutes at 94ºC	
MgCl2 (25mM)	1.5	30 seconds at 94ºC	x30 cycles
P_0cre forward (10µM)	1.25	1 minute at 50ºC	
P_0cre reverse (10µM)	1.25	1 minute at 72ºC	
dNTPs (10mM)	0.5	10 minutes at 72ºC	
Taq	0.2	PCR sizes: 500bp	
H_2O	13.05		
DNA (HOTSHOT)	1		
Final volume	25		
DMSO	1.25		

Rosa26 WT			
Sample	Volume (ml)	PCR conditions	
Buffer 5X	5	4 minutes at 94ºC	
MgCl2 (25mM)	1.5	15 seconds at 94ºC	x36 cycles
Rosa26 WT forward (10µM)	1.25	40 seconds at 60ºC	
Rosa26 WT reverse (10µM)	1.25	40 seconds at 72ºC	
dNTPs (10mM)	0.5	2 minutes at 72ºC	
Taq	0.2	PCR sizes: 350bp	
H2O	12.05		
DNA (HOTSHOT)	2		
DMSO	1.25		
Final volume	25		

c-Jun^{OE}			
Sample	Volume (ml)	PCR conditions	
Buffer 5X	5	5 minutes at 94ºC	
MgCl2 (25mM)	1.5	30 seconds at 94ºC	x34 cycles
c-Jun^{OE} forward (10µM)	1.25	45 seconds at 55ºC	
c-Jun^{OE} reverse (10µM)	1.25	1 minute at 72ºC	
dNTPs (10mM)	0.5	7 minutes at 72ºC	
Taq	0.2	PCR sizes: 271bp	
H2O	12.05		
DNA (HOTSHOT)	2		
DMSO	1.25		
Final volume	25		

c-Jun$^{f/f}$			
Sample	Volume (ml)	PCR conditions	
Buffer 5X	5	2 minutes at 94ºC	
MgCl2 (25mM)	1.5	40 seconds at 94ºC	x35-37 cycles
c-Jun$^{f/f}$ forward (10µM)	1.25	40 seconds at 57ºC	
c-Jun$^{f/f}$ reverse (10µM)	1.25	1 minute at 72ºC	
dNTPs (10mM)	0.5	7 minutes at 72ºC	
Taq	0.2	PCR sizes: 271bp	
H2O	14.3		
DNA (HOTSHOT)	1		
Final volume	25		

2.2.5 Surgical

Tools used for surgeries and dissections were bought from Fine Science Tools (Germany). These included number 2, 3, 5 forceps, curved forceps, crushing forceps, spring scissors, bone crushing scissors and fine scissors. Isofluorane, sterile drapes and sutures were provided by the Biological Services Unit (BSU) at University College London (UCL). Veterinary autoclips were obtained from VET-TECH. Bupivacaine was diluted 1:10 in sterile saline bought from the BSU.

2.2.6 Functional recovery tests

The wooden walking beam was made by UCL estates. 180gsm paper used for footprints, black paint and pencils were bought from Ryman (UK). Canon Pixma Scanner used to scan and analyse footprints was purchased from Office Depot (UK).

2.2.7 Histology

Glutaraldehyde, Agar 100 Resin, MNA, DDSA, BDMA, Tissue Tek OCT compound and rubber coffin moulds were bought from Agar Scientific. DPX mountant was from Merck Biosciences. Propylene oxide, osmium tetroxide, uranyl acetate, lead citrate, Na_2HPO_4 and NaH_2PO_4 were bought from Sigma.

2.2.8 Immunohistochemistry

Paraformaldehyde was bought from Fluka Chemicals Ltd. Triton-X-100 was bought from Sigma. Fluoromount-G was bought from SouthernBiotech. Superfrost slides were bought from Fisher Scientific. Mouse serum was bought from Serotec.
For a list of primary and secondary antibodies used in both Immunofluorescence and Western blotting, please see tables listed in section 2.2.2.

2.2.9 Molecular biology

Genotyping: EDTA disodium salt, ethidium bromide and sodium hydroxide were bought from Sigma. Taq DNA-polymerase, dNTPs, 100mM dNTP set and Agarose were bought from Invitrogen Limited. TAE 50X buffer was bought from VWR. 100bp DNA ladder was bought from Fisher Scientific Limited (Loughborough, UK).

Western blotting: Bis-Acrylamide 19:1, 1.5M Tris HCl, 0.5M Tris HCl, mini protean tank system, semi-dry transfer system and Chemidoc were bought from Bio-rad Laboratories. 15ml and 50ml Falcon tubes were bought from BD Biosciences. 5ml, 10ml and 25ml stripettes were bought from Costar. Nitrocellulose Hybond membrane, ECL and ECL Prime were bought from Amersham. Semi-skimmed milk powder was bought from Sigma. BCA protein assay, Halt protease inhibitior cocktail and EDTA were bought from Thermoscientific.

2.2.10 Tissue Culture

Tissue culture 35mm dishes, 4 well plates and centrifuge tubes were bought from VWR, UK. Round 13mm coverslips were bought from BDH (Lutterworth). Transferrin, selenium, putrescine, triiodothyronine (T3), thyroxine (T4), progesterone, dexamethasone, BSA, insulin, AraC, PLL, laminin, RPMI medium and Percoll were bought from Sigma. NRG1 was bought from R&D Systems. Collagenase was bought from Worthington. DMEM, Ham's F-12 medium and L15 medium were bought from Invitrogen Ltd. Trypsin, trypsin/EDTA and penicillin were bought from PAA. FBS was bought from Perbio. Forskolin was bought from Calbiochem. Horse serum was bought from Jackson Immunoresearch.

2.3 List of methods

2.3.1 Genotyping

DNA was extracted from fresh mouse ear notches, or for re-genotyping tail extracts were used. The tissue sample was incubated in 75µl of HotSHOT (recipe in section 2.2.1) solution for 1 hour at 95°C. This solution was then neutralised by adding 75µl of neutralising agent (recipe in section 2.2.1) and vortexing for 20s. The master mixes were made up according to the recipes above in section 2.2.4.2.

For Rosa26 WT and c-Jun^{OE} PCR reactions, 23µl of master mix and 2µl of extracted DNA were pipetted into thin walled PCR reaction tubes.

For P_0cre reactions, 24µl of master mix and 1µl of extracted DNA was pipetted into thin walled PCR tubes.

For c-Jun f/f PCR reactions, 21µl of master mix, and 4µl of extracted DNA were pipetted into thin walled PCR tubes.

2.3.2 Peripheral nerve surgeries and dissections

All peripheral nerve surgeries were carried out in accordance to Home Office Guidelines (UK) with the use of 2% isofluorane at the time of surgeries and when wounds were closed, bupivacaine diluted 1:10 in saline was administered. All wounds were closed using autoclips. All animals were culled using Schedule 1.

2.3.2.1 Uninjured sciatic nerve dissections

Sciatic nerves were dissected from WT, OE/+ and OE/OE mouse pups at postnatal (P) day 1, P7 and P21 for Western blot, Immunofluorescence and Electron Microscopy analyses.

For Immunofluorescence analysis, both nerves were dissected from WT, OE/+ and OE/OE animals at P7 and P60 and embedded in OCT compound (Tissue-Tek) ready for cryosectioning. P60 uninjured nerve samples were also dissected for teased nerve fibre preparation.

For Western blots, both nerves were dissected out from animals at P1, P7 and P60 from WT, OE/+ and OE/OE mice and put into clean eppendorf tubes before snap freezing them in liquid nitrogen. These nerves were then stored at -80°C ready for protein extraction. Western blot analysis was done by pooling both nerves from 6 animals at P1, both nerves from 3 animals at P7 and using 1 nerve from P60 mice.

For electron microscosopy (EM) studies, both nerves from WT, OE/+ and OE/OE mice at P1, P7, P21 and P60 were fixed inside the culled animal using EM fixative solution containing glutaraldehyde and PFA, before being dissected out and stored in fixative solution at 4°C ready to be processed for EM.

2.3.2.2 Crush injury

For sciatic nerve injuries, 6-10 week old mice (WT, OE/+ and OE/OE) had their right sciatic nerves exposed, which were crushed at the level of the sciatic notch, using fine forceps. The muscle was carefully put back in place to cover the nerve and bupivacaine diluted in saline 1:10 was administered to the muscle area before closing the wound.

The mice were allowed to recover for 1 day (D), 7D or 14D following injury. The distal stump of the nerve was dissected out from the crush point and separated into the first 0-2mm and the remaining 2-6mm. These segments were used for Western blot analysis by placing nerve segments into clean eppendorf tubes and snap freezing them in liquid nitrogen before storing them at -80°C ready for protein extraction.

The contralateral uninjured nerve was also dissected and divided into two 5mm segments- one of which was snap frozen for Western blot analysis, and the other was embedded in OCT compound ready for cryosectioning.

Some of the mice that had sciatic nerve crush surgeries were allowed to recover for 14D, 28D or 70D before dissecting out their sciatic nerves. From these mice, the distal stump was dissected 5.5mm from the crush point and fixed in the culled mouse using EM fixative solution containing 2.5% glutaraldehyde and 2% PFA for 15 minutes, before being dissected out and stored in fixative solution at 4°C overnight to a few days before being processed for EM.

WT, OE/+ and OE/OE mice that had sciatic nerve crush surgeries were also allowed to recover for 70D post crush for studying functional recovery through a series of behavioural tests at various time points. The nerves from these mice were then analysed for EM, in the same way as described above.

2.3.2.3 Transection injury

For all sciatic nerve transection injuries, 6-10 week old WT and cKO mice had their right sciatic nerves exposed, then were transected at the level of the sciatic notch, using fine scissors. The muscle was carefully put back in place to cover the nerve and bupivacaine diluted in saline 1:10 was administered to the muscle area before closing the wound.
These operated mice were allowed to recover for 1 hour, 6 hours, 48 hours or 2.5D depending on the experiment.

For teased nerve fibre preparations, only the first 2mm (0-2mm) which included the injury site of proximal stump was dissected out. This was then fixed for 10 minutes in 4% PFA and washed three times for 5 minutes each with 1XPBS. Samples were stored at 4°C ready to be teased out.

For Immunofluorescence analysis, the sciatic nerve of these injured mice was exposed at the transection site after 1 hour, 6 hours and 48 hours. In nerve transection experiments there was a clear separation of the intact nerve into a proximal and distal stump. From the proximal stumps, a 6mm segment beginning at the injury site was excised and cut into further 2mm segments (0-2mm, 2-4mm and 4-6mm). These individual segments were embedded separately in moulds using OCT compound ready for cryosectioning. A 6mm piece of the contralateral uninjured nerve of these mice was also dissected and embedded in OCT compound ready for analysis.

For Western blot analysis at 6 hours after nerve transection, the first 3mm of the proximal and distal stump was dissected out and 6mm of the contralateral uninjured nerve. These samples were placed into eppendorf tubes and snap frozen in liquid nitrogen before being stored at -80°C ready for protein extraction.

For L4 DRG (uninjured and injured) Western blots and immunofluorescence analyses, WT and cKO mice were allowed to recover for 48 hours following sciatic nerve transection. The L4 DRGs (uninjured and injured) from these mice were then dissected by excising the whole spine from the mouse to break away the vertebrae in

order to expose the spinal cord and DRGs. The L4 DRGs (both the injured and uninjured) were located and excised, carefully removing as much connective tissue and nerve roots as possible. The L4 DRGs were either snap frozen in liquid nitrogen or embedded in OCT compound for cryosectioning. Samples were stored at -80°C ready for processing.

For L4 DRG neuronal cultures, WT and cKO mice were allowed to recover for 2.5D following sciatic nerve transection. Only the L4 injured DRGs from these mice were dissected by excising the whole spine from the mouse to break away the vertebrae in order to expose the spinal cord and DRGs. L4 DRG cultures were made from the injured right L4 DRGs and plated both on PLL/laminin or PLL/myelin coated coverslips to analyse the conditioned growth response from these DRG neurons.

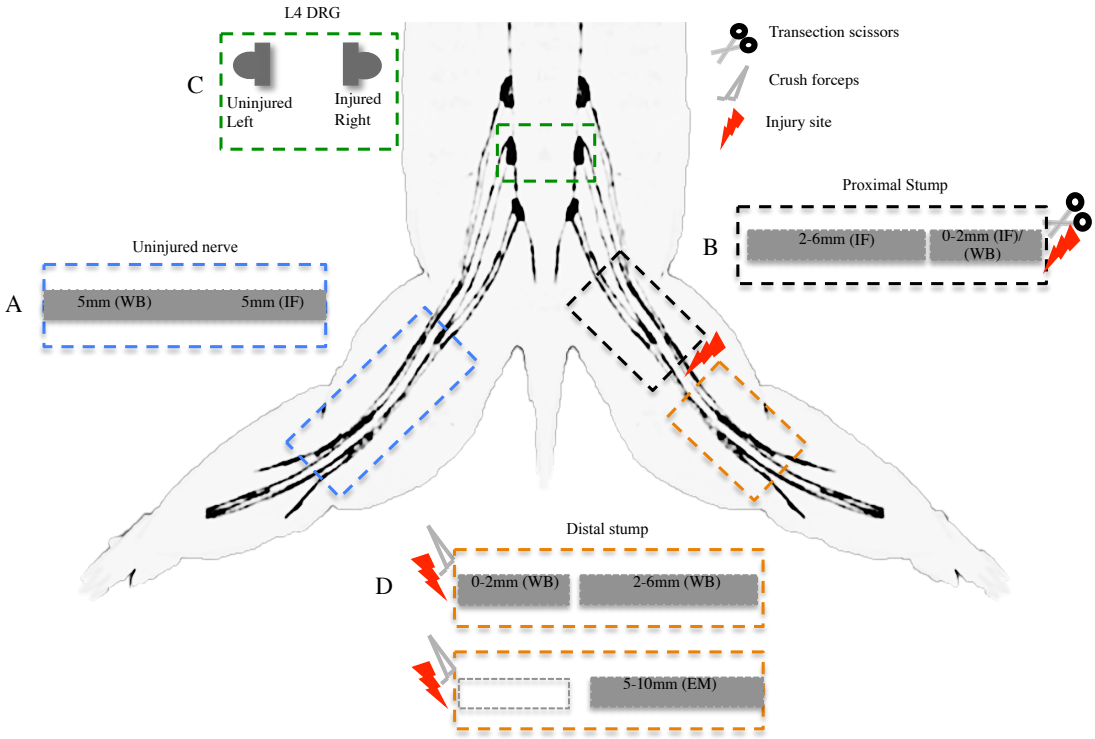

Figure 2.2 | Summary diagram showing the different types of peripheral nerve surgeries and how the tissue was processed
The control for all peripheral nerve experiments was the contralateral uninjured nerve (A) (blue dotted box). Depending on the experiment, the sciatic nerve was either transected (scissor symbol) or crushed (grey forceps symbol) at the sciatic notch (shown by the red lightning bolt). For sciatic nerve transection experiments, the proximal stump (B) (black dotted box) was processed for immunofluorescence in 2mm segments, or for Western blot analysis. The L4 DRGs (C) (green dotted box) were dissected for immunofluorescence, Western blot analysis or culture. For sciatic nerve crush experiments, the distal stump (D) (bottom orange dotted box) was used for electron microscopy, and Western blot analysis.

2.3.2.4 Conditioning lesion injury

The right sciatic nerve was exposed in the same way as for nerve crush or transection surgeries. The first surgery involved transecting the right sciatic nerve at mid-thigh level. The muscle was carefully put back in place to cover the nerve and bupivacaine diluted in saline 1:10 was administered to the muscle area before closing the wound. The mice were allowed to recover for 2.5D after the initial surgery. 2.5D following this initial nerve transection at mid-thigh level, the right sciatic nerve was re-exposed, and the second injury (viz sciatic nerve crush at the sciatic notch), was performed using fine crushing forceps. Again, the muscle was put back in place, and bupivacaine diluted in saline 1:10 was administered. The mice were allowed to recover for a further 2.5D. This method is similar to the one described by McQuarrie et al., 1977.
The sciatic nerves from these mice were dissected and removed from the injury site at the sciatic notch (where the crush injury was performed). The sciatic nerves were fixed for 2 hours in 4%PFA, washed 3 times with PBS before being embedded in 15% sucrose overnight at 4°C ready for embedding in OCT the following day. These sciatic nerve moulds were then used for 10µm thick longitudinal cryosections.

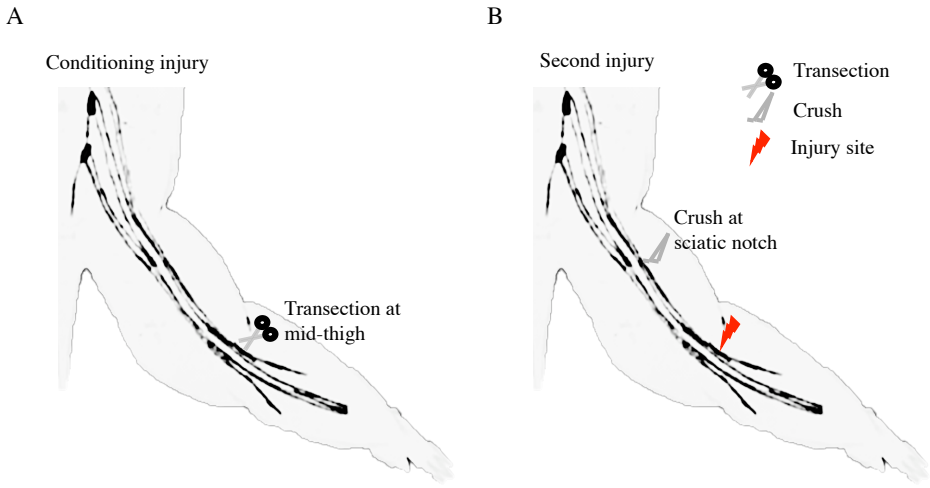

Figure 2.3 | Summary diagram to show how surgeries for conditioned lesion experiments *in vivo* were performed
Schematic representation of how conditioning lesion peripheral nerve surgeries were done in WT and cKO mice. (A) The conditioning injury is the first surgery done on the mouse which is a sciatic nerve transection at mid-thigh level. The mouse is allowed to recover before a second injury is carried out. (B) The second injury is a sciatic nerve crush at the sciatic notch. The mouse is again allowed to recover.

2.3.3 Behavioural tests

Sciatic functional index (SFI): Paw prints were taken from 6 week old mice to calculate the SFI. The SFI formula correlates mouse paw prints with nerve function as described by Inserra et al., 1998. The hindlimb paws of the mice were painted on the plantar surface with black paint. Mice then walked down a 54cm x 5cm wooden track lined with 180gsm highly absorbent paper (Goldline). Prints were subsequently scanned using a Canon pixma scanner to generate digital paw prints. Toe spread (the distance between the first and fifth toes) and print length (the distance between the third toe and the heel) were measured using ImageJ and Microsoft Excel was used to convert the measurements into SFI values using an established formula (Inserra et al., 1998). An SFI value of -100 represents complete loss of function. This is summarised in Figure 2.4 below.

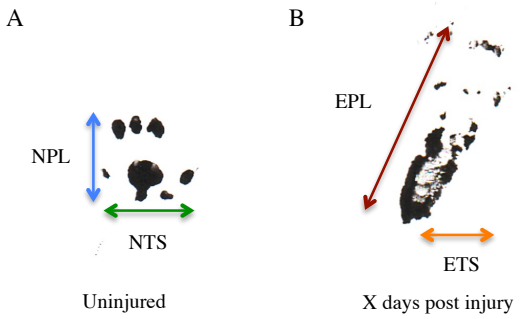

Figure 2.4 | Summary diagram showing typical mouse footprints used in SFI analysis
Scanned mouse footprints to show the typical print seen in an uninjured (A) and injured situation (B). SFI is determined by several parameters that include the Normal Print Length (NPL), the Normal Toe Spread (NTS) seen in (A) and the Experimental Print Length (EPL), Experimental Toe Spread (ETS) seen in (B). In a normal uninjured situation (A), the NPL is short and NTS is long, whereas after injury, the length of the footprint (EPL) becomes elongated, and the spread of the toes (ETS) gets shorter.

$$SFI = 118.9(ETS-NTS/NTS)-51.2(EPL-NPL/NPL)-7.5$$

ETS = Experimental Toe Spread

NTS = Normal Toe Spread

EPL = Experimental Print Length

NPL = Normal Print Length

Toe spread reflex: Each mouse was carefully lifted from the tail and given a score of 0 or 1 based on how well they were able to spread each of their toes apart. A score of 0 meant no spreading of the toes at all, and a score of 1 meant a full toe spread. The toe of the uninjured side was always used as control and compared when giving a score (Siconolfi et al, 2001).

Toe pinch test: As mice were lifted from the tail they were allowed to grip onto the cage with their forelimbs and the 3rd, 4th and 5th digits of the hindlimbs were pinched. The retraction of the paw from the stimulus was recorded as a positive response. This is a modification of the method first described by Collier et al., 1961.

2.3.4 Electron microscopy

Sciatic nerves processed for EM were from WT, OE/+ and OE/OE samples that had been dissected at different ages from P1-P60, and also samples that came from sciatic nerve crush experiments.

The nerves were fixed for 15 minutes inside the dissected mouse leg in fixative solution made up of 2% PFA, 2.5% glutaraldehyde diluted in 0.1M cacodylate buffer. The nerves were then transferred into 5ml bijous to be fixed in fixative solution for a further 24 hours at 4°C. The nerves were washed in 0.1M cacodylate buffer three times for 15 minutes each. They were then osmicated by adding 1% osmium tetroxide (1:1 ratio of osmium tetroxide in dH_2O and 0.2M cacodylate buffer) for 1.5 hours at 4°C. The nerves were rinsed twice for 15 minutes each using distilled water. To remove water from the samples, they were washed in progressively higher percentage alcohol solutions. 25% for 5 minutes, 50% for 5 minutes, 70% for 5 minutes, 90% for 10 minutes, 100% for 10 minutes repeated four times and finally propylene oxide for 10 minutes repeated three times. The nerves were then incubated in a 25:75 mixture of resin:propylene oxide for 1 hour at room temperature (RT). They were then changed into a 50:50 mixture of resin:propylene oxide for 1 hour at RT. The final change was into a 75:25 mixture of resin:propylene for 1 hour at RT. Nerves were blocked in resin and left shaking O/N at RT. These nerves were re-blocked the following day with fresh resin for 2 hours at RT. A change into fresh resin was carried out before the nerves were finally embedded in fresh resin and left in the oven for 24 hours at 37°C.

2.3.5 Cryosectioning

Dissected samples used for cryosectioning had been embedded in OCT compound and frozen in the gas phase of liquid nitrogen and stored at -80°C. The blocks obtained were mounted onto a chuck using OCT compound.
5μm or 10μm thick serial tissue sections (depending on the experiment) were cut using a Bright M100487 cryostat (Bright, UK) and collected on Superfrost Plus microscope slides before being stored at -80°C ready for Immunofluorescence. 8-10 sections per slide were collected serially onto Superfrost Plus slides.

2.3.6 Immunofluorescence

For teased nerve fibre preparations, Superfrost Plus slides were post fixed using 100% acetone for 10 minutes at RT. Slides were washed for 10 minutes with 1XTBS three times. Teased fibres were blocked with 5%BSA/0.2%Triton-X-100/1XTBS for 30 minutes before adding c-Jun antibody diluted in 1%BSA/0.2% Triton-X-100/1XTBS for 24 hours at RT in a humidified chamber (see table 2.2.2.1). c-Jun antibody was drained off and slides were then washed for 10 minutes with 1XTBS three times before adding the corresponding secondary antibody diluted in 1%BSA/0.2%Triton-X-100/1XTBS at RT for 1 hour (see table 2.2.2.2). Slides were washed for 10 minutes with 1XTBS three times before adding L1 antibody diluted in 1%BSA/0.2%Triton-X-100/1XTBS at RT for 1 hour. Slides were washed again for 10 minutes with 1XTBS three times. L1 antibody was drained off and slides were then washed for a further 10 minutes with 1XTBS three times before adding the corresponding secondary antibody and DAPI diluted 1%BSA/0.2%Triton-X-100/1XTBS at RT for 1 hour (see table 2.2.2.2). Slides were washed for a final 10 minutes with 1XTBS three times before mounting with Citifluor and viewing the slides. Slides were sealed with clear nail polish.

Superfrost slides with tissue sections were left to thaw for 5-10 minutes at RT. These cryosections were then fixed for 4 minutes in 4% PFA at RT followed by washing three times for 5 minutes each with 1XPBS. Sections were incubated in a sequence of 50% Acetone/H_2O, 100% Acetone and 50% Acetone/H_2O for 2 minutes each, then washed three times in 1XPBS, once every 5 minutes. They were blocked for 1 hour at

RT in 1XPBS solution containing 5% GS in a humidified chamber. The blocking agent was removed, and primary antibodies (see table 2.2.2.1) were diluted in 1XPBS/0.1% BSA and left incubating overnight at 4°C. Sections were washed three times in 1XPBS. Appropriate secondary antibodies and DAPI (see table 2.2.2.2) were diluted in 1XPBS/0.1% BSA and incubated for 1 hour at RT in the dark. The secondary antibody was removed and sections were washed three times with 1XPBS for 5 minutes each. Slides were mounted using Citifluor and sealed with nail polish. To determine if any signal was due to non-specific antibody binding from secondary antibodies, primary antibodies were omitted from one sample in each experiment.

For some antibodies (c-Jun, Sox10 and F480) a different protocol was used. Superfrost slides with tissue sections were left for 5-10 minutes to thaw at RT. Nerve sections were fixed with 4% PFA for 10 minutes at RT, followed by three 5 minutes washes with 1XPBS. Sections were blocked for 1 hour at RT using 10%HS/0.2%Triton-X-100/1XPBS. Primary antibodies (see table 2.2.2.1) were diluted in blocking solution and left incubating overnight at 4°C. The antibodies were drained off and then sections were washed three times using 1xPBS. Appropriate secondary antibodies and DAPI (see table 2.2.2.2) were diluted in blocking solution and left for 1 hour at RT, before washing sections three times with 1xPBS every 5 minutes. Fluoromount G was used to mount slides and sealed with clear nail polish.
Specifically for Krox20 and Ki67 immunofluorescence, the same protocol as above was used. However, the secondary antibody used was anti rabbit biotin which was left for 2 hours at RT followed after washing by a third layer (see table 2.2.2.2), streptavidin cy3, which was also left for 2 hours at RT. DAPI in these cases was added at the same time as the third layer.

For Superfrost Plus slides with longitudinal sections for immunolabelling with CGRP, Galanin and NF200, a separate protocol was used. The tissue sections on these slides were allowed to thaw for 5-10 minutes at RT before being fixed for 5 minutes at RT with 4%PFA/PB. The slides were then washed for 2 minutes in 0.1M PB. Slides were then incubated for 2 minutes each in the following solutions: 50% Acetone/H_2O, 100% Acetone and 50% Acetone/H_2O. Following this, slides were washed twice for 2 minutes each in 0.1M PB and then for a further 2 minutes in 0.1M PB/0.1%BSA.

Slides were blocked for 30 minutes with 5%GS/0.1M PB at RT in a humidified chamber. Primary antibodies (a combination of either anti CGRP/ anti NF200 or anti Galanin/ anti NF200 see table 2.2.2.1) were diluted in 0.1M PB/0.1%BSA and left at 4°C for 24 hours. Slides were washed in 0.1M PB/ 0.1%BSA for 2 minutes. They were washed again twice in 0.1M PB for 2 minutes each time. The slides were then washed for a further 2 minutes with 0.1M PB/0.1%BSA. Appropriate secondary antibodies and DAPI (see table 2.2.2.2) were diluted in mouse serum (1:50) in 0.1M PB at RT. The following washing steps were four times in 0.1M PB for 2 minutes each and then a final 2 minutes in 0.1M PB before mounting slides using CitiFluor and sealing them with clear nail polish.

Macrophage cultures and Schwann cell cultures were immunolabeled by fixing the coverslips with 4% PFA for 10 minutes at RT. They were then washed 6x 1 minute washes with 1x PBS and blocked using 10% HS/ADS/0.2%Triton-X-100 for 1 hour at RT. Appropriate primary antibodies (see table 2.2.2.1) were diluted in the blocking solution and left overnight at 4ºC. The coverslips were again washed for 6x 1 minute with 1x PBS and then incubated with secondary antibodies and DAPI (see table 2.2.2.2), diluted in blocking solution for 1 hour at RT in the dark. The coverslips were again washed for 6x 1 minute with 1x PBS and mounted using Citifluor and sealed with nail polish.

Coverslips from injured L4 DRGs cultures were immunolabelled with Tuj1 and DAPI (to label nuclei) after being fixed in 4%PFA for 15 minutes. They were then washed by serially dipping each coverslip into universal tubes containing 1XPBS, three times each. Coverslips were blocked for 1 hour at RT in a humidified chamber with 0.2%Triton-X-100/ADS. Primary antibody Tuj1 (see table 2.2.2.1) was diluted in blocking solution and added to coverslips overnight at 4ºC. Coverslips were then washed by serially dipping each coverslip into universal tubes containing 1XPBS, three times each. Appropriate secondary antibody and DAPI (see table 2.2.2.2) were diluted in blocking solution and added to coverslips for 1 hour at RT. Coverslips were washed for a final time by serially dipping each coverslip into universal tubes containing 1XPBS, three times each. These were then mounted using Citifluor and sealed with clear nail polish.

2.3.7 Western Blotting

Sciatic nerves from newborn, adult or surgically operated mice along with L4 DRGs that were transferred to tubes containing nine 10B lysing matrix beads and 100µl of RIPA lysis buffer (see recipe in section 2.2.1). Samples were placed in a Fastprep fp120 homogeniser for 45 seconds at speed 6, chilled on ice and then re-homogenised for a second time with the same settings. Lysates were then centrifuged at 4°C at 13,000rpm for 2 minutes before collecting the supernatants and transferring them to new eppendorf tubes. These were then centrifuged again at the same settings and this time the collected supernatants were stored at -80°C. 10µl from each sample was transferred to a new eppendorf tube to use for the BCA protein assay.

A BCA protein assay (Thermo Scientific Pierce BCA Protein Assay) was carried out to determine how much sample would need to be added to 5X laemmli buffer and load 10µg of protein sample onto 8% or 10% acrylamide gels. The gels were run using the mini Protean II gel electrophoresis system at graded voltages starting at 60V for 30 minutes, 70V for another 30 minutes, 90V for 30 minutes and 120V for the final stage. These gels were then transferred to nitrocellulose membranes using the Biorad semi-dry transfer system set to 25V for 45 minutes. Membranes were blocked in 5% milk in TBS-T for 1 hour at RT and subsequently incubated overnight at 4°C with primary antibodies (see table 2.2.2.3) diluted in 5% milk TBS-T or 5% BSA in TBS-T. Primary antibodies were removed and membranes were washed three times for 10 minutes each with TBS-T. HRP-conjugated secondary antibodies were added for 1 hour at RT in 5% milk (see table 2.2.2.4). Secondary antibodies were removed and membranes were washed three times for 10 minutes each with TBS-T. The membranes were subsequently developed with ECL detection reagent using the Chemidoc MP system.

2.3.8 Tissue culture methods

2.3.8.1 Myelin extraction

(adapted from Nicolo Musner and Norton and Poduslo 1973)

Two brains from WT mice were homogenised in 1ml of 0.32M homogenizing sucrose (diluted in sterile ddH_2O) using a glass homogeniser and glass pestle (roughly 7-10 strokes).

Using sterile glass pipettes, 1ml of 0.32M tissue suspension was added on top of 1ml of 0.85M sucrose solution. This was then centrifuged for 30 minutes at 4°C and spun at 34,000rpm (75000g) using a Beckman Optima TLX Rotor TLS 55.

The interphase (crude myelin membranes) was pipetted into a new clean centrifuge tube and filled to the top (roughly 2ml) with sterile water (osmotic shock). This was then centrifuged at 13,000rpm for 15 minutes at 4°C. The supernatant was discarded and the resulting pellet was re-suspended in sterile water (roughly 2ml). This was then centrifuged again at 13,000rpm for 15 minutes at 4°C. The cloudy supernatant fluid was discarded and the resulting pellet was re-suspended in 1ml 0.32M homogenizing sucrose and carefully added on top of 1ml 0.85M sucrose. This was then centrifuged at 34,000rpm for 30 minutes at 4°C, re-suspending the resulting interphase layer in sterile water (roughly 2ml). This was centrifuged at 34,000rpm for 15 minutes at 4°C. The resulting pellet of myelin was re-suspended in 50µl of sterile water and stored at -20°C until required for use.

To determine how much myelin to use on each coverslip and the dilution needed, a BCA protein (myelin) assay was carried out. The stock solution of myelin should be a 10µg/ml solution.

2.3.8.2 Coating coverslips and dishes

PLL: 13mm coverslips were coated at least 1 week prior to being used with PLL at a concentration of 1mg/ml. This was done by adding 25ml of PLL to a dish full of sterile 13mm coverslips, which were kept on a shaker for 24 hours at RT. The PLL was then removed and coverslips were washed with 6 changes of sterile ddH_2O over 3 days on the shaker. The coverslips were then individually dried on coverslip racks in the hood overnight. They were stored dessicated, ready for use.
35mm culture dishes were coated on the same day as the intended use with PLL at a concentration of 100µg/ml. This was done by adding 2-3ml of PLL onto each dish which was left in the hood for 2 hours. The PLL was then removed and dishes were washed 3 times with ddH_2O. They were subsequently stored and dessicated at RT ready for use.

Laminin: Laminin (1mg/ml) was diluted 1:50 in DMEM to have a working concentration of 20µg/ml for coverslips, and diluted 1:100 for coating dishes. Laminin was added either as a 50µl drop onto the surface of the 13mm coverslip or 1ml was added to 35mm dishes to coat the entire surface. This was left on for at least 1 hour in the hood, before removal just prior to plating cells.

Myelin: Myelin was diluted in ddH_2O to generate a 1µg/ml stock solution and added as a 50µl drop to coat the surface of a PLL coated 13mm coverslip. This was left overnight in the hood to dry, ready to be used the next day for the experiment.

2.3.8.3 Mouse Schwann cell culture from pups

Sciatic nerves from mouse pups (P8-P10) were dissected and placed in L15 medium on ice. The nerves were desheathed by removing epineurium and connective tissue using forceps. These desheathed nerves were digested in a 1:1 mixture of trypsin (0.25%) and collagenase (10µg/ml). Subsequently, they were incubated for 2 hours at 37°C/5%CO_2. They were then triturated ten times with a blue eppendorf tip and a further ten times with a yellow eppendorf tip. The reaction was stopped using DMEM and 5% HS. After centrifugation at 1000rpm for 10 minutes, the cell pellet was re-suspended in defined medium (DM) (Meier et al., 1999), containing 10^{-6}M insulin and 5%HS and plated in 25µl drops onto coverslips coated with PLL/laminin (10µg/ml). Cells were incubated at 37°C/5%CO_2 and allowed to adhere for 24 hours. After 24 hours, the medium was topped up with DM/0.5% HS (controls), or DM with NRG1 (10ng/ml) alone, or DM with NRG1 (10ng/ml) and dbcAMP (10^{-3}M) for 48 hours.

2.3.8.4 Adult mouse Schwann cell culture

Sciatic nerves were dissected from at least two adult mice, de-sheathed and placed into a 35mm tissue culture dish containing L15 on ice. They were then cut into 2mm segments and transferred to a separate dish containing enzyme cocktail (see section 2.2.1) at least 1 hour in the incubator at 37°C/5%CO_2. The cells were triturated with a blue eppendorf tip ten times followed by twenty times with a yellow tip after 1 hour. The segments were re-incubated for a further 1 hour at 37°C/5%CO_2 until fully digested. The reaction was stopped with DMEM/5%HS and the cells plated in DM/HI/ 0.5% HS (see DM recipe in section 2.2.1) on coverslips in 25µl drops. The cells were left in the incubator for 48 hours at 37°C/5%CO_2, being topped up 24 hours after plating.

2.3.8.5 Macrophage culture

Making sure the culled animal was well secured, the abdominal skin was pulled upwards and a small incision was made with scissors over the abdominal area, whilst trying not to pierce the abdominal wall itself. 5ml of sterile 1XPBS using a 23G

needle was injected into the incision, whilst at the same time massaging the abdomen of the mouse to ensure that the injected PBS is being moved around within the cavity. A sterile Pasteur pipette was inserted into the abdominal cavity and the liquid inside slowly withdrawn, being careful only to take liquid and nothing else. This was collected in a sterile 5ml Falcon tube and the cells were spun for 10 minutes at 1000rpm. The cells were then re-suspended in warm RPMI medium with 10%FBS and cultured for at least 24 hours on coverslips in 25µl drops at 37°C/5%CO_2.

2.3.8.6 Conditioning lesion L4 DRG culture

In the following section, "L4 injured DRG" refer to L4 DRGs dissected from the right side of the mouse where the sciatic nerve had been transected.

L4 DRG cultures were made from the injured right L4 DRGs and plated both on PLL/laminin or PLL/myelin coated coverslips to analyse the conditioned growth response from these DRG neurons. WT and cKO mice were allowed to recover for 2.5D following sciatic nerve transection. Mice had undergone a sciatic nerve transection at the level of the sciatic notch and allowed to recover for 2.5 days following this injury.

24 hours prior to culling the mouse, extracted brain myelin (see section 2.3.8.1) at a concentration of 1µg/ml was plated onto 13mm PLL coated coverslips and left to dry overnight in the tissue culture hood.

Only the L4 injured DRGs from these mice were dissected by excising the whole spine from the mouse to break away the vertebrae in order to expose the spinal cord and DRGs. The injured L4 DRGs were located and excised, carefully removing as much of the connective tissue and nerve roots as possible. The cleaned injured L4 DRGs were placed into a clean 35mm dish containing L15 on ice before replacing the L15 with 300µl trypsin and 300µl collagenase per one L4 DRG. The injured L4 DRGs were left in the incubator at 37°C/5%CO_2 for 2 hours and in the meantime two sets of fire polished glass pipettes were being made by fire polishing for 2 seconds and 5 seconds. Laminin (10µg/ml) 1:50 in DMEM was plated on 13mm coverslips and left in the hood for 2 hours. One Percoll gradient per L4 DRG was made by mixing 4ml of L15 and 1ml of Percoll in a 15ml Falcon tube. L4 DRGs were mechanically triturated 4 times using the 2 second fire polished glass pipette and then

four times with the 5 second fire polished glass pipette. The reaction was stopped by adding 100µl warm HS to each of the 35mm dish. 700µl of this L4 DRG mixture was gently pipetted on top of the Percoll gradient. Centrifugation was carried out at 1400rpm for 8 minutes using brake setting 1. The supernatants were very carefully and slowly removed and discarded leaving behind 500µl of solution in the falcon tube. 2ml of L15 was added to this 500µl solution and the tube was gently tapped to re-suspend the cells. Following this, they were centrifuged at 2300rpm for 2 minutes using brake setting 9. The supernatant was carefully and slowly removed leaving behind a small volume (~10µl), which was re-suspended in 100µl DRG medium (DM/0.5%HS/50mM glucose). Cells were counted in a haemocytometer and ~40 cells/µl were plated onto the PLL/laminin or PLL/myelin coated coverslips in 25µl drops left at 37°C/5%CO_2 overnight, topping up with 500µl DRG medium the following day. These were left for 20 hours if on PLL/laminin and 48 hours if on PLL/myelin before fixation was carried out ready for immunolabelling.

2.3.9 Microscopy and quantification

Stained tissue sections and coverslips using immunofluorescence were all examined using a Nikon Labophot 2 fluorescence microscope.
All statistical analysis is represented relative to a WT control, in most cases being the contralateral uninjured nerves, unless specified otherwise.

2.3.9.1 Sciatic nerve analysis and quantification

5μm thick uninjured sciatic nerve sections from WT, OE/+ and OE/OE mice at different developmental stages were quantified using images taken at x25 magnification with a Nikon Labophot 2 fluorescence microscope. The number of DAPI, Sox10, Krox20 and Ki67 positive cells were quantified using Cell Counter plugin in ImageJ software. The experiment was repeated at least 3 times and at least 3 independent sections were counted. The average of the results from each experiment was used to calculate the standard error of the mean (with results being plotted on a bar chart).

5µm thick transverse uninjured and proximal stump nerve tissue sections from both WT and cKO mice were quantified using a Nikon Labophot 2 fluorescence microscope at x63 magnification. Different areas along a distance of 6mm of the proximal stump (cut nerve) and the contralateral uninjured nerve were analysed 1 hour, 6 hours and 48 hours after nerve transection. The percentage of c-Jun positive nuclei was counted as a percentage of the total nuclei present. The experiment was repeated 3 times. The average of the results from each experiment was used to calculate the standard error of the mean (with results being plotted on a bar chart).

The transverse sections at 48 hours after nerve transection were also used to determine the expression of macrophage population using antibodies to the general macrophage marker F4/80. For these analyses, images were taken at a magnification of x25 magnification and then the Cell Counter plugin within ImageJ was used to quantify the percentage of F4/80 positive macrophages. The experiment was repeated 3 times. The average of the results from each experiment was used to calculate the standard error of the mean (with results being plotted on a bar chart).

Teased nerve fibres were quantified using antibodies to c-Jun and L1 (Remak Schwann cell marker) as described in Hantke et al., 2014, as well as identification by phase contrast microscopy of c-Jun positive Myelin fibres. The number of c-Jun and L1 positive fibres were counted at x63 magnification using a Nikon Labophot 2 fluorescence microscope. The experiment was repeated 3 times. The average percentages of c-Jun positive Remak and Myelin Schwann cells were used to calculate the standard error of the mean, with results being plotted on a bar chart.

2.3.9.2 DRG analysis

Images were taken at x25 magnification using a Nikon Labophot 2 fluorescence microscope with its digital camera (model: DXM1200, Nikon) and ACT-1 acquisition software (Nikon). The number of c-Jun, ATF-3, p-STAT3 Tyr705, p-STAT3 Ser727 and GAP-43 positive immunofluorescent neurons across independent sections at least 100μm apart were counted representing the entire L4 DRG. Immunolabeling with NF200 antibody was used to identify and quantify the total number of neurons in each section. The number of c-Jun, ATF-3, p-STAT3 ser727, p-STAT3 tyr705 and GAP-43 positive neurons 48 hours after sciatic nerve cut, were then expressed as a percentage of the total number of neurons on each section using the Cell Counter plugin in ImageJ software. Strongly expressing neurons were identified as those that were immunofluorescently labelled more intensely than the signal present in the contralateral uninjured L4 DRG sections**.** The experiment was repeated three times. The average of the results from each experiment was used to calculate the standard error of the mean (with results being plotted on a bar chart).

2.3.9.3 Conditioning lesion *in vivo* analysis

Slides were marked along nerve sections at 2mm and 3mm from the crush site using permanent marker pens. These marked distances were found under the microscope (Nikon Labophot 2 fluorescence microscope) at x25 magnification, and the number of positively immunofluorescently labelled CGRP and galanin axon fibres were counted. Positive regenerating axons were those that crossed the "X" visible under the microscope lens. At least four individual sections per slide per genotype were counted and normalised to each other by nerve width. The width of the nerve was determined by using the size of the field of view under the microscope (shown in Figure 2.5).
The experiment was repeated at least three times. The average of the results from each experiment was used to calculate the standard error of the mean (with results being plotted on a bar chart).

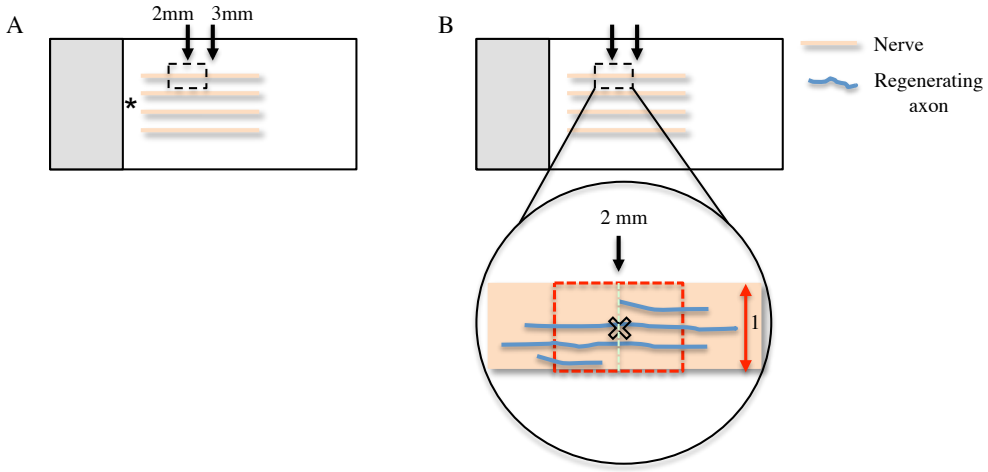

Figure 2.5 | Summary diagram for analysis of conditioning lesion *in vivo*
Schematic representation of how regenerating axons were quantified. (A) Distances of 2mm and 3mm from the crush site (marked with *) were marked along the nerve sections (black arrows). (B) Under the microscope at a magnification of x25 regenerating axons (blue) were quantified. Firstly, the width of the nerve (red double headed arrow) was noted in relation to the grid present in the lens of microscope (red dotted box) and given a width of 1. All nerve sections were normalised this way. Regenerating axons were only counted as positive if the entirety of the axon crossed the "X" which again is visible down the microscope lens and moves as the field of view is moved. An imaginary line (green) down the middle of the nerve was made to define the area of nerve where regenerating axons were counted from.

2.3.9.4 Schwann cell, macrophage and fibroblast culture analysis

Coverslips with Schwann cells, macrophages and fibroblasts from both WT and c-Jun cKO nerves were analysed and quantified using a Nikon Labophot 2 fluorescence microscope. Images were taken at x25 magnification from 15 individual fields across coverslips using a digital camera (model: DXM1200, Nikon) and ACT-1 acquisition software (Nikon). The number of Schwann cells, macrophages and fibroblasts expressing c-Jun were expressed as a percentage of total cells using the Cell Counter plugin in ImageJ software. A summary of how the quantification was done is shown below in Figure 2.6.

The experiment was repeated at least three times. The average of the results from each experiment was used to calculate the standard error of the mean, with results being plotted on a bar chart.

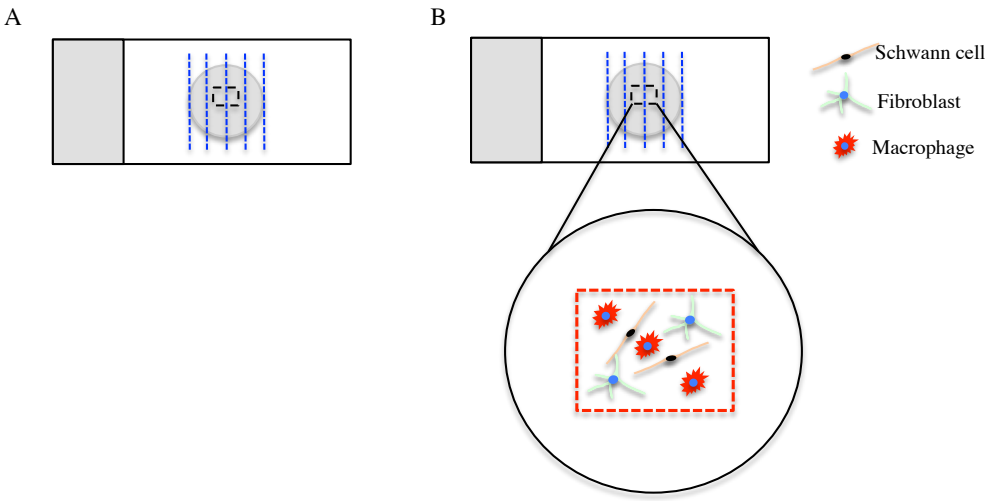

Figure 2.6 | Summary diagram for Schwann cell, fibroblast and macrophage culture analysis
Schwann cell, fibroblast and macrophage cultures were analysed in the same way. (A) Slides with cultured coverslips were divided up equally as shown by the blue dotted in lines. This was to make sure that the same area of the coverslip was not imaged and therefore quantified multiple times. (B) A magnified image of the red dotted rectangle which shows the field of view down the microscope lens.

2.3.9.5 Conditioning lesion DRG cultures

The coverslips fluorescently labelled using Tuj1 and DAPI were analysed in several different ways. Images of the entire population of neurons on these coverslips were taken at x25 magnification using a digital camera (model: DXM1200, Nikon) and ACT-1 acquisition software (Nikon). The number of neurons on each coverslip on both PLL/laminin and PLL/myelin from WT and cKO mice were counted using DAPI to identify the nucleus and Tuj1 for the neuronal processes. The neurons counted were divided into subgroups:-

1. Does the neuron have neurites and if so how many? A neurite for the purpose of this analysis was defined as any process longer than half the diameter of the cell body of that particular neuron. If there are neurites, how many are there?
2. Does the particular neuron being analysed have any supporting glial cells associated with it? Association with the neuron in terms of this analysis was defined as any cell within the distance of the diameter of the neuronal cell body
3. The length of the longest neurite was measured (in μm) using the tracing program in NeuronJ.

The experiment was repeated twice and the average of the results from each experiment was used to calculate the standard error of the mean, with results being plotted on a bar chart using Prism 6. The analysis carried out in shown in Figure 2.7.

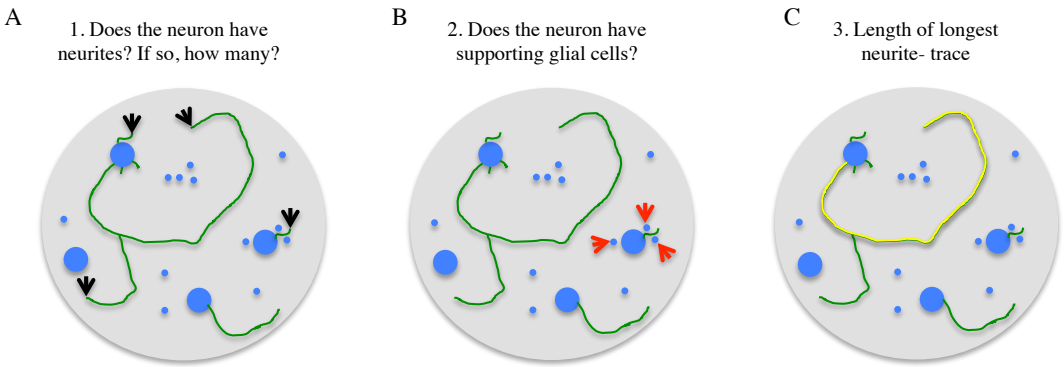

Figure 2.7 | Summary diagram for conditioned lesion L4 DRG culture analysis
Schematic representation of the step-by-step process of analysing conditioned lesion DRG cultures. Each panel A-C represents a magnified area on a coverslip on which cultured neurons are plated. They represent both PLL/laminin and PLL/myelin coverslips. (A) Diagram to show how neurons are identified by using DAPI which is blue, and the black arrowheads represent the processes from the neuron which would be counted as processes as their lengths are longer than half the diameter of the cell body of that neuron. (B) Diagram to show how supporting glial cells are counted as being associated with the neuron on or not based on their proximity to the cell body or process, as depicted by the red arrowheads. (C) Diagram to show how the NeuronJ software was used to trace the length of the longest neurite as depicted by the yellow line along the neurite.

2.3.9.6 Western blot analysis and quantification

All Western blot membranes were analysed using Bio-rad software Imagelab which converts the signal visible on a membrane into pixels. These values were then normalised to those of the reference genes, which in the case of Chapters 3 and 4 was firstly Calnexin and then GAPDH. These values were then expressed as a fold change relative to WT levels in arbitrary units (au). These experiments were repeated at least three times unless stated otherwise. The average of the results from each experiment was used to calculate the standard error of the mean, with results being plotted on a bar chart. A One-way ANOVA was performed using Prism 6. A p value of <0.0001, unless stated otherwise was considered to be statistically significant.

For Western blot analysis in Chapters 5 and 6, GAPDH was the only reference gene used for normalisation. For cases where phosphorylation levels were analysed, the total protein present of the phosphorylated protein of interest, was used for normalisation. These values were then expressed as a fold change relative to WT levels in arbitrary units (au). These experiments were repeated at least three times unless stated otherwise. The average of the results from each experiment was used to calculate the standard error of the mean (with results being plotted on a bar chart).

3. The effect of Schwann cell c-Jun overexpression throughout postnatal development into adulthood

3.1 Introduction

Normal function of peripheral nerves is strongly determined by the correct development of all peripheral nerve components which include axons, Schwann cells and connective tissue sheaths, along with the integrity of the communication network between all these components (Kaplan et al., 2009). Most of the studies carried out in this field have used animal models. Understanding the concomitant development of peripheral nerves (Schwann cells, axons, connective tissue) is important for further study of peripheral nerve injury and repair (Kaplan et al., 2009; Jessen and Mirsky 2016). The transcription factor c-Jun is involved in nerve development and has a particularly important role in controlling the response of Schwann cells following nerve injury to promote nerve repair (Parkinson et al., 2008; Arthur-Farraj et al., 2012; Fontana et al., 2012; Jessen et al., 2015; Jessen and Mirsky, 2016).

Although there is some evidence to suggest the importance and significance of interfering with levels of Schwann cell c-Jun expression (Parkinson et al., 2008), it was of interest to find out the possible effects of c-Jun overexpression in Schwann cells from early development into adulthood.

The transcription factor c-Jun, part of the AP-1 complex, regulates key cellular processes including proliferation and apoptosis in response to JNK and RAS/MAPK signalling (Chakraborty et al., 2015). c-Jun is an immediate early gene that is important in negative regulation of myelination (Parkinson et al., 2008), Schwann cell proliferation (Mirsky et al., 2008) and promotion of successful peripheral nerve regeneration, through the formation of repair Bungner Schwann cells following nerve injury (Arthur-Farraj et al., 2012; Jessen et al., 2015).
Elevated levels of c-Jun are also seen in a number of neuropathic conditions both in humans (Hutton et al., 2011) and animal studies (Hantke at al., 2014; Klein et al., 2014), where no cut or crush injuries are involved.

To address the importance of c-Jun elevation in Schwann cells, Schwann cell c-Jun overexpressing mice (OE/+ and OE/OE) were used (please see Chapter 2, section 2.2.3 for further details). These mice overexpress c-Jun in Schwann cells specifically in a gene-dose dependent manner. These mice have therefore been useful both in characterising the development of mouse nerves *in vivo*, and also in assessing the effect of increased c-Jun expression in Schwann cells on peripheral nerve injury and remyelination.

The objective of this chapter is to increase understanding of the significance of c-Jun expression, in Schwann cells. The results presented below address the effects of elevated levels of Schwann cell c-Jun on several aspects of nerve development including: (i) radial sorting, (ii) myelination, (iii) cell proliferation and (iv) nerve architecture.

3.2 Results

In the following sections, "development" refers to postnatal stages (P) 1-21.

3.2.1 c-Jun is overexpressed specifically in Schwann cells only

c-Jun is up-regulated during nerve development (Parkinson et al., 2008), and is vital for successful nerve repair following injury (Arthur-Farraj et al., 2012; Jessen et al., 2015). The evidence to suggest that c-Jun is an important negative regulator of myelination was shown *in vitro* (Parkinson et al., 2008), however a mouse model that has c-Jun conditionally ablated from Schwann cells did not show any obvious effect on myelination (Arthur-Farraj et al., 2012).

To address the significance of c-Jun elevation in Schwann cells *in vivo*, new c-Jun overexpressing mice, (both OE/+ and OE/OE) were used. This mouse provides a novel tool for elevating Schwann cell c-Jun *in vivo*, in a gene-dose dependent manner, which will prove useful in studies of nerve development and nerve injury and repair. As the P_0Cre transgene is activated from E13.5-E14.5 in the mouse (Feltri et al., 2002), the c-Jun overexpressing mice were useful for characterising the early influences postnatally of c-Jun elevation in Schwann cells.

This chapter aims to characterise the OE/+ and OE/OE mice at different stages through postnatal development (P1-P21) to adulthood at P60.

To confirm that c-Jun was overexpressed in Schwann cells, Western blot analysis and immunofluorescent labelling of WT, OE/+ and OE/OE nerves were performed at P1 and P7. From the result shown in Figure 3.1, it is clear from Western blot analysis, both at P1 and P7, that there is a significant 3 fold elevation from P1 WT to OE/+ in c-Jun protein expression (Figure 3.1A and 3.1B), and that this is further increased at P7 where it reaches 5 fold elevation compared to WT levels (Figure 3.1C and 3.1D). This elevation in c-Jun expression in sciatic nerves of P7 mice is higher in the OE/OE mouse (7 fold) compared to WT levels. This confirms the expectation and suggests very strongly that the c-Jun overexpressing mouse is a suitable subject of inquiry into the effects of c-Jun overexpression. The results showing the differences in Schwann cell c-Jun elevation in OE/+ and OE/OE mice compared to WT, correlates with the

presence of an extra copy of the c-Jun^{OE} transgene in OE/OE mice compared to the single copy in OE/+ mice. To confirm that this elevated c-Jun expression seen in OE/+ and OE/OE nerves (Figure 3.1A-D) was in Schwann cells, two different types of peripheral nerves were used: (i) brachial nerves and (ii) sciatic nerves. The brachial nerves were dissected from WT and OE/+ mice at P7 and immunofluorescently labelled with Sox10 used as a Schwann cell marker (Kuhlbrodt et al., 1998; Finzsch et al., 2010), and c-Jun, while DAPI was used as nuclear marker. (Figure 3.1E). From these results, it was clear that c-Jun overexpression seen in the overexpressing mice (OE/+ and OE/OE) by Western blot in Figure 3.1A-D, was specific to Schwann cells.

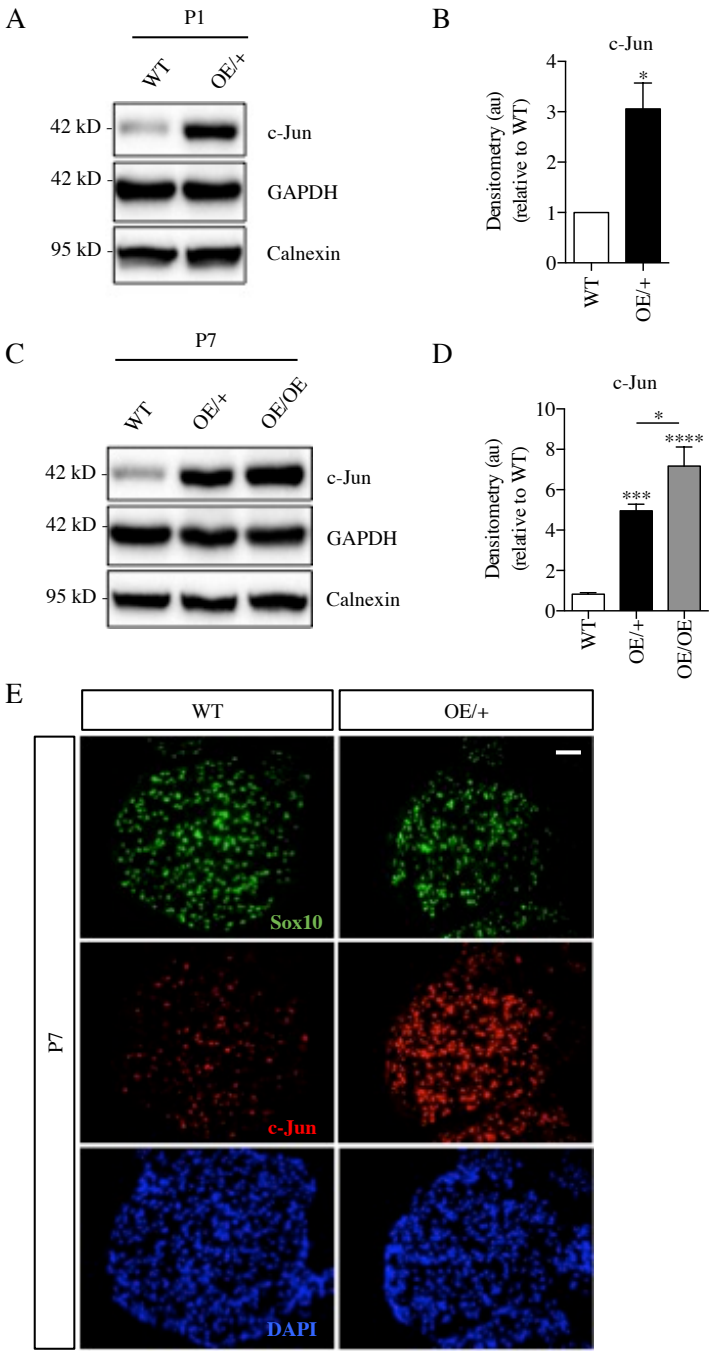

Figure 3.1 | c-Jun is significantly overexpressed specifically in peripheral nerve Schwann cells in OE/+ and OE/OE compared to WT

(A) Representative Western blot image of nerve extracts from P1 WT and OE/+ nerves to show the levels of c-Jun expression. GAPDH and calnexin are used as reference genes. (B) Graph to quantify c-Jun levels of OE/+ nerves at P1 relative to WT. c-Jun was normalised to calnexin and GAPDH, and then expressed as a fold change relative to WT. WT (n=3) and OE/+ (n=3); Mann-Whitney test, p=0.0286. (C) Representative Western blot image of nerve extracts from P7 WT, OE/+ and OE/OE nerves to show the levels of c-Jun expression. GAPDH and calnexin are used as reference genes. (D) Graph to quantify c-Jun levels of OE/+ and OE/OE nerves at P7 relative to WT. c-Jun was normalised to calnexin and GAPDH, and then expressed as a fold change relative to WT. WT (n=3), OE/+ (n=3) and OE/OE (n=3); One-way ANOVA with Tukey comparison, $p<0.0001$. All statistical analysis is represented relative to WT unless shown otherwise. (E) Representative immunofluorescence images from brachial nerves of WT and OE/+ mice at P7 to show that c-Jun overexpression is specifically in Schwann cells. These 5µm thick cryosections were fluorescently immunolabelled with Sox10 (Schwann cell marker) and c-Jun antibodies and with DAPI to label nuclei. Scale bar represents 50µm.

From Figure 3.1 there is strong evidence to show that in c-Jun overexpressing mice, the expression of Schwann cell c-Jun is higher compared to WT levels. To demonstrate that the c-Jun overexpressing transgene is working, a series of *in vitro* experiments were carried out using WT and OE/+ mice (Figure 3.2).
WT and OE/+ Schwann cell cultures were cultured in DM/0.5% HS (control), DM/0.5%HS/dbcAMP (10^{-3}M) or a combination of DM/0.5%HS/NRG1 (10ng/ml)/ dbcAMP (10^{-3}M), for 48 hours before being fixed and immunolabelled with Sox10 and c-Jun antibodies and with DAPI to label nuclei.

When Schwann cells are plated and exposed to basal conditions *in vitro*, they constitutively express c-Jun (De Felipe and Hunt, 1994; Stewart, 1995; Shy et al., 1996; Parkinson et al., 2004; Parkinson et al., 2008). For this reason, no obvious difference was seen in c-Jun expression between WT and OE/+ Schwann cell cultures under control conditions.
cAMP elevation down-regulates expression of genes, such as c-Jun, that are normally suppressed during myelination. dbcAMP (a cell permeable cAMP analogue) was used to activate the cAMP pathway *in vitro* (Jessen et al., 1987; Mokuno et al., 1988; Morgan et al., 1991; Parkinson et al., 2004; Parkinson et al., 2008; Arthur-Farraj et al., 2011). When WT and OE/+ Schwann cell cultures were treated with DM/0.5%HS/dbcAMP (10^{-3}M), there was an obvious down-regulation of c-Jun seen in WT cultures, however in OE/+ cultures c-Jun levels remained elevated and were similar to those seen in the control. This is strongly indicative of the fact that in the WT culture, endogenous levels of c-Jun are down-regulated in the presence of dbcAMP, however in OE/+ cultures, due to the presence of the transgenic c-Jun overexpression, c-Jun remains elevated (Figure 3.2).

NRG1 is a critical axon-derived survival and mitogenic signal that Schwann cells are reliant on (Jessen and Mirsky, 2005). NRG1 axon-associated signalling also drives Schwann cell division prior to myelination at least *in vivo* (Jessen and Mirsky, 2005).
In vitro, NRG1 alone, applied exogenously to mouse Schwann cell cultures does not induce myelin protein expression, although NRG1 promotes myelination *in vivo* (Jessen and Mirsky, 2008; Arthur-Farraj et al., 2011).

Activation of the cAMP pathway alone (*in vitro*) can mimic axonal signals that normally suppress myelination inhibitory signals *in vivo*, (such as c-Jun), however in the mouse, in order to suppress myelination inhibitory signals and elevate the expression of myelin related genes, NRG1 and cAMP pathways need to be activated together.

When WT and OE/+ cultures were exposed to DM/0.5%HS/NRG1 (10ng/ml)/ dbcAMP (10^{-3}M) (Figure 3.2), the increased elevation of c-Jun in overexpressing Schwann cells (OE/+) suggested that in the presence of axonal signals that would normally supress c-Jun during myelination *in vivo*, did not do so in the OE/+ mice (Parkinson et al., 2008; Jessen and Mirsky, 2008; Arthur-Farraj et al., 2011). This is expected due to the fact that the c-Jun overexpressing transgene has different genetic control elements than the endogenous gene (see Chapter 2, section 2.2.3).

The obvious down-regulation of c-Jun protein expression seen in WT cells treated with a combination of NRG1 and dbcAMP, in comparison to the lack of down-regulation seen in OE/+ cells when both WT and OE/+ cultures were compared to the control, indicate that transgenic c-Jun is still overexpressed in OE/+ cells (Figure 3.2).

In summary, the results shown in Figures 3.1 and 3.2 provide proof *in vivo* and *in vitro* that the c-Jun overexpressing transgene is active in both OE/+ and OE/OE mice, and that c-Jun levels are elevated in a gene-dose dependent manner.

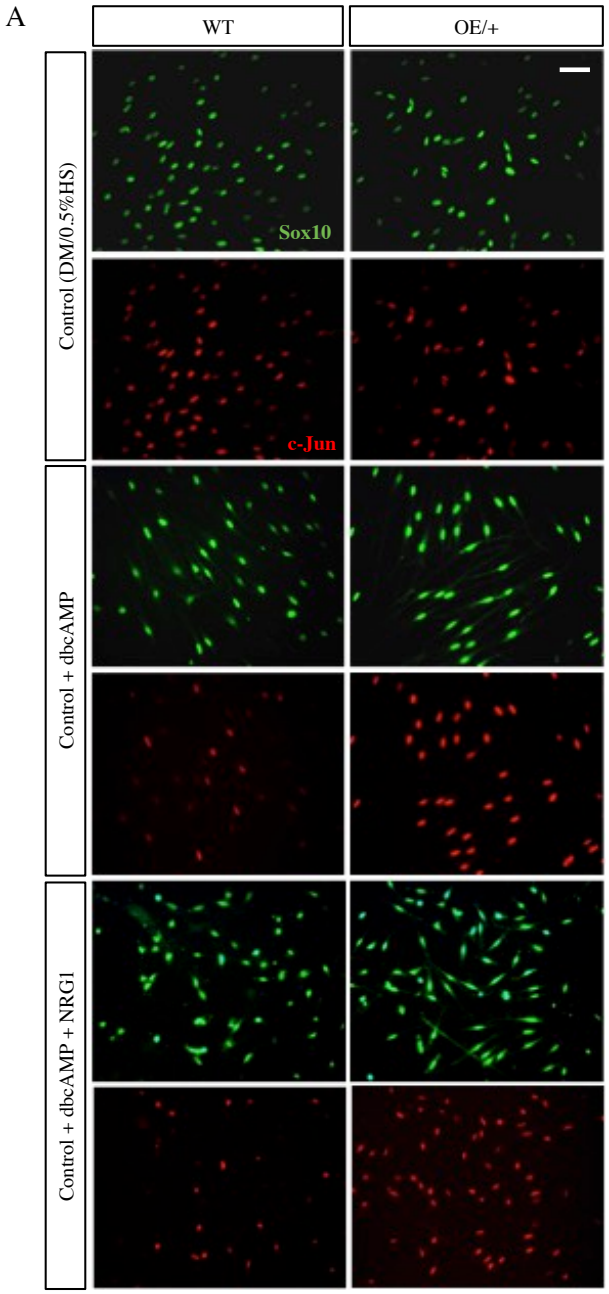

Figure 3.2 | Endogenous Schwann cell c-Jun expression *in vitro* is down-regulated by dbcAMP and NRG1 yet transgenic c-Jun overexpression is maintained

(A) Immunofluorescence images taken at x25 magnification showing Schwann cell cultures from P8-P10 old WT and OE/+ nerves. Scale bar represents 50μm. These cultures were treated with DM/0.5%HS (control), DM/0.5%HS/ dbcAMP (10^{-3}M) and DM/0.5%HS/ dbcAMP (10^{-3}M) NRG1 (10ng/ml) and cultured for 48 hours in vitro. dbcAMP was added in order to mimic the activation of the cAMP pathway that occurs *in vivo*. The combination of dbcAMP and NRG1 was added in order to mimic axonal signals that normally activate myelination signals *in vivo*, but also suppress c-Jun. The cultures were then fixed ready for fluorescent immunolabelling with Sox10 (Schwann cell marker) and c-Jun antibodies, to determine the amount of transgenic c-Jun that was overexpressed in Schwann cells in OE/+ compared to WT cultures.

The normal development of peripheral nerves is heavily reliant on the correct functioning of Schwann cells and their integrity for bidirectional cross-talk with axons (Lobsiger et al., 2002; Kaplan et al., 2009).

The regulation of c-Jun levels and the times at which its expression is present or absent during nerve development is key. Results so far have shown that the c-Jun overexpressing mouse elevates c-Jun in a gene-dose dependent manner in Schwann cells. Schwann cells have a major role in peripheral nerve development. Therefore, to further assess these effects, many different parameters of WT OE/+ and OE/OE mice were analysed from electron microscope images. Each developmental time point (P1, P7 and P21), was analysed in turn (shown in Figures 3.3-3.5) to determine the effects of elevated c-Jun in Schwann cells.

3.2.2 Overexpression of c-Jun in Schwann cells does not have an obvious effect on nerve development at P1

Figure 3.3A shows representative electron microscopy images from P1 WT, OE/+ and OE/OE at a low magnification of x3000 to show the overall nerve cytoarchitecture and at higher magnification of x10000 to focus on finer details of the nerve.

At P1, the total number of axons >1.5μm in diameter (regardless of whether they were non-myelinated or myelinated) was quantified in WT, OE/+ and OE/OE nerves. There was a tendency towards fewer axons being present in the nerve in OE/OE mice compared to both WT and OE/+ (Figure 3.3B). This decrease in the number of axons in OE/OE (666) mice compared to WT (894) was however not statistically significant**.** The number of myelinated axons present in WT (454), OE/+ (364) and OE/OE (229) nerves was not significantly different (Figure 3.3C), although suggestive of the fact that elevated levels of c-Jun in Schwann cells may affect the timing of the onset of myelination.

As previously mentioned, once Schwann cell families are formed, a process termed radial sorting occurs, where individual large diameter axons are isolated and become ensheathed and associated with one Schwann cell in a 1:1 relationship (Webster et al., 1973; Jessen and Mirsky, 2005; Monk et al., 2015; Feltri et al., 2016). Schwann cell families are highlighted by red outlines in Figure 3.3A.

When the percentages of radially sorted axons (inclusive of myelinated and non-myelinated axons >1.5μm in diameter) were quantified in WT, OE/+ and OE/OE mice at P1, there was a lower percentage of axons being radially sorted in OE/OE (56%) compared to WT (73%) and OE/+ (68%), although this was not statistically significant (Figure 3.3D). These results could indicate that c-Jun elevation in Schwann cells is affecting radial sorting, but that this effect may only become statistically significant later on in development, as radial sorting begins perinatally and continues to P10 (Feltri et al., 2016). This becomes clearer in results discussed later.

The total number of non-myelinated axons >1.5μm in diameter (whether in a 1:1 relationship with a Schwann cell or part of a Remak bundle or Schwann cell family), was not statistically different in all three genotypes WT (440), OE/+ (509) and OE/OE

(437) at P1 (Figure 3.3E). Myelin competent axons are defined as those that are non-myelinated and >1.5μm in diameter in a 1:1 relationship with a Schwann cell and therefore radially sorted. These are the axons that can later become myelinated. In OE/OE (142) nerves there seemed to be fewer axons that are non-myelinated and >1.5μm in diameter in a 1:1 relationship with a Schwann cell, compared to WT (222) and OE/+ (229), but again this difference did not reach statistical significance (Figure 3.3F). The number of non-myelinated axons >1.5μm in diameter in Remak bundles or Schwann cell families is also slightly higher in OE/OE (295) compared to OE/+ (280) and more obviously so when compared to WT (218), yet these differences do not reach statistical significance (Figure 3.3G). This slight difference in the number of non-myelinated axons (Figure 3.3E-G) may suggest a possible delay in myelination, which correlates with the number of myelinated axons quantified in WT, OE/+ and OE/OE nerves (Figure 3.3C).

Following on from the results already shown, the percentages of non-myelinated and myelinated axons were not statistically different between with WT, OE/+ and OE/OE nerves on day 1 (P1) (Figure 3.3H), indicating that this early postnatally, c-Jun elevation in Schwann cells does not significantly affect the ability of axons to be myelinated.

c-Jun elevation in P1 c-Jun overexpressing nerves is already substantially elevated compared to WT (Figure 3.1B). There is already evidence in the literature implicating the role of c-Jun in Schwann cell proliferation (Parkinson et al., 2008; Arthur-Farraj et al., 2011; Blom et al., 2014). Keeping in mind the results already shown above (Figure 3.1B) and the literature, it is surprising that the number of Schwann cell nuclei quantified per nerve profile in WT (263), OE/+ (284) and OE/OE (309) nerves was only marginally different and did not reach statistical significance (Figure 3.3I). This may indicate, however, that there are other drivers of cell proliferation that may be more important.

At P1 there was no statistically significant difference in nerve area between WT, OE/+ and OE/OE (Figure 3.3J).

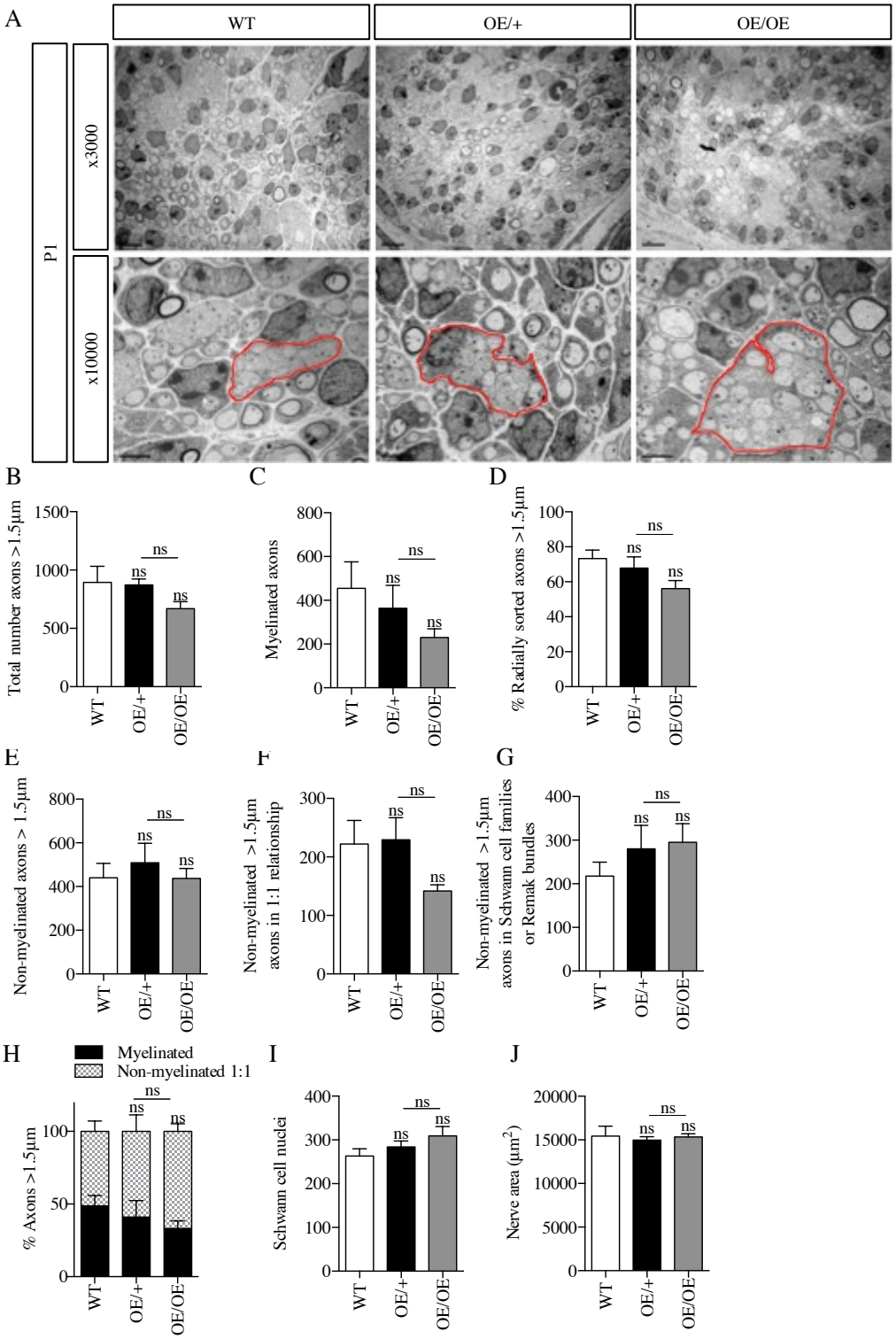

Figure 3.3 | Developmental characterisation of WT, OE/+ and OE/OE nerves at P1

(A) Representative electron microscopy images taken at x3000 and x10000 magnification to show more detail of the ultrastructure of WT, OE/+ and OE/OE nerves at P1. The red outlines highlight examples of Schwann cell families. Scale bar represents 5µm (x3000) and 2µm (x10000). Graphs shown in panels B-J are all quantified from WT (n=5), OE/+ (n=4) and OE/OE (n=5) mice at P1. (B) Graph to quantify the total number of axons >1.5µm per nerve profile. (C) Graph to quantify the number of myelinated axons per nerve profile. (D) Graph to quantify the percentage of axons >1.5µm that are segregated per nerve profile. (E) Graph to quantify the number of non-myelinated axons >1.5µm per nerve profile. (F) Graph to quantify the number of non-myelinated axons >1.5µm that are in a 1:1 relationship per nerve profile. (G) Graph to quantify the number of non-myelinated axons >1.5µm that are in Schwann cell families or Remak bundles per nerve profile. (H) Graph to quantify the percentage of 1:1 >1.5µm myelinated compared to non-myelinated axons per nerve profile. (I) Graph to quantify the number of Schwann cell nuclei per nerve profile. (J) Graph to show the nerve area. One-way ANOVA with Tukey comparison. All statistical analysis in all graphs is represented relative to WT unless shown otherwise.

In summary, the electron microscopy analysis presented in Figure 3.3 shows that although c-Jun is elevated substantially in OE/+ and OE/OE Schwann cells at P1 compared to WT, this is not enough to cause significant effects on Schwann cell biology, nor nerve development. Keeping in mind the arguments put forward at P1 of the likely expected outcomes of c-Jun elevation on various aspects of peripheral nerve development including: (i) Schwann cell proliferation, (ii) radial sorting and (iii) myelination, the next postnatal development stage P7, was analysed in the same way as P1.

3.2.3 c-Jun overexpression in Schwann cells causes a transient delay in radial sorting, yet a severe inhibition in myelination at P7

Figure 3.4A shows representative electron microscopy images both at low magnification of x3000 to show the gross ultrastructure of P7 WT, OE/+ and OE/OE nerves, as well as at higher magnification of x10000 that allows focus on finer details on the nerve cytoarchitecture. The nerve cytoarchitecture as depicted by electron microscope images show more obvious differences at P7, unlike what was seen at P1 (Figure 3.3A). Specifically, differences that were obvious between WT, OE/+ and OE/OE nerves at P7 were: (i) the reduced presence of myelinated axons in both OE/+ and OE/OE nerves, (ii) the presence of larger Remak bundles or Schwann cell families specifically in OE/OE nerves, (iii) the reduced myelin thickness in OE/+ and OE/OE and (iv) the visible increase in collagen, specifically in OE/OE nerves compared to both WT and OE/+. These differences are explained in more detail below (Figure 3.4).

The total number of axons >1.5μm in diameter regardless of whether they were non-myelinated or myelinated quantified at P7, showed a statistically significant decline from WT (3573) to OE/+ (2940) to OE/OE (2325), respectively as seen in Figure 3.4B.

The higher the c-Jun elevation in Schwann cells, the lower the number of myelinated axons there are in the nerve, from WT myelinated axons at 3385, compared to 2247 in OE/+ and 1054 in OE/OE nerves shown in Figure 3.4C. These differences were statistically significant when compared to WT levels, but also when compared between OE/+ and OE/OE.

Radial sorting is a process that takes place over a relatively long period of time throughout perinatal and postnatal development, with completion expected around P10 (Feltri et al., 2016). To this effect, by P7, radial sorting should almost be complete, which is what is observed in WT and OE/+ nerves where the percentage of radially sorted axons is 97% and 92% respectively. However, in OE/OE nerves, this percentage is statistically significantly lower at 79% (Figure 3.4D). This is the first indication of the detrimental effects of c-Jun elevation on radial sorting.

The number of non-myelinated axons >1.5μm in diameter (those that were in a 1:1 relationship with a Schwann cell, or part of a Remak bundle or Schwann cell family), were all statistically significantly elevated in OE/OE nerves compared to WT (Figure 3.4E-G). Yet, in OE/+ nerves, these differences were not of statistical significance compared to WT, except for the number of non-myelinated axons >1.5μm in diameter that were in a 1:1 relationship with a Schwann cell (Figure 3.4F), where these, were also higher in OE/+ (483) compared to WT (113).
Therefore as would be expected, the percentage of axons that are >1.5μm in diameter whether myelinated or non-myelinated, were also statistically significantly different, between WT, OE/+ and OE/OE nerves at P7 (Figure 3.4H). The higher the elevation of Schwann cell c-Jun (OE/+ and OE/OE), the higher the percentage of non-myelinated axons present, or inversely, the lower the percentage of myelinated axons present (Figure 3.4H).

The number of Schwann cell nuclei quantified in OE/OE (808) was significantly elevated compared to WT (413). The number of Schwann cell nuclei in OE/+ nerves was also statistically significantly elevated compared to WT nerves, 589 and 413 respectively, as shown in Figure 3.4I.

A 5 fold elevation of c-Jun in Schwann cells (OE/+) is enough to delay myelination, and higher levels of 7 fold c-Jun elevation in Schwann cells (OE/OE), has a significantly more detrimental effect on the ability of Schwann cells to myelinate (Figure 3.4C-G). Elevated levels of Schwann cell c-Jun also have a clear impact on the thickness of myelin sheaths present around those axons that have been myelinated. Levels of c-Jun expression above the norm, cause myelin sheaths around axons to be considerably thinner. Myelin sheaths present in OE/+ and OE/OE nerves are statistically thinner compared to WT as shown in Figure 3.4J.

The nerve area of WT (44907μm^2), OE/+ (48221μm^2) and OE/OE (51994μm^2), was not significantly different, although there is a trend towards OE/OE nerves being bigger (Figure 3.4K).

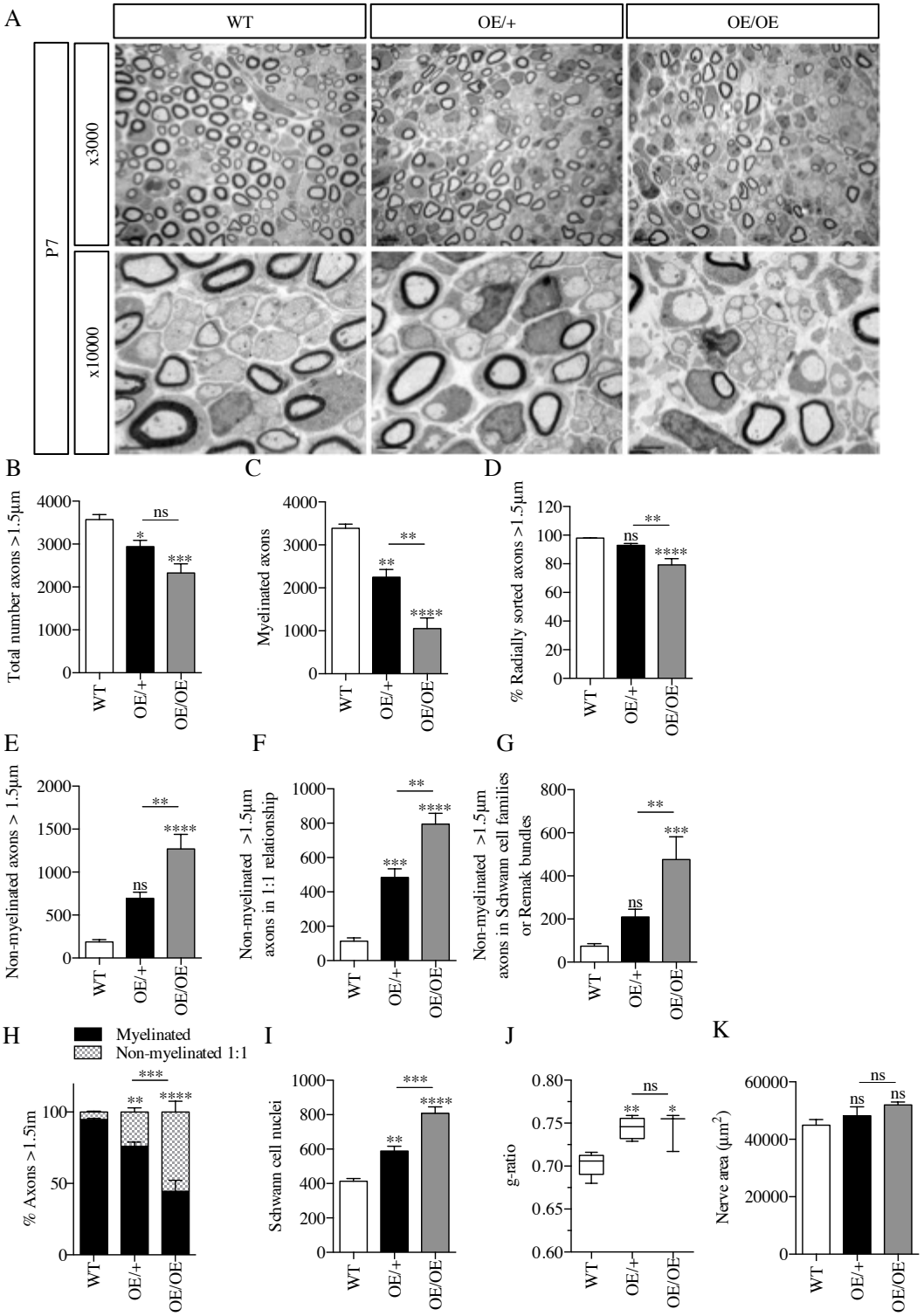

Figure 3.4 | Developmental characterisation of WT, OE/+ and OE/OE nerves at P7
(A) Representative electron microscopy images taken at x3000 and x10000 magnification to show more detail of the ultrastructure of WT, OE/+ and OE/OE nerves at P7. Scale bar represents 5µm (x3000) and 2µm (x10000). Graphs shown in panels B-K are all quantified from WT (n=5), OE/+ (n=5) and OE/OE (n=5) mice at P7. (B) Graph to quantify the total number of axons >1.5µm per nerve profile. (C) Graph to quantify the number of myelinated axons per nerve profile. (D) Graph to quantify the percentage of axons >1.5µm that are segregated per nerve profile. (E) Graph to quantify the number of non-myelinated axons >1.5µm per nerve profile. (F) Graph to quantify the number of non-myelinated axons >1.5µm that are in a 1:1 relationship per nerve profile. (G) Graph to quantify the number of non-myelinated axons >1.5µm that are in Schwann cell families or Remak bundles per nerve profile. (H) Graph to quantify the percentage of 1:1 >1.5µm myelinated compared to non-myelinated axons per nerve profile. (I) Graph to quantify the number of Schwann cell nuclei per nerve profile. (J) Graph to show the g-ratio. (K) Graph to show the nerve area. One-way ANOVA with Tukey comparison, $p<0.0001$. All statistical analysis in all graphs is represented relative to WT unless shown otherwise.

In summary, the results presented in Figure 3.4, highlight the potentially detrimental effects that very high levels of c-Jun in Schwann cells may have on Schwann cell function and nerve development.

These findings corroborate previous findings from Parkinson et al., 2008 that show the negative effect of elevated Schwann cell c-Jun on myelination *in vitro*. However, the results presented here provide evidence for this effect *in vivo* as well.
Specifically, radial sorting and myelination are inhibited in OE/OE nerves, which can still be seen later in development. However in OE/+ nerves, this is only a transient delay, as will be discussed later.

To determine whether these differences seen in c-Jun overexpressing mice compared to WT are maintained or diminished, a later developmental time point of P21 in WT, OE/+ and OE/OE nerves, was characterised in the same way as P1 and P7.

3.2.4 Radial sorting and myelination are still delayed in OE/OE nerves, yet seem comparable between WT and OE/+ nerves at P21

At closer examination of electron microscopy images taken from P21 WT, OE/+ and OE/OE nerves, both at low magnification of x3000 and at higher magnification of x10000 (Figure 3.5A), the differences visible in P7 nerves (Figure 3.4A), were no longer apparent between WT and OE/+ nerves. However, the OE/OE nerve ultrastructure was still very different to the WT nerve (Figure 3.5A). Although at a glance, WT and OE/+ nerve cytoarchitecture seem similar (Figure 3.5A), OE/OE nerves have very significant changes in their nerve architecture, such as: (i) the obvious increase in collagen, (ii) the reduced thickness in myelin sheaths, (iii) the presence of many non-myelinated large diameter axons (both radially sorted and part of Remak bundles), and (iv) the irregular structure of the Remak bundles. By P21, no Schwann cell families were visible in WT, OE/+ or OE/OE nerves as expected (Webster et al., 1973), however in OE/OE nerves, there was the presence of slightly irregular Remak bundles compared to both WT and OE/+ nerves, as highlighted in Figure 3.5A with red outlines**.** These changes seen in OE/OE nerves at P21 (Figure 3.5) appear to be an exaggerated change in the phenotype which had started to appear at P7 (Figure 3.4).

WT and OE/+ nerves at P21 were more similar to each other compared to that seen at P7 (Figure 3.4). The total number of axons >1.5μm in diameter, both non-myelinated and myelinated, quantified in WT and OE/+ were not significantly different, 4180 and 4229 respectively, however there was a notable decrease in OE/OE (3338) compared to WT (4229) (Figure 3.5B).

The number of myelinated axons in WT and OE/+ nerves at P21 is very similar, at 4110 and 3990 respectively. This is a strong indication that lower fold elevation of Schwann cell c-Jun (OE/+) does not have as great a negative effect on myelination when compared to a higher Schwann cell c-Jun elevation, such as the one seen in OE/OE (1912) nerves, where there is a significant decline compared to both WT and OE/+ nerves (Figure 3.5C). This is a strong indication that the very high levels of c-Jun present in OE/OE Schwann cells strongly inhibit myelination *in vivo*, which was previously suggested by the work of Parkinson et al., 2008.

Radial sorting in normal nerves should be complete by P10, therefore the percentage of radially sorted axons at P21 should be 100%. From the analysis shown in Figure 3.5D, WT and OE/+ nerves were almost entirely radially sorted at 99% and 98% respectively, unlike OE/OE nerves where only 84% of larger axons were radially sorted. This difference between OE/OE and WT and OE/+ nerves was statistically significant.

In line with this, the number of non-myelinated axons >1.5μm in diameter were 69 in WT, 239 in OE/+ and 1425 in OE/OE nerves. There was no statistical difference between WT and OE/+, however in OE/OE nerves, the number of non-myelinated axons >1.5μm in diameter was significantly higher than WT and OE/+ (Figure 3.5E). The number of non-myelinated axons >1.5μm that were in a 1:1 relationship with a Schwann cell (Figure 3.5F) or in Remak bundles (Figure 3.5G), was not significantly different between WT and OE/+. In OE/OE nerves the number of non-myelinated axons >1.5μm in diameter (including those that form a 1:1 relationship with a Schwann cell or part of a Remak bundle), is significantly higher compared to WT and OE/+ (Figure 3.5E-G), further confirming the severe inhibitory myelination phenotype seen with very high Schwann cell c-Jun levels.

The percentage of large calibre axons that were myelinated (WT 98% and OE/+ 94%) or unmyelinated (WT 2% and OE/+ 6%) were similar in WT and OE/+ nerves. There was a significant decrease in the percentage of myelinated axons in OE/OE (57%) nerves and conversely a significant increase in the percentage of non-myelinated axons in OE/OE (43%), compared to WT and OE/+ nerves (Figure 3.5H).

The number of Schwann cell nuclei counted in OE/+ compared to WT, though still slightly elevated in OE/+ (409) compared to WT (311), was not significantly different (Figure 3.5I), yet at P7 (Figure 3.4I) these differences were notably elevated in OE/+ (589) compared to WT (413). It seems that by P21, Schwann cell proliferation seen in OE/+ nerves has ceased. The number of Schwann cell nuclei quantified in P21 OE/OE (745) nerves was statistically higher compared to WT and OE/+ nerves (Figure 3.5I).

The reduced myelin sheath thickness between OE/+ and OE/OE nerves compared to WT remained significantly different (Figure 3.5J).

The nerve areas of WT (91368μm^2), OE/+ (99166μm^2) and OE/OE (112536μm^2), were not significantly different to each other, although there is still a trend towards OE/OE nerves being bigger (Figure 3.5K).

The comparison of all these parameters between WT and OE/+ nerves indicates that Schwann cells can withstand moderate levels of c-Jun elevation without significant detrimental effects, yet, a very high elevation in Schwann cell c-Jun can be detrimental, as is seen when comparing WT and OE/OE nerves (Figure 3.5).

OE/OE nerve development is severely impaired due to the substantially high levels of Schwann cell c-Jun. All the significant changes between WT and OE/OE nerves noted at P7 (Figure 3.4) were more pronounced at P21 (Figure 3.5), contrary to what was seen in OE/+ nerves.

By P21, the initial transient delay in myelination seen in OE/+ nerves compared to WT at P7, was no longer evident, yet in these same nerves, the thickness of myelin sheaths remained significantly thinner in OE/+ compared to WT. Although the data presented would suggest that in OE/OE nerves radial sorting is affected (Figure 3.5D), the presence of Remak bundles in these nerves, albeit slightly abnormal in form suggests that they eventually form. Myelination inhibition observed in OE/OE nerves at P7 (Figure 3.4) was still present at P21, but also more prominent compared to WT and OE/+ nerves (Figure 3.5). Myelin sheath thickness of the myelinated axons present in OE/OE nerves, was also significantly thinner than in WT nerves.

The importance of myelin sheath thickness may prove to be important in sensory and motor reflexes. Myelin sheath formation is crucial for saltatory conduction, therefore one could assume that if such conduction velocity studies were carried out, they may provide more of an insight into how detrimental thinner myelin sheaths seen in OE/+ and OE/OE nerves may be (Figures 3.4J and 3.5J). Notwithstanding such future work, behavioural studies give an indication of how nerve conduction/transmission has been affected in the OE/+.

There is strong indication from the results presented so far, that Schwann cells are tolerant of moderately high levels of c-Jun, such as those present in OE/+ nerves, and to a certain extent the higher levels expressed in OE/OE nerves. This conclusion is based on the lack of significant differences in OE/+ nerves compared to WT, except for those seen in g-ratios. There is also strong evidence to show that myelination and

radial sorting were only temporarily delayed in OE/+ nerves, but severely inhibited in OE/OE nerves. Therefore, this implies that there is a gene-dose dependent effect of Schwann cell c-Jun expression on both the function of Schwann cells and nerve development. Most importantly however is the obvious confirmation of previous *in vitro* studies, now done *in vivo* using a novel transgene expression dependent mouse model.

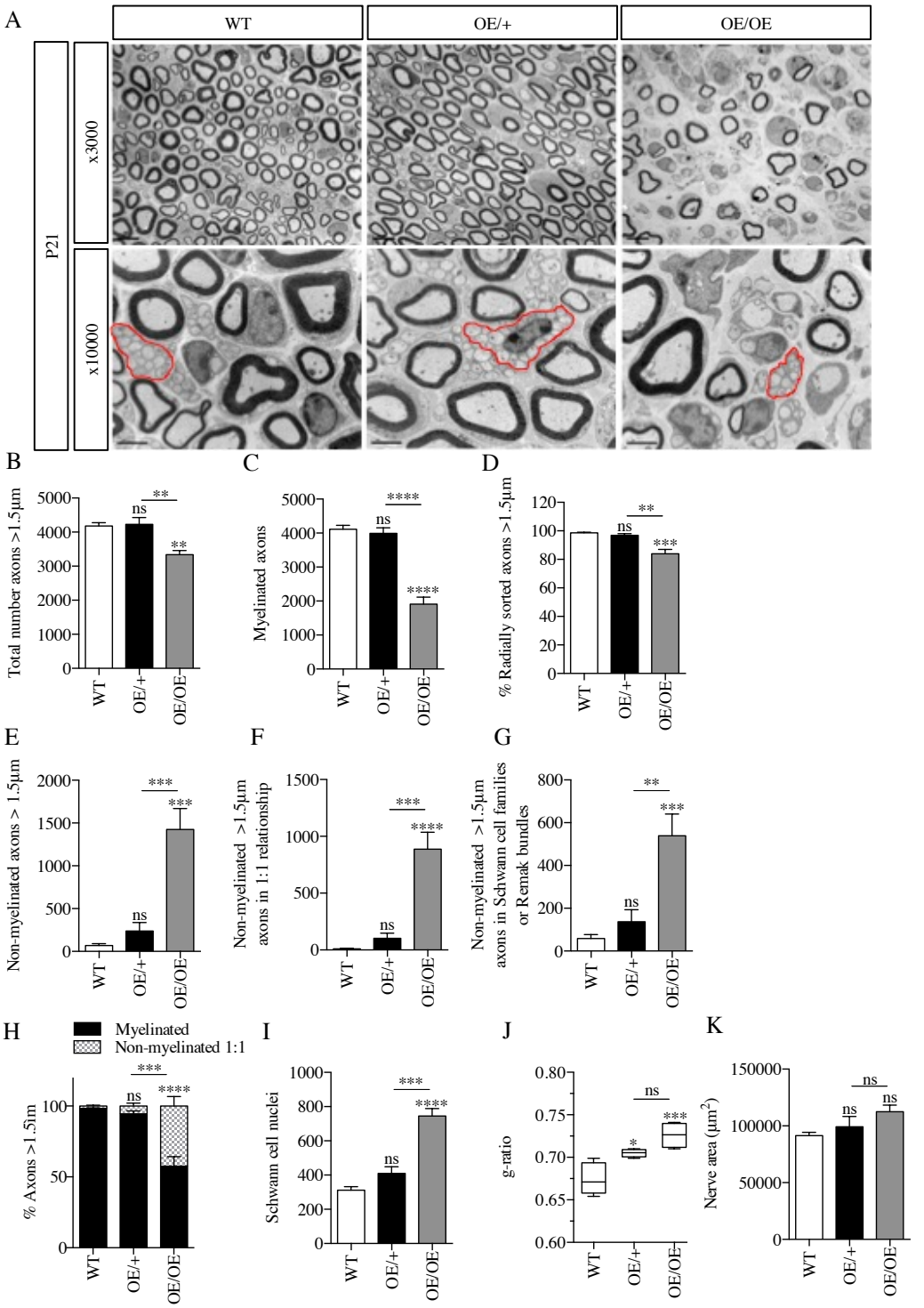

Figure 3.5 | Characterisation of WT, OE/+ and OE/OE nerves at P21

(A) Representative electron microscopy images taken at x3000 and x10000 magnification to show more detail of the ultrastructure of WT, OE/+ and OE/OE nerves at P21. The red outlines show the presence of normal Remak bundles in WT and OE/+ nerves, yet slightly irregular arrangements of Remak bundles in OE/OE nerves. Scale bar represents 5µm (x3000) and 2µm (x10000). Graphs shown in panels B-K are all quantified from WT (n=5), OE/+ (n=4) and OE/OE (n=4) mice at P21. (B) Graph to quantify the total number of axons >1.5µm per nerve profile. (C) Graph to quantify the number of myelinated axons per nerve profile. (D) Graph to quantify the percentage of axons >1.5µm that are segregated per nerve profile. (E) Graph to quantify the number of non-myelinated axons >1.5µm per nerve profile. (F) Graph to quantify the number of non-myelinated axons >1.5µm that are in a 1:1 relationship per nerve profile. (G) Graph to quantify the number of non-myelinated axons >1.5µm that are in Schwann cell families or Remak bundles per nerve profile. (H) Graph to quantify the percentage of 1:1 >1.5µm myelinated compared to non-myelinated axons per nerve profile. (I) Graph to quantify the number of Schwann cell nuclei per nerve profile. (J) Graph to show the g-ratio. (K) Graph to show the nerve area. One-way ANOVA with Tukey comparison, $p<0.0001$. All statistical analysis in all graphs is represented relative to WT unless shown otherwise.

So far, as has been shown in this chapter, there is strong evidence that Schwann cells can withstand moderately high levels of c-Jun elevation, such as those seen in OE/+ mice, yet levels that exceed those seen in OE/+ such as those in OE/OE, can prove to be detrimental to the proper functioning of the Schwann cell, and therefore ultimately the nerve itself. Based on this, it is now clear that at least from P1-P21, c-Jun levels in OE/+ and OE/OE Schwann cells remain elevated. c-Jun in Schwann cells has a multi-faceted role, with the key one being its function in successful nerve regeneration, as shown by the work of Arthur-Farraj et al., 2012.

For this reason, it would be crucial to find out if c-Jun levels in OE/+ remain elevated into adulthood (P60) and whether the nerves of these mice still resemble those of WT ones. It is as important to assess whether or not very high c-Jun elevation in Schwann cells seen in in OE/OE mice, affect nerve development or if these nerves end up resembling those of WT mice. The characterisation of adult P60 OE/+ and OE/OE compared to WT mice is fundamental as it could prove to be a useful tool *in vivo* for studying elevated c-Jun levels in peripheral nerve injury and regeneration.

3.2.5 Elevated levels of c-Jun in Schwann cells down-regulate myelin related genes

As previously shown using *in vitro* studies by the work of Parkinson et al., 2008, c-Jun is a negative regulator of myelination. It was therefore decided to investigate whether c-Jun overexpression in Schwann cells (OE/+ and OE/OE) results in down-regulation of myelin genes. A crucial myelination transcription factor, that unlike c-Jun, is a positive regulator of myelination, is Krox20 (Topilko et al., 1994; Murphy et al., 1996; Zorick et al., 1999; Ghislain et al., 2002; Jessen and Mirsky, 2005; Parkinson et al., 2008; Woodhoo et al., 2009). With this in mind, sciatic nerve cryosections from WT, OE/+ and OE/OE nerves at P7 were immunofluorescently labelled using Sox10 (Schwann cell marker) and Krox20 (marker of myelination) antibodies and with DAPI to label nuclei, to determine whether high levels of c-Jun expression in OE/+ and OE/OE nerves caused a down-regulation in Krox20 expression compared with WT nerves (Figure 3.6). Clear and significant down-regulation of Krox20 expression in Schwann cells is seen in OE/+ (43%) and OE/OE (24%) compared to WT (60%) levels as well as a significant decrease between OE/+ and OE/OE nerves. The quantification for the representative immunofluorescence images (Figure 3.6A) is shown in Figure 3.6B. To show how Krox20/Sox10 positive Schwann cells were quantified, a magnified image is shown in Figure 3.6C, with white arrowheads to highlight positive Krox20/Sox10 cells.

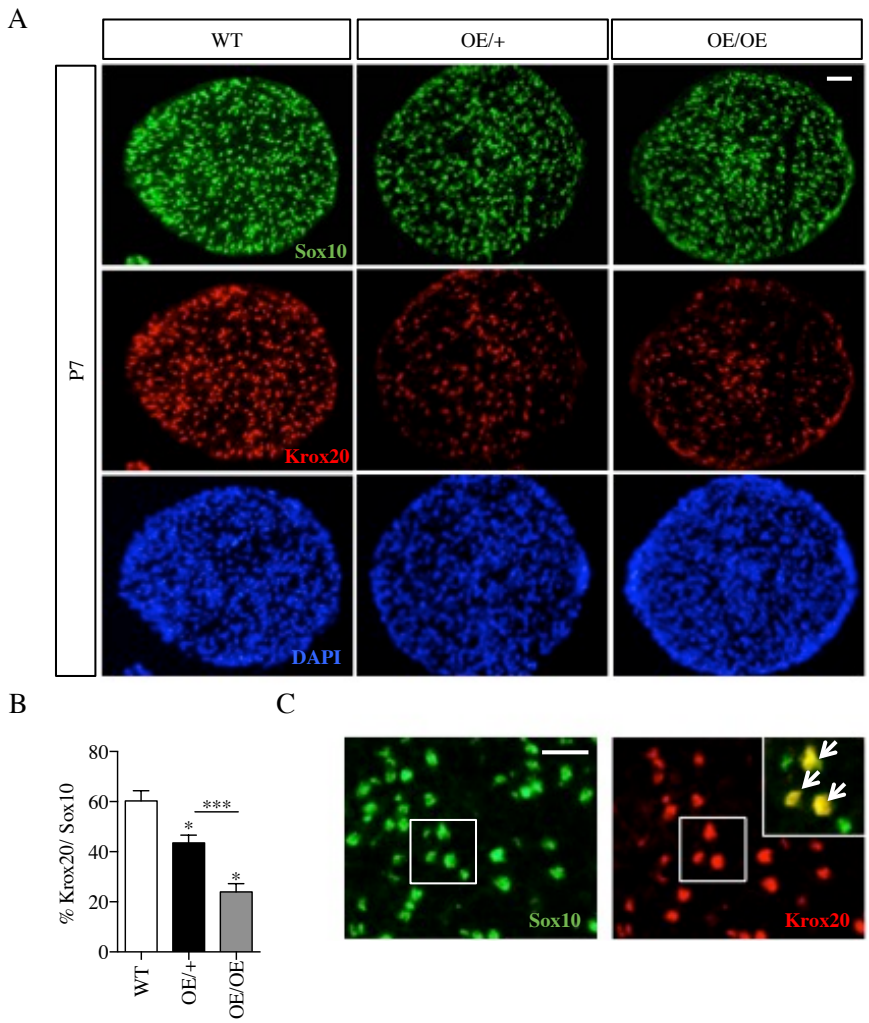

Figure 3.6 | Elevated levels of c-Jun in Schwann cells at P7 results in significant down-regulation of Krox20 in Schwann cells

(A) Representative immunofluorescence images taken at x25 magnification show the different levels of Krox20 expression in WT, OE/+ and OE/OE nerves at P7. Transverse sections of P7 sciatic nerves immunolabelled with Sox10 (Schwann cell marker) and Krox20 (marker of myelination) antibodies and with DAPI to label nuclei. Scale bar represents 50µm. (B) Graph to quantify the percentage of positively labelled Krox20/Sox10 cells in WT, OE/+ and OE/OE nerves. WT (n=6), OE/+ (n=4) and OE/OE (n=3); One-way ANOVA with Tukey comparison, p=0.0002. All statistical analysis is represented relative to WT unless shown otherwise. (C) Magnified immunofluorescence images of P7 nerve to show how Krox20/Sox10 positive cells were quantified. Scale bar represents 25µm.

Figure 3.1A-B shows that c-Jun is elevated in overexpressing mouse nerves as early as P1. For this reason, nerve extracts from WT, OE/+ and OE/OE sciatic nerves were analysed by Western blot both at P1 and P7 for Krox20 expression. Unlike the results seen in Figure 3.6, Western blot results of Krox20 expression in OE/+ and OE/OE nerves, were not significantly down-regulated at P1, nor at P7 (Figure 3.7). Although the results in Figures 3.6 and 3.7 appear not to agree with each other, they are not necessarily contradictory. At P7 the Western blot analysis (Figure 3.7C-D), shows that there is a slight decrease in Krox20 expression in OE/OE mice compared to WT, even though this does not reach statistical significance. No statistical analysis was done on P1 Western blot results as this experiment was only repeated twice. For further discussion of this, please see section 3.3.

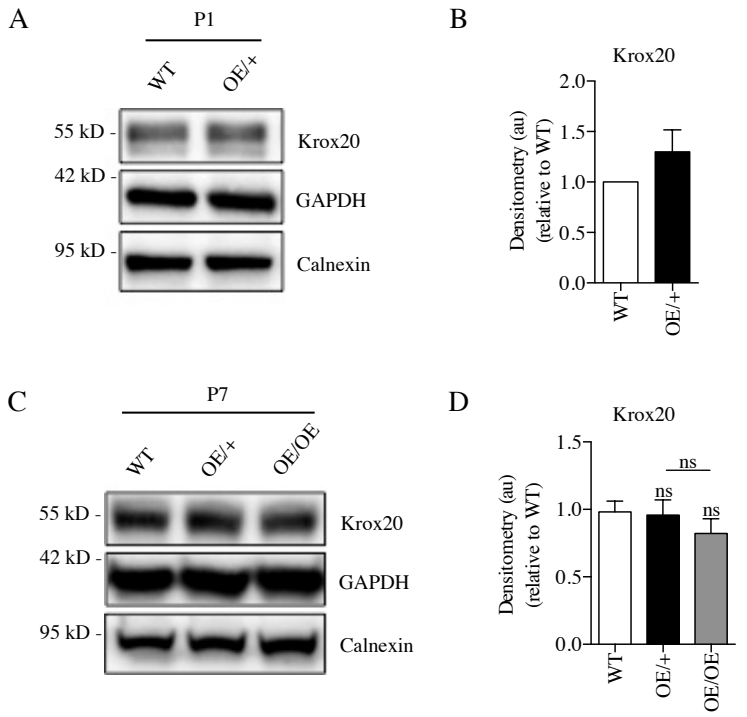

Figure 3.7 | Krox20 levels remain unaffected in OE/+ and OE/OE nerves by elevated c-Jun levels at P1 and P7
(A) Representative Western blot image of nerve extracts from P1 WT and OE/+ nerves to show the levels of Krox20 expression. GAPDH and calnexin are used as reference genes. (B) Graph to quantify Krox20 levels of OE/+ nerves at P1 relative to WT. c-Jun was normalised to calnexin and GAPDH, and then expressed as a fold change relative to WT. WT (n=2) and OE/+ (n=2); no statistical analysis. (C) Representative Western blot image of nerve extracts from P7 WT, OE/+ and OE/OE nerves to show the levels of Krox20 expression. GAPDH and calnexin are used as reference genes. (D) Graph to quantify Krox20 levels of OE/+ and OE/OE nerves at P7 relative to WT. Krox20 was normalised to calnexin and GAPDH, and then expressed as a fold change relative to WT. WT (n=3), OE/+ (n=3) and OE/OE (n=3); One-way ANOVA with Tukey comparison. All statistical analysis is represented relative to WT unless shown otherwise.

If c-Jun elevation in Schwann cells causes down-regulation of pro-myelin transcription factors such as Krox20, what happens to the expression of myelin proteins in these nerves? To address this, a myelin protein that is a major component of peripheral nerve myelin sheaths, Mpz, was analysed (Mirsky et al., 1980; Jessen and Mirsky, 1991; Jessen et al., 1991; Cheng and Mudge, 1996; Corfas et al., 2004).

Western blot analysis of P1 and P7 nerve extracts from WT, OE/+ and OE/OE mice showed that early on after birth (P1), there was no significant decrease in the levels of Mpz expression between WT and OE/+ nerves (Figure 3.8A-B). This similarity of Mpz expression in WT and OE/+ nerves was maintained at P7, yet levels of Mpz expression in OE/OE nerves at this time point were significantly less compared to both WT and OE/+ levels (Figure 3.8C-D). These results, unlike at P1, suggest that a 7 fold c-Jun elevation (OE/OE) in Schwann cells compared to WT may have a detrimental effect on myelin protein expression. This result is in line with the evidence shown earlier (Figure 3.4C) where OE/OE nerves have fewer myelinated axons, therefore the nerve extracts from these mice might be expected to have lower overall levels of Mpz expression.

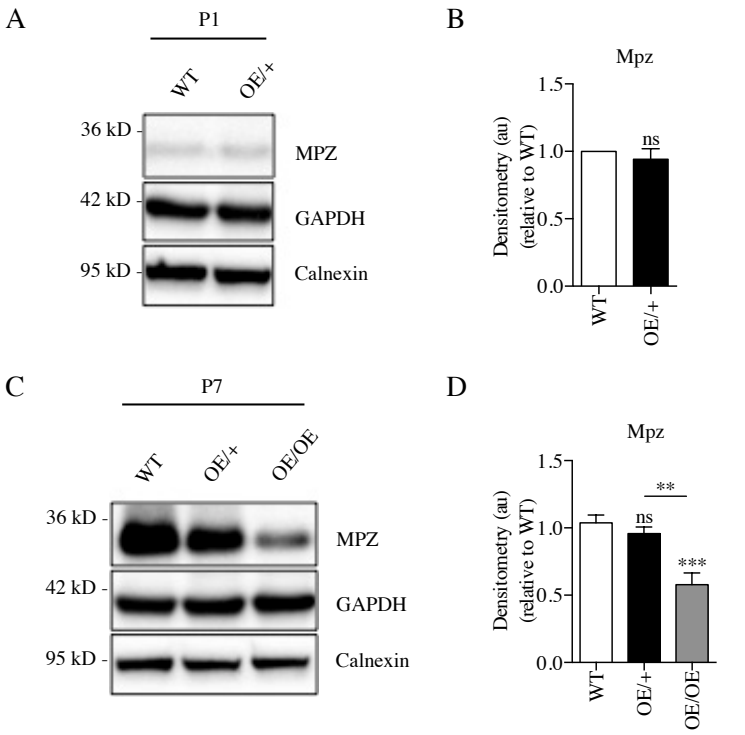

Figure 3.8 | Mpz levels remain constant in OE/+ nerves compared to WT at P1 and P7 but are significantly downregulated in OE/OE nerves compared to WT at P7

(A) Representative Western blot image of nerve extracts from P1 WT and OE/+ nerves to show the levels of Mpz expression. Mpz is used to show how a myelin-related protein is affected by increased levels of transgenic c-Jun. GAPDH and calnexin are used as reference genes. (B) Graph to quantify Mpz levels of OE/+ nerves at P1 relative to WT. Mpz was normalised to calnexin and GAPDH, and then expressed as a fold change relative to WT. WT (n=3) and OE/+ (n=3); Mann Whitney test, p=0.6825. (C) Representative Western blot image of nerve extracts from P7 WT, OE/+ and OE/OE nerves to show the levels of Mpz expression. GAPDH and calnexin are used as reference genes. (D) Graph to quantify Mpz levels of OE/+ and OE/OE nerves at P7 relative to WT. Mpz was normalised to calnexin and GAPDH, and then expressed as a fold change relative to WT. WT (n=3), OE/+ (n=3) and OE/OE (n=3); One-way ANOVA with Tukey comparison, $p<0.0001$. All statistical analysis is represented relative to WT unless shown otherwise.

3.2.6 Overexpression of Schwann cell c-Jun results in increased Schwann cell proliferation

c-Jun elevation is associated with increased cell proliferation in many tissues (Schreiber et al., 1999; Vleugel et al., 2006; Mirsky et al., 2008; Arthur-Farraj et al., 2011; Ma et al., 2012). For this reason, it was of interest to see whether c-Jun increased cell proliferation in overexpressing mouse nerves (OE/+ and OE/OE),

Cyclin D1 is an important cell cycle regulatory switch in proliferating cells and is therefore used as a marker of cell proliferation (Baldin et al., 1993; Diehl, 2002; Stacey, 2003; Klein and Assoian, 2008; Duronio and Xiong, 2013; Porrello et al., 2014). For this reason, P7 WT, OE/+ and OE/OE nerve extracts were probed with Cyclin D1 antibody to see if there was an increase in cell proliferation in OE/+ and OE/OE nerves. Surprisingly, there was no significant increase in cell proliferation, regardless of c-Jun elevation in Schwann cells as shown in Figure 3.9A-B.

Although Cyclin D1 expression in WT, OE/+ and OE/OE nerves did not show significant differences in cell proliferation, possibly due to the fact that Cyclin D1 recognises proliferating cells in fewer stages of the cell cycle than some other markers, it was still worth investigating cell proliferation using a different proliferation marker. Another reason for the lack of proliferation difference seen using Cyclin D1 as a marker, may be due to the fact that other pathways might be the major drivers of proliferation at this stage in development.

Ki67 is another commonly used nuclear protein that is expressed in proliferating mammalian cells and is able to recognise proliferating cells at more stages of the cell cycle than Cyclin D1 (Lopez et al., 1991; Scholzen and Gerdes, 2000; Hoos et al., 2001; Porrello et al., 2014; Sobecki et al., 2016). To determine whether Schwann cell c-Jun elevation causes proliferation within Schwann cells specifically, nerve cryosections from P7 WT, OE/+ and OE/OE were fluorescently immunolabelled with Sox10 and Ki67, and with DAPI as shown in Figure 3.9C-E. Sox10 was used as a marker for recognising Schwann cells, therefore allowing for specific localisation of Ki67 and Sox10 positive cells, unlike Western blot analysis where different cell types cannot be determined. The percentage of proliferating Schwann cells in OE/OE nerves was significantly higher compared to both WT and OE/+ nerves. These results

demonstrate that in P7 nerves, when c-Jun is elevated in Schwann cells to the extent seen in OE/OE nerves (7 fold), cell proliferation is increased as determined by the percentage of Ki67 positive Schwann cells (Figure 3.9C-E).

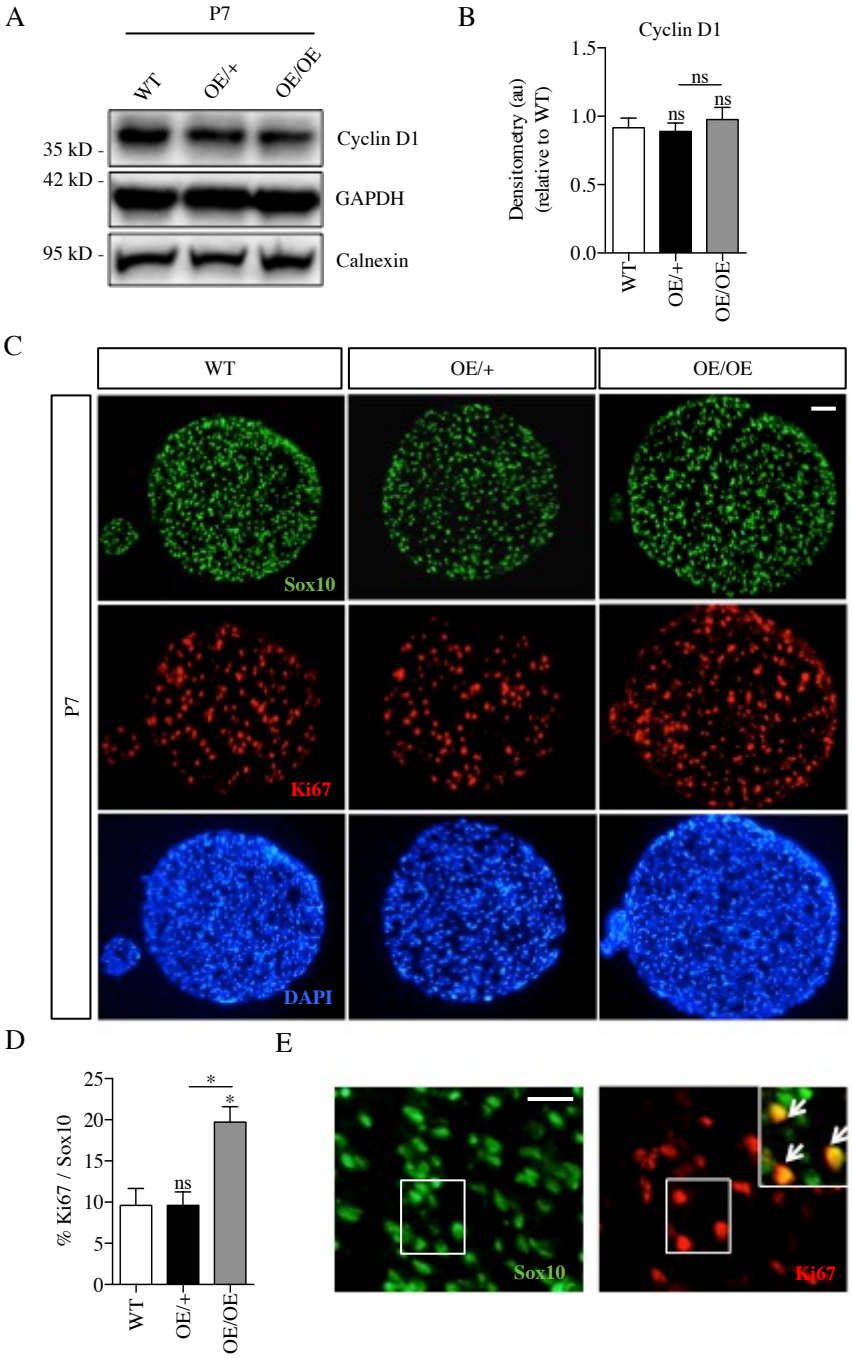

Figure 3.9 | Elevated levels of c-Jun in Schwann cells at P7 suggest a modest effect on cell proliferation
(A) Representative Western blot image of nerve extracts from P7 WT, OE/+ and OE/OE nerves to show the levels of Cyclin D1 expression. Cyclin D1 is used as a marker of cell proliferation. GAPDH and calnexin are used as reference genes. (B) Graph to quantify Cyclin D1 levels of OE/+ and OE/OE nerves at P7 relative to WT. Cyclin D1 was normalised to calnexin and GAPDH, and then expressed as a fold change relative to WT. WT (n=3), OE/+ (n=3) and OE/OE (n=3); One-way ANOVA with Tukey comparison. (C) Representative immunofluorescence images taken at x25 magnification show the different proliferation rates in WT, OE/+ and OE/OE nerves at P7. Transverse sections of P7 sciatic nerves immunolabelled with Sox10 (Schwann cell marker) and Ki67 (marker of proliferating cells) antibodies and DAPI to label nuclei. Scale bar represents 50µm. All statistical analysis is represented relative to WT unless shown otherwise. (D) Graph to quantify the percentage of positively labelled Ki67/Sox10 cells in WT, OE/+ and OE/OE nerves. WT (n=6), OE/+ (n=4) and OE/OE (n=3); One-way ANOVA with Tukey comparison, p=0.0121. All statistical analysis is represented relative to WT unless shown otherwise. (E) Magnified immunofluorescence images of P7 nerve to show how Ki67/Sox10 positive cells were quantified. Scale bar represents 25µm.

3.2.7 c-Jun elevation in OE/+ and OE/OE Schwann cells is maintained at P60

c-Jun was clearly shown to be elevated in both OE/+ and OE/OE nerves, specifically in Schwann cells (Figure 3.1). Longitudinal nerve cryosections from P60 WT, OE/+ and OE/OE nerves were immunolabelled with c-Jun and Sox10 antibodies, and DAPI to label nuclei (Figure 3.10A), and nerve protein extracts probed with c-Jun antibodies (Figure 3.10B-C), to show that c-Jun was still elevated in both OE/+ and OE/OE nerves at P60, and that this elevation was specific to Schwann cells, as indicated in earlier results in this chapter. As expected, both immunofluorescence and Western blot analysis clearly showed c-Jun elevation specifically in Schwann cells in OE/+ and OE/OE nerves relative to WT. Although the immunofluorescence images were not quantified, it was obvious that Schwann cells in WT nerves express the lowest level of c-Jun, and progressively higher levels are expressed in OE/+ and OE/OE nerve Schwann cells, as determined by co-localisation of c-Jun signal with Sox10 (Schwann cell marker) (Figure 3.10A).

The representative Western blot image in Figure 3.10B and its quantification in 3.10C show an obvious elevation in c-Jun expression in both OE/+ and OE/OE nerves compared to WT. This elevation of OE/+ compared to WT is 6 fold, yet the elevation in OE/OE nerves compared to WT is 19 fold. This suggests that Schwann cell c-Jun levels are maintained in OE/+ and OE/OE nerves compared to WT levels at P60.

At P60, whilst the comparative elevation in c-Jun in OE/+ and OE/OE nerves compared to WT c-Jun expression may seem high compared to P1 and P7, it should be remembered that the comparative increases in c-Jun seen have been measured against WT c-Jun expression in mice of the same age (ie. P1 OE/+ and OE/OE relative to P1 WT, P7 OE/+ and OE/OE relative to P7 WT, etc.). It is known that c-Jun levels expressed earlier on postnatally (P1 and P7) in WT, are much higher than at P60 a time at which endogenous c-Jun levels are very low at P60 (Parkinson et al., 2008). This finding is also highlighted in Figure 3.10D-E above. For this reason, c-Jun may be elevated in OE/+ and OE/OE Schwann cells equally throughout the different ages of the mouse lifespan, beginning from the point at which transgenic P_0cre is activated driving Cre recombinase at E13.5-14.5 (Feltri et al., 1999). Nevertheless, to confirm this idea, analysis such as by Western blot would need to be

done using WT, OE/+ and OE/OE nerves from different aged mice and compared together at the same time on the same membrane.

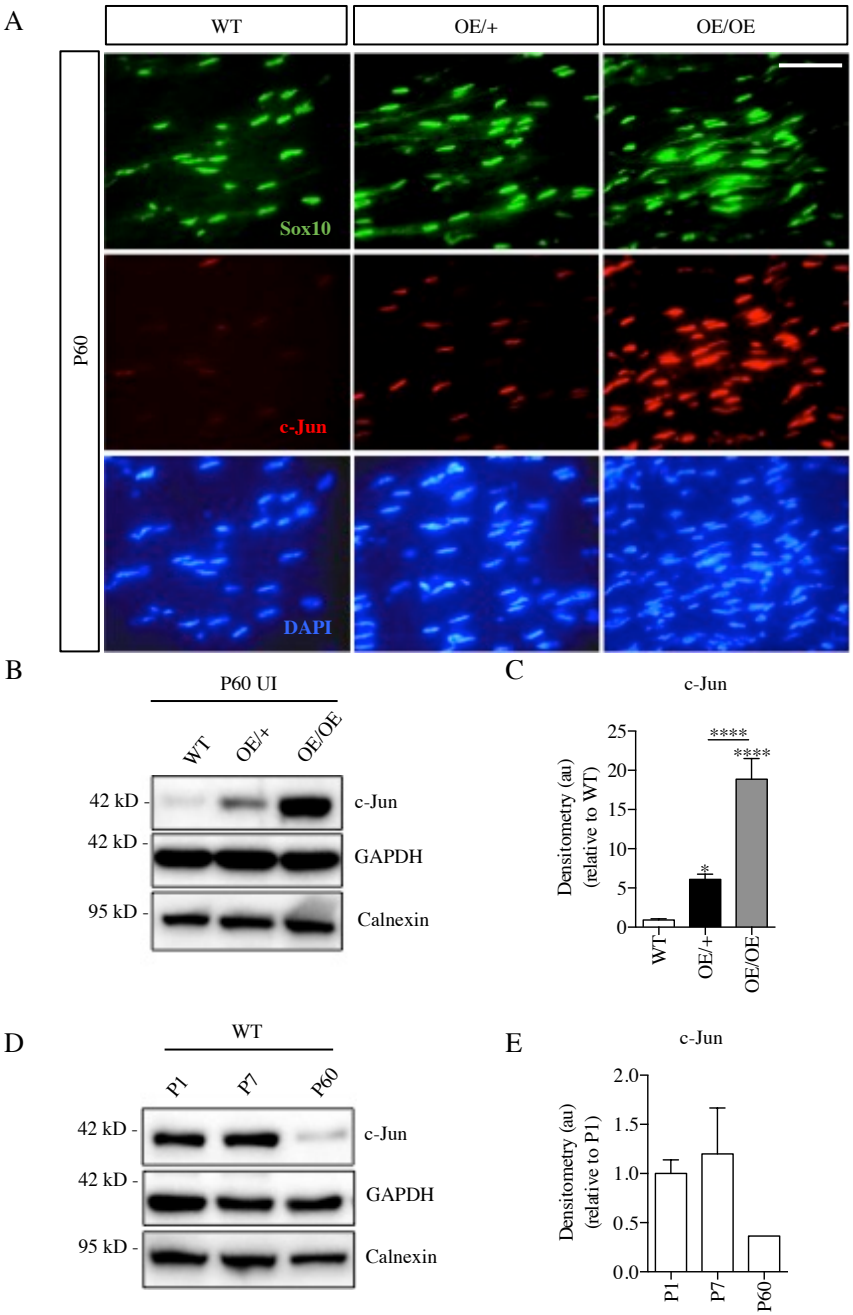

Figure 3.10 | c-Jun is overexpressed specifically in Schwann cells

(A) Representative immunofluorescence images taken at x63 magnification show the different levels of c-Jun expression in Schwann cells at P60 in uninjured nerves. Longitudinal sections of P60 sciatic nerves were immunolabelled with Sox10 (Schwann cell marker) and c-Jun antibodies and with DAPI to label nuclei. These images show that the c-Jun overexpressing transgene is working and maintained at P60. Scale bar represents 25µm. (B) Representative Western blot image of nerve extracts from P60 WT, OE/+ and OE/OE nerves to show the levels of c-Jun expression. c-Jun is used to show that the c-Jun overexpressing transgene is working and maintained at P60. GAPDH and calnexin are used as reference genes. (C) Graph to quantify c-Jun levels of OE/+ and OE/OE nerves at P60 relative to WT. c-Jun was normalised to calnexin and GAPDH, and then expressed as a fold change relative to WT. WT (n=5), OE/+ (n=4) and OE/OE (n=5); One-way ANOVA with Tukey comparison, $p<0.0001$. All statistical analysis is represented relative to WT unless shown otherwise. (D) Representative Western blot image of nerve extracts from P1, P7 and P60 WT nerves to show the levels of c-Jun expression. GAPDH and calnexin are used as reference genes. e-Jun expression in WT nerves declines from early postnatal stages (P1-P7) to adulthood (P60). (E) Graph to quantify c-Jun levels of OE/OE nerves at P60 and P300 and WT at P300, relative to WT P60 levels. c-Jun was normalised to calnexin and GAPDH, and then expressed as a fold change relative to WT P1. P1 (n=3), P7 (n=3), P60 (n=1); no statistical analysis.

3.2.8 The nerve architecture of adult OE/+ nerves is nearly normal compared to WT, yet OE/OE nerves continue to show abnormalities at P60

The integrity of peripheral nerves is strongly determined by the proper development and function of its components including Schwann cells, axons and connective tissue. Nerves of OE/OE mice began to show abnormalities such as increased Schwann cell nuclei, impaired radial sorting of axons, increased number of non-myelinated axons (both in a 1:1 relationship with a Schwann cell but also in Remak bundles and Schwann cell families), axons with thinner myelin sheaths, increased appearance of collagen and also a larger nerve area. These changes became evident from electron microscopy analysis at P7 (Figure 3.4), and were more prominent by P21 (Figure 3.5). In contrast however, in OE/+ nerves, these changes seemed to be mild compared to those seen in OE/OE nerves, in relation to WT. However at P7 (Figure 3.4) there was a suggestion of delayed radial sorting and myelination, but unlike in OE/OE nerves, this became almost normal by P21 (Figure 3.5).
The question then arises: do OE/+ nerves remain almost normal regardless of their c-Jun elevation at P60, and do OE/OE nerves adopt a more abnormal phenotype? To address these questions, electron microscopy analysis of P60 WT, OE/+ and OE/OE nerves was undertaken in the same manner as that shown in Figures 3.3-3.5.

When dissecting OE/OE nerves from the mouse, the most striking feature is the obvious increase in nerve size, compared to WT and OE/+ nerves. This difference is highlighted by photographs shown in Figure 3.11A, taken inside the mouse, and then overlaid on 1mm x 1mm gridded paper. Analysis of WT, OE/+ and OE/OE nerve areas at P7 (Figure 3.4K) and P21 (Figure 3.5K) indicated a marginal yet insignificant increase in both OE/+ and OE/OE nerve size compared to WT. Furthermore, the magnified electron microscopy images at P7 (Figure 3.4A) and P21 (Figure 3.5A) indicated that there was more collagen and extracellular matrix in OE/OE nerves compared to WT and OE/+ nerves. Representative electron microscopy images shown in Figure 3.11B highlight the differences in the ultrastructure of OE/OE nerves compared to both WT and OE/+, which look very similar to each other. Already this analysis is indicative of the fact that, at P60, c-Jun elevation in Schwann cells of OE/OE nerves is having a strong effect on nerve development and ultimately function,

but that the elevated levels of c-Jun in OE/+ nerves are not enough to cause a detrimental effect.

The nerve area was therefore measured from WT, OE/+ and OE/OE nerves at P60 (Figure 3.11C). It showed that WT and OE/+ nerves were almost the same size, 123604μm^2 and 120121μm^2, the size of OE/OE nerves was 245090μm^2 , significantly larger than both WT and OE/+ nerves.

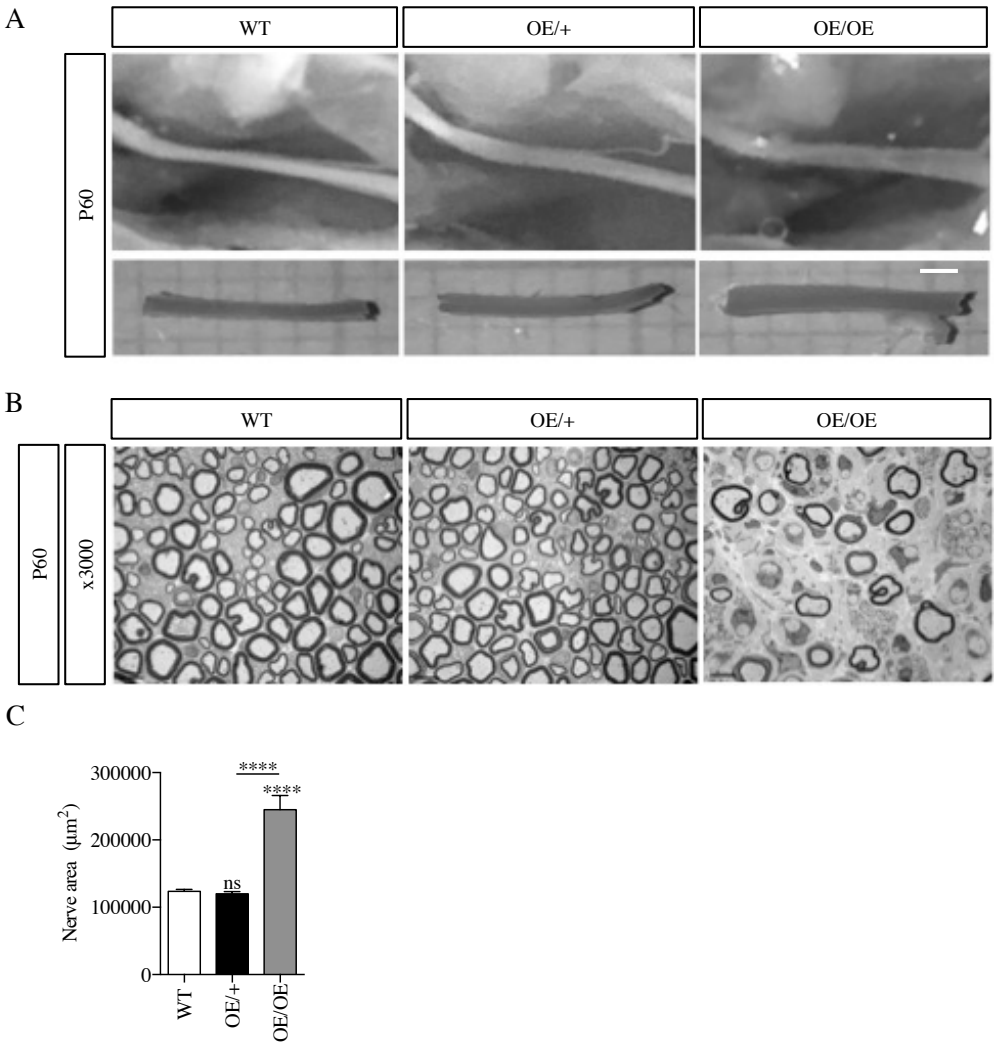

Figure 3.11 | Nerve areas of WT and OE/+ mice are similar, but OE/OE is substantially larger at P60
(A) Representative photographs taken of WT, OE/+ and OE/OE nerves inside the mouse, which were then placed along 1x1mm ruled paper to see the differences in nerve thickness. Scale bar represents 1mm. (B) Representative electron microscopy images taken at x3000 magnification to show the ultrastructure of WT, OE/+ and OE/OE nerves at P60. Scale bar represents 5µm. (C) Graph to show the nerve area of WT (n=5), OE/+ (n=5) and OE/OE (n=3) mice at P60. One-way ANOVA with Tukey comparison, $p<0.0001$. All statistical analysis is represented relative to WT unless shown otherwise.

Higher magnification electron microscopy images shown in Figure 3.12A reveal even more the differences between OE/OE nerve architecture compared to WT and OE/+ mice. Further in depth analysis of electron microscopy was carried out, as shown in Figure 3.12, that highlighted very distinct differences of OE/OE nerves compared to WT and OE/+ nerves, yet also showed how similar WT and OE/+ nerves are at P60.

The number of axons >1.5μm in diameter, both myelinated and unmyelinated were virtually the same between WT and OE/+ nerves, 4574 and 4572 respectively (Figure 3.12B). The total number of axons >1.5μm in diameter (both non-myelinated and myelinated) that were quantified in OE/OE (3870) nerves were significantly lower compared to WT (4574) and OE/+ (4572) (Figure 3.12B).

In line with this, the number of myelinated axons between WT and OE/+ was not significantly different, 4552 and 4533, respectively, yet it was significantly lower in OE/OE (1784) nerves compared to both WT and OE/+ (Figure 3.12C).

The inhibitory effect seen on radial sorting and on myelination of axons present in OE/OE nerves was already visible at P7 (Figure 3.4) and P21 (Figure 3.5), but became even more obvious and pronounced at P60, where the percentage of axons >1.5μm that were radially sorted was significantly lower at 72% in OE/OE nerves compared to WT and OE/+ at 99% (Figure 3.12D).

The results above indicate that at P60 c-Jun elevation seen in OE/OE nerves (19 fold), is enough to impair radial sorting and myelination.

In line with this, the number of non-myelinated axons >1.5μm in diameter (both in a 1:1 relationship with a Schwann cell and part of a Remak bundle), was significantly higher in OE/OE nerves compared to WT and OE/+ (Figure 3.12E-G). These results may indicate that an excess of Schwann cell c-Jun elevation (19 fold) such as that seen in P60 OE/OE nerves, affects the number of axons that are myelin competent and may therefore explain the increased numbers in non-myelinated 1:1 axons (1028 compared to 1 in WT and OE/+), Figure 3.12F. However, it is important to note that this is not a definitive conclusion because there is no data presented in this thesis showing what the levels of c-Jun elevation between P21 and P60 are. In order to conclude the level of Schwann cell c-Jun elevation that is detrimental, Western blot analysis of P60 WT nerves would need to be directly compared to levels of c-Jun present in OE/OE nerves at P1 and P7 and later time points. This has not been addressed in this thesis.

c-Jun also affects the ability of axons to be radially sorted**,** shown by the increase in the number of large diameter non-myelinated axons present in Remak bundles (1046 compared to 22 in WT and 37 in OE/+), Figure 3.12G.
The percentage of axons >1.5μm in diameter that were either myelinated or non-myelinated in WT and OE/+ nerves, was the same where 99% of their nerves were myelinated, and the remaining 1% were non-myelinated (Figure 3.12H). These results are similar to those seen at P21 (Figure 3.5H).

c-Jun elevation in OE/+ Schwann cells is not substantial enough to cause an increase in Schwann cell proliferation as the number of Schwann cell nuclei present in WT and OE/+ was similar, 205 and 254 respectively, and not significantly different (Figure 3.12I). However, c-Jun elevation in OE/OE nerves, resulted in a significant increase in Schwann cell nuclei to 1308 compared to WT and OE/+ (Figure 3.12I).

Myelin sheath thickness as determined by g-ratio analysis was also, as expected, significantly thinner in OE/OE nerves compared to both WT and OE/+ nerves shown in Figure 3.12J, and also thinner in OE/+ nerves compared to WT.

Unlike the small effect seen in OE/+ nerves compared to WT, in OE/OE nerves, the effects of elevated Schwann cell c-Jun were unambiguous, resulting in a strong phenotype (Figure 3.12). All morphometric analyses carried out on WT and OE/+ nerves indicated no difference between these nerves apart from significantly thinner myelin sheaths, even though the Schwann cells of OE/+ nerves have significantly elevated c-Jun levels compared to WT. However, as earlier results in this chapter (Figures 3.4 and 3.5) indicated, levels of Schwann cell c-Jun in OE/OE nerves has strong effects on nerve function and development.

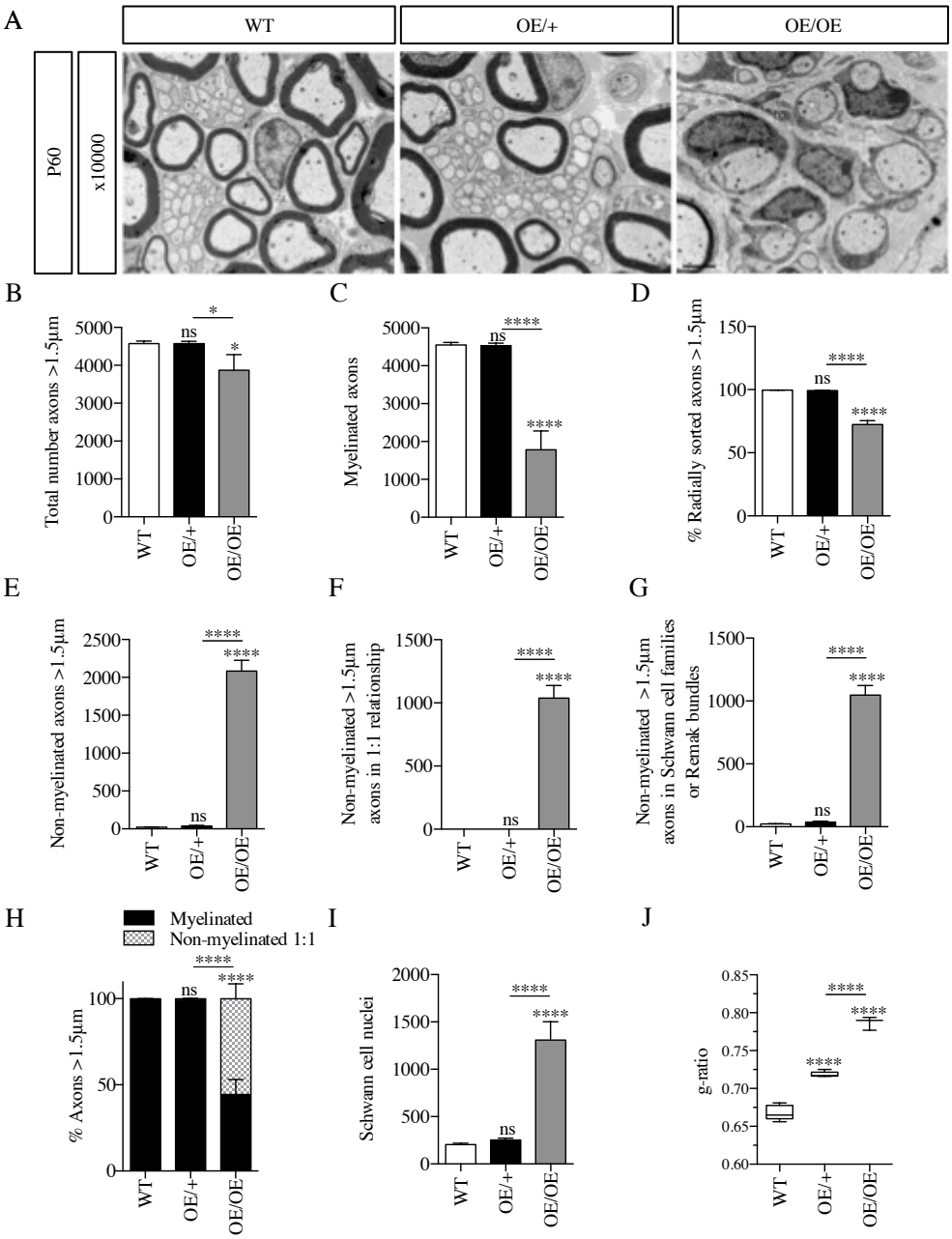

Figure 3.12 | Characterisation of WT, OE/+ and OE/OE nerves at P60

(A) Representative electron microscopy images taken at x10000 magnification to show more detail of the ultrastructure of WT, OE/+ and OE/OE nerves at P60. Scale bar represents 1µm. Graphs shown in panels B-J are all quantified from WT (n=5), OE/+ (n=5) and OE/OE (n=3) mice at P60. (B) Graph to quantify the total number of axons >1.5µm per nerve profile. (C) Graph to quantify the number of myelinated axons per nerve profile. (D) Graph to quantify the percentage of axons >1.5µm that are segregated per nerve profile. (E) Graph to quantify the number of non-myelinated axons >1.5µm per nerve profile. (F) Graph to quantify the number of non-myelinated axons >1.5µm that are in a 1:1 relationship per nerve profile. (G) Graph to quantify the number of non-myelinated axons >1.5µm that are in Schwann cell families or Remak bundles per nerve profile. (H) Graph to quantify the percentage of 1:1 >1.5µm myelinated compared to non-myelinated axons per nerve profile. (I) Graph to quantify the number of Schwann cell nuclei per nerve profile. (J) Graph to show the g-ratio. One-way ANOVA with Tukey comparison, $p<0.0001$. All statistical analysis in all graphs is represented relative to WT unless shown otherwise.

Analysis carried out by JA Gomez-Sanchez.

3.2.9 c-Jun elevation in OE/+ and OE/OE nerves down-regulates the expression of Krox20 and Mpz in WT nerves at P60

As previously mentioned, c-Jun in Schwann cells is an important negative regulator of myelination, and results so far strongly support this idea. In development an important driver of myelination, Krox20, was mildly down-regulated in Schwann cells in the presence of elevated levels of c-Jun seen in OE/+ and OE/OE nerves, as confirmed by immunofluorescence experiments (Figures 3.6). With this is mind, Krox20 levels were also analysed in P60 WT, OE/+ and OE/OE nerves to determine whether or not c-Jun elevation in Schwann cells still had a negative effect on this pro-myelin factor. Immunofluorescence images in Figure 3.13A from longitudinal nerve sections show that although c-Jun is still elevated in OE/+ nerves compared to WT, these levels do not seem to be enough to result in a down-regulation of Krox20 expression. Although this result is not quantified, it matches Western blot analysis of WT and OE/+ nerves shown in Figure 3.13B-C, which also suggest that Krox20 levels are very similar. However, in contrast to this, (seen both in Figure 3.13A immunofluorescence images, and later confirmed by Western blot analysis in Figure 3.13B-C), Krox20 expression in OE/OE nerve Schwann cells is significantly down-regulated. This suggests that in mature P60 WT and OE/+ nerves, c-Jun does not seem to have a negative effect on Krox20, and therefore myelination. Yet, in OE/OE nerves, the c-Jun elevation present in these Schwann cells is 19 fold compared to WT (Figure 3.10B), which is enough to down-regulate Krox20 expression. In order to confirm the effects of c-Jun elevation in Schwann cells on Krox20 expression, an immunofluorescence experiment would need to be carried out where individual myelinated fibres would be immunolabelled with myelin basic protein (MBP) and Krox20 in order to decipher how much Krox20 was present in myelinated fibres.

An important component of myelin sheaths that insulate axons is Mpz. Levels of Mpz in OE/OE nerves were shown to be down-regulated in development compared to WT, and in OE/+ nerves where these levels did not seem to be very different (Figure 3.8). As expected, Western blot analysis of protein extract from WT, OE/+ and OE/OE nerves shown in Figure 3.13D-E, clearly demonstrate that Mpz levels are unaltered between WT and OE/+ nerves, regardless of c-Jun elevation being maintained, yet, in

OE/OE nerves, there is a significant down-regulation in Mpz expression compared to WT. This down-regulation of Mpz in OE/OE nerves compared to WT is expected due to the fact that in OE/OE nerves there are fewer myelin sheaths present. This decrease is of significance as is shown in Figure 3.13D-E.

On one hand these results indicate that at P60 where c-Jun elevation is still maintained to a higher degree in OE/+ nerves compared to WT, these levels are not high enough to affect expression of Krox20 nor Mpz. On the other hand, as was suggested in development, c-Jun elevation present in P60 OE/OE nerves appear to strongly down-regulate expression of Krox20 and therefore Mpz, compared to WT levels. This indicates that levels of c-Jun in Schwann cells as high as those in OE/OE nerves, may continue to impair nerve function.

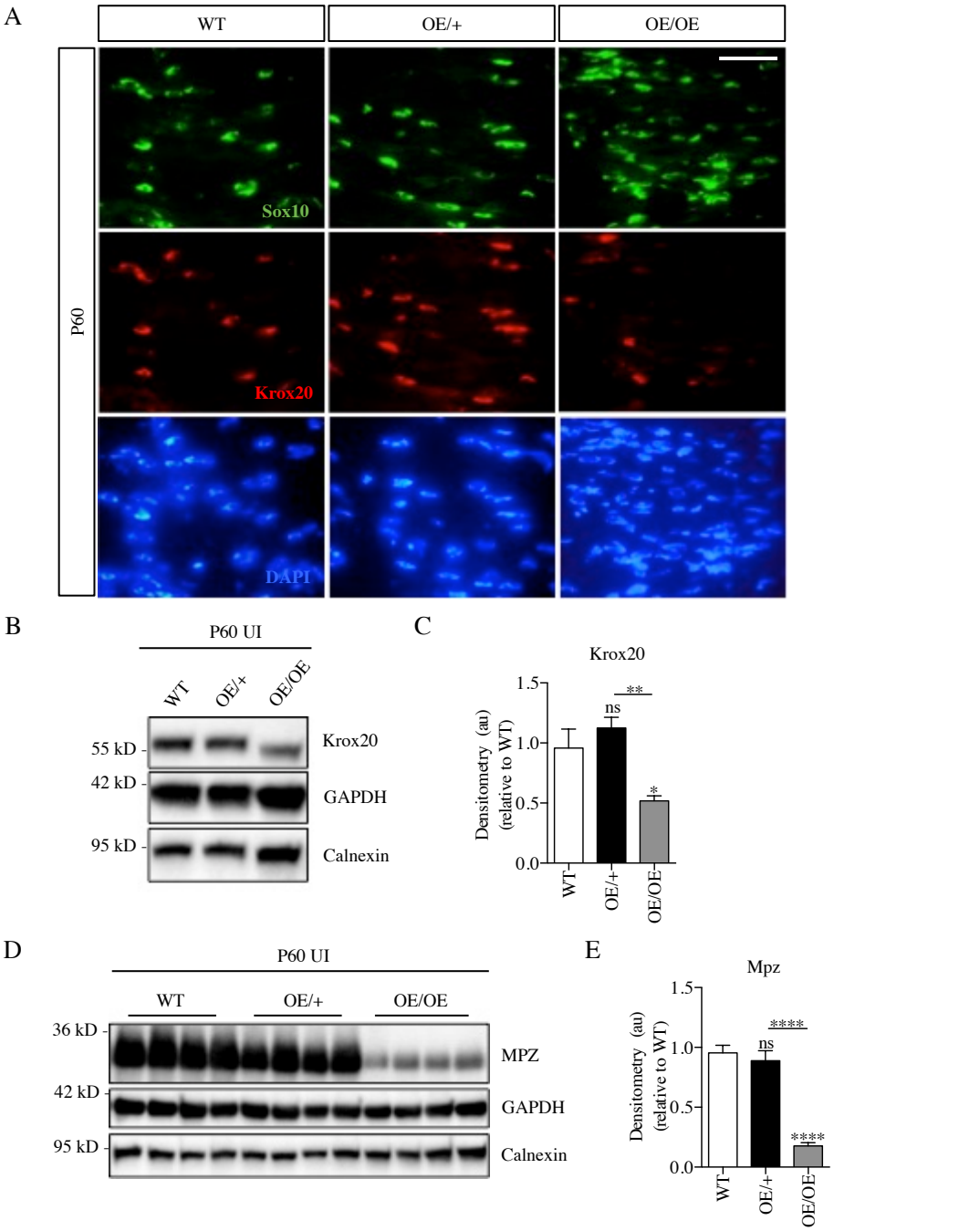

Figure 3.13 | High levels of c-Jun overexpression in Schwann cells cause down-regulation of positive regulators of myelination and myelin proteins

(A) Representative immunofluorescence images taken at x63 magnification show the different levels of Krox20 expression in Schwann cells at P60 in uninjured nerves of WT, OE/+ and OE/OE nerves. Longitudinal sections of P60 sciatic nerves were immunolabelled with Sox10 (Schwann cell marker) and Krox20 (marker of myelination) antibodies and with DAPI to label nuclei. Scale bar represents 25µm. (B) Representative Western blot image of nerve extracts from P60 WT, OE/+ and OE/OE nerves to show the levels of Krox20 expression. GAPDH and calnexin are used as reference genes. (C) Graph to quantify Krox20 levels of OE/+ and OE/OE nerves at P60 relative to WT. Krox20 was normalised to calnexin and GAPDH, and then expressed as a fold change relative to WT. WT (n=5), OE/+ (n=4) and OE/OE (n=5); One-way ANOVA with Tukey comparison, $p<0.0001$. (D) Representative Western blot image of nerve extracts from P60 WT, OE/+ and OE/OE nerves to show the levels of Mpz expression. Mpz is used to show how a myelin-related protein is affected by increased levels of transgenic c-Jun. GAPDH and calnexin are used as reference genes. (E) Graph to quantify Mpz levels of OE/+ and OE/OE nerves at P60 relative to WT. Mpz was normalised to calnexin and GAPDH, and then expressed as a fold change relative to WT. One-way ANOVA with Tukey comparison, $p<0.0001$. All statistical analysis is represented relative to WT unless shown otherwise.

3.2.10 c-Jun elevation in OE/OE nerves causes more cell proliferation compared to WT and OE/+ nerves at P60

In development, there was some evidence to suggest that Schwann cells in OE/OE nerves that express very high levels of c-Jun would continue to proliferate. Yet in OE/+ nerves, although there seemed to be a slight increase in cell proliferation, this never reached significance (Figure 3.9). A similar outcome is seen at P60 in WT, OE/+ and OE/OE nerves (Figure 3.14). Western blot analysis of protein extracts from WT, OE/+ and OE/OE nerves indicates strong expression of Cyclin D1 compared to both WT and OE/+, which is of statistical significance (Figure 3.14A-B). There is a 3.5 fold increase in Cyclin D1 expression in OE/OE nerves, compared to WT. This suggests that cells are still proliferating in OE/OE nerves, but not significantly so in OE/+ nerves.

To determine whether it was specifically Schwann cells that were proliferating in P60 OE/OE nerves, transverse cryosections of WT, OE/+ and OE/OE nerves were fluorescently immunolabelled with another proliferation marker Ki67 and Sox10 to identify Schwann cells, with DAPI to label nuclei. Quantification from these immunofluorescence images (shown in Figure 3.14C), showed that there was a significant elevation in Schwann cells of OE/OE nerves expressing Ki67 at 2.6% compared to OE/+ at 1.6% and WT at 0.7% (Figure 3.14D). Although there was a slight elevation in OE/+ Schwann cell proliferation, similar to that of the Western blot in Figure 3.14, this did not reach significance. Therefore, the results from both Western blot and immunofluorescence analysis using two different markers of proliferation, lean towards the fact that in OE/OE nerves, cells are continuously proliferating, in particular Schwann cells. High levels of Schwann cell c-Jun such as those seen in OE/OE nerves, continue to drive cell proliferation.

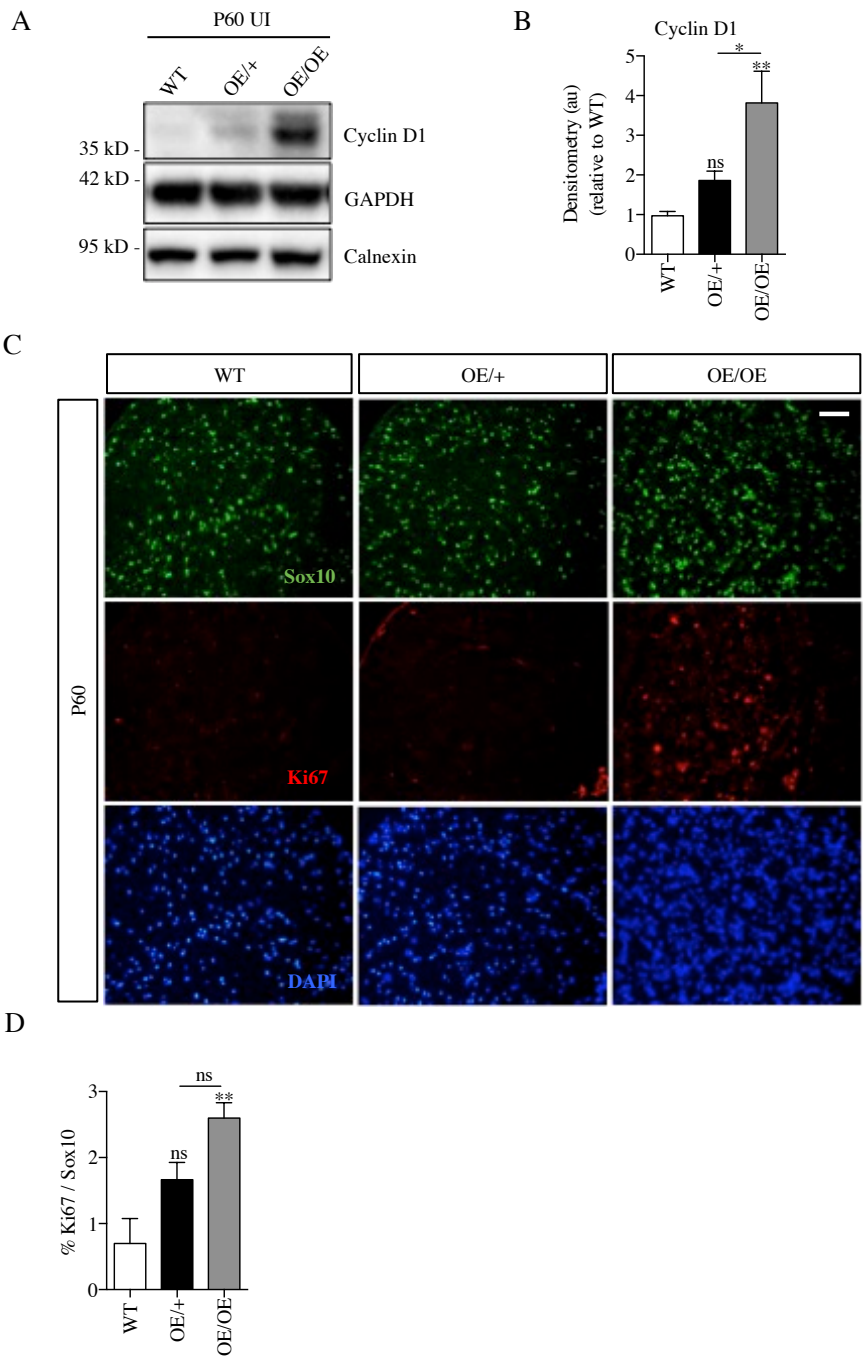

Figure 3.14 | High levels of c-Jun overexpression in Schwann cells causes proliferation of cells in OE/+ and OE/OE nerves at P60

(A) Representative Western blot image of nerve extracts from P60 WT, OE/+ and OE/OE nerves to show the levels of Cyclin D1 expression. Cyclin D1 is used as a marker for cell proliferation and how these levels are affected by increased levels of transgenic c-Jun. GAPDH and calnexin are used as reference genes. (B) Graph to quantify Cyclin D1 levels of OE/+ and OE/OE nerves at P60 relative to WT. Cyclin D1 was normalised to calnexin and GAPDH, and then expressed as a fold change relative to WT. WT (n=4) and OE/+ (n=4) and OE/OE (n=4); One-way ANOVA with Tukey comparison, p=0.0071. (C) Representative immunofluorescence images taken at x25 magnification show the different levels of Ki67 expression in Schwann cells at P60 in uninjured WT, OE/+ and OE/OE nerves. Transverse sections of P60 sciatic nerves were immunolabelled with Sox10 (Schwann cell marker) and Ki67 (marker of proliferating cells) antibodies and with DAPI to label nuclei. Scale bar represents 50μm. (D) Graph to quantify the percentage of Ki67/ Sox10 positive cells in WT, OE/+ and OE/OE P60 uninjured nerves. WT (n=3), OE/+ (n=3) and OE/OE (n=5); One-way ANOVA with Tukey comparison, p=0.0042. All statistical analysis is represented relative to WT unless shown otherwise.

3.2.11 c-Jun elevation in OE/OE nerves results in early formation of onion bulbs and increased collagen

The extracellular matrix and its components including collagen form a complex matrix network in which axons and supportive cells are found. It is critical in several cell functions such as proliferation, migration and differentiation. It also provides mechanical and structural support (Gonzalez-Perez et al., 2013).

Previous results shown in this chapter have strongly indicated that cell proliferation is increased in OE/OE nerves (Figure 3.14). There was also a strikingly visible increase in OE/OE nerve size upon dissection (Figure 3.11). It was therefore of interest to see whether or not any of these noticeable changes had any effect on the extracellular matrix. In order to answer this question, electron microscope images from P60 WT, OE/+ and OE/OE nerves (Figure 3.15A) were analysed using ImageJ software to determine the percentage of extracellular matrix present within each nerve, quantified as shown in the green highlighted images in Figure 3.15A. From the quantification shown in Figure 3.15B, it is evident that c-Jun elevation in Schwann cells present in OE/OE nerves, is enough to cause abnormalities in these nerves, including an increase in the amount of extracellular matrix. There is a significantly higher percentage of extracellular matrix in OE/OE nerves at 54% compared to WT (13%) and OE/+ (20%). This could be a possible explanation for the visible nerve size increase seen in OE/OE mice compared to both WT and OE/+ (Figure 3.15).

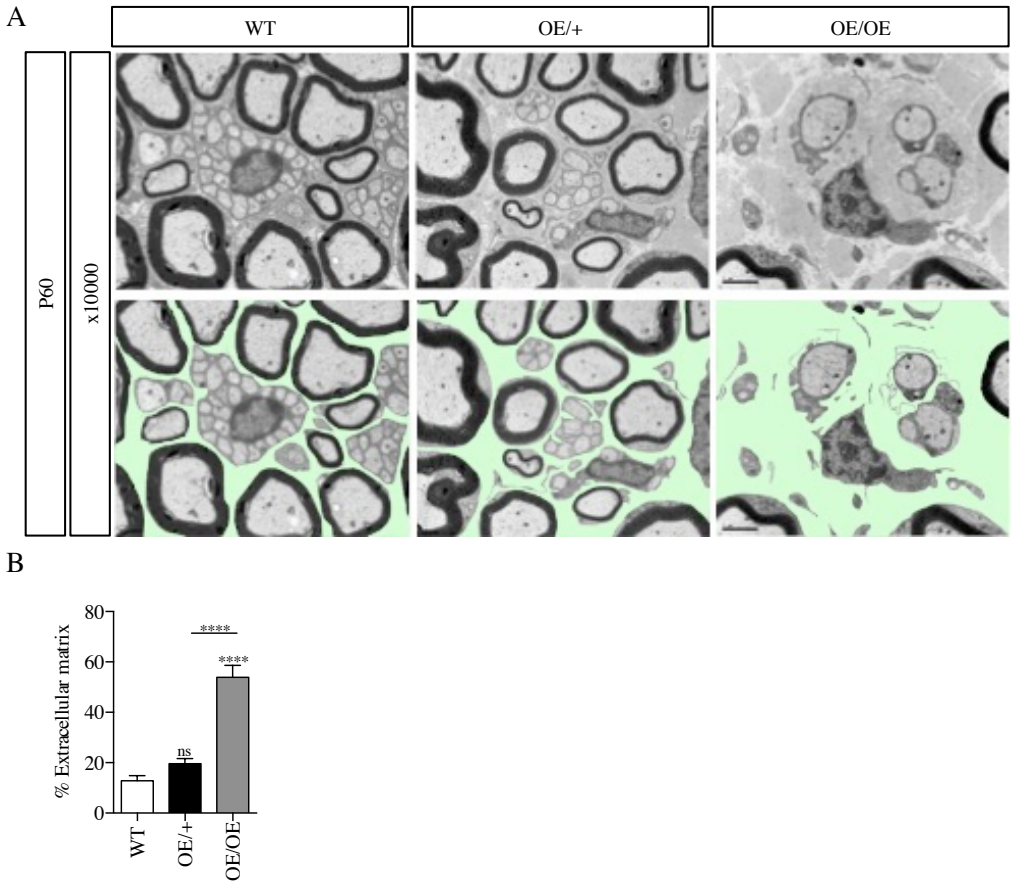

Figure 3.15 | Overexpression of Schwann cell c-Jun substantially increases the amount of extracellular matrix within the nerve of OE/OE mice

(A) Representative electron microscopy images taken at x10000 magnification to show more detail of the ultrastructure of WT, OE/+ and OE/OE nerves at P60. In particular these images highlight the increase in extracellular matrix with progressively high expression of Schwann cell c-Jun. Scale bar represents 1µm. The panels below (A) show the same electron microscopy images to highlight (green) how the % extracellular matrix was determined. (B) Graph to quantify the percentage of extracellular matrix present in WT, OE/+ and OE/OE uninjured nerves at P60, per nerve profile. WT (n=5), OE/+ (n=5) and OE/OE (n=3); One-way ANOVA with Tukey comparison, $p<0.0001$. All statistical analysis is represented relative to WT unless shown otherwise.

Another prominent feature of OE/OE nerves to the eye with x20000 magnified electron microscopy images shown in Figure 3.16A, is the presence of the early formation of onion bulbs. Onion bulbs are formed by concentric layers of Schwann cell cytoplasm around myelinated or non-myelinated axons, usually visible in peripheral nerve neuropathies (Sereda et al., 1996; Naba et al., 2000).

Unregulated, increased cell proliferation can result in tumour formation with a potentially malignant outcome. c-Jun is a known oncogene associated with increased cell proliferation in other tissues (Vleugel et al., 2006). Cell cycle progression is controlled by many regulatory signalling networks, one of them being the RAS-RAF-MEK-ERK pathway (Samatar and Poulikakos, 2014). Results presented so far show that cell proliferation, as determined by the two different markers (Cyclin D1 and Ki67) of proliferation, is significantly increased in OE/OE nerves that have substantially high levels of c-Jun elevation in Schwann cells (Figures 3.9 and 3.14) compared to WT nerves. To this effect, P60 WT, OE/+ and OE/OE nerves were analysed by Western blot to see if ERK was more highly activated (as determined by its phosphorylation), in OE/OE nerves compared to WT and OE/+. The Western blot results in Figure 3.16B-C show an obvious and significant 2 fold increase in ERK phosphorylation in OE/OE nerves compared to both WT and OE/+. This is a strong indication that elevated levels of Schwann cell c-Jun may lead to increased ERK activation, caused by an increase in cell proliferation, or through another mechanism.

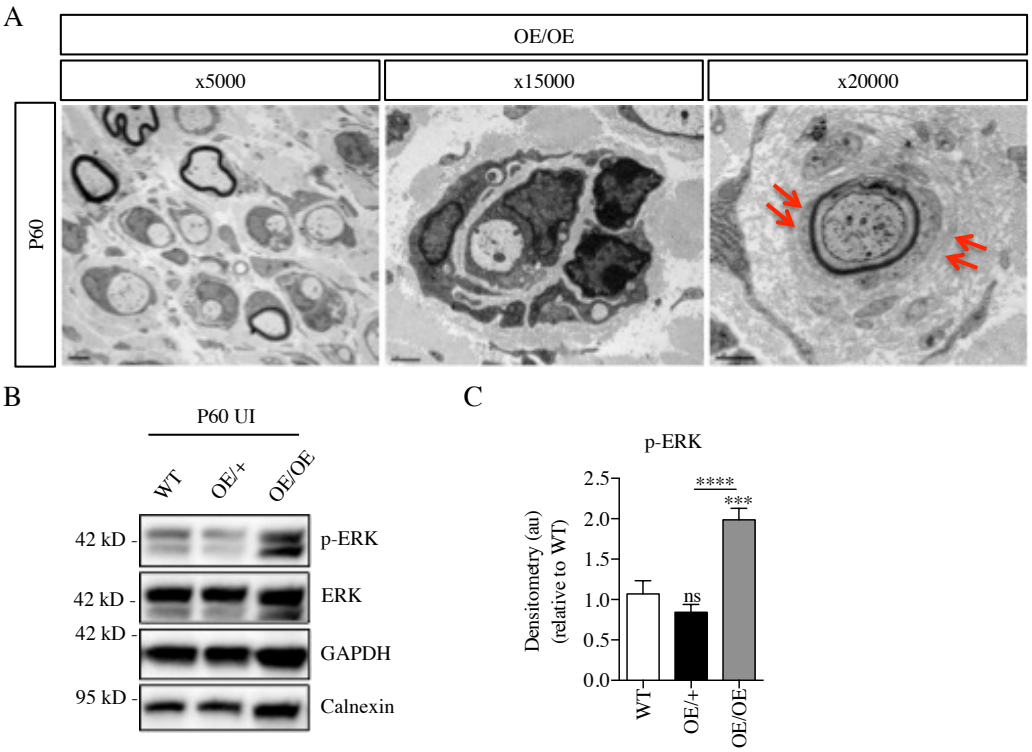

Figure 3.16 | P60 nerves of OE/OE mice show signs of nerve abnormalities reminiscent of peripheral nerve neuropathies

(A) Enlarged representative electron microscopy images taken at various magnifications to show more greater detail of some of the abnormalities seen in uninjured P60 OE/OE nerves. x5000 (Scale bar represents 2µm), x15000 and x20000 (Scale bar represents 1µm). Concentric layers of Schwann cell cytoplasm are highlighted by the red arrows. (B) Representative Western blot images of P60 WT, OE/+ and OE/OE protein extract to show levels of p-ERK. Western blots were probed with p-ERK, ERK, GAPDH and calnexin. GAPDH and calnexin were used as loading controls. Blots were normalised to ERK and then expressed as a fold change relative to WT. (D) Graph to show the fold elevation of p-ERK relative to WT levels. WT (n=3), OE/+ (n=4) and OE/OE (n=4); One-way ANOVA with Tukey comparison, $p<0.0001$. All statistical analysis is compared to WT, unless otherwise shown.

3.3 Discussion

The results presented in this chapter show that the new c-Jun overexpressing mouse, bred to create a model for elevating c-Jun only in Schwann cells in a gene-dose dependent manner, has been achieved successfully. Particularly what needs to be highlighted is the fact that this c-Jun elevation is seen specifically in Schwann cells (Figures 3.1 and 3.10) and the gene-dose dependent manner of its elevation compared to WT levels, is maintained from early on postnatally (P1-P7) (Figure 3.1) and maintained into adulthood (P60) (Figure 3.10).

Increases in cell proliferation (Schwann cells alike) shown in Figures 3.9C-E and 3.14C-D indicate that it may be of interest to see if later on into the mouse's life span, Schwann cells present in OE/OE mice still continue to proliferate, or if they cease to do so. If cell proliferation from early on in development (P7) is still continuing into adulthood (P60) and already causes such evident modifications in nerve architecture and function, this could suggest that cell proliferation even later into the lifespan of the mouse may result in the formation of possible tumours, as c-Jun is also an oncogene (Vleugel et al., 2006; Gomez-Sanchez et al., 2013).

In summary, morphometric analysis of electron microscopy images at P1, P7, P21 and P60 (Figures 3.3-3.5 and 3.11-3.12), showed that in OE/+ mice, myelination was transiently delayed at P7 specifically, even though it seemed almost normal at P1 and P21. By P60, WT and OE/+ nerves were almost indistinguishable, apart from the difference in myelin sheath thickness (Figure 3.12J). In contrast to this, in OE/OE mice, myelination was severely impaired from P7 onwards, even into adulthood, where the abnormal nerve phenotype was more exaggerated (Figures 3.4-3.5 and 3.11-3.12). As expected, this is a strong *in vivo* proof of the previous *in vitro* work showing the importance of c-Jun in Schwann cells as a negative regulator of myelination (Jessen and Mirsky, 2008; Parkinson et al., 2008; Arthur-Farraj et al., 2012;).

A question that arises from the work presented in this chapter is whether or not levels of c-Jun in OE/OE nerves continue to increase after P60, or if levels begin to decline

as the mouse gets older, similar to that seen in WT ageing mice (Painter et al., 2014). This experiment could be carried out using P60 WT and OE/OE mice as "young" and P300 WT and OE/OE mice as "old" to determine whether or not c-Jun levels also decrease in old mice, regardless of the fact they already have elevated levels of Schwann cell c-Jun.

The lack of correlation between immunofluorescence and Western blot results regarding Krox20 expression, may be due to the fact that in immunofluorescent labelling it is possible to determine Schwann cell nuclei specifically and therefore Krox20 nuclear expression, whereas in Western blot analysis, both nuclear and cytoplasmic expression is detected. These differences between immunofluorescence and Western blot analysis may indicate a possible further role that c-Jun has of determining nuclear localisation of Krox20, however this is highly speculative and has not been addressed in this thesis. An alternative way of determining the extent of the effect of c-Jun overexpression in Schwann cells on Krox20 expression, would be to carry out immunofluorescence and Western blot analysis at other postnatal time points such as P1 and P21 and compare these results with those seen at P7. This premise is not addressed in this thesis.
The lack of down-regulation of Krox20 seen in OE/+ nerves compared to WT (Figure 3.13) would suggest that c-Jun does not affect myelin protein expression in nerves. However, it is important to note, that the conclusions drawn from results in Figure 3.13 do stand true, due to the fact that although myelin sheaths in OE/+ nerves are thinner, the presence of myelin sheaths around axons, means that Krox20 is still able to have a pro-myelin effect in OE/+ nerves at P60.

Results in this chapter have shown, most notably in Figures 3.11 and 3.12, that regardless of the c-Jun fold elevation seen in Schwann cells of OE/+ mice, these nerves seem to develop normally, similarly to WT. This is the first crucial piece of evidence that makes this mouse model so useful in studying c-Jun elevation in Schwann cells in an uninjured, but also injured situation.

The activation of ERK as determined by its phosphorylation has also been strongly implicated in models of both inherited and infectious neuropathies (Tapinos et al.,

2006; Fischer et al., 2008; Nadra et al., 2008; Napoli et al., 2012), therefore suggesting that if at P60 some onion bulbs in early formation are already visible, they are likely to become more complex later on and hence a peripheral neuropathy can ensue. Upon closer inspection of older P300 OE/OE mouse nerves by electron microscopy, there seem to be more onion bulbs visible, yet they do not seem to have become more advanced in their formation (unpublished observations SV Fazal and JA Gomez-Sanchez).

More ERK activation also occurs in Schwann cell tumours that develop in Neurofibromatosis (NF1) (Napoli et al., 2012; Gomez-Sanchez et al., 2013). With this in mind, OE/OE nerves that showed a clear increase in ERK activation (Figure 3.16B-C) were further analysed at electron microscopy level for the presence of any tumours, as well as at the point of dissection, to see if any tumours were visible as lumps on the nerves, DRGs or spinal cord (Gomez-Sanchez et al., 2013). Both at electron microscopy and anatomical level, neither such tumours, nor any structures reminiscent of tumours were noticed.

The suggested conclusions drawn above regarding ERK signalling have been focused on its elevation in OE/OE nerves particularly and the potential significance of this, however it is also important to remember that ERK activation is involved in many other aspects of Schwann cell biology, including: (i) its activation in Schwann cells at the injury site and throughout the distal stump following nerve injury (Sheu et al., 2000; Harrisingh et al., 2004; Napoli et al., 2012), (ii) its continuous activation which can override the signals that end myelination, where myelin growth is continuous (Sheean et al., 2014; Birchmeier and Bennett, 2016) and (iii) its strongly maintained expression which can result in demyelination (Napoli et al., 2012). These observations highlight the complexity of ERK signalling in various aspects of Schwann cell biology, which have not been addressed in this thesis.

In conclusion, the evidence presented so far would highlight the fact that: (i) c-Jun is a negative regulator of myelination as determined by its elevation in Schwann cells causing a down-regulation of myelin genes, (ii) increased levels of Schwann cell c-Jun increase cell proliferation, (iii) substantial elevation of c-Jun in Schwann cells causes morphogenetic changes to the nerve and its composition, suggesting possible neuropathies later on and (iv) Schwann cells are tolerant of large elevations in c-Jun

levels as shown in OE/+ nerves, which seem to look very similar to WT nerves, therefore providing a potentially useful model for studying the impact of overexpression of c-Jun in Schwann cells in nerve injury and regeneration.

Further observations on P60 WT and OE/+ nerves in injury and regeneration is the subject of the next chapter.

4. The role of elevated Schwann cell c-Jun following nerve injury

4.1 Introduction

With the astounding influence of Schwann cell c-Jun on successful nerve regeneration following injury, it was only natural to enquire further and carry out a series of regeneration assays using the new c-Jun overexpressing mouse (OE/+). The following chapter determines whether or not increased levels of Schwann cell c-Jun following injury induce a faster regenerative programme, and if this elevation of c-Jun in Schwann cells seen following injury, is maintained in OE/+ nerves compared to WT. The characterisation of adult P60 WT and OE/+ nerves shown in Chapter 3, justified the regeneration studies *in vivo* using a mouse model that elevates c-Jun in a gene-dose dependent manner specifically in Schwann cells.

Schwann cell c-Jun is an important regulator of the injury response, triggering crucial events that need to take place to create the repair Bungner Schwann cells that favour successful nerve regeneration (Arthur-Farraj et al., 2012; Jessen et al., 2015; Jessen and Mirsky, 2016). From regeneration experiments conducted in mice that conditionally lack Schwann cell c-Jun (cKO), the importance of c-Jun in Schwann cells for nerve regeneration became evident. Following nerve crush injury, it became clear, that in mice lacking Schwann cell c-Jun, functional recovery assays (as defined by sensory and motor tests) that include: (i) toe pinch assay, (ii) toe spread reflex and (iii) SFI analysis, were all significantly delayed compared to WT (Arthur-Farraj et al., 2012).

As c-Jun is a key amplifier of the repair Schwann cell phenotype, increasing its levels in Schwann cells might be an appropriate approach for improving nerve repair and testing whether or not functional recovery is faster. To test this hypothesis, regeneration studies were carried out in P60 WT and OE/+ mice using a nerve crush injury model as described in Chapter 2, section 2.3.2.2. Evidence shown in Chapter 3 clearly highlighted the obvious differences in OE/OE adult nerves compared to both WT and OE/+, therefore making OE/OE mice an unsuitable candidate to study nerve regeneration.

4.2 Results

4.2.1 c-Jun expression remains elevated in OE/+ nerves compared to WT, following nerve injury

As discussed in Chapter 3, the c-Jun overexpressing mouse, OE/+ in particular, which is the focus of this chapter, is a unique *in vivo* model that allows for c-Jun elevation in Schwann cells specifically. This c-Jun overexpression is present in early postnatal development and maintained into adulthood in OE/+ nerves.

To determine whether c-Jun is still elevated in OE/+ nerves compared to WT following nerve injury, injured P60 WT and OE/+ nerves were analysed by Western blot 1D, 7D and 14D following nerve crush. The outcome of this experiment is summarised in Figure 4.1. From the representative Western blot image shown in Figure 4.1A, there is a clear graded increase in c-Jun elevation in WT nerves from uninjured, through to 7D crush where it reaches a peak elevation that appears to be maintained at 14D following crush. c-Jun expression in OE/+ nerves following injury also follows a graded increase from 1D through to 14D post crush, however the elevation seen in these nerves is considerably higher than that seen in WT nerves (Figure 4.1B). From the quantification of the Western blot, the ratio of c-Jun elevation between OE/+ and WT at 1D (3.5 fold) is highest compared to (2 fold) seen at 7D and 14D after crush (Figure 4.1B).

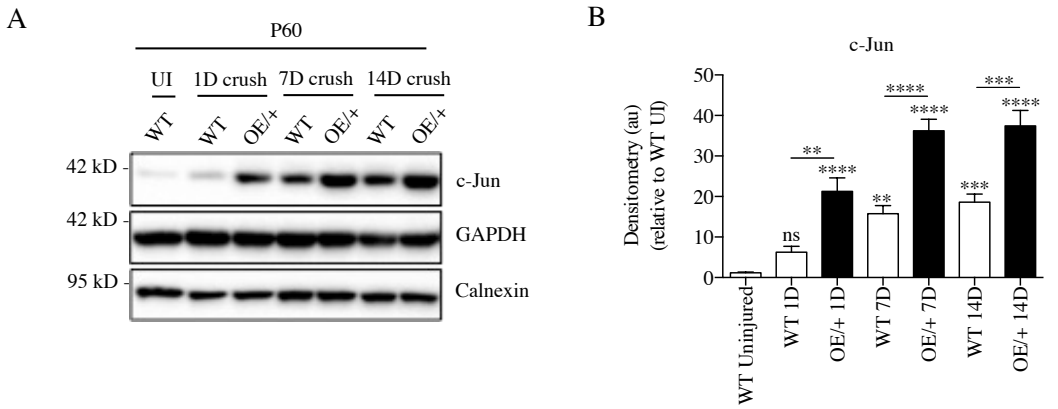

Figure 4.1 | Analysis of c-Jun expression in WT and OE/+ nerves following sciatic nerve crush injury
(A) Representative Western blot image of nerve extracts from WT and OE/+ uninjured, 1D, 7D and 14D crushed nerves to show the levels of c-Jun expression. GAPDH and calnexin are used as reference genes. (B) Graph to quantify c-Jun levels of WT and OE/+ nerves at 1D, 7D and 14D following sciatic nerve crush relative to WT uninjured. c-Jun was normalised to calnexin and GAPDH, and then expressed as a fold change relative to WT uninjured. WT (n=4) and OE/+ (n=4); One-way ANOVA with Tukey comparison, $p<0.0001$. All statistical analysis is represented relative to WT uninjured, unless shown otherwise.

4.2.2 Overexpression of c-Jun in OE/+ nerves results in down-regulation of Krox20 and Mpz compared to WT following nerve injury

An important constituent of myelin sheaths that wrap around axons, is the myelin protein, Mpz. Results described in Chapter 3 highlighted that increased c-Jun expression in Schwann cells, caused a decrease in Mpz expression. Bearing in mind these results, it was therefore interesting to see whether or not Mpz levels were also down-regulated in OE/+ nerves after injury.

As expected, following nerve crush injury in WT nerves, the levels of Mpz expression decrease during the time when severed axons with their associated myelin is broken down through Schwann cell autophagy and macrophage phagocytosis (Gomez-Sanchez et al., 2015), as seen in the representative Western blot and its quantification in Figure 4.2A-B.
In OE/+ nerves, this decrease in Mpz expression from 1D to 14D after crush is also seen, similarly to that in WT nerves. However, in OE/+ nerves, this decrease in Mpz expression is of significance at 7D and 14D after crush where its decrease compared to WT is 2.4 fold and 5 fold, respectively (Figure 4.2B). This suggests that maintenance of c-Jun elevation to very high levels in OE/+ nerves, at different time points following nerve injury (1D-14D, shown in Figure 4.1), is enough to down-regulate Mpz levels to lower levels than that seen in normal WT nerves at these time points (Figure 4.2A-B), which may indicate faster myelin clearance.

These results are in line with work that demonstrated that the lack of c-Jun in Schwann cells results in a delay in myelin clearance through the regulation of Schwann cell autophagy (Gomez-Sanchez et al., 2015).

Another important myelin related gene is Krox20. Results described in Chapter 3 showed that overexpression of c-Jun in Schwann cells results in a significant down-regulation of Krox20 in uninjured nerves. In Western blot analysis shown in Figure 4.2A-B, Mpz levels are not significantly different between WT and OE/+ nerves at 1D after crush, but this difference is more striking at 7D and 14D after nerve injury.

For these reasons, Krox20 levels were analysed by Western blot 7D and 14D after nerve crush in both WT and OE/+ nerves. These results are shown in Figure 4.2C-F. Following nerve injury, c-Jun is up-regulated very highly which results in a down-regulation of Krox20, during the time which axons and their associated myelin are broken down (Arthur-Farraj et al., 2012; Jessen and Mirsky, 2016).

Therefore, in keeping with this reasoning, Krox20 levels were lower in OE/+ nerves than in WT, though this only reached significance at 14D after nerve crush, being only a trend at 7D following crush (Figure 4.2C-F). In uninjured nerves, c-Jun is highly elevated in OE/+ nerves compared to WT. The further increase in these c-Jun levels seen after injury resulted in significantly lower levels of Krox20.

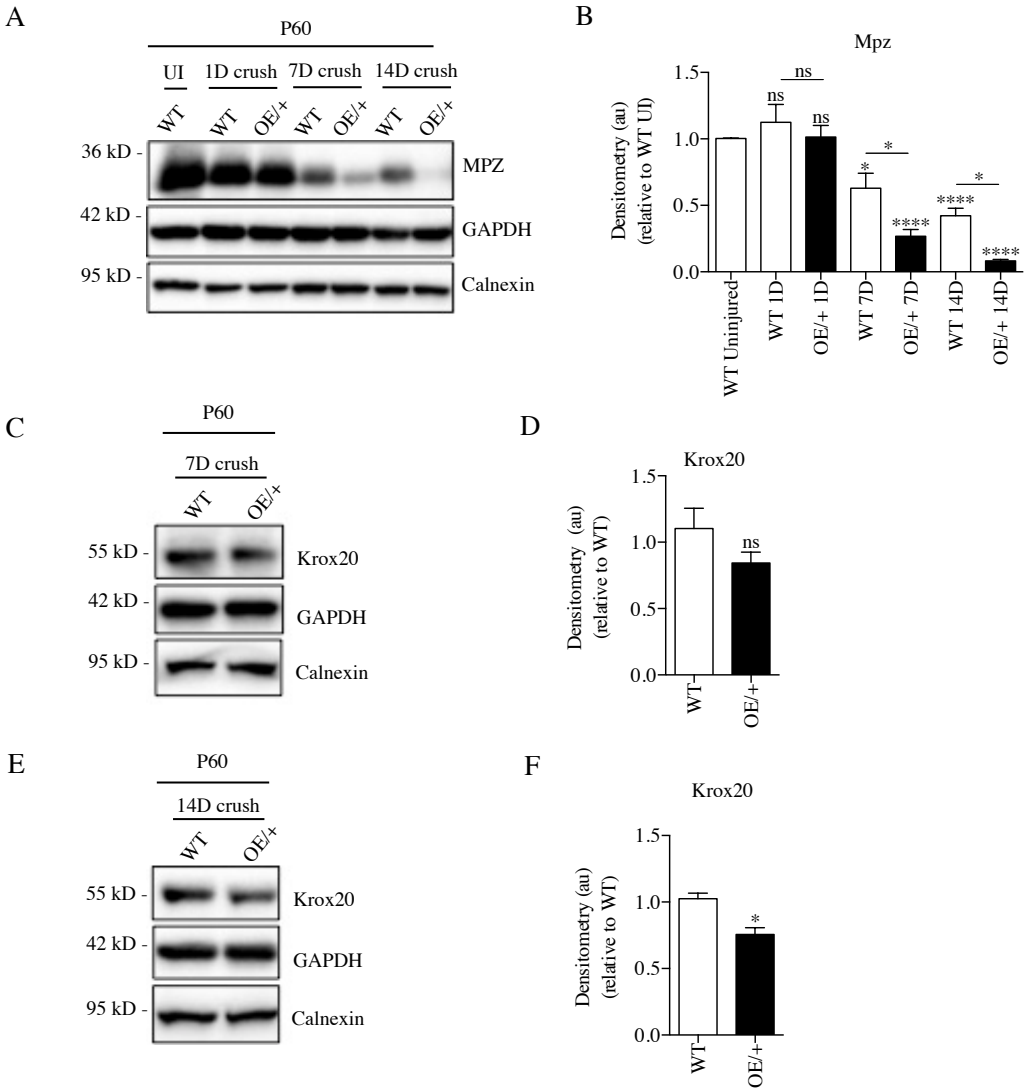

Figure 4.2 | Analysis of Mpz and Krox20 expression in WT and OE/+ nerves following sciatic nerve crush injury
(A) Representative Western blot image of nerve extracts from WT and OE/+ uninjured, 1D, 7D and 14D crushed nerves to show the levels of Mpz expression. Mpz is used to show how a myelin-related protein is affected by increased levels of transgenic c-Jun. GAPDH and calnexin are used as reference genes. (B) Graph to quantify Mpz levels of WT and OE/+ nerves at 1D, 7D and 14D following sciatic nerve crush relative to WT uninjured. Mpz was normalised to calnexin and GAPDH, and then expressed as a fold change relative to WT uninjured. WT (n=4) and OE/+ (n=4); One-way ANOVA with Tukey comparison, $p<0.0001$. (C) Representative Western blot image of nerve extracts from WT and OE/+ 7D crushed nerves to show the levels of Krox20 expression. Krox20 is used as a marker of re-myelination. GAPDH and calnexin are used as reference genes. (D) Graph to quantify Krox20 levels of WT and OE/+ nerves 7D following sciatic nerve crush relative to WT. Krox20 was normalised to calnexin and GAPDH, and then expressed as a fold change relative to WT. WT (n=4) and OE/+ (n=4); Mann Whitney test, $p=0.2900$. (E) Representative Western blot image of nerve extracts from WT and OE/+ 14D crushed nerves to show the levels of Krox20 expression. Krox20 is used as a marker of re-myelination. GAPDH and calnexin are used as reference genes. (F) Graph to quantify Krox20 levels of WT and OE/+ nerves 14D following sciatic nerve crush relative to WT. Krox20 was normalised to calnexin and GAPDH, and then expressed as a fold change relative to WT. WT (n=4) and OE/+ (n=4); Mann Whitney test, $p=0.0286$. All statistical analysis is represented relative to WT.

4.2.3 Re-myelination after injury in OE/+ is delayed compared WT nerves

In order for successful axonal regeneration to occur, the terrain, into which new axons must grow into, needs to be prepared. Schwann cells play a crucial part in this process. Injury induces Schwann cell reprogramming to form a new support cell known as a repair Bungner Schwann cell by: (i) down-regulating myelin genes, (ii) up-regulating trophic factors and cytokines, (iii) clearing myelin debris through the process of myelinophagy (Schwann cells) and phagocytosis (macrophages) and (iv) forming the regeneration tracks known as the bands of Bungner which act as a guide for the regenerating axons to reach their targets (Arthur-Farraj et al., 2012; Gomez-Sanchez et al., 2015; Jessen and Mirsky, 2016).

Prior to sciatic nerve injury, WT and OE/+ nerves were very similar to each other both at macroscopic and microscopic levels (Chapter 3, Figure 3.16). For this reason, the nerve cytoarchitecture of WT and OE/+ nerves following nerve injury was analysed by electron microscopy in a similar way to that of uninjured WT and OE/+ nerves shown in Chapter 3, Figure 3.16.

The time points chosen for electron microscopy analysis were 14D, 28D and 70D following nerve crush, selected on the basis of the different stages through which the re-myelination process takes place following nerve injury. This was to focus more on how elevation of c-Jun in Schwann cells following nerve injury may affect re-myelination.

By 14D following sciatic nerve injury in the mouse, the majority of myelin debris from axonal break down is thought to have been cleared away by Schwann cell mediated autophagy also known as myelinophagy, and phagocytosis through the recruitment of macrophages (Perry et al., 1992; Vargas et al., 2010; Gomez-Sanchez et al., 2015).

Further in depth analysis of WT and OE/+ nerves at electron microscopy level following nerve injury revealed some differences that could be explained by the maintained levels of c-Jun overexpression following nerve injury in OE/+ nerves

(Figure 4.1), and also the down-regulation of myelin-related genes in OE/+ nerves (Figure 4.2). Although several aspects of P60 WT and OE/+ uninjured nerves were very similar (Chapter 3, Figure 3.16), it later becomes apparent that WT and OE/+ nerves do not display the same initial responses to nerve injury. The gross nerve cytoarchitecture shown at x3000 magnification and the finer details shown at a higher magnification in Figure 4.3A, reveals differences between WT and OE/+ nerves 14D following injury in, (i) the number of myelinated axons present, (ii) the increase in extracellular matrix and (iii) increase in large diameter axons that are non-myelinated, seen more prominently in OE/+ nerves compared to WT.

The number of Schwann cell nuclei is statistically significantly higher in OE/+ nerves compared to WT, 906 and 635 respectively (Figure 4.3B). The number of myelinated axons is statistically significantly less in OE/+ (566) compared to WT (3110) (Figure 4.3C). Therefore the same is true for the percentage of myelinated axons in OE/+ (25%) compared to WT (93%) (Figure 4.3D). The number of non-myelinated axons>1.5μm in diameter is significantly higher in OE/+ (1642) nerves compared to WT (225) (Figure 4.3E).

Not surprisingly, this means that the number of non-myelinated axons >1.5μm in diameter (which includes those in a 1:1 relationship with a Schwann cell and those part of a regenerating axon bundle), are all statistically significantly higher in OE/+ nerves compared to WT (Figure 4.3F-G).

The myelin thickness of the myelinated axons present in OE/+ nerves is also substantially thinner compared to WT (Figure 4.3H), which is of statistical significance. The significant decrease in myelin thickness in OE/+ nerves could be due to the lower expression of pro-myelin genes such as Krox20 shown in Figure 4.2C-F. Although the nerve areas of WT and OE/+ mice were similar prior to nerve injury, it was important to see if this similarity was present post nerve injury. The nerve areas between WT and OE/+ 14D following nerve crush were not significantly different at 122694μm^2 and 127933μm^2 respectively (Figure 4.3I).

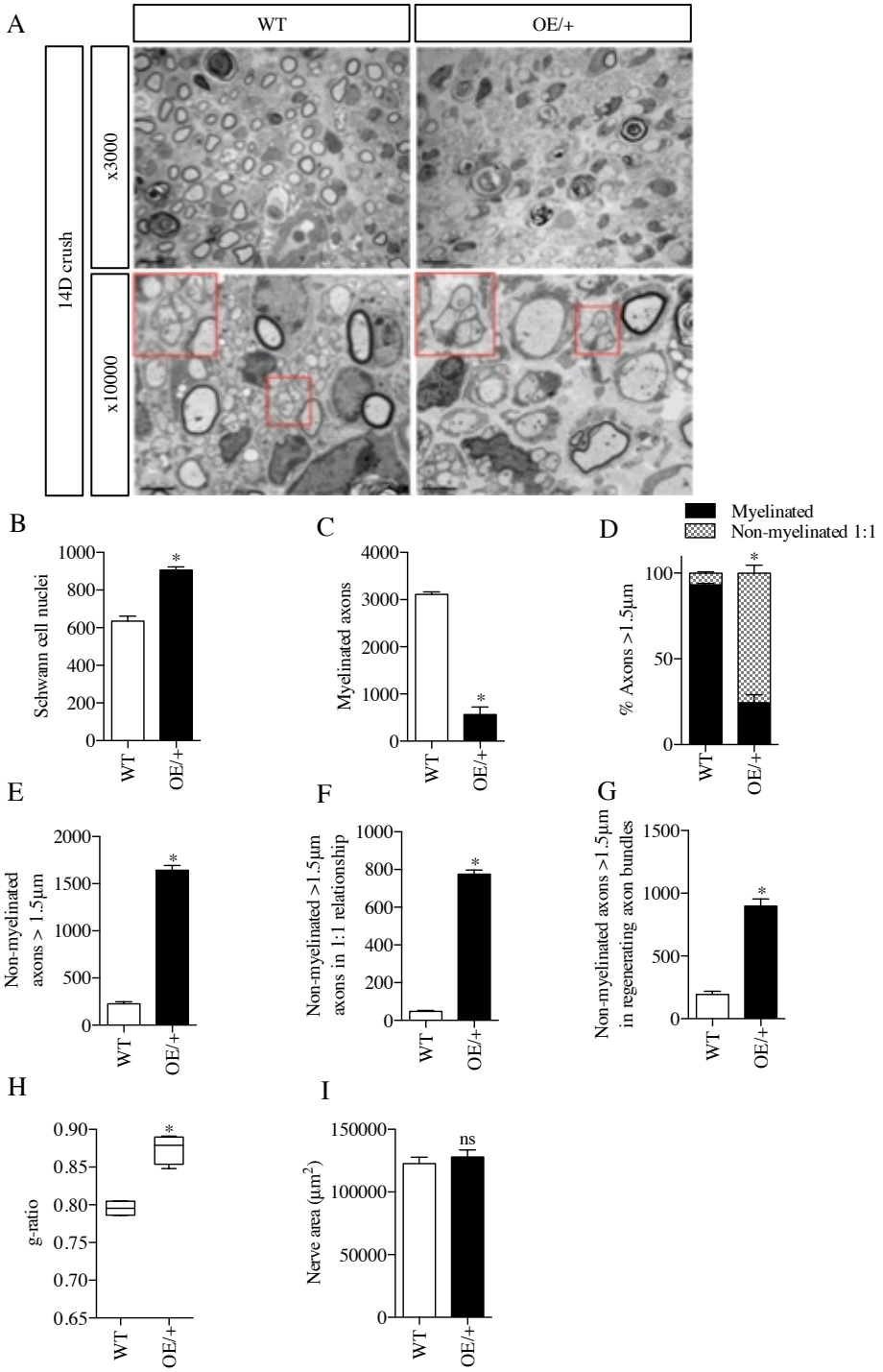

Figure 4.3 | Characterisation of WT and OE/+ 14D following sciatic nerve crush

(A) Representative electron microscopy images taken at x3000 and x10000 magnification to show more detail of the ultrastructure of WT and OE/+ nerves 14D following nerve crush. The red outlines show examples of regenerating axon bundles. Scale bar represents 5µm (x3000) and 1µm (x10000). Graphs shown in panels B-I are all quantified from WT (n=4) and OE/+ (n=4) 14D following nerve crush. An example of a regenerating axon bundle is highlighted in the red boxes in panel A. (B) Graph to quantify the number of Schwann cell nuclei per nerve profile. Mann Whitney test, p=0.0286. (C) Graph to quantify the number of myelinated axons per nerve profile. Mann Whitney test, p=0.0286. (D) Graph to quantify the percentage of myelinated compared to non-myelinated 1:1 axons per nerve profile. Mann Whitney test, p=0.0286. (E) Graph to quantify the number of non-myelinated axons >1.5µm per nerve profile. Mann Whitney test, p=0.0286. (F) Graph to quantify the number of non-myelinated axons >1.5µm that are in a 1:1 relationship per nerve profile. Mann Whitney test, p=0.0286 (G) Graph to quantify the number of non-myelinated axons >1.5µm that are in regenerating axon bundles per nerve profile. Mann Whitney test, p=0.0286. (H) Graph to show the g-ratio of WT and OE/+ nerves. Mann Whitney test, p=0.0286. (I) Graph to show the nerve area of WT and OE/+ mice at 14D after sciatic nerve crush. Mann Whitney test, p=0.6571. All statistical analysis in all graphs is represented relative to WT.
Analysis carried out by JA Gomez-Sanchez.

By 28D following sciatic nerve crush in the WT mouse, the process of re-myelination is normally well underway, by which point some Schwann cells have begun to myelinate newly regenerating axons whilst others remain in close contact with growing axons to provide them with the necessary support needed for correct target re-innervation (Ma et al., 2011; Gaudet at al., 2011; Svennigsen and Dahlin, 2013).

The nerve cytoarchitecture of WT and OE/+ nerves 28D following nerve crush, as depicted by electron microscopy images in Figure 4.4A, highlights some visible differences including fewer myelinated axons, thinner myelin sheaths and more extracellular matrix in OE/+ nerves compared to WT.

Schwann cell nuclei are still very significantly higher in OE/+ (1279) compared to WT (605). This could be in line with the reasoning that in WT nerves, by this point in the re-myelination process, negative regulators of myelination such as c-Jun are suppressed in Schwann cells, whereas, in OE/+ nerves these levels are maintained, hence increasing Schwann cell proliferation (Figure 4.4B).

The total number of myelinated axons quantified in WT and OE/+ nerves at 28D following crush, is overall higher compared to 14D following nerve crush, indicating recovery following nerve injury. More important, however, is the fact that the ratio of myelinated axons between WT and OE/+ at 28D is less than the ratio of myelinated axons between WT and OE/+ at 14D following crush injury. At 28D following nerve crush, the differences in numbers of myelinated axons between WT and OE/+ are 4330 and 2772 (statistically significant) respectively (Figure 4.4C).
The percentage of non-myelinated axons is statistically significantly higher in OE/+ (25%) compared to WT (2%) nerves, and conversely, the percentage of myelinated axons is statistically significantly lower in OE/+ (75%) compared to WT (98%) nerves (Figure 4.4D).
In line with the aforementioned results, the overall numbers of non-myelinated axons >1.5μm in diameter (which includes those in a 1:1 relationship with a Schwann cell and those part of a regenerating axon bundle), are also greater in both WT and OE/+ nerves compared to 14D following crush. However, when comparing the individual ratios 28D following nerve crush of (i) non-myelinated axons (both in 1:1 relationship

with a Schwann cell and in regenerating axon bundles), between WT and OE/+ nerves, it is clear that these are all statistically significantly higher in OE/+ nerves compared to WT (Figure 4.4E-G). Non-myelinated axons are 899 in OE/+ nerves compared to 79 in WT nerves (Figure 4.4E). Non-myelinated axons in 1:1 relationships with Schwann cells or present in regenerating axon bundles are 541 and 308 respectively in OE/+ nerves, compared to 2 and 69 respectively in WT nerves, all differences being statistically significant (Figure 4.4F-G).

Myelin sheath thickness of the fewer myelinated axons present in OE/+ (0.803) nerves still remain significantly thinner compared to WT (0.716) (Figure 4.4H) suggesting negative regulation of pro-myelin genes by c-Jun elevation in Schwann cells.

Similarly to what was seen at 14D post nerve crush, the areas of WT and OE/+ nerves are not significantly different, 132075μm^2 and 139193μm^2, respectively as shown in Figure 4.4I.

The results described in Figure 4.4 suggest a significant recovery in the re-myelination process in OE/+ nerves 28D following nerve injury, though not to the same extent as that of WT nerves.

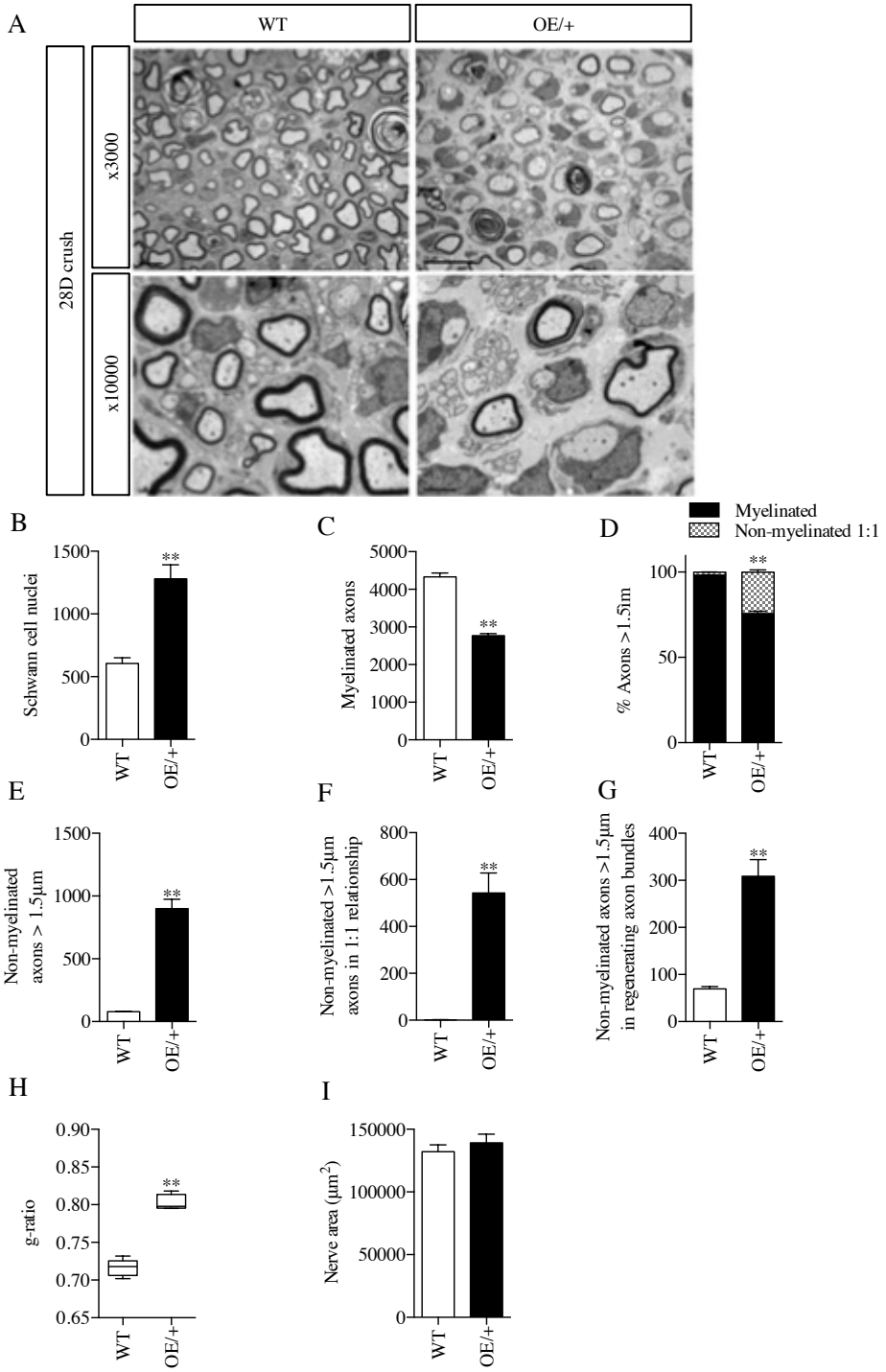

Figure 4.4 | Characterisation of WT and OE/+ 28D following sciatic nerve crush

(A) Representative electron microscopy images taken at x3000 and x10000 magnification to show more detail of the ultrastructure of WT and OE/+ nerves 28D following nerve crush. Scale bar represents 5µm (x3000) and 1µm (x10000). Graphs shown in panels B-I are all quantified from WT (n=5) and OE/+ (n=5) 28D following nerve crush. (B) Graph to quantify the number of Schwann cell nuclei per nerve profile. Mann Whitney test, p=0.0079. (C) Graph to quantify the number of myelinated axons per nerve profile. Mann Whitney test, p=0.0079. (D) Graph to quantify the percentage of myelinated compared to non-myelinated 1:1 axons per nerve profile. Mann Whitney test, p=0.0079. (E) Graph to quantify the number of non-myelinated axons >1.5µm per nerve profile. Mann Whitney test, p=0.0079. (F) Graph to quantify the number of non-myelinated axons >1.5µm that are in a 1:1 relationship per nerve profile. Mann Whitney test, p=0.0079. (G) Graph to quantify the number of non-myelinated axons >1.5µm that are in regenerating axon bundles per nerve profile. Mann Whitney test, p=0.0079. (H) Graph to show the g-ratio of WT and OE/+ nerves. Mann Whitney test, p=0.0079. All statistical analysis in all graphs is represented relative to WT. (I) Graph to show the nerve area of WT and OE/+ mice at 28D after sciatic nerve crush. Mann Whitney test, p=0.3095. .All statistical analysis in all graphs is represented relative to WT.

Analysis carried out by JA Gomez-Sanchez.

By 70D post nerve injury, the nerve cytoarchitecture should therefore be similar to that of uninjured nerves in both WT and OE/+ as re-myelination is complete. For this reason and as was expected, the electron microscope images shown in Figure 4.5A both at x3000 and x10000 magnification, are very similar between WT and OE/+ nerves apart from the presence of slightly fewer myelinated axons, and those that are myelinated, are more thinly myelinated in OE/+ nerves compared to WT.

The number of Schwann cells quantified 70D following nerve crush in WT and OE/+ nerves are significantly different, 427 and 651 respectively (Figure 4.5B). An important comparison to note, however, is that the overall numbers of Schwann cells quantified in both WT and OE/+ nerves are lower at 70D post crush compared to 28D post crush. This result is expected due to the fact that during peripheral nerve regeneration (following nerve crush), similar to what is seen in development (Grinspan et al. 1996; Nakao et al. 1997; Syroid et al. 1996; Yang et al., 2008), excess Schwann cells that are not in contact with axons are removed by apoptosis to ensure the correct ratio between Schwann cells and axons (Yang et al., 2008).

The number of myelinated axons present in WT and OE/+ nerves are not significantly different (Figure 4.5C). To this effect, the percentage of myelinated and non-myelinated axons are also very similar in both WT and OE/+ nerves.
The percentage of myelinated and non-myelinated axons >1.5μm in diameter is similar between WT and OE/+ nerves. The percentage of myelinated axons is 99% in WT compared to 98% in OE/+ nerves, and the inverse is true of non-myelinated axons (Figure 4.5D).
Although the number of non-myelinated axons >1.5μm in diameter (both in a 1:1 relationship with a Schwann cell or in regenerating axon bundles), are not statistically different between WT and OE/+ nerves 70D following nerve crush, they do show a trend towards more non-myelinated axons being present in OE/+ nerves, as shown in Figure 4.5E-G.

Myelin sheath thickness as determined by g-ratio, remains significantly thinner in OE/+ (0.797) nerves compared to WT (0.712) (Figure 4.5H). c-Jun elevation in OE/+

nerves is therefore still having an effect on the thickness of myelin sheaths, suggesting that it still has a negative regulatory effect on pro-myelin signals.

The nerve areas of WT and OE/+ are almost the same, 108829μm^2 and 107572$\mu m^{2,}$ respectively (Figure 4.5I). More importantly however, the nerve cytoarchitecture along with different aspects of the nerve analysed 70D following injury are strongly indicative of the fact that OE/+ nerves regain a very similar morphological phenotype as WT nerves.

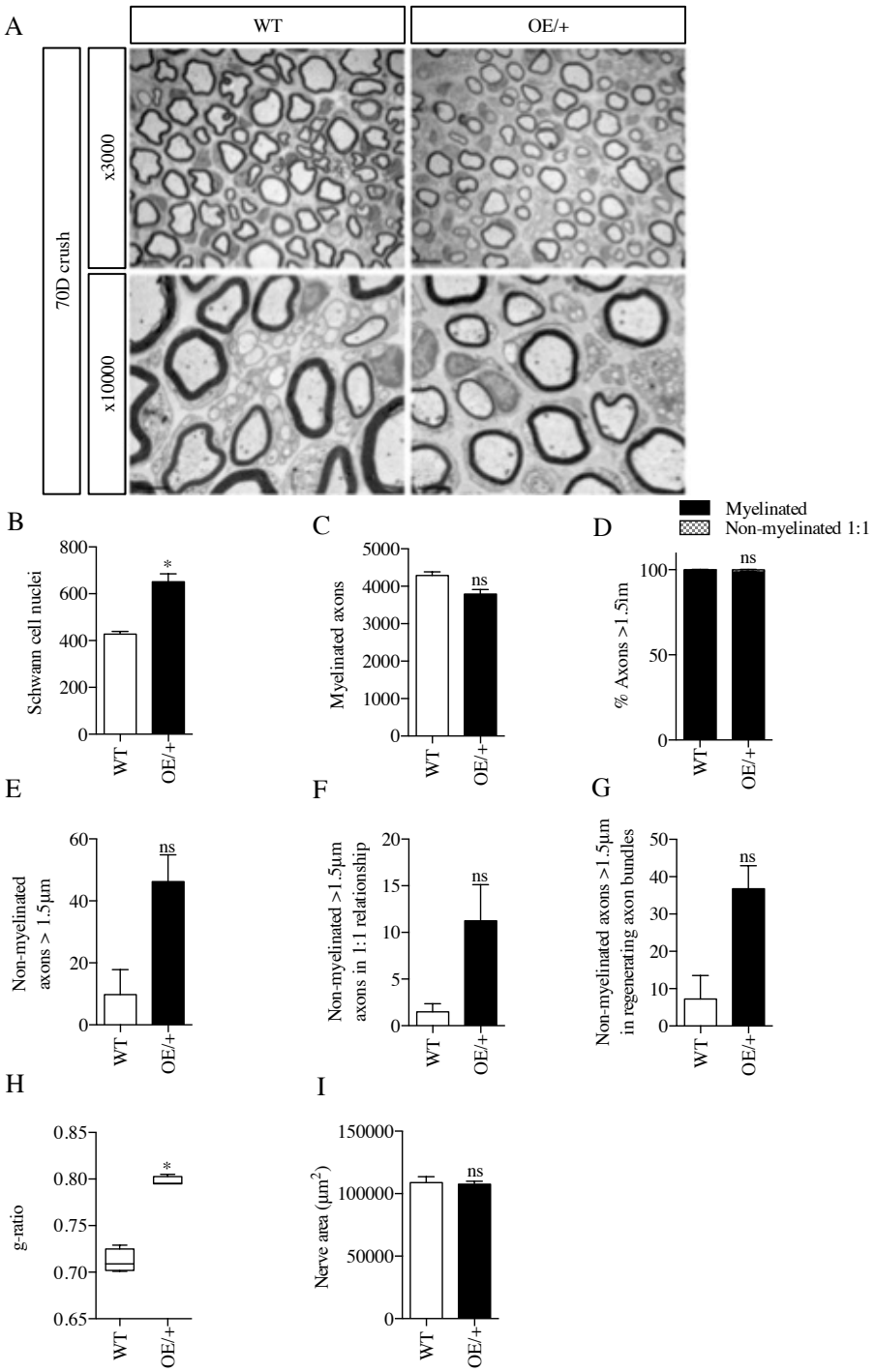

Figure 4.5 | Characterisation of WT and OE/+ 70D following sciatic nerve crush

(A) Representative electron microscopy images taken at x3000 and x10000 magnification to show more detail of the ultrastructure of WT and OE/+ nerves 70D following nerve crush. Scale bar represents 5µm (x3000) and 1µm (x10000). Graphs shown in panels B-I are all quantified from WT (n=6) and OE/+ (n=5) 70D following nerve crush. (B) Graph to quantify the number of Schwann cell nuclei per nerve profile. Mann-Whitney test, p=0.0286. (C) Graph to quantify the number of myelinated axons per nerve profile. Mann-Whitney test, p=0.0571. (D) Graph to quantify the percentage of myelinated compared to non-myelinated 1:1 axons per nerve profile. Mann-Whitney test, p=0.0571. (E) Graph to quantify the number of non-myelinated axons >1.5µm per nerve profile. Mann-Whitney test, p=0.0857. (F) Graph to quantify the number of non-myelinated axons >1.5µm that are in a 1:1 relationship per nerve profile. Mann-Whitney test, p=0.1143. (G) Graph to quantify the number of non-myelinated axons >1.5µm that are in regenerating axon bundles per nerve profile. Mann-Whitney test, p=0.0571. (H) Graph to show the g-ratio of WT and OE/+ nerves. Mann Whitney test, p=0.0286. (I) Graph to show the nerve area of WT and OE/+ mice at 28D after sciatic nerve crush. Mann Whitney test, p=0.9004. All statistical analysis is represented relative to WT.

Analysis carried out by JA Gomez-Sanchez.

4.2.4 Sensory functional recovery is delayed in OE/+ nerves compared to WT following nerve crush injury

The toe pinch assay is a common way to test sensory recovery in mice following nerve injury (Collier et al., 1961; Arthur-Farraj et al., 2012; Painter et al., 2014). The assay is carried out by pinching toes 3, 4 and 5 of the mice individually and observing the response (further details in Chapter 2, section 2.3.3). Sensory nerve conduction is reliant on both non-myelinated and myelinated axons (Schmalbruch, 1986).

The results of this analysis in WT and OE/+ mice is represented in two ways: (i) the percentage of animals of each genotype that showed a response on a particular day post nerve crush injury, and from which toe this response was observed, and (ii) the first day following nerve crush injury where a response was seen from the genotypes of mice studied. These results are shown in Figure 4.6.

In toe 3 a small percentage (25%) of WT mice showed a response to a toe pinch by day 15 post injury, compared to day 17 in OE/+ (Figure 4.6A). When taking into account the average time in days per genotype where a response to toe pinch (on toe 3) was noted (Figure 4.6B), WT mice responded earlier (day 17) on average compared to OE/+ mice (day 19).

In toe 4, WT and OE/+ responses are seen on day 17 after injury (Figure 4.6C). When considering the average response to toe pinch per genotype, WT mice responded one day earlier compared to OE/+ mice (Figure 4.6D), which is of statistical significance.

Finally, in toe 5, the responses seen to toe pinch were similar to those in toe 3, where WT and OE/+ mice showed responses by day 15 and 17 post surgery respectively (Figure 4.6E). However when taking into account the average response in days per genotype (Figure 4.6F), WT mice responded by day 16 post injury whereas OE/+ mice responded 18 days after injury. This difference is statistically significant.

These results are an indication that OE/+ mice show delayed regain of sensory function compared to WT mice.

The results from the toe pinch assay, a measure of sensory recovery are clear cut yet unexpected given the previous work of Arthur-Farraj et al., 2012. Their work showed that the lack of c-Jun elevation in Schwann cells after injury significantly delayed and impaired regeneration because of slower initial axon outgrowth after injury.

With this in mind, the expected outcome would be that the higher the elevation of Schwann cell c-Jun such as that seen in OE/+ nerves, the faster the recovery compared to WT nerves. However, it is important to note that in OE/+ nerves, evidence is presented showing that re-myelination following injury is retarded compared to WT, therefore making the delay in sensory functional recovery in OE/+ mice, less surprising. The data presented above therefore implies that increased c-Jun expression in Schwann cells alone is not sufficient to result in faster functional recovery.

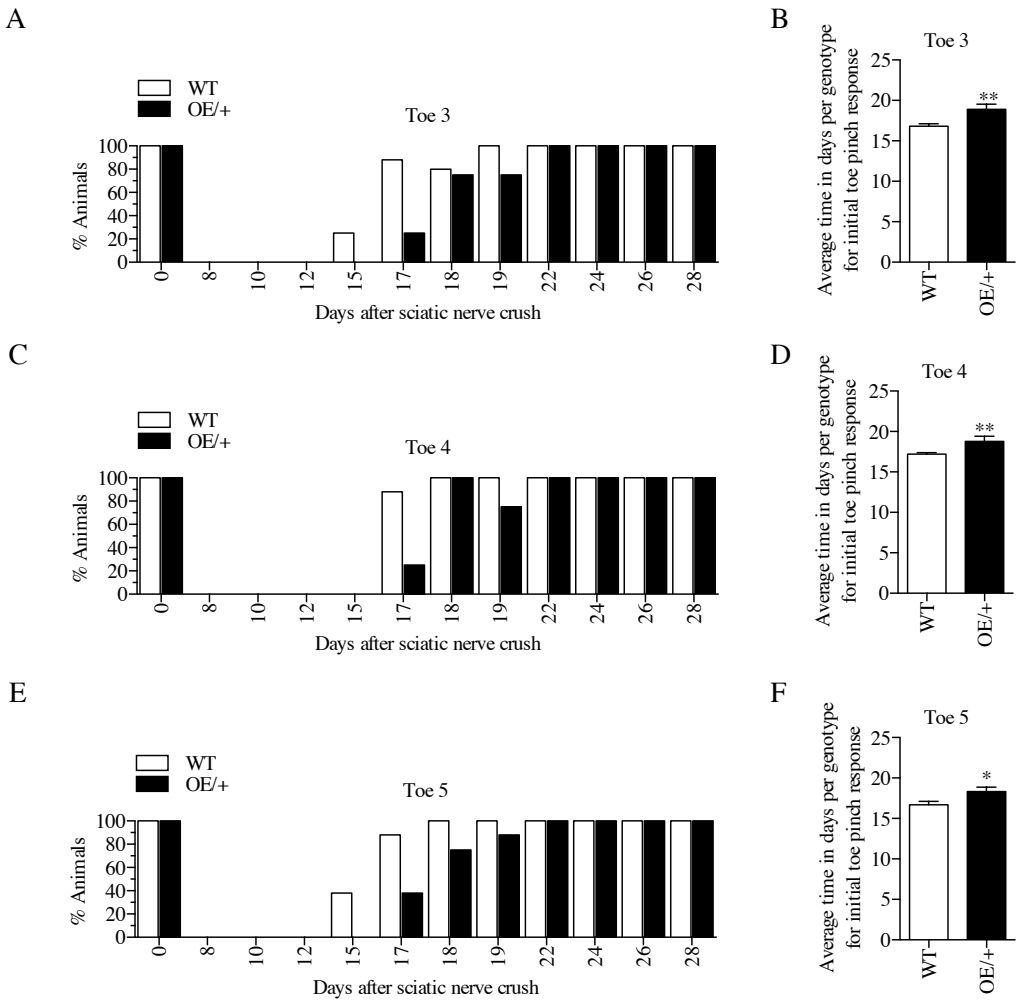

Figure 4.6 | Sensory functional recovery following a crush injury is delayed in OE/+ compared to WT mice
Sensory function following different days post sciatic nerve crush was tested in WT (n=10) and OE/+ (n=9) using the toe pinch assay. (A) Graph to show the percentage of WT and OE/+ mice that responded to a toe pinch test specifically on toe 3. (B) Graph to show the average time in days per genotype for the initial day on which a toe pinch response in toe 3 specifically, is seen in WT and OE/+ mice. Mann-Whitney test, p=0.0056. (C) Graph to show the percentage of WT and OE/+ mice that responded to a toe pinch test specifically on toe 4. (D) Graph to show the average time in days per genotype for the initial day on which a toe pinch response in toe 4 specifically, is seen in WT and OE/+ mice. Mann-Whitney test, p=0.0043. (E) Graph to show the percentage of WT and OE/+ mice that responded to a toe pinch test specifically on toe 5. (F) Graph to show the average time in days per genotype for the initial day on which a toe pinch response in toe 5 specifically, is seen in WT and OE/+ mice. Mann-Whitney test, p=0.0404. All statistical analysis is represented relative to WT unless shown otherwise.

4.2.5 Motor functional recovery is delayed in OE/+ nerves compared to WT following nerve crush injury

A common way to test motor recovery following a sciatic nerve injury is using the toe-spread reflex. Injured mice are analysed as explained in Chapter 2, section 2.3.3 by way of a toe-spread reflex, in response to the mouse being lifted by the tail. This is a measure of motor function as described by Siconolfi et al, 2001. Motor coordination is reliant on large diameter, myelinated axons as these insulated axons conduct nerve impulses very rapidly by a process known as saltatory conduction (Virchow, 1854; Ranvier, 1871).

A graph summarising the toe spread reflex responses seen in WT and OE/+ mice over several days following sciatic nerve crush injury is shown in Figure 4.7A. There is an obvious delay in OE/+ mice spreading their toes to the same extent as WT mice between days 11 and 18 post nerve injury, but by day 21, both WT and OE/+ are fully recovered. This delay in the toe spread reflex of OE/+ mice compared to WT is only of significance at 14 and 15 days post injury.

This difference in response to nerve injury between WT and OE/+ could be due to the elevation of c-Jun in Schwann cells of OE/+ nerves. This maintained increase of c-Jun elevation appears to has an effect on the presence of fewer myelinated axons in OE/+ nerves compared to WT (Figures 4.3C and 4.4C), which is an indication of delayed re-myelination following nerve injury. As motor function is reliant on myelinated axons, the presence of fewer of these axons in OE/+ nerves, whilst those that are present are more thinly myelinated, may provide a reason why OE/+ motor functional recovery is delayed compared to WT.

A

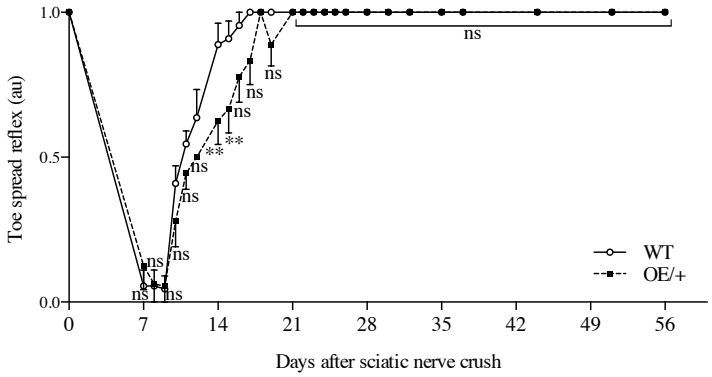

Figure 4.7 | Motor functional recovery following a crush injury is delayed in OE/+ mice compared to WT
Motor function following different days post sciatic nerve crush was tested in WT and OE/+ mice using the toe spread reflex. (A) Graph to show the toe spread reflex of WT and OE/+ mice on different days post sciatic nerve crush. WT (n=10) and OE/+ (n=9); Two-way ANOVA with Bonferroni comparison, $p<0.0001$. All statistical analysis is represented relative to WT.

4.2.6 Following nerve injury, WT and OE/+ mice regain functional recovery as determined by sensory-motor assays

Sciatic functional index (SFI) is a technique used to determine sensory-motor functional recovery following nerve injury. Injured WT and OE/+ mice were made to walk along a wooden track whilst leaving footprints on paper that was later scanned and analysed in the same was as described by Inserra et al.,1998. Typical footprints seen in WT and OE/+ at the most significantly different days following nerve injury are shown in Figure 4.8. It is clear from these representative footprint scanned images taken from WT and OE/+ mice at 0, 7, 18, 21, 28 and 70 days post injury that in OE/+ mice, recovery is seen similar to WT based on the similarities between the footprints over time.

The previous work of Arthur-Farraj et al., 2012 demonstrated that lack of Schwann cell c-Jun was detrimental to successful nerve regeneration. The results presented in Chapter 3 show clearly that the new and novel mouse model has been successfully developed to overexpress Schwann cell c-Jun in a gene-dose dependent manner.
Taking this information into account, it was of interest to see whether elevated levels of c-Jun seen in OE/+ nerves accelerated sensory-motor functional recovery compared to WT.

These results of sensory-motor function are summarised in the graph shown in Figure 4.9A. Full functional recovery as determined by SFI is reached by day 35 post surgery in both WT and OE/+, even though the WT response is faster than OE/+ mice, particularly at day 21, however this is not of statistical significance. Full functional recovery has been determined as and when the SFI has reached the same baseline result seen as at day 0, as this serves as the uninjured control. Although both WT and OE/+ respond similarly to each other to nerve crush injury, as seen between day 0 and day 11, by day 14 post injury, the WT appears to be recovering faster, until day 35 post injury where both WT and OE/+ responses are the same. The responses are then maintained through the duration of the experiment until day 70 post injury.

In summary, the sensory and motor functional recovery assays shown in Figures 4.6-4.9 would suggest that high Schwann cell c-Jun elevation seen in OE/+ mice seems to delay the functional recovery modestly compared to WT.

A

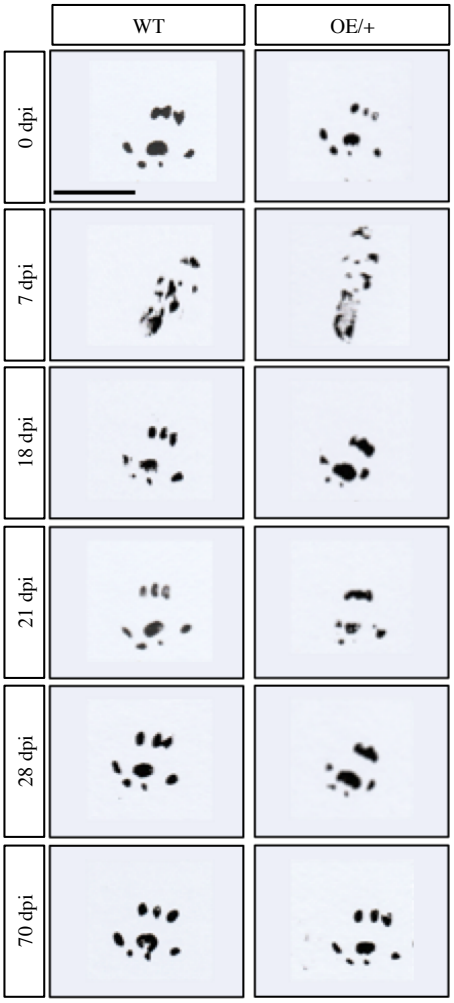

Figure 4.8 | Typical footprints from WT and OE/+ mice following sciatic nerve crush injury
(A) Representative scanned footprint images from WT and OE/+ mice from day 0 (uninjured), 7, 18, 21, 28 and 70 days post injury (dpi). The footprints seen in WT and OE/+ return to normal, comparable to day 0. These were used to analyse the normal toe spread, normal print length, experimental toe spread and experimental toe length. Scale bar represents 1cm.

A

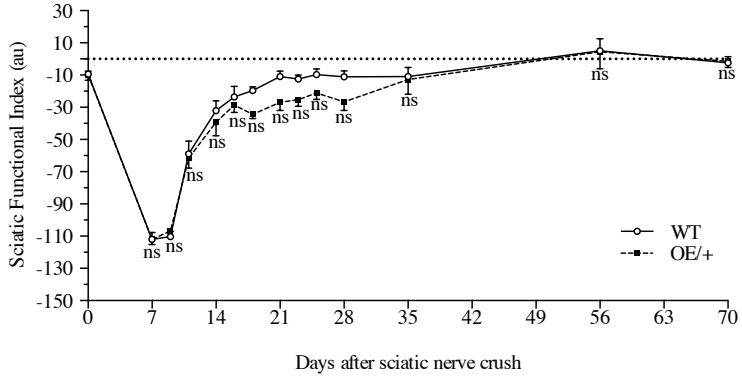

Figure 4.9 | Sensory-motor function was delayed in OE/+ mice compared to WT, following nerve crush injury
Sensory-motor function following different days post sciatic nerve crush was tested in WT and OE/+ mice using the sciatic functional index (SFI). (A) Graph to show how SFI changed over time following nerve crush injury in OE/+ mice compared to WT. WT (n=10) and OE/+ (n=9); Two-way ANOVA with Bonferroni comparison, $p<0.0001$. All statistical analysis is represented relative to WT.

4.3 Discussion

Although Western blot analysis of nerves at 28D and 70D post injury has not been carried out, it is plausible to posit that in the WT at these time points c-Jun levels would have decreased because axons have fully regenerated and begun to myelinate, which suppresses the elevation of c-Jun. However in OE/+ nerves, it is likely that this elevation seen at 14D, would be maintained at 28D and 70D following crush.

An obvious line of enquiry that would be crucial to investigate is the number of macrophages present in OE/+ nerves following injury. Due to the sustained increase in c-Jun expression following nerve injury in OE/+ nerves, and the indication that myelin clearance may be faster in these nerves, it is possible to hypothesise that there would be more macrophages present after injury.

Some evidence presented in this chapter would strongly indicate that myelin clearance might be faster in OE/+ nerves. There is already some pilot data to suggest that myelin clearance is in fact faster in OE/+ nerves following a short term injury as determined by the number of intact myelin rings, which are significantly fewer in OE/+ nerves compared to WT (unpublished observations SV Fazal and JA Gomez-Sanchez). Therefore it would be worth investigating whether or not autophagy specific genes were up-regulated more readily in OE/+ nerves compared to WT, in line with the work published by Gomez-Sanchez et al., 2015.

The results presented in Figures 4.6-4.9 that addressed functional recovery in WT and OE/+ mice using various sensory and motor tests, showed somewhat unexpected results. Bearing in mind the generally accepted role of c-Jun in nerve regeneration, where the lack of its presence in Schwann cells is detrimental to nerve regeneration (Arthur-Farraj et al., 2012), with the corollary of the up-regulation of Schwann cell c-Jun in a gene-dose dependent manner, faster functional recovery might have been expected. This was not seen in OE/+ nerves compared to WT. In hindsight, the modest delay in sensory and motor functional recovery seen in OE/+ mice compared to WT is not as unexpected as originally thought since there is a clear delay in the onset of myelination in the Schwann cells that surround the regenerating axons. It is

important to note, that in OE/+ mice, even though functional recovery is delayed following nerve injury compared to WT, these mice still do regain full functional recovery, comparable to WT. These functional studies suggest therefore, that this new c-Jun overexpressing (OE/+) mouse could be useful in other regeneration studies.

As expected, c-Jun levels remain elevated in OE/+ nerves following injury compared to WT as shown in Figure 4.1. For this reason the OE/+ mouse provides a platform upon which further studies can be carried out in models where c-Jun expression needs to be elevated or maintained. c-Jun expression in Schwann cells is not only down-regulated during normal nerve development, but it also declines in the distal stumps of severed nerves after chronic injury and in aged adult nerves (Parkinson et al., 2008; Painter et al., 2014; Jessen and Mirsky, 2016). In order to study the effects of maintenance of c-Jun levels in both uninjured (to study ageing induced c-Jun decline) nerves and long term injured nerves (where c-Jun normally declines), the OE/+ mouse provides a robust tool in addressing these questions.

Other evidence suggests that OE/+ mice can be useful in assessing the rate of axonal regeneration immediately after nerve injury. After nerve crush injury, when the numbers of regenerating axons are quantified in WT and OE/+ nerves using peptides as markers of regeneration at the short time point of 3D post crush, there are more regenerating axons in OE/+ nerves compared to WT (personal communication JA Gomez-Sanchez). For this reason, it would be interesting to study whether or not OE/+ DRG neurons are able to switch from a "signalling" mode to a "growth" mode more readily compared than WT neurons. This is discussed further in Chapter 6.

An important aspect of the nerve injury response that should be addressed in OE/+ mice is whether or not there is less death of injured neurons. The work of Arthur-Farraj et al., 2012 demonstrated that in mice that had c-Jun conditionally knocked out of their Schwann cells, there was a marked increase in the death of injured DRG neurons. For this reason, it can be hypothesised that if c-Jun levels are elevated in Schwann cells following injury, as seen in the OE/+ mouse, these mice may exhibit less death of injured neurons and c-Jun in this instance would act to prevent neuronal death.

Another obvious line of enquiry would be to look at the number of macrophages present in OE/+ nerves following injury. The increase in Schwann cell numbers in OE/+ nerves, might indicate a higher presence of macrophages in these nerves compared to WT. If there are already more Schwann cells in OE/+ nerves following injury, these would in turn release more Schwann cell-derived chemotactic molecules such as MCP-1 and LIF that attract macrophages (Tofaris et al., 2002).

5. Nerve transection elevates c-Jun expression in proximal stump Schwann cells

5.1 Introduction

As already mentioned, c-Jun is an immediate early gene that is rapidly expressed by Schwann cells after nerve injury (Shy et al., 1996; Parkinson et al., 2004; Raivich et al., 2004). It is widely accepted that c-Jun acts as a global regulator of peripheral nerve injury and highly important in determining the successful reprogramming of Schwann cells into repair Bungner cells which are essential for successful peripheral nerve regeneration after injury (Arthur-Farraj et al., 2012; Jessen et al., 2015; Jessen and Mirsky, 2016). Work so far has focused on c-Jun elevation in distal stump Schwann cells after periods from 1 hour to several days after injury. However little is known about the role of c-Jun levels in Schwann cells of the proximal stump early after nerve injury.

The c-Jun conditional knockout (cKO) mouse model (Behrens et al., 2002; Arthur-Farraj et al., 2012) was used for determining the importance of c-Jun up-regulation in proximal stump Schwann cells after peripheral nerve transection. As explained in Chapter 2 (section 2.2.3), the cKO mouse has c-Jun conditionally knocked out only in Schwann cells when the P_0-Cre transgene activates Cre-mediated recombination between E13.5 and E14.5.
The significance of this early expression of c-Jun in Schwann cells after sciatic nerve transection remains to be explored.

The following chapter is focused on the defining what happens to Schwann cell c-Jun levels in the proximal stump following sciatic nerve transection.

5.2 Results

5.2.1 c-Jun is elevated in proximal stump cells following short-term injury

Sciatic nerve transection elevates levels of c-Jun expression in WT proximal stump cells as early as 1 hour after injury. This is reflected by immunofluorescent labelling of proximal stump tissue of WT mice from the first 6mm of the proximal stump including the injury site (Figure 5.1A). The immunofluorescence images show the different levels of c-Jun expression 1 hour after nerve transection, along different distances of the proximal stump starting from the injury site (0-2mm). It is clear from both the immunofluorescence images and quantification (Figures 5.1A and C) that the injury site has the highest c-Jun expression in proximal stump cells, whereas 1 hour after sciatic nerve transection, the further away from the injury site, the lower the expression of c-Jun in these cells. These levels of c-Jun in WT proximal cells are relative to the very low expression seen in the contralateral uninjured nerve (Figure 5.1B), which is quantified in Figure 5.1C.

It is evident from the quantification that following nerve injury, there is a very strong c-Jun elevation in proximal stump cells as early as 1 hour after the injury, compared to uninjured levels, namely from as little as 7% in the uninjured nerve, to as high as 72% in the first 2mm of the proximal stump (Figure 5.1C). Further away from the injury site at 2-4mm there is also a significant increase in c-Jun expression to 46% compared to the uninjured levels. However at a distance of 4-6mm, this elevation is no longer seen.

These results demonstrate that c-Jun expression in WT proximal cells is very high as early as 1 hour after injury, with the maximal expression being nearest to the injury site. However the further away from the injury site, the lower this level of expression becomes, as summarised in Figure 5.1.

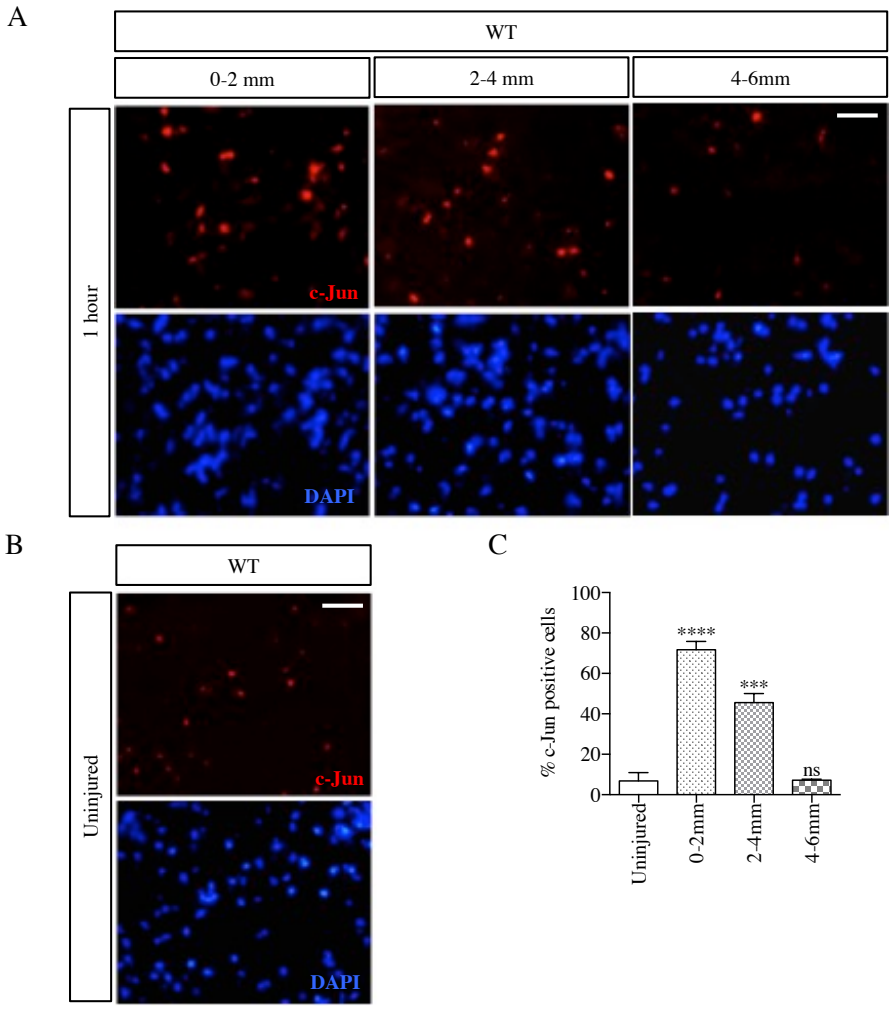

Figure 5.1 | c-Jun expression in proximal stump cells 1 hour after sciatic nerve transection
(A) 5µm thick sciatic nerve cryosections were immunolabelled with c-Jun antibody and with DAPI to label nuclei. Immunofluorescence images taken at x25 magnification showing the population of proximal stump cells expressing c-Jun at different distances along the nerve from the transection site, 1 hour after injury. The proximal stump is divided into three 2mm segments. (B) Immunofluorescence images taken at x25 magnification showing the population of cells expressing c-Jun in a contralateral uninjured WT nerve. The contralateral uninjured nerve is used for comparison. Scale bar represents 50µm. (C) Quantification of the percentage of c-Jun positive cells in the proximal stumps of WT mice 1 hour after nerve transection. WT (n=3) and cKO (n=3), One-way ANOVA with Sidak comparison, $p<0.0001$). All statistical analysis is compared to WT uninjured levels.

c-Jun elevation in WT proximal stump cells is rapid in response to sciatic nerve transection, however is this elevation maintained after longer periods of injury? To address this, the same analysis was carried out as in Figure 5.1 but at 6 hours after sciatic nerve transection. Again, the elevation of c-Jun in proximal stump cells was compared to uninjured levels. 6 hours after sciatic nerve transection, the elevation of c-Jun in proximal stump cells within the first 2mm segment was 63% (Figure 5.2B), which was similar to the percentage of c-Jun expression at this same distance 1 hour after nerve injury (Figure 5.2C). Interestingly, at the 6 hour time point, c-Jun expression in the 2-4mm and 4-6mm segments was also elevated (28% and 29% respectively). This was lower than after 1 hour in the 2-4mm segment, but there was an increase at 4-6mm compared to at 1 hour. The increases in c-Jun expression seen along different distances from the injury site at 6 hours were significantly higher compared to uninjured levels (Figure 5.2).

These current results indicate that c-Jun expression in WT proximal stump cells is very rapid and is not only maintained, but also spreads along cells further from the injury site. Do these cells still express c-Jun as highly as the initial elevation seen at 1 hour in the first 2mm, or at 6 hours in the next 4-6mm, or do these cells reach a maximal elevation which then begins to decline after longer periods following injury? To address this hypothesis, WT sciatic nerves were transected and the mice were allowed to recover for 48 hours before their proximal stumps were analysed in the same way as 1 hour and 6 hours after sciatic nerve transection. These results are shown in Figure 5.3.

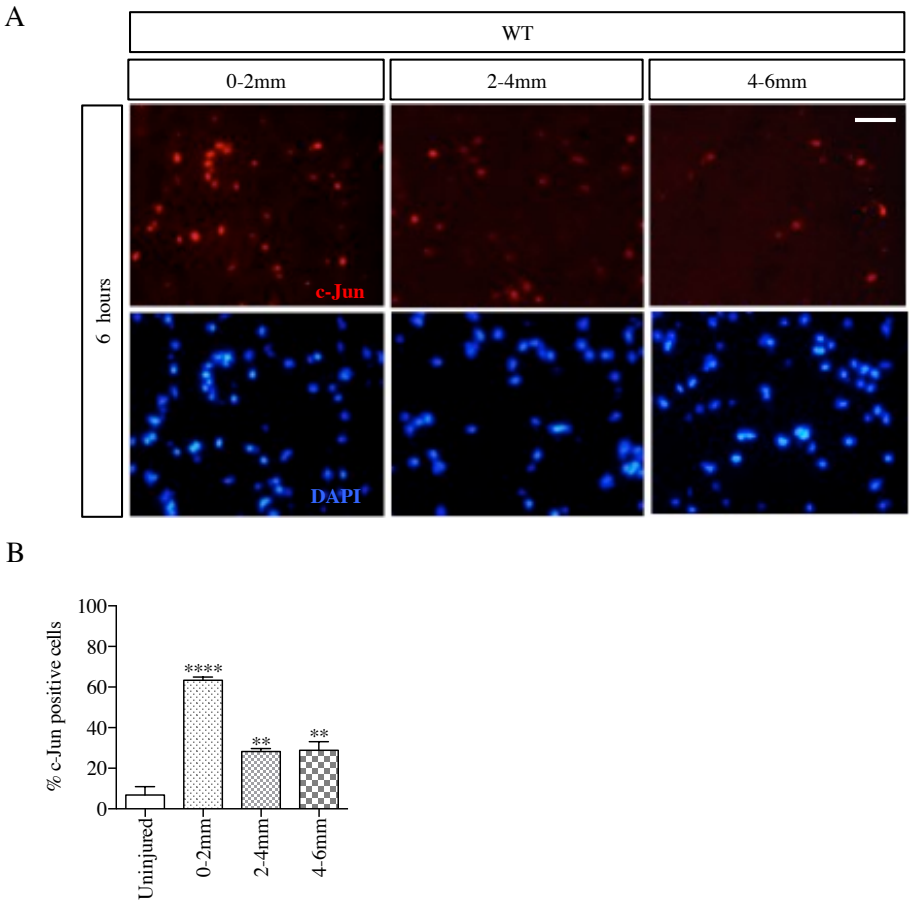

Figure 5.2 | c-Jun expression in proximal stump cells 6 hours after sciatic nerve transection
(A) 5µm thick sciatic nerve cryosections were immunolabelled with c-Jun antibody and with DAPI to label nuclei. Immunofluorescence images taken at x25 magnification showing the population of proximal stump cells expressing c-Jun at different distances along the nerve from the transection site, 6 hours after injury. The proximal stump is divided into three 2mm segments. The contralateral uninjured nerve is used for comparison. Scale bar represents 50µm. (B) Quantification of the percentage of c-Jun positive cells in the proximal stumps of WT mice 6 hours after nerve transection. WT (n=3) and cKO (n=3), One-way ANOVA with Sidak comparison, $p<0.0001$. All statistical analysis is compared to WT uninjured levels.

Allowing proximal stump cells to respond to a longer injury produced surprising results. WT proximal cells maintain their c-Jun expression at 65% in the first 2mm, and also an increase is seen to 44% and 38% in 2-4mm and 4-6mm respectively (Figure 5.3). This is a significant increase compared to the 7% c-Jun expression seen in cells of uninjured nerves. This would suggest that there is maintenance of c-Jun expression in proximal stump cells nearest to the injury site, but that also there is a spread in the percentage of cells expressing c-Jun further from the injury site.

The importance and significance of this rapid response in c-Jun elevation in proximal stump cells is unknown, as is the reason for the visible maintenance in c-Jun elevation over a period of 48 hours. Nevertheless it can be hypothesised that these cells have elevated c-Jun following sciatic nerve transection, and that this is maintained, to assist the neuronal response to injury.

The sciatic nerve is composed of many cell populations including (Schwann cells, which form the largest majority) but also endoneurial fibroblasts, blood vessels, and resident macrophages (Jurecka et al., 1975; Weinberg et al., 1978; Hirose et al., 1986).

Since elevation of c-Jun in Schwann cells is important in nerve regeneration, to determine the number of Schwann cells in the c-Jun positive population after injury, the percentage of c-Jun positive cells in the proximal stump of WT and cKO mice was compared. This mouse has c-Jun deleted only in Schwann cells, see below (Figure 5.4).

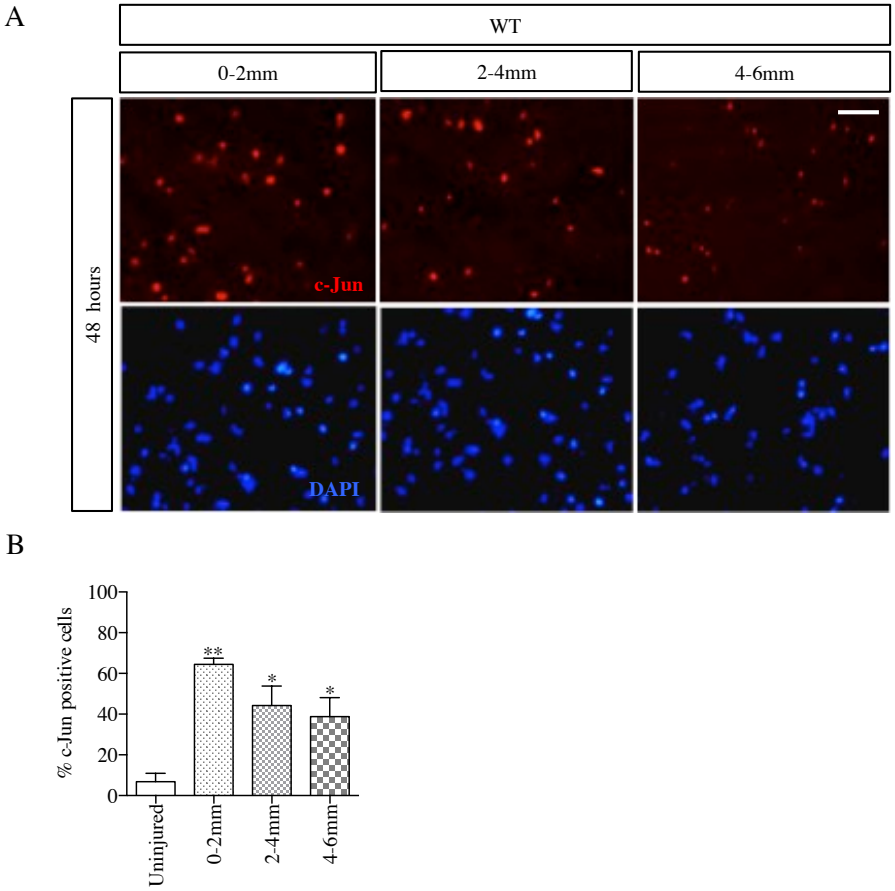

Figure 5.3 | c-Jun expression in proximal stump cells 48 hours after sciatic nerve transection
(A) 5µm thick sciatic nerve cryosections were immunolabelled with c-Jun antibody and with DAPI to label nuclei. Immunofluorescence images taken at x25 magnification showing the population of proximal stump cells expressing c-Jun at different distances along the nerve from the transection site, 48 hours after injury. The proximal stump is divided into three 2mm segments. The contralateral uninjured nerve is used for comparison. Scale bar represents 50µm. (B) Quantification of the percentage of c-Jun positive cells in the proximal stumps of WT mice 48 hours after nerve transection. WT (n=3) and cKO (n=3), One-way ANOVA with Sidak comparison, $p=0.0030$ denotes significance. All statistical analysis is compared to WT uninjured levels.

5.2.2 c-Jun is conditionally knocked out specifically from Schwann cells

The following experiments address the specificity of the cKO mouse model. Sciatic nerves from adult 6-8 week old WT and cKO mice were dissected and dissociated to produce mixed Schwann cell and fibroblast cultures. These cells were cultured for 48 hours *in vitro* before being fixed and fluorescently labelled with Sox10 (a Schwann cell marker) and c-Jun antibodies and the nuclear dye DAPI.

Immunofluorescence images of these WT and cKO Schwann cell and fibroblast cultures in Figure 5.4 show the cells that labelled positively for Sox10 (Schwann cell marker) are c-Jun positive in WT cultures, however c-Jun negative in cKO cultures. The magnified images in Figure 5.4C show clearly the positive co-localisation of Sox10/c-Jun positive Schwann cells in WT, but not in cKO cultures. Quantification of the percentage of Schwann cells that expressed c-Jun in both WT and cKO cultures are seen in Figure 5.4B, confirming that c-Jun is not expressed by Schwann cells from the cKO mouse. To quantify the number of fibroblasts expressing c-Jun in WT and cKO cultures, morphology was used as depicted in Figure 5.4D. The graph in Figure 5.4E also confirms that c-Jun in only knocked out of Schwann cells in the cKO model and not in other cells such as fibroblasts as these expressed c-Jun equally in WT and cKO cultures.

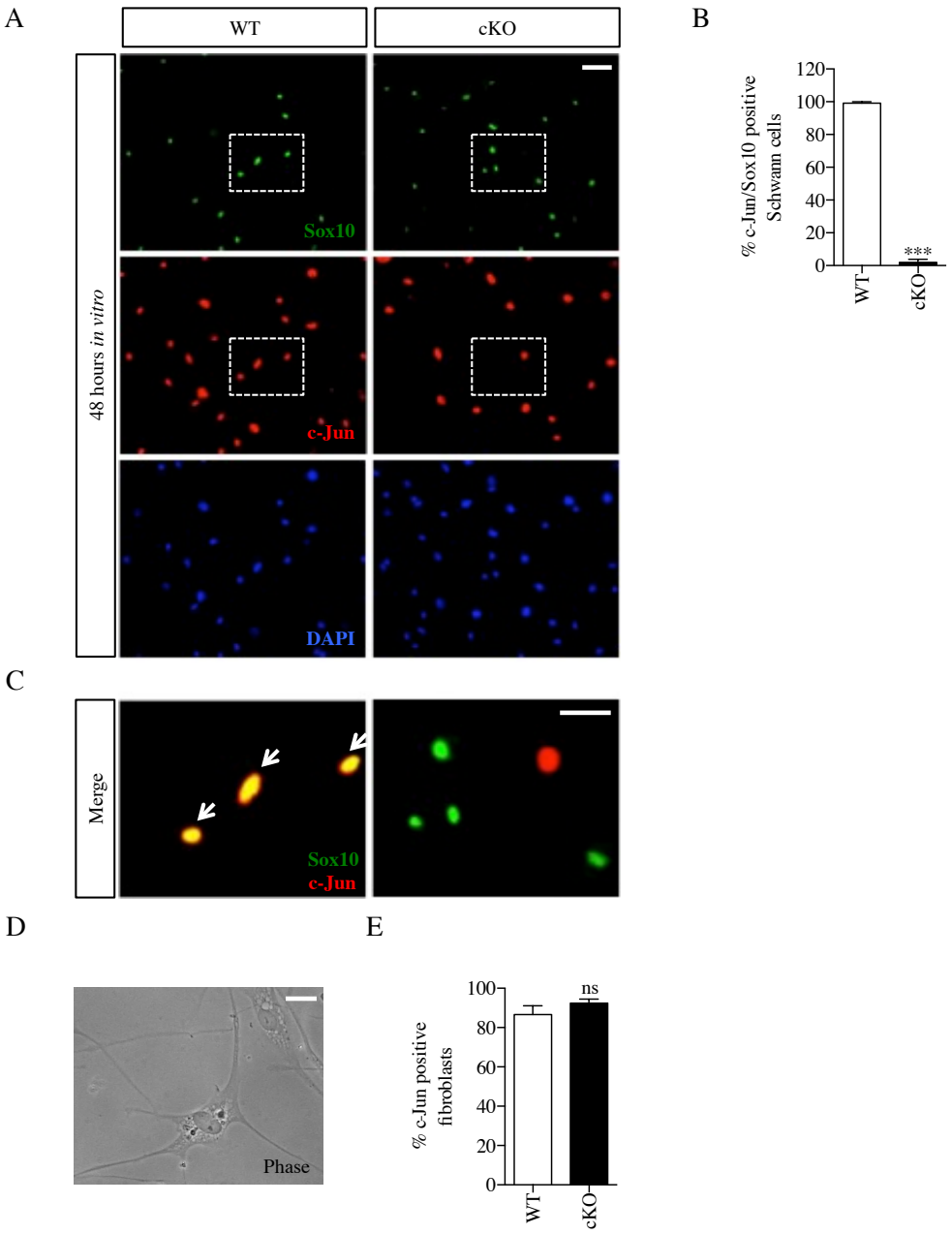

Figure 5.4 | 48 hours adult Schwann cell and fibroblast culture using sciatic nerves from WT and cKO mice
(A) Immunofluorescence images taken at x25 magnification showing the population of Schwann cells that express c-Jun after 48 hours in vitro. Schwann cells were cultured from both adult WT and cKO mice. Coverslips with cultured Schwann cells and fibroblasts were immunolabelled with c-Jun and Sox10 (Schwann cell marker) antibodies and with DAPI to label nuclei. The white boxes highlight areas that are magnified to show co-localisation of Sox10/c-Jun positive cells. Scale bar represents 50µm. (B) Quantification of the percentage of c-Jun positive Schwann cells in both WT and cKO cultures. WT (n=3) and cKO (n=3); Mann-Whitney test, p=0.0002). (C) Magnified immunofluorescence images from (A) to demonstrate Sox10/c-Jun co-localisation indicated specifically by white arrowheads. Scale bar represents 25µm (D) Phase contrast image taken at x63 magnification to show how fibroblasts were identified in culture. Scale bar represents 50µm. (D) Quantification of c-Jun positive fibroblasts in WT and cKO cultures. WT (n=3) and cKO (n=3); Mann-Whitney test, p=0.3308. All statistical analysis is compared to WT.

To further demonstrate the effective c-Jun ablation specifically from Schwann cells in the cKO mouse model, pure macrophages were cultured for 24 hours *in vitro* from the peritoneal cavity of both WT and cKO mice. These macrophage cultures were later fixed and fluorescently labelled with F4/80 (a general macrophage marker) and c-Jun antibodies and with DAPI to label nuclei. Immunofluorescence images in Figure 5.5 show that there is equal c-Jun expression in macrophages from WT and cKO mice, further confirming specific ablation of c-Jun only in Schwann cells. This is quantified in Figure 5.5B.

Thus, results shown in Figures 5.4 and 5.5 validate use of the cKO model to determine the percentage of c-Jun expression in proximal stump Schwann cells after sciatic nerve transection.

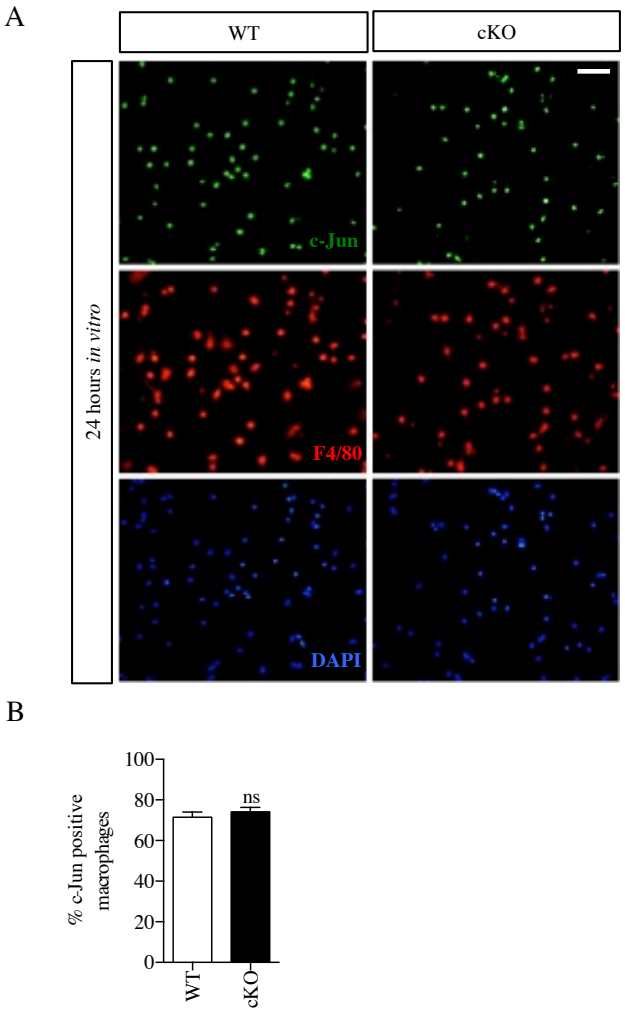

Figure 5.5 | 24 hours peritoneal macrophage cultures using adult WT and cKO mice
(A) Immunofluorescence images taken at x25 magnification showing the population of peritoneal macrophages that express c-Jun after 24 hours in vitro. Macrophages were cultured from both WT and cKO mice. Cultures were immunolabelled with c-Jun and F4/80 (general macrophage marker) antibodies and with DAPI to label nuclei. Scale bar represents 50μm. (B) Quantification of the percentage of F4/80 positive macrophages expressing c-Jun. WT (n=3) and cKO (n=3); Mann-Whitney test p=0.4291. All statistical analysis is compared to WT.

5.2.3 Macrophage recruitment in the proximal stump is similar in both WT and cKO mice 48 hours after sciatic nerve transection

In peripheral nerves, myelin break down is a universal result of a wide range of conditions, one of which being sciatic nerve transection. The work establishing the role of macrophages in injured nerves is mainly done through analysis of the distal portion of the nerve that undergoes Wallerian degeneration. A commonly accepted idea about macrophages, is that following nerve injury whether transection or crush, they are recruited to the injury site through the release of Schwann cell factors such as MCP-1 and LIF (Tofaris et al., 2002), to start to break down myelin through the process of phagocytosis (Perry et al., 1993). In more recent work however, it has been shown that the initial phase of myelin breakdown (5-7 days) (Perry et al., 1993) is carried out through the process of autophagy by Schwann cells (Gomez-Sanchez et al., 2015), rather than phagocytosis as originally thought (Perry et al., 1993). Activated macrophages that invade injured nerves breakdown myelin by phagocytosis (Hirata and Kawabuchi, 2002; Ramaglia et al., 2008; Vargas et al., 2010; Dubový et al., 2013). This modified explanation of the role of macrophages in myelin clearance does not however negate their importance in the proximal stump following short-term injury. Work from Arthur-Farraj et al., 2012 demonstrated that initial macrophage recruitment in the distal stump of the nerve following injury was lower in the cKO compared to WT in the first 3mm of the distal stump but not more distally, therefore perhaps adding to the impairment of successful nerve regeneration.

From experiments shown in Figure 5.6 where macrophage numbers were quantified in the proximal stump 48 hours after sciatic nerve transection, it is evident that the numbers between WT and cKO are not significantly different (Figure 5.6C). This further confirms that in the cKO proximal stump, the population of macrophages present may also be expressing c-Jun, which would affect the results of c-Jun elevation in WT proximal stump cells in Figure 5.3B.

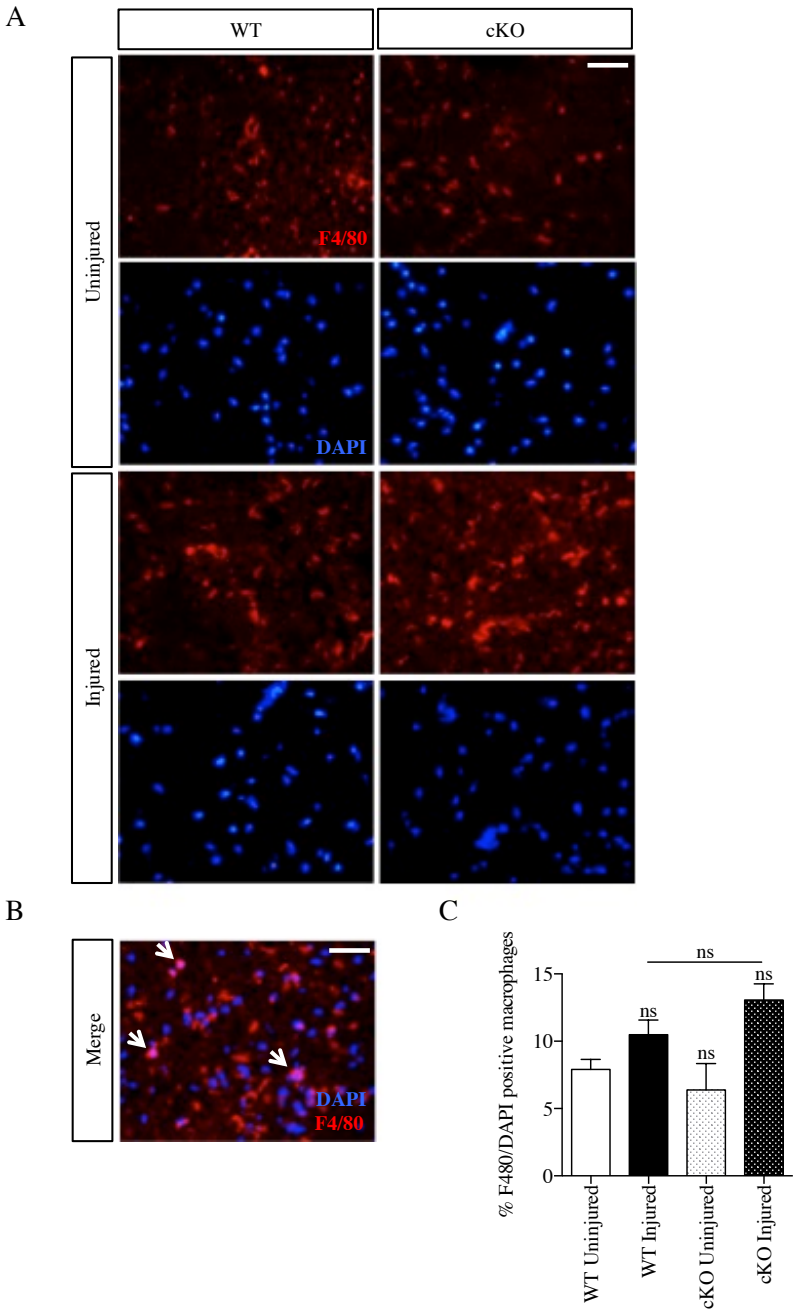

Figure 5.6 | Percentage of F480 positive macrophages in proximal stump 48 hours after nerve
(A) Immunofluorescence images taken at x25 magnification showing tissue sections of WT and cKO proximal stump 48 hours after sciatic nerve. These sections were immunolabelled with F4/80 (general macrophage marker) antibody and with DAPI to label nuclei. The contralateral uninjured nerves were used as controls. Scale bar represents 50µm. (B) Merged immunofluorescence image to show how positive F4/80 cells were quantified in transverse sections. Scale bar represents 50µm. (C) Quantification of the percentage of F4/80 positive macrophages in uninjured and injured nerves 48 hours after nerve transection in WT and cKO mice. WT (n=3) and cKO (n=3); One-way ANOVA with Tukey comparison, p=0.0206. All statistical analysis is compared to WT uninjured levels, unless otherwise shown.

5.2.4 Rapid c-Jun elevation is localised to proximal stump Schwann cells

To address exactly what the percentage of Schwann cells of the proximal stump specifically express c-Jun following sciatic nerve transection, the results shown in Figures 5.1-5.3 (analysis in WT mice), was also performed in the cKO mice. The use of the cKO allowed the percentage of Schwann cells in the proximal stump that express c-Jun after (1 hour, 6 hours and 48 hours) nerve transection to be determined exactly. The percentage of c-Jun expression in cKO uninjured nerves and proximal stumps reflects the total percentage of c-Jun positive cells and includes other cells in the nerve other than Schwann cells, as confirmed in Figures 5.4 and 5.5. Therefore, to determine the percentage of c-Jun elevation in Schwann cells only 1 hour, 6 hours and 48 hours after injury in the proximal stump, c-Jun percentages from cKO mice were subtracted from the total percentages quantified in WT nerves. The graph in Figure 5.7A is a summary of the c-Jun elevation seen in Schwann cells only at different times after injury and along the different distances from the injury site.
The significance of this c-Jun elevation specifically in Schwann cells following injury, may be implicated in the ability of DRG neurons to respond to sciatic nerve transection, which will be discussed in Chapter 6.

Though it is now clear that at 1 hour and 6 hours after injury in the first 2mm the percentage elevation of c-Jun in proximal stump Schwann cells is maintained at 62%, there is a decrease in this elevation at 48 hours down to 45% which is due to the fact that at this time point more macrophages, which also express c-Jun are likely to have been recruited to the injury site. The percentage of c-Jun elevation seen in the next 2-4mm segment is slightly higher at 1 hour (43%) whereas at 6 hours and 48 hours this is less (27%). Finally, at the 4-6mm segment, c-Jun expression is lowest at 1 hour (7%) and increases significantly to 27% at 6 hours and 48 hours. A summary diagram is shown in Figure 5.7B to illustrate these changes in Schwann cell c-Jun expression in proximal stumps over time and along distances from the injury site.

A

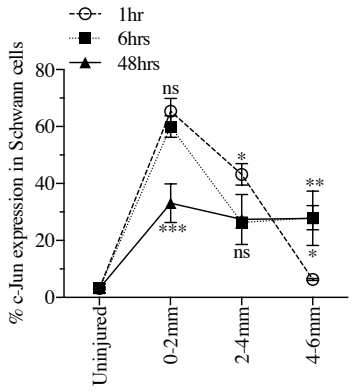

B

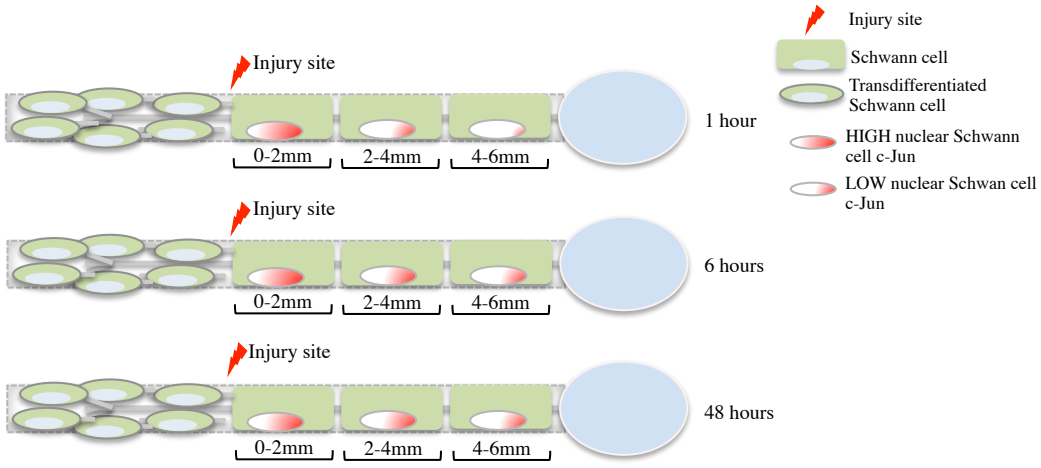

Figure 5.7 | c-Jun expression in proximal stump Schwann cells increases in time and space
(A) Quantification of the percentage of c-Jun expression in WT proximal stump Schwann cells from uninjured levels to 1 hour, 6 hours and 48 hours following nerve transection, at different distances from the transection site. WT (n=3) and cKO (n=3); Two-way ANOVA with Sidak comparison, $p<0.0001$. Statistical analysis is all relative to 1 hour at each distance. (B) Summary diagram to show how levels of c-Jun expression in WT proximal stump Schwann cells change within time and along different distances from the injury site.

5.2.5 c-Jun elevation after injury is equal in Remak and Myelin Schwann cells

Schwann cells mature into two distinct subpopulations depending on axon size and signals from them to form Myelin or Remak Schwann cells. Myelin Schwann cells form a 1:1 relationship with an axon, whereas Remak Schwann cells ensheath several axons. Figure 5.1 shows that WT proximal stump Schwann cells express c-Jun highly 1 hour after sciatic nerve transection, however from these results it is not clear whether the expression of c-Jun seen is in Myelin or Remak Schwann cells. To answer this question, teased nerve fibre preparations were taken from both WT and c-Jun cKO proximal stumps 1 hour (first 2mm) following nerve transection, where highest c-Jun elevation was observed. These were fixed and fluorescently immunolabelled using L1 as a Remak Schwann cell marker (Hantke et al., 2014), c-Jun and DAPI to label nuclei, while the morphology of the nerve fibre under phase contrast optics was used to determine which cells were myelinating Schwann cells. Immunofluorescence images in Figure 5.8A reveal some weak c-Jun expression in 24% of WT uninjured nerves, which then increases to 73% after injury, conversely to what is seen in the cKO nerves where there is no c-Jun expression in Remak Schwann cells. This difference in the WT was statistically significant compared to WT uninjured nerves (Figure 5.8B).

Immunofluorescence images in Figure 5.8C show the lack of c-Jun expression in uninjured Myelin Schwann cells, but the elevation of c-Jun in these cells can still be detected after injury in the WT. This elevation in WT teased fibre preparations from uninjured (2%) to injured (45%) was also statistically significant as shown in Figure 5.8D. The lack of c-Jun expression in both uninjured and injured nerves of the c-Jun cKO, further demonstrates that the specificity of this c-Jun expression after nerve transection is within Schwann cells.

Therefore c-Jun is expressed to very high levels and rapidly following nerve injury, equally in Remak and Myelin Schwann cells. This c-Jun elevation in proximal stump Schwann cells increases further away from the injury site with time, but the initial elevation at the injury site is maintained over several hours.

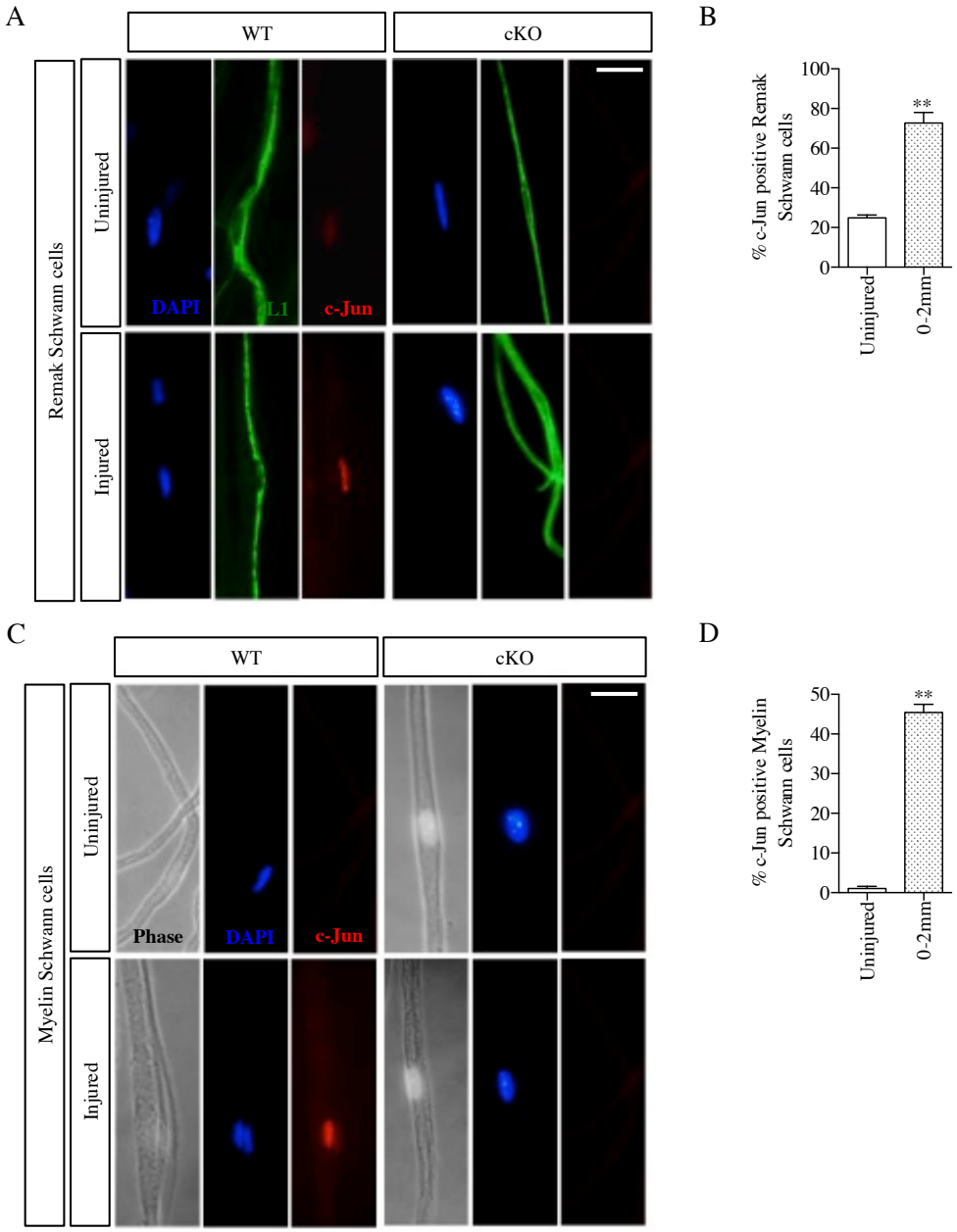

Figure 5.8 | Teased nerve fibres 1 hour after nerve transection from 0-2mm of WT and cKO proximal stumps
(A) Immunofluorescence images taken at x63 magnification showing teased fibres 1 hour after sciatic nerve transection from the site most proximal to the injury (0-2mm) using both WT and cKO mice. Teased fibre preparations were immunolabelled with L1 (Remak Schwann cell marker) and c-Jun antibodies and with DAPI to label nuclei. (B) Quantification of the percentage of Remak Schwann cells expressing c-Jun 1 hour after injury in WT and cKO sciatic nerves. WT (n=3) and cKO (n=3); Student T-test, p=0.0087). Scale bar represents 50µm. (C) Immunofluorescence images taken at x25 magnification showing teased fibres 1 hour after sciatic nerve transection from the site most proximal to the injury (0-2mm) using both WT and cKO mice. Teased fibre preparations were immunolabelled with c-Jun antibody and with DAPI to label nuclei. Phase contrast was used to determine Myelin Schwann cells. (D) Quantification of the percentage of Myelin Schwann cells expressing c-Jun 1 hour after injury in WT and cKO sciatic nerves. Student T-test, p=0.0012. Scale bar represents 50µm. 200 cells were quantified from each genotype. All statistical analysis is compared to WT uninjured levels.

In summary, proximal stump Schwann cells express very high levels of c-Jun as early as 1 hour following sciatic nerve transection. These levels are maintained near the injury site, and with longer time point after injury, c-Jun levels become more and more elevated further from the injury site. c-Jun expression in proximal stump Schwann cells is equally present in Remak and Myelin Schwann cells following nerve injury. Schwann cell c-Jun however does not affect the expression of retrograde axonal injury signals to the neuronal cell body.

5.3 Discussion

Schwann cell c-Jun is an important determining factor in the response to nerve injury, most notably its role in the cellular reprogramming of Remak and Myelin Schwann cells into repair Bungner Schwann cells (Arthur-Farraj et al., 2012; Fontana et al., 2012; Jessen et al., 2015; Jessen and Mirsky, 2016).

The results presented in this chapter shed some light on the role of Schwann cell c-Jun in the proximal stump in contrast to previous work on the distal stump, in determining the role of Schwann cell c-Jun in nerve regeneration. Although work from Arthur-Farraj et al., 2012 shows that high levels of Schwann cell c-Jun result in Schwann cells being reprogrammed into functionally distinct repair Bungner Schwann cells that aid nerve regeneration, one could question whether the high levels of c-Jun expression seen in proximal stump Schwann cells would result in the same effect. One important difference to reiterate is that when the Schwann cell c-Jun elevation seen in this chapter at short time points after injury in the proximal stump, and is compared with levels seen at longer time points after injury in the distal stump, the levels of c-Jun seen measured by Western blotting in proximal stump Schwann cells are much lower than those seen in the distal stump Schwann cells that become repair Bungner Schwann cells (unpublished observations JA Gomez-Sanchez).

The results presented here do not determine the signalling cascade through which these effects take place following c-Jun elevation in Schwann cells following injury, however the work of Charlotta Lindwall Blom and others published in 2014 using Schwann cell experiments confirmed that nerve injury induced Schwann cell c-Jun activation is JNK independent.

Inflammatory cytokines such as LIF, IL-6 and TNFα that are expressed following nerve injury have been shown to activate MAPKs or the JAK/STAT signalling pathway, both of which are strongly implicated in neuronal activation (Sheu et al., 2006; Qiu et al., 2005). IL-6 is thought to modulate neuronal outgrowth through the activation of the JAK/STAT signalling pathway within the axon, which leads to an increase in the level of p-STAT3 and hence this is subsequently retrogradely transported back to the soma, where it promotes the up-regulation of GAP-43 (Qiu et al., 2005). With this in mind, it would be interesting to see if levels of such

inflammatory cytokines are different in the proximal stump of cKO mice compared to WT, as this could be important in determining the possible role of levels of c-Jun expression in proximal stump Schwann cells after injury, and their role in neuronal cell body response to axotomy, when many genes associated with regeneration are expressed in DRG neurons within hours following nerve injury (Lindwall et al., 2004; Qiu et al., 2005; Zou et al., 2009). Although macrophages also express these inflammatory cytokines, their numbers in the nerve only rise significantly 48 hours after nerve transection (Stoll et al., 1989; Perry et al., 1987).

The experiments in the following chapter address the question of whether c-Jun dependent signalling from the proximal stump Schwann cells controls the growth response of neurons.

6. Schwann cell c-Jun dependent neuronal activation in response to nerve injury

6.1 Introduction

As previously mentioned, in contrast to central nerves, peripheral nerves have the remarkable ability to re-generate (albeit to a limited extent) following nerve injury. This is due to the glial cells of peripheral nerves and also the responses of the neuronal cell body to axotomy (Abe and Cavalli, 2008). Following nerve injury, DRG neurons express many RAGs that are crucial for successful neuronal outgrowth, unlike in the CNS, where this is not seen to the same extent (Chandran et al., 2016). Peripheral nerve injury causes neurons to switch from a signalling mode to a growth one, which promotes successful peripheral nerve regeneration (Navarro et al., 2007; Abe and Cavalli, 2008).

Further evidence highlighting the importance of the response of peripheral neurons to injury, is the work which demonstrated that following a conditioning lesion of the peripheral branch of DRG neurons, the intrinsic molecular changes that take places, are sufficient to cause the central axons of DRG neurons to regenerate (McQuarrie, 1985; Neumann and Woolf, 1999).

The neuronal cell body response to peripheral nerve injury is as important as that of the cells proximal to the injury site. In the Chapter 5, following sciatic nerve transection, c-Jun was elevated in proximal stump Schwann cells as early as 1 hour following nerve injury, and this elevation was maintained up to 48 hours later. The time course of this proximal stump Schwann cell c-Jun elevation is suggestive of the fact that c-Jun is present in Schwann cells at the necessary time required to drive a signalling cascade that would result in neuronal activation. It was therefore of interest to see whether or not the early and rapid elevation of proximal stump Schwann cell c-Jun following nerve injury, was sufficient to affect the neuronal cell body response to nerve axotomy and whether c-Jun elevation in proximal stump Schwann cells has a role in the crucial switch of DRG neurons from signalling to growth.

6.2 Results

6.2.1 RAG expression in L4 DRG neurons following sciatic nerve transection

Is proximal stump Schwann cell c-Jun elevation important for the up-regulation of well known RAGs following sciatic nerve transection? To address this question, sciatic nerves from WT and cKO mice were transected at the sciatic notch and these mice were allowed to recover for 48 hours after the transection before being culled (as described in Chapter 2, section 2.3.2.3). The L4 DRG neurons (uninjured and injured) from WT and cKO mice were analysed by immunofluorescence and Western blot for the expression of several known RAGs which included c-Jun, ATF3, p-STAT3 Tyr705, p-STAT3 Ser727 and GAP43 in the neuronal soma (Figures 6.1-6.10). For all L4 DRG immunofluorescence quantification presented below, the most strongly expressing neurons were determined as defined in Chapter 2, section 2.3.9.2.

An obvious RAG candidate to analyse was c-Jun, and its expression in neurons following nerve transection. The cKO mouse model is only a knockout of c-Jun in Schwann cells (Figures 5.4 and 5.5); therefore it was of interest to see if proximal stump Schwann cell c-Jun was important for neuronal c-Jun expression. Previous studies have shown the importance of neuronal c-Jun activation following nerve injury to promote successful nerve regeneration through use of a neuronal c-Jun knockout mouse (Raivich et al., 2004; Makwana et al., 2010; Fontana et al., 2012). With this in mind, it was valid to address the question of whether proximal stump Schwann cell c-Jun affects neuronal c-Jun expression, ultimately affecting nerve regeneration. Figure 6.1A shows nuclear expression of c-Jun in L4 uninjured and injured DRG neurons 48 hours after sciatic nerve transection. From the representative immunofluorescence images shown in Figure 6.1A, it is clear that levels of c-Jun expression in uninjured L4 DRG neurons of WT and cKO mice are barely detectable, yet as expected, there is a clear elevation of nuclear c-Jun expression in neurons following nerve transection.

This elevation of neuronal c-Jun appears to be similar in both WT and cKO injured L4 DRG neurons (Figure 6.1A), yet upon closer inspection through quantification of this c-Jun expression (Figures 6.1B and 6.1C), there is a mild decrease in c-Jun expression in the cKO mouse following injury. This mild decrease in neuronal c-Jun expression in the cKO does not reach significance (Figure 6.1B) when counting c-Jun/NF200 positive neurons, regardless of their signal intensity where WT levels are 51% compared to cKO levels of 47%. Nevertheless, as seen in Figure 6.1C, if these c-Jun expression levels are quantified by analysing only the strongest expressing c-Jun positive neurons, the mild decrease of c-Jun expression seen in the cKO becomes statistically significant, decreasing from 35% in the WT to 29% in the cKO neurons. Although there is only a modest decrease seen in neuronal c-Jun expression 48 hours following sciatic nerve transection in the cKO mouse, this may be of significance later on in the regenerative process, as there is a body of evidence that shows how important c-Jun is both in neurons (Makwana et al., 2004; Fontana et al., 2012) and Schwann cells of the distal stump (Parkinson et al., 2008; Arthur-Farraj et al., 2012).

Western blot analysis of WT and cKO L4 DRGs (uninjured and injured) 48 hours after sciatic nerve transection (Figure 6.2) supported the findings from Figure 6.1. The c-Jun band seen in cKO injured DRG lane in the representative Western blot image (Figure 6.2A) is less intense compared to the WT one. Important to note however is that the levels of c-Jun expression in L4 uninjured DRGs from WT and cKO mice are equal, therefore further indicating that c-Jun is only knocked out of Schwann cells in the cKO model, which is seen both in the immunofluorescence quantification (Figures 6.1B and 6.1C) and Western blot quantification (Figure 6.2B). Western blot quantification agrees with the immunofluorescence quantification where a mild decrease is seen in cKO mice, although this does not reach significance when normalised to WT uninjured levels (Figure 6.2B).

Although there is a mild decrease seen in c-Jun expression in DRG neurons following sciatic nerve injury, this may be enough to affect the rate of neuronal outgrowth. This possible hypothesis that lack of Schwann cell c-Jun decreases neuronal outgrowth after injury will be addressed later in this chapter.

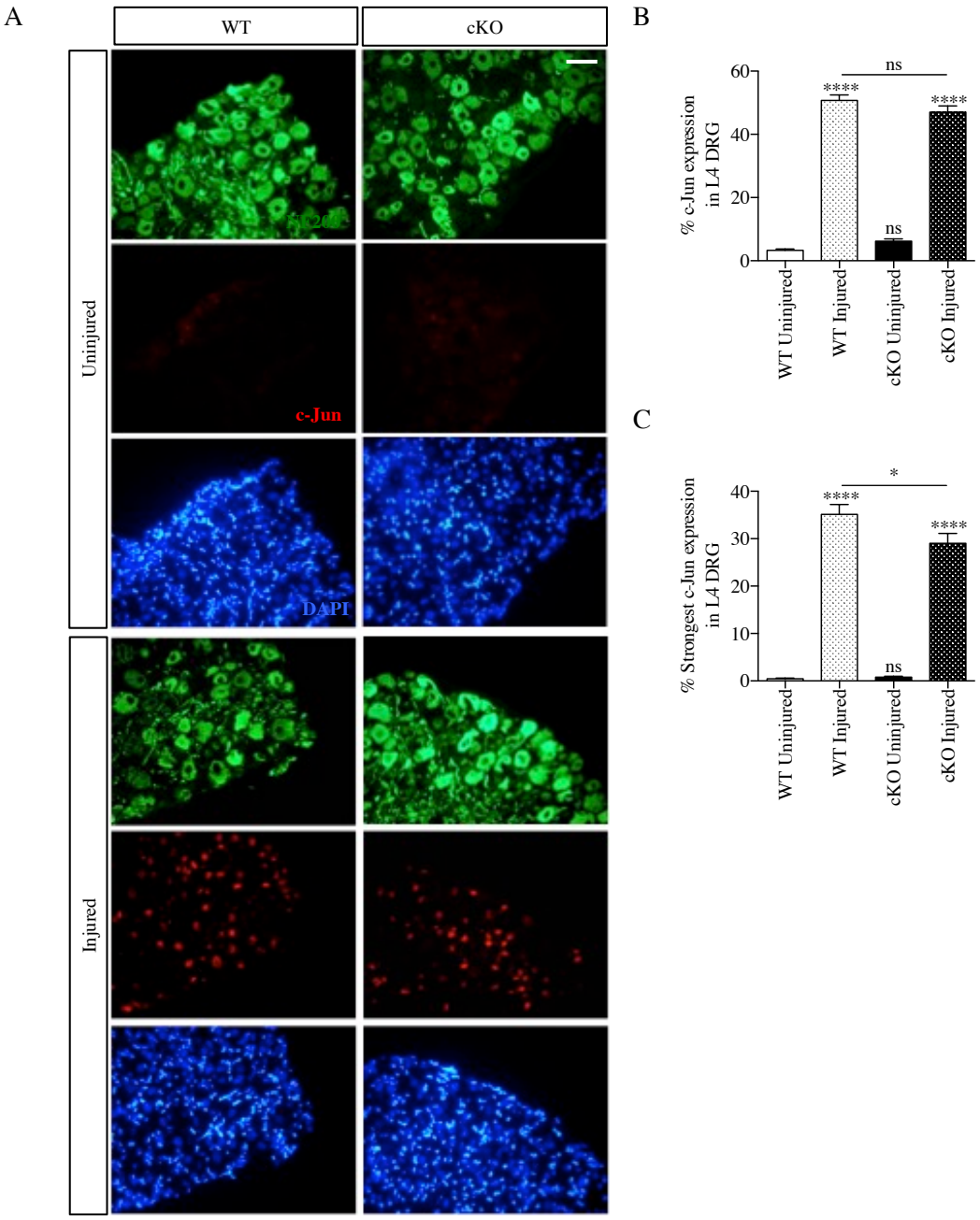

Figure 6.1 | c-Jun expression in L4 DRGs 48 hours after sciatic nerve transection
(A) 5µm thick L4 DRGs (uninjured and injured) cryosections from WT and cKO were immunolabelled with NF200 (neuronal marker) and c-Jun antibodies and with DAPI to label nuclei. Immunofluorescence images taken at x25 magnification showing the population of neurons (NF200 positive) that were also c-Jun positive in L4 uninjured and injured DRGs. (B) Quantification of the percentage of c-Jun/NF200 positive neurons in WT and cKO L4 uninjured and injured DRG neurons. WT (n=4) and cKO (n=4); One-way ANOVA with Tukey comparison, $p<0.0001$. (C) Quantification of the percentage of the strongest c-Jun/NF200 positive neurons in WT and cKO L4 uninjured and injured DRG neurons. One-way ANOVA with Tukey comparison, $p<0.0001$). All statistical analysis is compared to WT uninjured levels, unless otherwise shown.

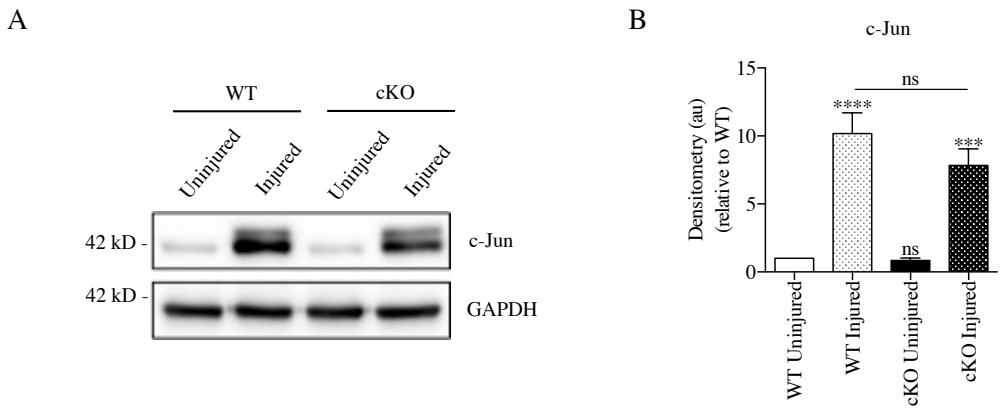

Figure 6.2 | Western blot of c-Jun expression in L4 DRGs 48 hours after sciatic nerve transection
(A) Representative Western blot of c-Jun expression in L4 uninjured and injured DRG protein extracts from WT and cKO mice 48 hours after sciatic nerve transection. GAPDH is used as a reference gene. (B) Quantification of the level of c-Jun expression in WT and cKO L4 uninjured and injured DRGs. c-Jun expression in normalised to GAPDH, and then expressed as a fold change relative to WT uninjured levels. WT (n=3) and cKO (n=3); One-way ANOVA with Tukey comparison, $p<0.0001$. All statistical analysis is compared to WT uninjured levels, unless otherwise shown.

Another important RAG transcription factor is ATF3. It is specifically expressed in neurons following injury and is associated with promoting neurite outgrowth, neurite elongation and cell survival (Nakagomi et al., 2003; Seijffers et al., 2007; Kiryu-Seo et al., 2008; Linda et al., 2011; Hunt et al., 2012; Fu and Killberg, 2012). This means that ATF3 is a very important RAG not only for these reasons, but also because it works with c-Jun to bring about certain aspects of effective regeneration (Fagoe et al., 2015). Analysis of ATF3 neuronal expression in L4 uninjured and injured DRG neurons from WT and cKO mice showed no difference in expression (Figure 6.3A-C). Whether analysing all neurons expressing ATF3 in WT and cKO (uninjured and injured) L4 DRG neurons (Figure 6.3B) or specifically the strongly positive ATF3 neurons (Figure 6.3C), no difference was observed. Levels of ATF3 expression seen in WT injured neurons were 45% compared to 43% in cKO injured DRG neurons (Figure 6.3B). When comparing only the most strongly expressing ATF3 neurons, WT injured levels were 22% compared to cKO injured levels of 23% (Figure 6.3C).
In conclusion, the lack of c-Jun in proximal stump Schwann cells is not enough to affect the up-regulation of ATF3 in DRG neurons following nerve injury.

The results depicted in Figure 6.3 were confirmed by Western blot analysis where a representative image is shown in Figure 6.4A and the quantification relative to WT uninjured levels in Figure 6.4B.
The results in Figures 6.3 and 6.4 suggest that neuronal ATF3 activation in L4 DRGs 48 hours after nerve transection is not determined by the presence of high and maintained levels of Schwann cell c-Jun expression in the proximal stump.

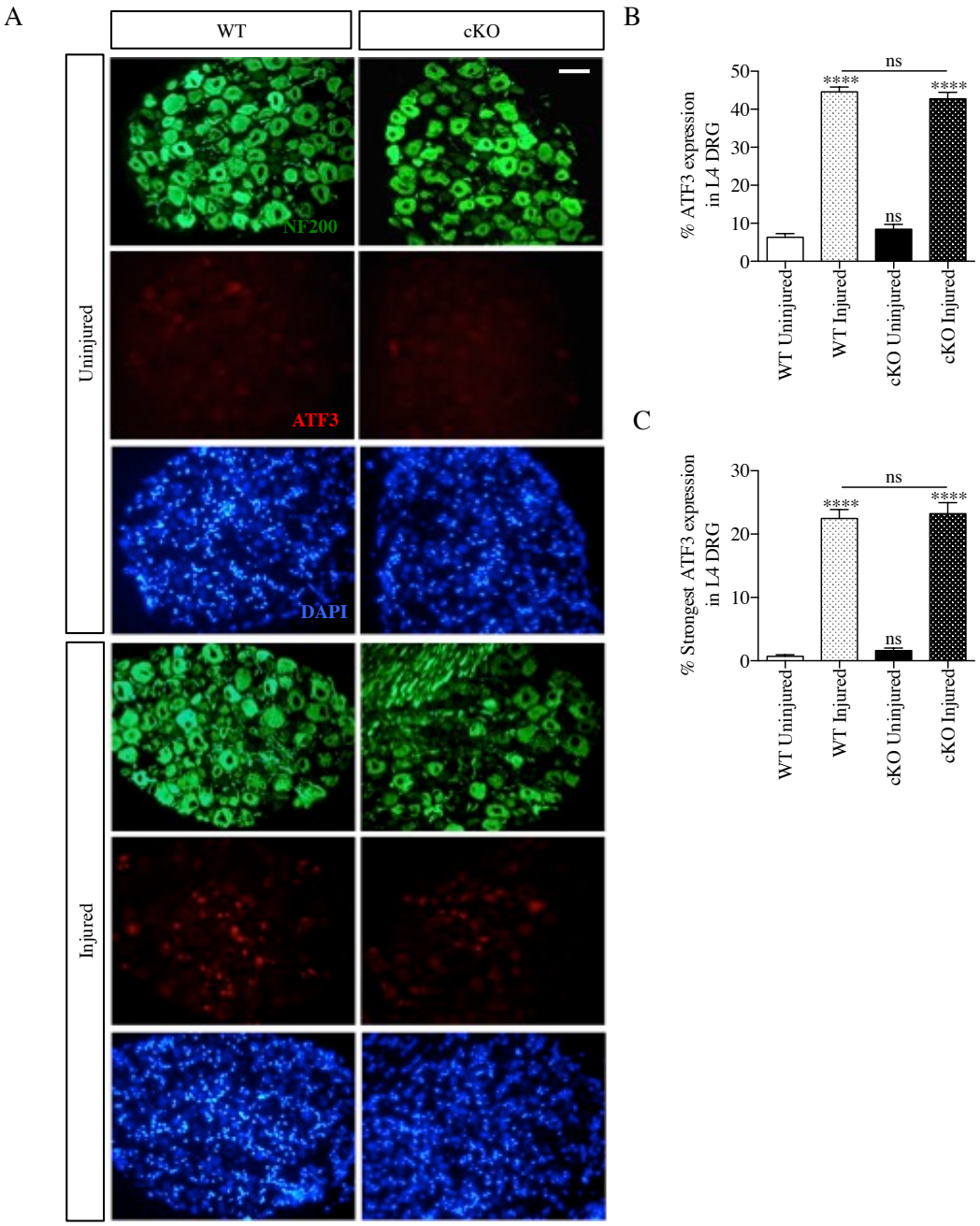

Figure 6.3 | ATF3 expression in L4 DRGs 48 hours after sciatic nerve transection
(A) 5µm thick L4 DRGs (uninjured and injured) cryosections from WT and cKO were immunolabelled with NF200 (neuronal marker) and ATF3 antibodies and with DAPI to label nuclei. Immunofluorescence images taken at x25 magnification showing the population of neurons (NF200 positive) that were also ATF3 positive in L4 uninjured and injured DRGs. (B) Quantification of the percentage of ATF3/NF200 positive neurons in WT and cKO L4 uninjured and injured DRG neurons. WT (n=4) and cKO (n=4); One-way ANOVA with Tukey comparison, $p<0.0001$. (C) Quantification of the percentage of the strongest ATF3/NF200 positive neurons in WT and cKO L4 uninjured and injured DRG neurons. One-way ANOVA with Tukey comparison, $p<0.0001$. All statistical analysis is compared to WT uninjured levels, unless otherwise shown.

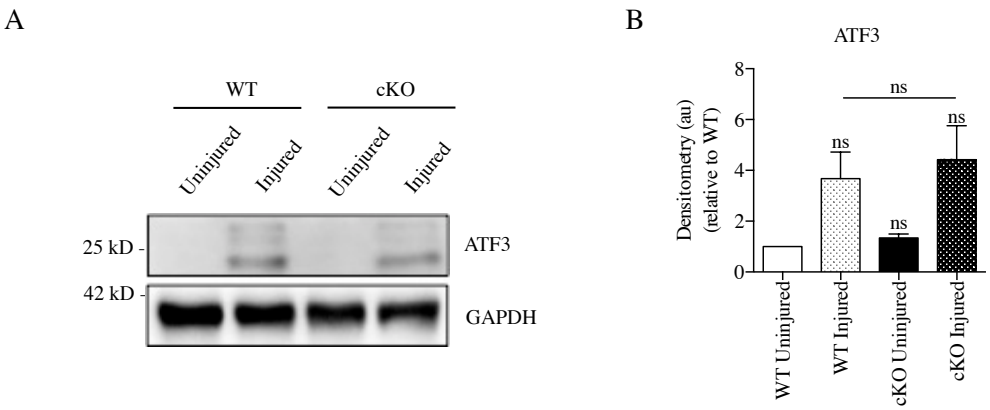

Figure 6.4 | Western blot of ATF3 expression in L4 DRGs 48 hours after sciatic nerve transection
(A) Representative Western blot of ATF3 expression in L4 uninjured and injured DRG protein extracts from WT and cKO mice 48 hours after sciatic nerve transection. GAPDH is used as a reference gene. (B) Quantification of the level of ATF3 expression in WT and cKO L4 uninjured and injured DRGs. ATF3 expression was normalised to GAPDH, and then expressed as a fold change relative to WT uninjured levels. WT (n=3) and cKO (n=3); One-way ANOVA with Tukey comparison, p=0.0533. All statistical analysis is compared to WT uninjured levels, unless otherwise shown.

STAT3, c-Jun and ATF3 are the most commonly investigated transcription factor RAGs that are expressed in response to nerve injury (Haas et al., 1999; Tsujino et al., 2000; Nakagomi et al., 2003; Raivich et al., 2004; Patodia and Raivich, 2012). This means that STAT3 is also a prime candidate for expression analysis in (uninjured and injured) L4 DRG neurons in WT and cKO mice following sciatic nerve transection. Classically, phosphorylation of STAT3 on the tyrosine 705 (Tyr705) residue is analysed (Lee et al., 2004; Qiu et al., 2005; Bareyre et al., 2011; Ben-Yaakov et al., 2012; Shin et al., 2012), yet phosphorylation of STAT3 on the serine 727 (Ser727) residue is also important, but not necessary for the translocation of STAT3 into the nucleus (Lee et al., 2009; Zhou and Too, 2013; Mandal et al., 2014). For these reasons, both Tyr705 and Ser727 phosphorylation of STAT3 were analysed in L4 DRG neurons of WT and cKO mice 48 hours after sciatic nerve transection (Figures 6.5-6.8). Immunofluorescence images in Figure 6.5A, along with their quantification in Figures 6.5B and 6.5C show that the lack of Schwann cell c-Jun expression after sciatic nerve transection does not affect the expression of p-STAT3 Tyr705 in (uninjured and injured) L4 DRG neurons. Though there was clear up-regulation of p-STAT3 Tyr705 in WT and cKO L4 DRG neurons 48 hours after injury, from 13% to 38% (WT) and 11% to 38% (cKO), this was not significantly different between WT and cKO mice (Figure 6.5B). Quantifying only the strongest p-STAT3 Tyr705 expressing neurons showed the same result (Figure 6.5C). These immunofluorescence results were confirmed by Western blot analysis, shown in Figure 6.6.

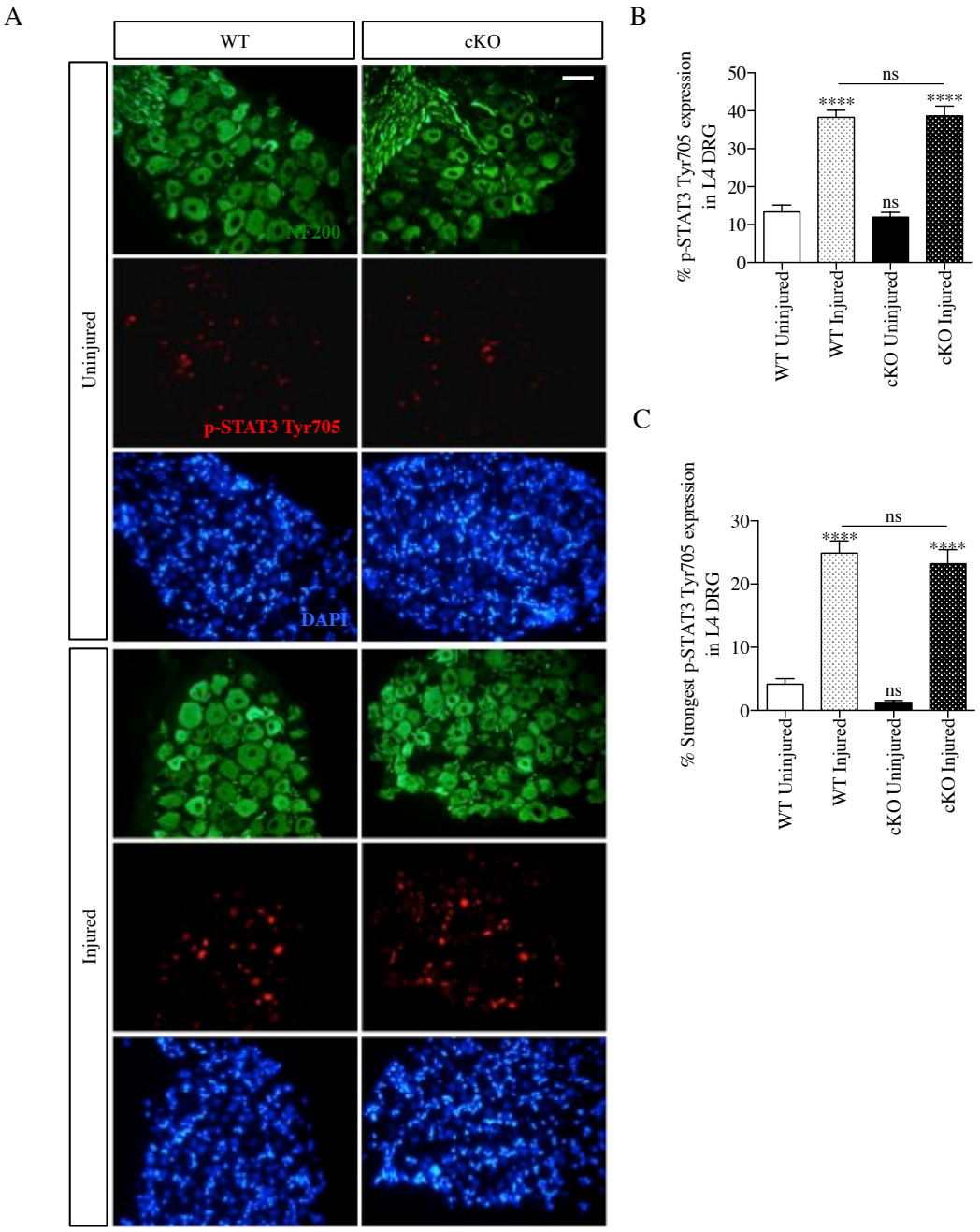

Figure 6.5 | p-STAT3 Tyr705 expression in L4 DRGs 48 hours after sciatic nerve transection
(A) 5µm thick L4 DRGs (uninjured and injured) cryosections from WT and cKO were immunolabelled with NF200 (neuronal marker) and p-STAT3 Tyr705 antibodies and with DAPI to label nuclei. Immunofluorescence images taken at x25 magnification showing the population of neurons (NF200 positive) that were also p-STAT3 Tyr705 positive in L4 uninjured and injured DRGs. (B) Quantification of the percentage of p-STAT3 Tyr705/NF200 positive neurons in WT and cKO L4 uninjured and injured DRG neurons. WT (n=3) and cKO (n=3); One-way ANOVA with Tukey comparison, $p<0.0001$. (C) Quantification of the percentage of the strongest p-STAT3 Tyr705/NF200 positive neurons in WT and cKO L4 uninjured and injured DRG neurons. One-way ANOVA with Tukey comparison, $p<0.0001$. All statistical analysis is compared to WT uninjured levels, unless otherwise shown.

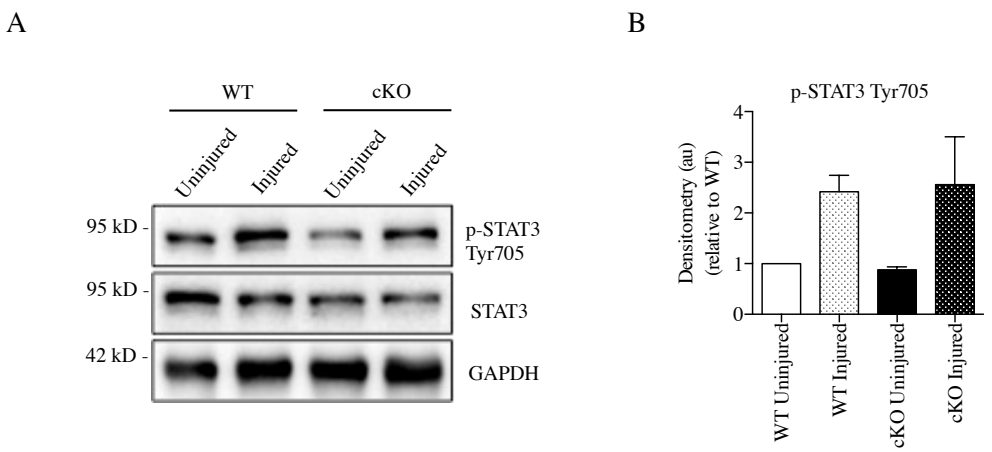

Figure 6.6 | Western blot of p-STAT3 Tyr705 expression in L4 DRGs 48 hours after sciatic nerve transection
(A) Representative Western blot of p-STAT3 Tyr705 expression in L4 uninjured and injured DRG protein extracts from WT and cKO mice 48 hours after sciatic nerve transection. GAPDH is used as a loading control, and the reference gene is STAT3. (B) Quantification of the level of p-STAT3 Tyr705 expression in WT and cKO L4 uninjured and injured DRGs. p-STAT3 Tyr705 expression was normalised to STAT3, and then expressed as a fold change relative to WT uninjured levels. WT (n=2) and cKO (n=2). No statistical analysis was carried out.

Quantification of p-STAT3 phosphorylation on the Ser727 residue was measured by counting the total number of positively labelled Ser727/NF200 neurons regardless of intensity. These results are shown in Figure 6.7A and 6.7B. A surprising outcome was that the uninjured levels in the cKO (29%) were higher than in the WT (20%), and that following nerve transection, there was no significant elevation seen in the injured L4 DRG neurons of WT (19%) and cKO (27%) mice.

It was unexpected to see that expression of p-STAT3 Ser727 was not higher after injury compared to uninjured levels as it is well documented that STAT3 becomes phosphorylated after injury on the Tyr705 residue, but this appears not to be the case for Ser727 in DRG neurons. Further analysis would be needed to elucidate the significance of this finding.

The result seen by immunofluorescence of p-STAT3 Ser727 expression in L4 DRG neurons of uninjured and injured mice was confirmed by Western blot analysis (Figure 6.8). The Western blot results (Figure 6.8) also showed that there was no higher expression of p-STAT3 Ser727 expression in L4 DRG neurons of WT and cKO mice in injured compared with uninjured levels.

The results above shown in Figures 6.5-6.8 suggest that the lack of Schwann cell c-Jun does not determine the phosphorylation of STAT3 (both Tyr705 and Ser727) in L4 DRG neurons following sciatic nerve injury.

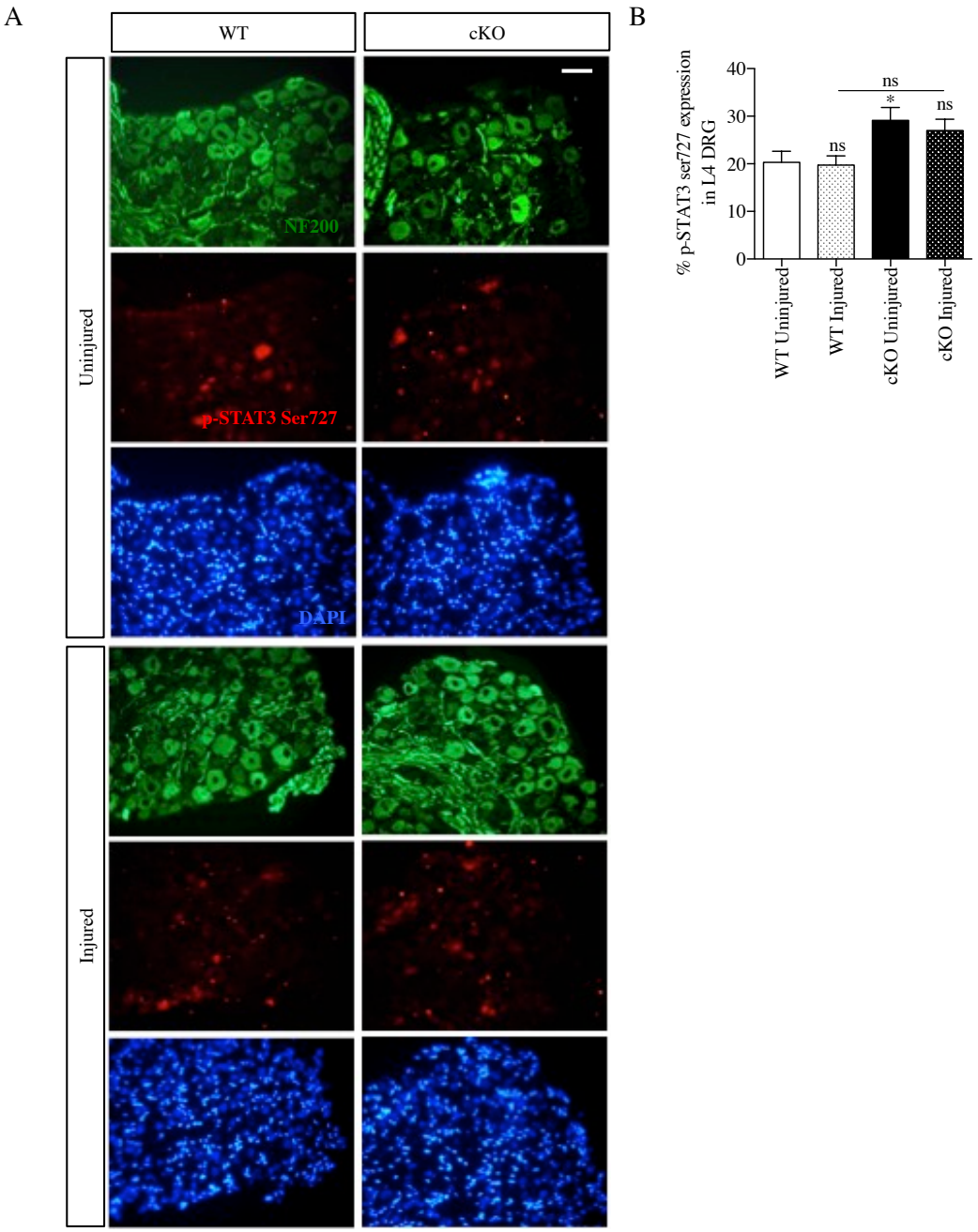

Figure 6.7 | p-STAT3 Ser727 expression in L4 DRGs 48 hours after sciatic nerve transection
(A) 5µm thick L4 DRGs (uninjured and injured) cryosections from WT and cKO were immunolabelled with NF200 (neuronal marker) and p-STAT3 Ser727 antibodies and with DAPI to label nuclei. Immunofluorescence images taken at x25 magnification showing the population of neurons (NF200 positive) that were also p-STAT3 Ser727 positive in L4 uninjured and injured DRGs. (B) Quantification of the percentage of p-STAT3 Ser727/NF200 positive neurons in WT and cKO L4 uninjured and injured DRG neurons. WT (n=3) and cKO (n=3); One-way ANOVA with Tukey comparison, p=0.0076. All statistical analysis is compared to WT uninjured levels, unless otherwise shown.

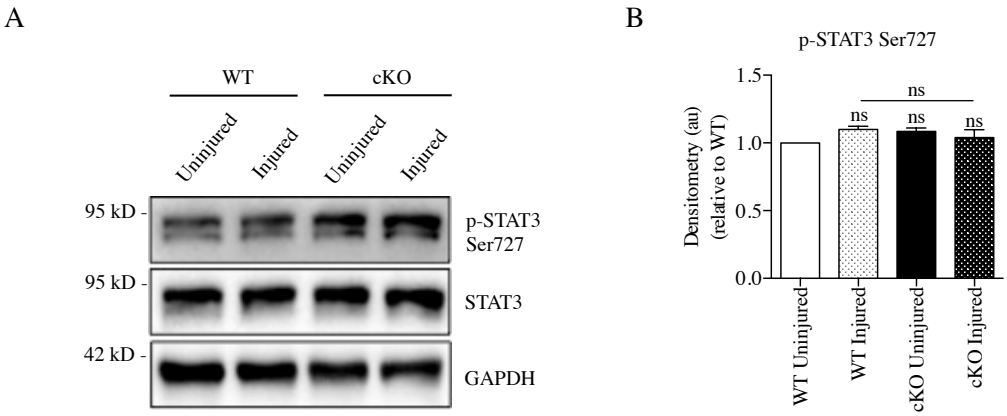

Figure 6.8 | Western blot of p-STAT3 Ser727 expression in L4 DRGs 48 hours after sciatic nerve transection
(A) Representative Western blot of p-STAT3 Ser727 expression in L4 uninjured and injured DRG protein extracts from WT and cKO mice 48 hours after sciatic nerve transection. GAPDH is used as a loading control, and the reference gene is STAT3. (B) Quantification of the level of p-STAT3 Ser727 expression in WT and cKO L4 uninjured and injured DRGs. p-STAT3 Ser727 expression was normalised to STAT3, and then expressed as a fold change relative to WT uninjured levels. WT (n=3) and cKO (n=3); One-way ANOVA with Tukey comparison, p=0.2287. All statistical analysis is compared to WT uninjured levels, unless otherwise shown.

A well-studied and characterised gene associated with successful nerve regeneration is GAP43, which is more strongly expressed in sensory neurons following nerve injury (Schreyer and Skene, 1993; Chong et al., 1994; Zhang et al., 2005; Hunt et al., 2012). The importance of GAP43 expression in neurons has been shown both *in vivo* and *in vitro* (Meiri et al., 1988; Woolf et al., 1990; Schreyer and Skene, 1991; Schreyer et al., 1997; Cafferty et al., 2004).

To determine whether or not Schwann cell c-Jun elevation in the proximal stump could act as a positive signal to the neuron to express more GAP43 following nerve injury and therefore increase the chances of successful nerve repair was one of importance. To do this, WT and cKO mice with transected sciatic nerves for 48 hours, had their L4 DRG neurons (uninjured and injured) dissected and analysed by immunofluorescent labelling and Western blot analysis (Figures 6.9 and 6.10).

GAP43 expression in L4 DRG (uninjured and injured) neurons 48 hours after nerve transection from WT and cKO mice was significantly higher in WT injured (59%) compared to cKO injured (47%) whereas the uninjured levels in WT and cKO were not significantly different, 31% and 29% respectively (Figures 6.9A and 6.9B). This significant decrease in GAP43 expression in injured cKO neurons compared to WT injured was maintained when quantifiying only the strongest GAP43/NF200 expressing neurons as shown in Figure 6.9C. The results in Figure 6.9 suggest that Schwann cell c-Jun in the proximal stump is having a small but significant effect on the expression of GAP43 in neurons 48 hours after injury. since the number of GAP43 positive neurons in the cKO injured L4 DRG is lower compared to WT.

Western blot analysis of GAP43 expression in L4 DRGs (uninjured and injured) of WT and cKO mice correlated with the immunofluorescence results shown in Figure 6.9, and although the decrease in GAP43 elevation seen in cKO mice compared to WT, 2.4 fold compared to 3.1 fold, respectively, did not reach significance the trend was clear (Figure 6.10). The quantification suggests that GAP43 is elevated less in cKO mice L4 DRG neurons following injury compared to those of WT mice.

The results from Figures 6.9 and 6.10 suggest that the lack of Schwann cell c-Jun in the proximal stump is affecting the ability of L4 DRG neurons to up-regulate GAP43

expression. This difference in expression of GAP43 between WT and cKO L4 DRG neurons may be important in determining the outcome of growth cone progression, which is not addressed in this thesis (Skene and Virag, 1989).

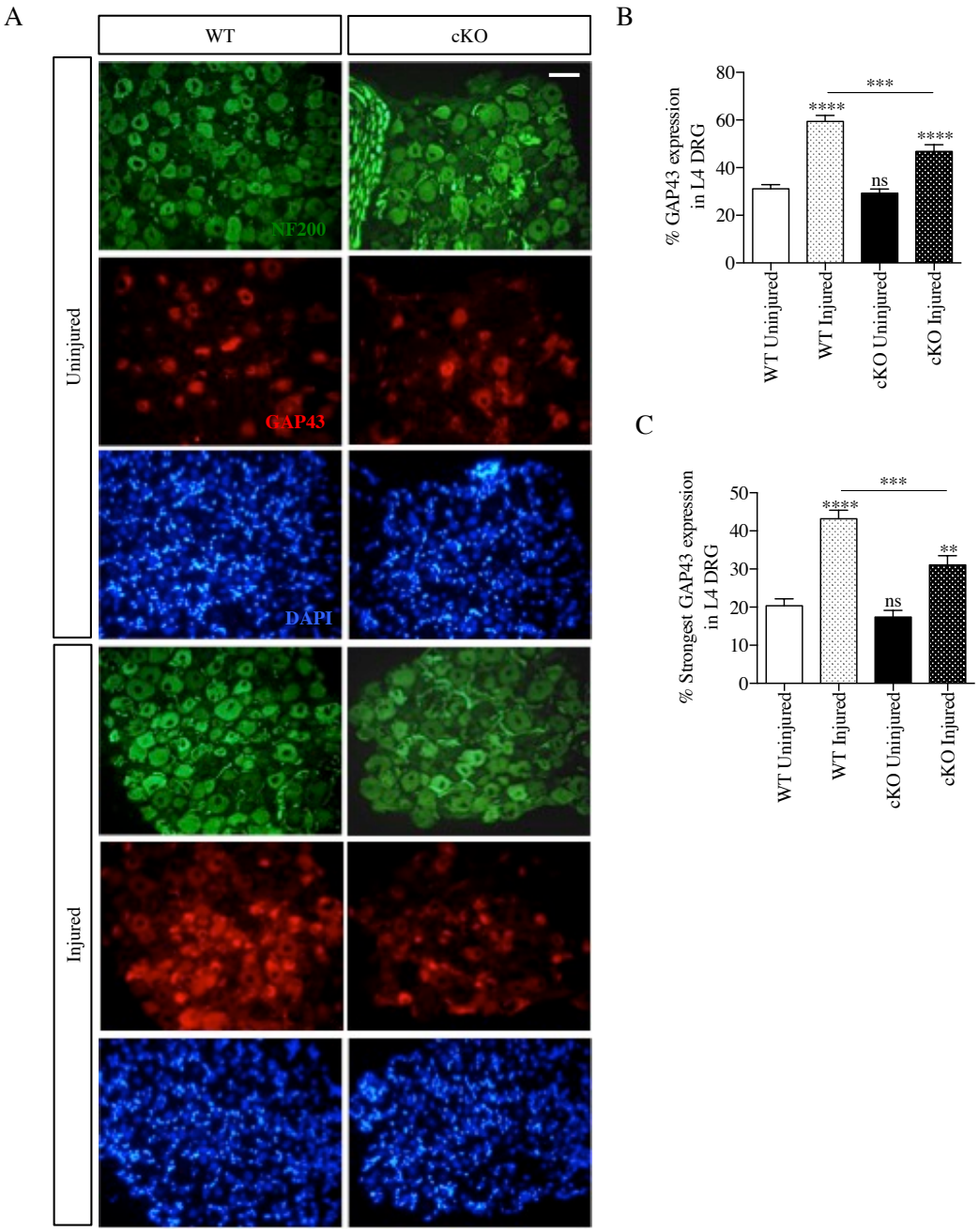

Figure 6.9 | GAP43 expression in L4 DRGs 48 hours after sciatic nerve transection
(A) 5µm thick L4 DRGs (uninjured and injured) cryosections from WT and cKO were immunolabelled with NF200 (neuronal marker) and GAP43 antibodies and with DAPI to label nuclei. Immunofluorescence images taken at x25 magnification showing the population of neurons (NF200 positive) that were also GAP43 positive in L4 uninjured and injured DRGs. (B) Quantification of the percentage of GAP43/NF200 positive neurons in WT and cKO L4 uninjured and injured DRG neurons. WT (n=3) and cKO (n=3); One-way ANOVA with Tukey comparison, $p<0.0001$. All statistical analysis is compared to WT uninjured levels, unless otherwise shown. (C) Quantification of the percentage of the strongest GAP43/NF200 positive neurons in WT and cKO L4 uninjured and injured DRG neurons. One-way ANOVA with Tukey comparison, $p<0.0001$. All statistical analysis is compared to WT uninjured levels, unless otherwise shown.

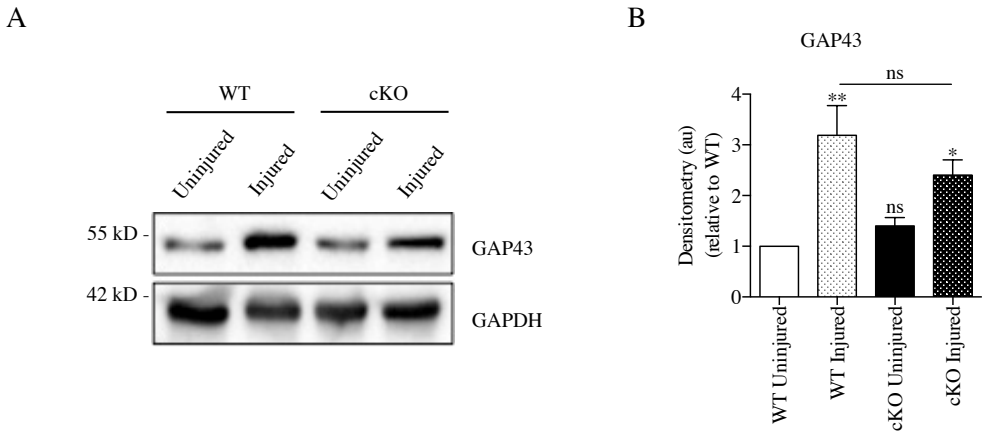

Figure 6.10 | Western blot of GAP43 expression in L4 DRGs 48 hours after sciatic nerve transection
(A) Representative Western blot of GAP43 expression in L4 uninjured and injured DRG protein extracts from WT and cKO mice 48 hours after sciatic nerve transection. GAPDH is used as a reference gene. (B) Quantification of the level of GAP43 expression in WT and cKO L4 uninjured and injured DRGs. GAP43 expression was normalised to GAPDH, and then expressed as a fold change relative to WT uninjured levels. WT (n=3) and cKO (n=3); One-way ANOVA with Tukey comparison, p=0.0014. All statistical analysis is compared to WT uninjured levels, unless otherwise shown.

Cytokine release has also been shown to induce expression of c-Jun, STAT3 and GAP43, so to address whether differential expression of some RAGs was due to macrophage populations, WT and cKO uninjured and injured L4 DRG neurons were quantified using F4/80 as a general macrophage marker, 48 hours after sciatic nerve transection. This experiment was repeated only twice, therefore no concrete conclusions can be drawn, but it provides a potential insight into what is happening. Levels of F4/80 expression were analysed by immunofluorescent labelling of L4 DRG sections and quantified to show that the level of macrophage expression in WT and cKO uninjured L4 DRGs was 21% and 27% respectively, and both levels were elevated to 41% (WT) and 42% (cKO) after sciatic nerve injury, shown in Figure 6.11. As the experiment was only done twice, the slight elevation of macrophages in the cKO uninjured may not be of significance because the presence of macrophages in the injured DRGs is very similar in WT and cKO mice.

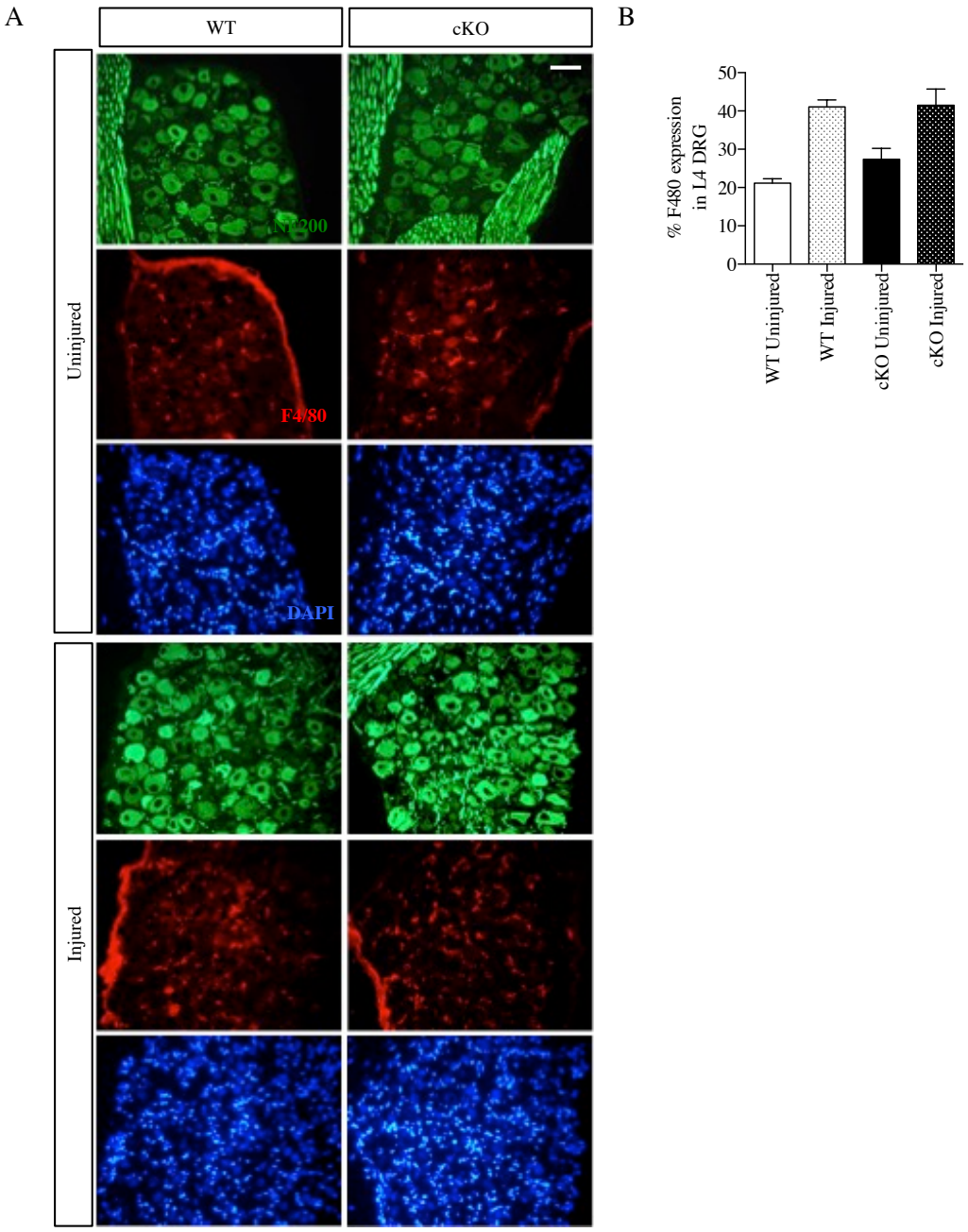

Figure 6.11 | Percentage of F480 positive macrophages in L4 DRGs 48 hours after sciatic nerve transection
(A) 5µm thick L4 DRGs (uninjured and injured) cryosections from WT and cKO were immunolabelled with NF200 (neuronal marker) and F4/80 (general macrophage marker) antibodies and with DAPI to label nuclei. Immunofluorescence images taken at x25 magnification showing the population of neurons (NF200 positive) that were also F4/80 positive in L4 uninjured and injured DRGs. (B) Quantification of the percentage of F4/80/NF200 positive neurons in WT and cKO L4 uninjured and injured DRG neurons. WT (n=2) and cKO (n=2). No statistical analysis was done.

6.2.2 Proximal stump Schwann cell c-Jun modestly affects neuronal outgrowth following a conditioning lesion *in vivo*

As mentioned earlier, axons of adult CNS nerves show very poor regeneration following nerve injury in contrast to those of peripheral nerves. The idea that increasing the ability of the neurons to respond to nerve injuries by upregulating important factors such as RAGs, is much discussed. CNS neurons following injury have limited expression of RAGs, compared to PNS neurons. As mentioned earlier, DRG neurons are unique in that they possess a single axon that is branched, with terminations both in the CNS and the PNS. A commonly used paradigm to increase the ability of CNS neurons to show axonal outgrowth following injury, is the "conditioning lesion paradigm". This is achieved by injuring the peripheral branch of DRG neurons before injuring the central branch, as the prior lesion of the peripheral branch primes the neuron to respond to the initial injury, so that when the central branch is injured, these primed neurons show some axonal outgrowth (McQuarrie, 1985; Ramer et al., 2000; Neumann et al., 2002; Qiu et al., 2002). Using this paradigm, motor neurons originating in the CNS and projecting to the PNS and peripheral branches of DRG neurons also show increased outgrowth after prior injury.

To address whether c-Jun elevation in proximal stump Schwann cells is important in the conditioning lesion effect, experiments were designed using WT and cKO mice. It is important to note however, that the following experiments were carried out only in the peripheral nerves, using the injury model described in Chapter 2, section 2.3.2.4. The comparison between the WT and cKO conditioning lesion effects is important as this is what would address the question of whether the absence of proximal stump Schwann cell c-Jun has a detrimental effect on the ability of neurons to be primed to an initial injury and therefore regenerate their injured axons. The effects from this lesion were analysed by assessing the number of positively regenerating axons using CGRP and galanin as markers for regenerating axons, at distances of 2mm and 3mm from the crush site in the PNS (sciatic notch). Although there is still extensive debate about which types of neurons both CGRP and galanin label, for the following experiments, they were used for analysis in the same way as Arthur-Farraj et al., 2012. These results are shown in Figures 6.12 and 6.13. The controls for these

experiments were a single crush for 2.5D, where regenerating axons were quantified in the same way as for the conditioning lesion experiment, using CGRP and galanin. (For full details of how the experiment was carried out and specific time points please refer to Chapter 2, section 2.3.1.4). Both CGRP and galanin primarily label sensory axons (Gibson et al., 1984; Li et al., 2004), yet this distinction is still widely debated as some suggest that both CGRP and galanin are also expressed in motor neurons (Holmes et al., 2000; Fontana et al., 2012).

A representative immunofluorescence image is shown in Figure 6.12A to demonstrate what CGRP positively labelled regenerating axons looked like. The number of CGRP positive regenerating axons in WT and cKO nerves 2.5D following nerve crush at 2mm are very similar, 6 and 5 respectively (Figure 6.12B). Following a conditioning lesion at this same distance of 2mm from the crush site, the number of CGRP positively labelled regenerating axons increases both in WT (14) and cKO (8) as shown in Figure 6.12C. In terms of the conditioning effect, this is working in both WT and cKO mice as there is an obvious increase in the number of positively labelled regenerating CGRP axons in both genotypes, when comparing 2.5D crush (Figure 6.12B) and conditioning lesion (Figure 6.12C). The marginal differences seen between WT and cKO CGRP positively labelled regenerating axons in the conditioning lesion experiment, suggest that Schwann cell c-Jun might have an effect on the priming of the DRG neurons to respond to the injury. However this does not reach significance, and it remains a trend (Figure 6.12C).

At a distance of 3mm from the crush site both at 2.5D after crush (Figure 6.12D) and following a conditioning lesion (Figure 6.12E), the number of positively labelled regenerating CGRP follow a similar trend to that seen at 2mm. The conditioning effect is still seen in both WT and cKO, where the number of WT regenerating axons increases from 2 (2.5D crush) to 7 (conditioning lesion) and cKO from 1 (2.5D crush) to 5 (conditioning lesion). Again this difference between WT and cKO conditioning lesion effect does not reach significance and remains a trend. One thing to note however, is that at a distance of 3mm compared to 2mm, there are fewer regenerating axons altogether in both WT and cKO, which is expected.

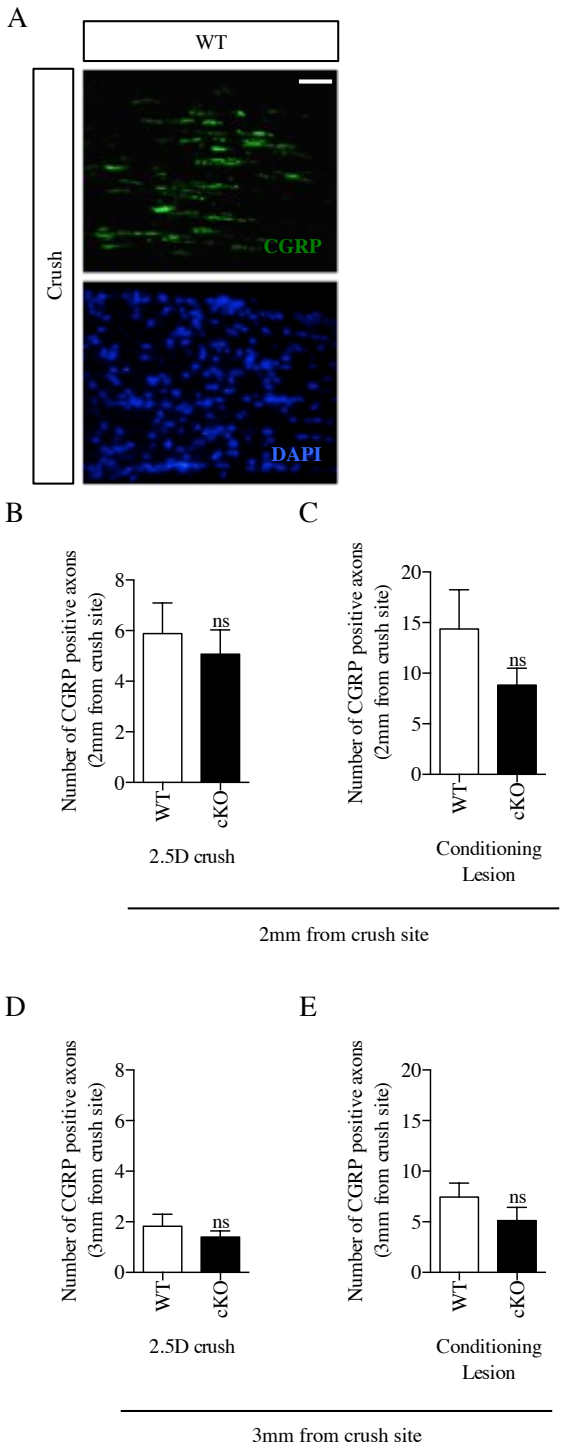

Figure 6.12 | CGRP positive axons in WT and cKO mice following crush and conditioned lesion *in vivo*
(A) 10µm thick longitudinal cryosections from 2.5D crushed WT sample. These sections were immunolabelled with CGRP (primarily recognises sensory neurons) antibody and with DAPI to label nuclei. A representative immunofluorescent image taken at x25 magnification to show an example of CGRP positively immunolabelled regenerating axons. Scale bar represents 50µm. (see Chapter 2, section 2.3.9.3 for full method of quantification) (B-C) Quantification to show the number of CGRP positively labelled regenerating axons at a distance of 2mm from the crush site were quantified. These CGRP positive axons were quantified from WT and cKO mice at 2.5D after crush (B) and following a conditioning lesion *in vivo* (C). (B) WT (n=4) and cKO (n=4); Mann-Whitney test, p=0.9714 /(C) WT (n=5) and cKO (n=5); Mann-Whitney test, p=0.6571. (D-E) Quantification to show the number of CGRP positively labelled regenerating axons at a distance of 3mm from the crush site were quantified. These CGRP positive axons were quantified from WT and cKO mice at 2.5D after crush (D) and following a conditioning lesion *in vivo* (E). (D) WT (n=4) and cKO (n=4); Mann-Whitney test, p=0.2063/ (E) WT (n=5) and cKO (n=5); Mann-Whitney test, p=0.3095. All statistical analysis is compared to WT.

Another commonly used marker to label regenerating axons is galanin. A representative immunofluorescence image is shown in Figure 6.13A to demonstrate what galanin positively labelled regenerating axons look like. WT and cKO nerve samples from 2.5D and conditioning lesion experiments used in CGRP analysis were also used to analyse the number of galanin positive axons. Figure 6.13 shows the results obtained from this analysis. Positively labelled galanin regenerating axons at 2mm from the crush site were higher in the conditioning lesion experiment in both WT and cKO nerves where positively labelled axons increased from 2 to 8 in WT and 2 to 6 in cKO (Figure 6.13B and 6.13C). There is no significant difference between these results, although a slight trend can be seen. At a distance of 3mm from the crush site, as was seen with CGRP labelled axons, overall the number of positive axons was less in both WT and cKO compared to the 2mm distance (Figure 6.13B-D). The analysis of galanin positive axons in WT and cKO mice both at 2.5D after crush and after conditioning lesion experiments show almost identical numbers in both situations (Figure 6.13D and 16.3E), suggesting that at this distance, Schwann cell c-Jun is not having a significant effect on the ability of galanin positive neurons to respond to the injury although numbers are small so this conclusion must be qualified.

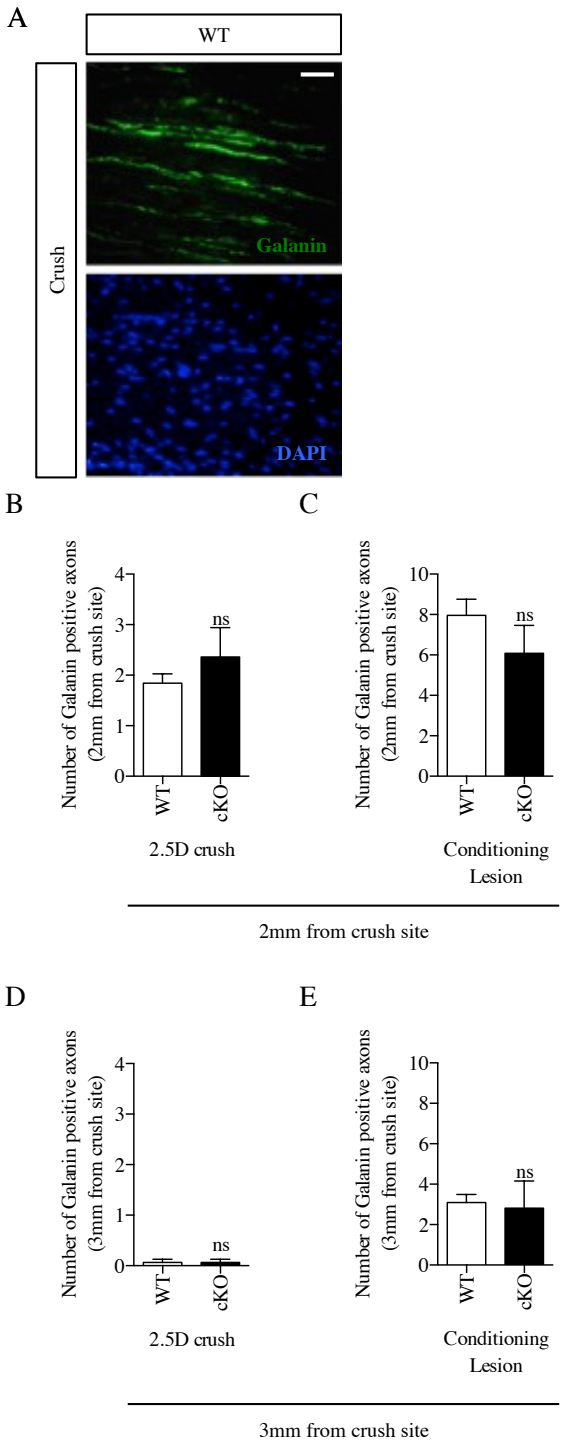

Figure 6.13 | Galanin positive axons in WT and cKO mice following crush and conditioned lesion *in vivo*
(A) 10µm thick longitudinal cryosections from 2.5D crushed WT sample. These sections were immunolabelled with galanin (recognises sensory and motorneurons) antibody and with DAPI to label nuclei. A representative immunofluorescent image taken at x25 magnification to show an example of galanin positively labelled regenerating axons. Scale bar represents 50µm. (see Chapter 2, section 2.3.9.3 for full method of quantification) (B-C) Quantification to show the number of galanin positively labelled regenerating axons at a distance of 2mm from the crush site were quantified. These galanin positive axons were quantified from WT and cKO mice at 2.5D after crush (B) and following a conditioning lesion *in vivo* (C). (B) WT (n=4) and cKO (n=4); Mann-Whitney test, p=0.5714 /(C) WT (n=5) and cKO (n=5); Mann-Whitney test, p=0.3429. (D-E) Quantification to show the number of galanin positively labelled regenerating axons at a distance of 3mm from the crush site were quantified. These galanin positive axons were quantified from WT and cKO mice at 2.5D after crush (D) and following a conditioning lesion *in vivo* (E). (D) WT (n=4) and cKO (n=4); Mann-Whitney test, p> 0.9999 / (E) WT (n=5) and cKO (n=5); Mann-Whitney test, p> 0.9999. All statistical analysis is compared to WT.

6.2.3 The effect of c-Jun elevation in proximal stump Schwann cells on neuronal outgrowth following a conditioning lesion *in vitro*

In vivo analysis of the number of regenerating axons determined by CGRP and galanin labelling (Figure 6.12 and Figure 6.13) suggested a possible trend towards the idea that Schwann cell proximal stump c-Jun expression might have a modest effect on the ability of neurons to regenerate following a conditioning lesion injury. With this in mind, it was of interest to see if this possible influence of Schwann cell c-Jun on neuronal outgrowth after a conditioning lesion could be tested using dissociated L4 DRG neurons in an *in vitro* model in which neurons are cultured on a permissive (PLL/laminin) and an inhibitory substrate (myelin) (for further details of the experimental procedure see Chapter 3, section 2.3.8.6).

To address this question, it was important to define certain parameters:
(i) the length of time the DRGs should be cultured for (ii) whether the myelin extracted is actually an inhibitory substrate (iii) whether both uninjured and injured L4 DRGs should be analysed and (iv) what concentration of myelin should be used.
Figure 6.14 summarises all the tests that were carried out using WT L4 DRGs to determine optimal culture conditions, although no quantification is shown. Figure 6.14A shows representative immunofluorescence images of WT uninjured L4 DRG neurons cultured on PLL/laminin for 24 hours or 48 hours to determine how much outgrowth was seen at these two time points. Several processes were seen at both time points, however at 48 hours the outgrowth was more evident. This experiment was repeated twice. Already by 24 hours considerable outgrowth seen from an injured L4 DRG, so this is why in Figure 6.14B, the WT uninjured and injured L4 DRGs were cultured for a shorter period of time of 20 hours. This was to test the effect of a conditioning lesion injury to the sciatic nerve on the amount of outgrowth from L4 DRG neurons on PLL/laminin and on a PLL/myelin surface in an uninjured and injured state. It is clear from this that at 20 hours after plating there in enough outgrowth from L4 DRG neurons plated on both PLL/laminin and PLL/myelin, but that injury induces more outgrowth in both situations. This difference between uninjured and injured is less obvious on PLL/myelin, therefore suggesting that myelin at a concentration of 10μg/ml is concentrated enough to inhibit axonal outgrowth.

This experiment was repeated twice, and from these results, the final test of what would be the best myelin substrate to use was determined by using only injured WT L4 DRG neurons. These neurons were cultured for 20 hours on four different substrates: (i) PLL/laminin as a positive control to show the culture was working (ii) PLL/myelin (10μg/ml) (iii) PLL/myelin (1μg/ml) (iv) PLL/laminin + myelin (1μg/ml). These experiments were repeated twice, and from the results in Figure 6.14C, it was clear that both concentrations of myelin had the same effect on outgrowth, and that whether myelin is present or not, the presence of laminin particularly overcomes the inhibitory effects of myelin. For these reasons, myelin was used at a concentration of 1μg/ml without laminin, however PLL/laminin was used in each experiment as a positive control.

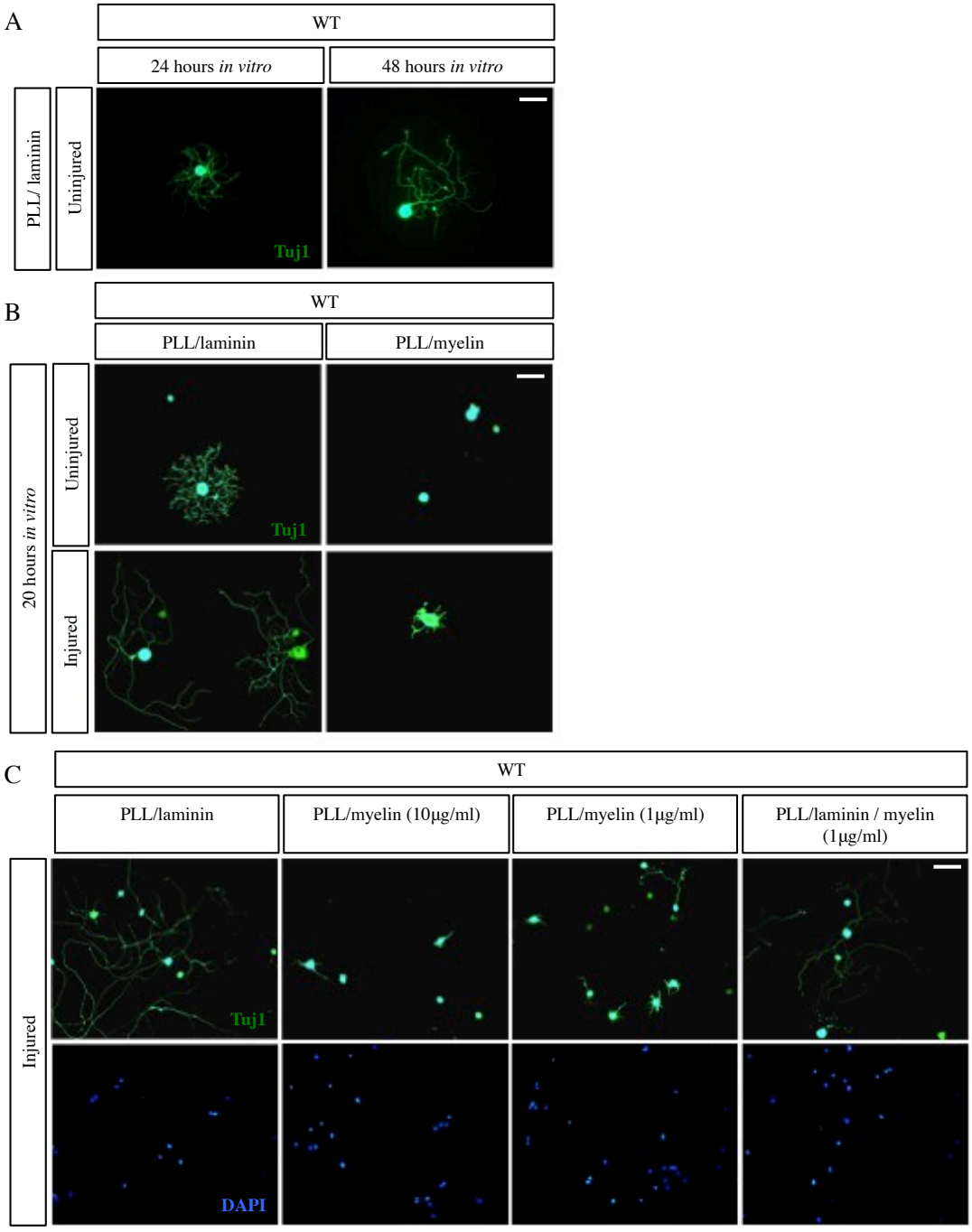

Figure 6.14 | Optimal DRG (conditioned lesion) culture conditions using PLL/laminin and PLL/myelin substrates
(A) 13mm round coverslips were fluorescently labelled with Tuj1 (neuronal marker) to determine the number of neurons present in the culture from WT uninjured L4 DRGs. These were cultured on PLL/laminin substrate for 24 hours or 48 hours *in vitro* before being fixed with 4% PFA. These are representative immunofluorescence images taken at x25 magnification. Scale bar represents 50µm. (B) 13mm round coverslips were fluorescently labelled with Tuj1 (neuronal marker) antibody to determine the number of neurons present in the culture from WT uninjured and injured (2.5D crush) L4 DRGs . Quantification not shown. These were cultured on PLL/laminin, PLL/myelin substrate for 20 hours *in vitro* before being fixed with 4% PFA. These are representative immunofluorescence images taken at x25 magnification. Scale bar represents 50µm. (C) 13mm round coverslips were fluorescently labelled with Tuj1 (neuronal marker) antibody and with DAPI (nuclear marker) to determine the number of neurons present in the culture from WT injured (2.5D crush) L4 DRGs. Quantification not shown. These DRGs were cultured on PLL/laminin or PLL/myelin (10µg/ml), PLL/myelin (1µg/ml) and PLL/laminin + myelin (1µg/ml) substrates for 20 hours *in vitro* before being fixed with 4% PFA. These are representative immunofluorescence images taken at x25 magnification. Scale bar represents 50µm.

Taking into account this information, L4 DRG cultures were prepared from both WT and cKO mice that had their sciatic nerves transected for 2.5D (conditioning injury) after which the injured L4 DRGs from these mice were dissociated and the neurons cultured for a further 20 hours (PLL/laminin) or 48 hours (PLL/myelin), which was the equivalent of the second injury *in vivo*. Figure 6.15A and 6.15B show immunofluorescence images of WT and cKO injured L4 DRG cultures on both PLL/laminin and PLL/myelin. It is clear that the growth seen on PLL/laminin is much greater than that seen on PLL/myelin. The cultures grown on PLL/laminin served as a positive control for the experiment, and no further analysis was carried out on these. From the WT and cKO myelin cultures, quantification of number of neurons with neurites with or without supporting cells and the length of the longest neurite with or without supporting cells, was carried out as described in Chapter 3, section 2.3.9.5. The quantification shown in Figure 6.15C and 6.15D demonstrates that the average number of neurons counted with neurites in each experiment from WT and cKO, was very similar regardless of whether these neurons had supporting cells associated with them or not. Of the neurons counted with neurites in both situations from WT and cKO mice (Figure 6.15E and 6.15F), it is clear that whether or not there are supporting glial cells around the neurons, the average length of the longest neurite is virtually the same between both genotypes. When there are no glial cells associated with the neurons, the length of the longest neurite in both WT and cKO is shorter overall, which is not surprising, as the glial cells can provide support to the neurons to be able to grow further and longer. The results shown in Figure 6.15 are preliminary as they were only repeated twice, however they indicate that *in vitro*, Schwann cell c-Jun does not affect the ability of neurons to grow on an inhibitory substrate following a conditioning lesion.

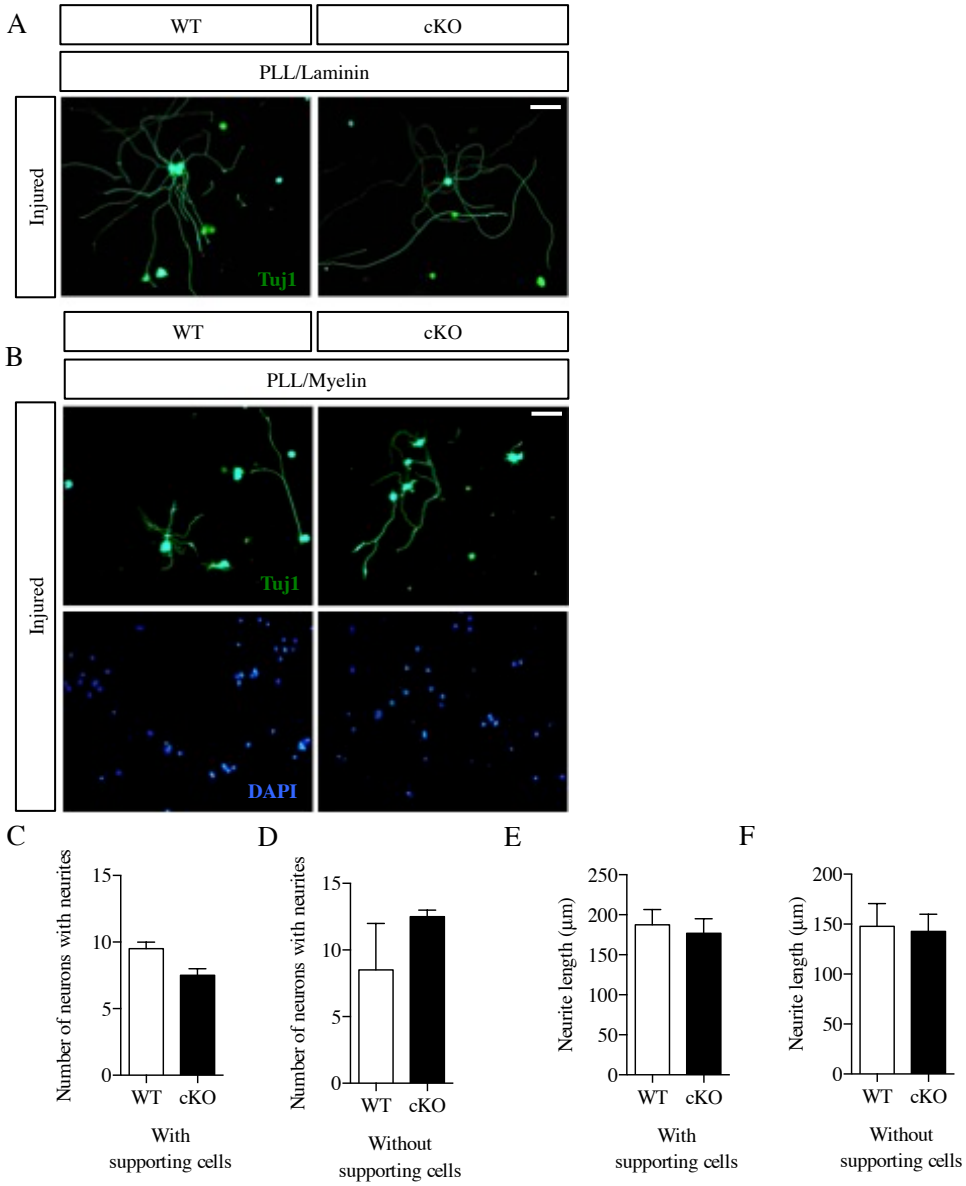

Figure 6.15 | Conditioned lesion L4 injured DRG cultures from WT and cKO mice
(A) 13mm round coverslips were fluorescently immunolabelled with Tuj1 (neuronal marker) antibody and DAPI to label nuclei, to determine the number of neurons present in the conditioned lesion L4 injured DRG culture from WT and cKO mice. These were cultured on PLL/laminin substrate for 20 hours *in vitro* before being fixed with 4% PFA. These are representative immunofluorescence images taken at x25 magnification. Scale bar represents 50µm. No quantification was made from these cultures, but they were used as a positive control to ensure that the culture was successful. (B) 13mm round coverslips were fluorescently labelled with Tuj1 (neuronal marker) antibody and with DAPI to label nuclei to determine the number of neurons present in the conditioned lesion L4 injured DRG culture from WT and cKO mice. These were cultured on PLL/myelin substrate for 20 hours *in vitro* before being fixed with 4% PFA. These are representative immunofluorescence images taken at x25 magnification. Scale bar represents 50µm. (C-D) Quantification of the number of neurons (Tuj1 positive) that had neurites as well as supporting glial cells associated (C) and the number of neurons that had neurites without the presence of supporting glial cells (D). This analysis was done both in WT and cKO cultures. (n=2, no statistical analysis was done). (E-F) Quantification of the length of the longest neurite of neurons (Tuj1 positive) that had supporting glial cells associated (C) and the length of the longest neurite of those neurons without supporting glial cells (E). This analysis was done both in WT and cKO cultures. WT (n=2) and cKO (n=2). No statistical analysis was done.

6.3 Discussion

Peripheral nerve injury causes activation of neurons resulting in a switch from a signalling mode to a growth one which promotes axonal outgrowth and successful peripheral nerve regeneration. The idea underlying this chapter was to try to understand the mechanisms through which this crucial switch takes place within the DRGs and whether Schwann cells might have a role to play. It is known that Schwann cells of the distal stump and c-Jun within these Schwann cells is important in successful peripheral nerve regeneration (Arthur-Farraj et al., 2012), however, results shown so far also suggest that Schwann cell c-Jun of the proximal stump might also be important in the process of peripheral nerve regeneration. Evidence is provided to support the idea that the lack of c-Jun in Schwann cells and therefore the lack of its up-regulation in Schwann cells of cKO mice, results in reduced levels of expression of certain RAGs, (particularly c-Jun and more strongly GAP43) in the DRGs. Both of these are important in the neuronal cell response to nerve injury (Abe and Cavalli, 2008; Ma and Willis, 2015; Chandran et al., 2016).

The rapid up-regulation of c-Jun seen in Schwann cells at the injury site as early as 1 hour after nerve transection, fits well with the early onset of RAG up-regulation that can be seen as early as 6 hours after nerve transection (Hunt et al., 2012). This strongly suggests that c-Jun would be present in Schwann cells at the necessary time required to drive a signalling cascade that would result in neuronal growth activation. Although the sciatic nerve is made up of many different cell types, the majority are Schwann cells and it is unlikely that at the early time point of 1 hour after nerve transection, invading cells such as macrophages would be present in significant numbers except at the immediate injury site, nevertheless these cell types should be taken into consideration at longer time points such as 48 hours after nerve transection.

Although it is rather surprising that lack of Schwann cell c-Jun does not cause a greater down-regulation in neuronal expression of c-Jun in injured L4 DRGs compared to WT (Figures 6.1-6.2), it is possible to conclude that even the modest difference in c-Jun expression shown is enough to alter the neuronal cell body response to axotomy. The effect of proximal stump Schwann cell c-Jun on its neuronal expression is likely to be important early on following nerve injury (up to 48

hours) when the neuron is primed to change its program from one of signal transmission to target tissues, to one of growth in response to nerve injury. This important regulatory effect of c-Jun elevation in neurons is strengthened by recent work (Chandran et al., 2016), which shows that c-Jun is at the hub of the gene regulatory network controlling the peripheral nerve injury induced axonal growth program.

The difference in uninjured levels of F4/80 seen between WT and cKO L4 DRGs may not be significant, although it may provide a possible explanation for the surprising result seen in p-STAT3 Ser727 expression levels. Although the differences between WT and cKO uninjured F4/80 levels in L4 DRG neurons are marginal (WT 21% and cKO 27%) and not significantly different, this slight increase in macrophage numbers in cKO might suggest that there are higher levels of cytokines such as TNF-α IL-1 and IL-6 present in the cKO and these are known to increase phosphorylation of STAT3 (Qiu et al., 2005; Nguyen et al., 2015).

Expression of GAP43 is an important part of the neuronal activation programme, as in its absence regeneration is impaired (Aigner et al., 1995). Figures 6.9 and 6.10 show that lack of Schwann cell c-Jun affects the expression of GAP43 in injured L4 DRG neurons, it would therefore be interesting to find out if this difference between WT and cKO is a transient one, or if it is maintained over long periods of time. Preliminary experiments in which analysis of cryosections of uninjured and injured (7D cut) WT and cKO L4 DRGs via immunofluorescent labelling with GAP43, NF200 and DAPI was carried out, suggest that this difference is a transient one. 7D following nerve cut, the levels of GAP43 expressed in L4 injured DRG neurons in WT and cKO are the same. This experiment was only repeated twice and was not analysed statistically (data not shown). It may be that levels of Schwann cell c-Jun in the proximal stump are important for the initial switch in the neuronal program from one of “transmission” to one of “growth” (Abe and Cavalli, 2008), but after this period, even though proximal stump c-Jun levels remain elevated, this is no longer critical/essential in terms of neuronal response to axotomy and in particular that of GAP43.

WT and c-Jun overexpressing mice, in particular OE/+ are very similar in terms of their nerve architecture, even though c-Jun is substantially elevated in Schwann cells. For this reason, in order to further elucidate the importance of Schwann cell c-Jun elevation in the proximal stump following injury and whether it has an effect in RAG expression, and therefore successful axonal regeneration, the OE/+ mouse could be analysed in a similar way as that shown in Figures 6.1-6.10. Preliminary data suggests that in terms of GAP43 expression (as this was most affected by lack of Schwann cell c-Jun), there seems to already be an increase in its neuronal expression in L4 uninjured DRGs compared to WT levels. This experiment has only been done once, and so is statistically insignificant, yet it would slot in very nicely with the hypothesis that high expression of Schwann cell c-Jun is important in the neuronal cell body response to nerve axotomy and determines the levels of expression of certain RAGs.
L4 DRG neurons from both WT and OE/+ mice could also be used to replicate the *in vitro* conditioning lesion model shown above (Figure 6.15), as well as creating DRG-Schwann cell co-cultures to determine if already elevated Schwann cell c-Jun in OE/+ mice would result in better initial axonal outgrowth compared to WT.

It is possible that although the lack of Schwann cell c-Jun has a modest effect *in vivo* on the ability of DRG neurons to respond to injury in the experiments tested here, this effect could be stronger if the conditioning lesion paradigm were carried out in the central nervous system, where the environment is shown to limit central nerve regeneration. Preliminary results suggest that when spinal cord sections are immunofluorescently labelled with cholera toxin B (CTB) following a conditioning lesion where firstly the sciatic nerve is cut and a crush is performed 7D later, at the level of T6 in the spinal cord, the number of axonal sprouts growing past the lesion in the CNS is higher in WT compared to cKO (unpublished observations Professor Elizabeth Bradbury). In these experiments the lack of Schwann cell c-Jun appears to be important in the conditioning lesion paradigm.

7. General discussion

Very early studies indicated the importance of Schwann cells in peripheral nerve development and following nerve injury. A key transcription factor that has a critical importance during development and following nerve injury where it amplifies the Schwann cell injury response is c-Jun. The work presented in this thesis has highlighted further the importance of the transcription factor c-Jun in Schwann cell biology.

The work presented in this thesis has used two contrasting mouse models to study the effect of levels of c-Jun expression in Schwann cells. First, c-Jun elevation in Schwann cells was studied using mice where these levels were overexpressed in a gene-dose dependent manner from development into adulthood, and the effects of this up-regulation following nerve injury (using sciatic nerve crush as a model) were also studied. Second, the rapid Schwann cell c-Jun elevation in the proximal stump following nerve transection was measured. To study effects of this elevation in the proximal stump on the neuronal cell body response to nerve injury, responses in proximal stump and in the neurons of the L4 DRG from mice in which c-Jun was conditionally ablated (cKO) from Schwann cells were compared with the response of neurons in the L4 DRG in WT nerves.

There is clear evidence from this and previous studies to suggest that controlling the levels of Schwann cell c-Jun elevation is crucial for the successful development and function of peripheral nerves, as well as peripheral nerve regeneration following injury (Chapters 3 and 4).

The new Schwann cell specific c-Jun overexpressing mice (OE/+ and OE/OE) characterised in Chapter 3 have provided further insight *in vivo* of the effects that c-Jun elevation in Schwann cells has on many aspects of nerve development and Schwann cell biology. Some of these findings corroborate previous results from *in vitro* work, showing that c-Jun is a negative regulator of myelination and the antagonistic relationship between Krox20 and c-Jun (Parkinson et al., 2008). One of the most important findings from the work shown in Chapter 3, which characterised OE/+ and OE/OE nerves, showed that the c-Jun elevation seen in Schwann cells of

uninjured nerves early in development is still maintained into adulthood. It is this maintenance of Schwann cell c-Jun elevation, particularly in OE/+ nerves, which provides an *in vivo* model to study the effects of c-Jun elevation in Schwann cells both at short and long time points following nerve injury, as described in Chapter 4. It is important to note as well, that this work has emphasised that excessive c-Jun elevation (OE/OE) is detrimental to nerve development and function, resulting in severe phenotypic abnormalities.

It is already well known that c-Jun is a key amplifier of the Schwann cell injury response (Arthur-Farraj et al., 2012), however through the evidence shown in the thesis, it has become clearer that c-Jun elevation in Schwann cells needs to be finely controlled, as excessive c-Jun elevation is detrimental both during nerve development and after injury.

Although at first glance it may seem that overexpressing Schwann cell c-Jun might be key to accelerating peripheral nerve regeneration because axon outgrowth after nerve injury is slower in cKO mice, at least initially, suggesting that elevating c-Jun levels further might promote faster axonal growth (Arthur-Farraj et al. 2012), the evidence shown above has highlighted that fact that the picture is more complex, This is because c-Jun expression affects aspects of Schwann cell biology, such as myelination, which are crucial to functional recovery. It may be important to design a system in which c-Jun elevation in Schwann cells can be finely regulated in a dose-dependent manner in order to achieve the maximum c-Jun elevation that promotes faster regeneration without significant effects on remyelination. This could be achieved using an inducible transgenic mouse, or by finding a drug delivery mechanism that can elevate c-Jun in a dose-dependent manner for a limited period of time after injury.

The levels of c-Jun elevation in Schwann cells after injury are important not only in determining the terrain into which newly regenerating axons grow, they may also however, be important in the proximal stump following a nerve transection in influencing the way in which the neuronal cell body responds to injury (Chapters 5 and 6).

Schwann cell c-Jun elevation in the proximal stump following nerve injury is rapid and maintained over several hours. This elevation has a mild effect on the ability of the neuronal cell body to express RAGs and therefore determine the neuronal outgrowth seen following injury. In order to confirm the importance of c-Jun elevation in proximal stump Schwann cells on the neuronal cell body response to injury, a wider analysis of RAG expression would need to be carried out, as this thesis looks at a few RAG candidates from the wide network that is known. It would also be interesting to use the c-Jun overexpressing mouse to determine whether or not with higher levels of c-Jun elevation, more RAG expression is seen in neurons, and whether this results in more neuronal outgrowth.

In conclusion, Schwann cell c-Jun following nerve injury in the proximal stump may be influencing the ability of neurons to respond to nerve injury, however a more in depth analysis would need to be carried out to confirm this finding.

The new Schwann cell specific c-Jun overexpressing mouse provides a robust tool for studying the importance of c-Jun elevation in Schwann cells following nerve injury. This is of importance; especially in the ageing process and following chronic nerve injury, where levels of c-Jun elevation falter. Further studies using this c-Jun overexpressing mouse might provide an insight into how c-Jun expression can be manipulated in a clinical setting, therefore translating work from the “bench side” to the “bedside”.

8. References

Abe, N., & Cavalli, V. (2008). Nerve injury signaling. Current Opinion in Neurobiology, 18(3), 276–283. https://doi.org/10.1016/j.conb.2008.06.005

Aguayo, AJ. Charron, L. Bray, GM. (1976a) Potential of Schwann cells from unmyelinated nerves to produce myelin: a quantitative ultrastructural and radiographic study. J Neurocytol **5**:565–573.

Aguayo, AJ. Martin, JB. & Gray, GM. (1972) Effects of nerve growth factor antiserum on peripheral unmyelinated nerve fibers. Acta Neuropathol. (Berl.) 20: 288-298.

Aigner, L., Arber, S., Kapfhammer, J. P., Laux, T., Schneider, C., Botteri, F., … Caroni, P. (1995). Overexpression of the neural growth-associated protein GAP-43 induces nerve sprouting in the adult nervous system of transgenic mice. Cell, 83(2), 269–278. https://doi.org/10.1016/0092-8674(95)90168-X

Ambron, R. T., & Walters, E. T. (1996). Priming events and retrograde injury signals. A new perspective on the cellular and molecular biology of nerve regeneration. Molecular Neurobiology, 13(1), 61–79. https://doi.org/10.1007/BF02740752

Aquino, J. B., Hjerling-Leffler, J., Koltzenburg, M., Edlund, T., Villar, M. J., & Ernfors, P. (2006). In vitro and in vivo differentiation of boundary cap neural crest stem cells into mature Schwann cells. Experimental Neurology, 198(2), 438–449. https://doi.org/10.1016/j.expneurol.2005.12.015

Armati, P. (2007). The Biology of Schwann Cells. Development, Differntiation and Immunomodulation, 1–264. https://doi.org/10.1017/CBO9780511541605

Arthur-Farraj, P. J., Latouche, M., Wilton, D. K., Quintes, S., Chabrol, E., Banerjee, A., … Jessen, K. R. (2012). c-Jun Reprograms Schwann Cells of Injured Nerves to Generate a Repair Cell Essential for Regeneration. Neuron, 75(4), 633–647. https://doi.org/10.1016/j.neuron.2012.06.021

Arthur-Farraj, P., Wanek, K., Hantke, J., Davis, C. M., Jayakar, A., Parkinson, D. B., … Jessen, K. R. (2011). Mouse schwann cells need both NRG1 and cyclic AMP to myelinate. Glia, 59(5), 720–733. https://doi.org/10.1002/glia.21144

Baldin, V., Lukas, J., Marcote, M. J., Pagano, M., & Draetta, G. (1993). Cyclin D 1 is a nuclear protein required for cell cycle progression in G1, 812–821.

Banner, L. R., & Patterson, P. H. (1994). Major changes in the expression of the mRNAs for cholinergic differentiation factor/leukemia inhibitory factor and its receptor after injury to adult peripheral nerves and ganglia. Proceedings of the National Academy of Sciences of the United States of America, 91(15), 7109–13. https://doi.org/10.1073/pnas.91.15.7109

Bareyre, F. M., Garzorz, N., Lang, C., Misgeld, T., Büning, H., & Kerschensteiner, M. (2011). In vivo imaging reveals a phase-specific role of STAT3 during central and peripheral nervous system axon regeneration. Proceedings of the National Academy of Sciences of the United States of America, 108(15), 6282–6287. https://doi.org/10.1073/pnas.1015239108

Barrette, B., Hébert, M.-A., Filali, M., Lafortune, K., Vallières, N., Gowing, G., … Lacroix, S. (2008). Requirement of Myeloid Cells for Axon Regeneration. Journal of Neuroscience, 28(38), 9363–9376. https://doi.org/10.1523/JNEUROSCI.1447-08.2008

Behrens, A., Sibilia, M., David, J. P., Möhle-Steinlein, U., Tronche, F., Schütz, G., & Wagner, E. F. (2002). Impaired postnatal hepatocyte proliferation and liver regeneration in mice lacking c-jun in the liver. EMBO Journal, 21(7), 1782–

1790. https://doi.org/10.1093/emboj/21.7.1782
Ben-Yaakov, K., Dagan, S. Y., Segal-Ruder, Y., Shalem, O., Vuppalanchi, D., Willis, D. E., … Fainzilber, M. (2012). Axonal transcription factors signal retrogradely in lesioned peripheral nerve. The EMBO Journal, 31(6), 1350–63. https://doi.org/10.1038/emboj.2011.494
Bermingham, J. R., Scherer, S. S., O'Connell, S., Arroyo, E., Kalla, K. A., Powell, F. L., & Rosenfeld, M. G. (1996). Tst-1/Oct-6/SCIP regulates a unique step in peripheral myelination and is required for normal respiration. Genes and Development, 10(14), 1751–1762. https://doi.org/10.1101/gad.10.14.1751
Birchmeier, C., & Bennett, D. L. H. (2016). Neuregulin/ErbB Signaling in Developmental Myelin Formation and Nerve Repair. Current Topics in Developmental Biology (1st ed., Vol. 116). Elsevier Inc. https://doi.org/10.1016/bs.ctdb.2015.11.009
Birchmeier, C., & Nave, K. A. (2008). Neuregulin-1, a key axonal signal that drives schwann cell growth and differentiation. Glia, 56(14), 1491–1497. https://doi.org/10.1002/glia.20753
Bixby, S., Kruger, G. M., Mosher, J. T., Joseph, N. M., & Morrison, S. J. (2002). Cell-intrinsic differences between stem cells from different regions of the peripheral nervous system regulate the generation of neural diversity. Neuron, 35(4), 643–656. https://doi.org/10.1016/S0896-6273(02)00825-5
Blanchard, A. D., Sinanan, A., Parmantier, E., Zwart, R., Broos, L., Meyer, D., … Mirsky, R. (1996). Oct-6 (SCIP/Tst-1) is expressed in Schwann cell precursors, embryonic Schwann cells, and postnatal myelinating Schwann cells: Comparison with Oct- 1, Krox-20, and Pax-3. Journal of Neuroscience Research, 46(5), 630–640. https://doi.org/10.1002/(SICI)1097-4547(19961201)46:5<630::AID-JNR11>3.0.CO;2-0
Blom, C. L., Martensson, L. B., Dahlin, L.B. (2014). Nerve-injury induced c-Jun activation in Schwann cells is JNK independent. Hindawi Publishing Corporation. http://dx.doi.org/10.1155/2014/392971
Bolin, L. M., Verity, a N., Silver, J. E., Shooter, E. M., & Abrams, J. S. (1995). Interleukin-6 production by Schwann cells and induction in sciatic nerve injury. Journal of Neurochemistry, 64(2), 850–858.
Brennan, A., Dean, C. H., Zhang, A. L., Cass, D. T., Mirsky, R., & Jessen, K. R. (2000). Endothelins control the timing of Schwann cell generation in vitro and in vivo. Developmental Biology, 227(2), 545–57. https://doi.org/10.1006/dbio.2000.9887
Britsch, S., Li, L., Kirchhoff, S., Theuring, F., Brinkmann, V., Birchmeier, C., & Riethmacher, D. (1998). The ErbB2 and ErbB3 receptors and their ligand, neuregulin-1, are essential for development of the sympathetic nervous system. Genes and Development, 12(12), 1825–1836. https://doi.org/10.1101/gad.12.12.1825
Buchser, W. J., Smith, R. P., Pardinas, J. R., Haddox, C. L., Hutson, T., Moon, L., … Lemmon, V. P. (2012). Peripheral nervous system genes expressed in central neurons induce growth on inhibitory substrates. PLoS ONE, 7(6). https://doi.org/10.1371/journal.pone.0038101
Bunge, M. B., Williams, A. K., & Wood, P. M. (1982). Neuron-schwann cell interaction in basal lamina formation. Developmental Biology, 92(2), 449–460. https://doi.org/10.1016/0012-1606(82)90190-7
Bunge, R. P. (1993). Expanding roles for the Schwann cell: ensheathment, myelination, trophism and regeneration. Current Opinion in Neurobiology, 3(5),

805–809. https://doi.org/10.1016/0959-4388(93)90157-T
Bunge, R. P., Bunge, M. B., & Bates, M. (1989). Movements of the Schwann cell nucleus implicate progression of the inner (axon-related) Schwann cell process during myelination. Journal of Cell Biology, 109(1), 273–284. https://doi.org/10.1083/jcb.109.1.273
Cafferty, W. B. J., Gardiner, N. J., Das, P., Qiu, J., McMahon, S. B., & Thompson, S. W. N. (2004). Conditioning injury-induced spinal axon regeneration fails in interleukin-6 knock-out mice. The Journal of Neuroscience : The Official Journal of the Society for Neuroscience, 24(18), 4432–43. https://doi.org/10.1523/JNEUROSCI.2245-02.2004
Cajal,R. (1928). Degeneration and regeneration of the nervous system. London, p484
Cattin, A. L., Burden, J. J., Van Emmenis, L., MacKenzie, F. E., Hoving, J. J. A., Garcia Calavia, N., … Lloyd, A. C. (2015). Macrophage-Induced Blood Vessels Guide Schwann Cell-Mediated Regeneration of Peripheral Nerves. Cell, 162(5), 1127–1139. https://doi.org/10.1016/j.cell.2015.07.021
Chakraborty, A., Diefenbacher, M. E., Mylona, A., Kassel, O., & Behrens, A. (2015). The E3 ubiquitin ligase Trim7 mediates c-Jun/AP-1 activation by Ras signalling. Nature Communications, 6, 6782. https://doi.org/10.1038/ncomms7782
Chandran, V., Coppola, G., Nawabi, H., Omura, T., Versano, R., Huebner, E. A., … Geschwind, D. H. (2016). A Systems-Level Analysis of the Peripheral Nerve Intrinsic Axonal Growth Program. Neuron, 89(5), 956–970. https://doi.org/10.1016/j.neuron.2016.01.034
Chaudhry, V. & Cornblath, D.R. (1992). Wallerian degeneration in human nerves: serial electrophysiological studies. Muscle and nerve, 15 (6), pp.687-693
Cheng, L., & Mudge, A. W. (1996). Cultured Schwann cells constitutively express the myelin protein P0. Neuron, 16(2), 309–319. https://doi.org/10.1016/S0896-6273(00)80049-5
Cho, Y., Sloutsky, R., Naegle, K. M., & Cavalli, V. (2013). Erratum: Injury-induced HDAC5 nuclear export is essential for axon regeneration (Cell (2013) 155 (894-908). Cell, 161(3), 691. https://doi.org/10.1016/j.cell.2015.04.019
Chong, M. S., Reynolds, M. L., Irwin, N., Coggeshall, R. E., Emson, P. C., Benowitz, L. I., & Woolf, C. J. (1994). GAP-43 expression in primary sensory neurons following central axotomy. The Journal of Neuroscience : The Official Journal of the Society for Neuroscience, 14(7), 4375–84. Retrieved from http://www.ncbi.nlm.nih.gov/pubmed/8027785
Coleman, M. P., Conforti, L., Buckmaster, E. A., Tarlton, A., Ewing, R. M., Brown, M. C., … Perry, V. H. (1998). An 85-kb tandem triplication in the slow Wallerian degeneration (Wlds) mouse. Proceedings of the National Academy of Sciences of the United States of America, 95(17), 9985–90. https://doi.org/10.1073/pnas.95.17.9985
Collier, H. J., Warner, B. T., & Skerry, R. (1961). MULTIPLE TOE-PINCH METHOD FOR TESTING ANALGESIC DRUGS BY.
Corfas, G., Velardez, M. O., Ko, C.-P., Ratner, N., & Peles, E. (2004). Mechanisms and Roles of Axon–Schwann Cell Interactions. The Journal of Neuroscience, 24(42), 9250–9260. https://doi.org/10.1523/JNEUROSCI.3649-04.2004
Cruz, C. D., & Cruz, F. (2007). The ERK 1 and 2 pathway in the nervous system: from basic aspects to possible clinical applications in pain and visceral dysfunction. Current Neuropharmacology, 5(4), 244–52. https://doi.org/10.2174/157015907782793630

D'Antonio, M., Droggiti, a, Feltri, M. L., Roes, J., Wrabetz, L., Mirsky, R., & Jessen, K. R. (2006). TGFbeta type II receptor signaling controls Schwann cell death and proliferation in developing nerves. Journal of Neuroscience, 26(33), 8417–8427. https://doi.org/10.1523/JNEUROSCI.1578-06.2006

Dailey, a T., Avellino, a M., Benthem, L., Silver, J., & Kliot, M. (1998). Complement depletion reduces macrophage infiltration and activation during Wallerian degeneration and axonal regeneration. The Journal of Neuroscience : The Official Journal of the Society for Neuroscience, 18(17), 6713–22. Retrieved from http://www.ncbi.nlm.nih.gov/pubmed/9712643

David, S., & Aguayo, A. J. (1981). Axonal Elongation into Peripheral Nervous System "Bridges" after Central Nervous System Injury in Adult Rats. Science, 214(4523), 931–933. https://doi.org/0036-8075/81/1120

Davies, S. J., Fitch, M. T., Memberg, S. P., Hall, a K., Raisman, G., & Silver, J. (1997). Regeneration of adult axons in white matter tracts of the central nervous system. Nature, 390(6661), 680–3. https://doi.org/10.1038/37776

Decker, L., Desmarquet-Trin-Dinh, C., Taillebourg, E., Ghislain, J., Vallat, J.-M., & Charnay, P. (2006). Peripheral myelin maintenance is a dynamic process requiring constant Krox20 expression. The Journal of Neuroscience : The Official Journal of the Society for Neuroscience, 26(38), 9771–9779. https://doi.org/10.1523/JNEUROSCI.0716-06.2006

DeFelipe, C., Hunt, S. P., De Felipe, C., & Hunt, S. P. (1994). The differential control of c-jun expression in regenerating sensory neurons and their associated glial cells. The Journal of Neuroscience : The Official Journal of the Society for Neuroscience, 14(5), 2911–23. Retrieved from http://www.ncbi.nlm.nih.gov/pubmed/8182448

Deng, T., & Karin, M. (1992). Construction expression protein transcription AP-1-responsive, 89(September), 8572–8576.

Dent, E. W., & Meiri, K. F. (1998). Distribution of phosphorylated GAP-43 (neuromodulin) in growth cones directly reflects growth cone behavior. Journal of Neurobiology, 35(3), 287–299. https://doi.org/10.1002/(SICI)1097-4695(19980605)35:3<287::AID-NEU6>3.0.CO;2-V

Diehl, J. A. (2002). Cycling to cancer with cyclin D1. Cancer Biology and Therapy, 1(3), 226–231. https://doi.org/10.4161/cbt.72

Doddrell, R. D. S., Dun, X.-P., Moate, R. M., Jessen, K. R., Mirsky, R., & Parkinson, D. B. (2012). Regulation of Schwann cell differentiation and proliferation by the Pax-3 transcription factor. Glia, 60(9), 1269–78. https://doi.org/10.1002/glia.22346

Dong, Z., Sinanan, A., Parkinson, D., Parmantier, E., Mirsky, R., & Jessen, K. (1999). Schwann cell development in embryonic mouse nerves. Journal of Neuroscience Research, 348(January), 334–348. https://doi.org/10.1002/(SICI)1097-4547(19990515)56:4<334::AID-JNR2>3.0.CO;2-# [pii]

Dubový, P., Jančálek, R., & Kubek, T. (2013). Role of inflammation and cytokines in peripheral nerve regeneration. International Review of Neurobiology (1st ed., Vol. 108). Elsevier Inc. https://doi.org/10.1016/B978-0-12-410499-0.00007-1

Duronio, R. J., & Xiong, Y. (2016). Signaling Pathways that Control Cell Proliferation, 1–13.

Dyck, PJ. & Hopkins, AP. (1972) Electron microscopic observations on degeneration and regeneration of unmyelinated fibres. Brain, 95, 223-234.

Erez, H., Malkinson, G., Prager-Khoutorsky, M., De Zeeuw, C. I., Hoogenraad, C. C., & Spira, M. E. (2007). Formation of microtubule-based traps controls the sorting

and concentration of vesicles to restricted sites of regenerating neurons after axotomy. Journal of Cell Biology, 176(4), 497–507. https://doi.org/10.1083/jcb.200607098

Fagoe, N. D., Attwell, C. L., Kouwenhoven, D., Verhaagen, J., & Mason, M. R. J. (2015). Overexpression of ATF3 or the combination of ATF3, c-Jun, STAT3 and Smad1 promotes regeneration of the central axon branch of sensory neurons but without synergistic effects. Human Molecular Genetics, 24(23), 6788–6800. https://doi.org/10.1093/hmg/ddv383

Feltri, M. L., D'Antonio, M., Previtali, S., Fasolini, M., Messing, A., & Wrabetz, L. (1999). P0-Cre transgenic mice for inactivation of adhesion molecules in Schwann cells. Annals of the New York Academy of Sciences. https://doi.org/10.1111/j.1749-6632.1999.tb08574.x

Feltri, M. L., Porta, D. G., Previtali, S. C., Nodari, A., Migliavacca, B., Cassetti, A., … Wrabetz, L. (2002). Conditional disruption of NL 1 integrin in Schwann cells impedes interactions with axons, 199–209. https://doi.org/10.1083/jcb.200109021

Feltri, M. L., Poitelon, Y., & Previtali, S. C. (2016). How Schwann Cells Sort Axons New Concepts. The Neuroscientist, 1(14), 1–14. https://doi.org/10.1177/1073858415572361

Finzsch, M., Schreiner, S., Kichko, T., Reeh, P., Tamm, E. R., Bösl, M. R., … Wegner, M. (2010). Sox10 is required for Schwann cell identity and progression beyond the immature Schwann cell stage. Journal of Cell Biology, 189(4), 701–712. https://doi.org/10.1083/jcb.200912142

Fischer, S. Martini, R. López-Vales, R. & David, S. (2008). Interactions between schwann cells and macrophages in injury and inherited demyelinating disease. Glia, 56(14), 1566–1577. https://doi.org/10.1002/glia.20766

Fontana, X., Hristova, M., Da Costa, C., Patodia, S., Thei, L., Makwana, M., … Behrens, A. (2012). C-Jun in Schwann cells promotes axonal regeneration and motoneuron survival via paracrine signaling. Journal of Cell Biology, 198(1), 127–141. https://doi.org/10.1083/jcb.201205025

Fowler, X., Dehority, R., Geary, M. B., & Elfar, J. C. (2015). Analysis of Myelin and Neurofilament Content in a Sciatic Nerve Crush Injury Model, 1(8), 1–5.

Friede, RL. & Bischhausen, R. (1980). The fine structure of stumps of transected nerve fibers in subserial sections.J Neurol Sci. Jan;44(2-3):181-203.

Fricker, F. R., Lago, N., Balarajah, S., Tsantoulas, C., Tanna, S., Zhu, N., … Bennett, D. L. H. (2011). Axonally derived neuregulin-1 is required for remyelination and regeneration after nerve injury in adulthood. The Journal of Neuroscience : The Official Journal of the Society for Neuroscience, 31(9), 3225–3233. https://doi.org/10.1523/JNEUROSCI.2568-10.2011

Friede, R. L. (1972). Control of myelin formation by axon caliber.(With a model of the control mechanism). Journal of Comparative Neurology, 144(2), 233–252.

Fu, L., & Kilberg, M. S. (2013). Elevated cJUN expression and an ATF/CRE site within the ATF3 promoter contribute to activation of ATF3 transcription by the amino acid response. Physiological Genomics, 45(4), 127–37. https://doi.org/10.1152/physiolgenomics.00160.2012

Garbay, B., Heape, A. M., Sargueil, F., & Cassagne, C. (2000). Myelin synthesis in the peripheral nervous system. Progress in Neurobiology, 61(3), 267–304. https://doi.org/10.1016/S0301-0082(99)00049-0

Garratt, A. N., Britsch, S., & Birchmeier, C. (2000). Neuregulin, a factor with many functions in the life of a Schwann cell. BioEssays, 22(11), 987–996.

https://doi.org/10.1002/1521-1878(200011)22:11<987::AID-BIES5>3.0.CO;2-5
Gaudet, A. D., Popovich, P. G., & Ramer, M. S. (2011). Wallerian degeneration: gaining perspective on inflammatory events after peripheral nerve injury. J. Neurotrauma, 8(1), 110. https://doi.org/10.1186/1742-2094-8-110
Ghislain, J., & Charnay, P. (2006). Control of myelination in Schwann cells: a Krox20 cis-regulatory element integrates Oct6, Brn2 and Sox10 activities. EMBO Reports, 7(1), 52–58. https://doi.org/10.1038/sj.embor.7400573
Ghislain, J., Desmarquet-Trin-Dinh, C., Jaegle, M., Meijer, D., Charnay, P., & Frain, M. (2002). Characterisation of cis-acting sequences reveals a biphasic, axon-dependent regulation of Krox20 during Schwann cell development. Development (Cambridge, England), 129(1), 155–166.
Gibson SJ, Polak JM, Bloom SR, Sabate IM, Mullberry PM, M. A. Ghatei, G. P. McGregor, J. F. B. J. S. Kelly, R. M. Evans, and M. G. Rosenfeld (1984) Calcitonin gene-related peptide immunoreactivity in the spinal cord of man and of eight other species. J. Neurosci. 4: 3 10 l-3 111.
Gomez-Sanchez, J. A., Carty, L., Iruarrizaga-Lejarreta, M., Palomo-Irigoyen, M., Varela-Rey, M., Griffith, M., … Jessen, K. R. (2015). Schwann cell autophagy, myelinophagy, initiates myelin clearance from injured nerves. Journal of Cell Biology, 210(1), 153–168. https://doi.org/10.1083/jcb.201503019
Gomez-Sanchez, J. A., Gomis-Coloma, C., Morenilla-Palao, C., Peiro, G., Serra, E., Serrano, M., & Cabedo, H. (2013). Epigenetic induction of the Ink4a/Arf locus prevents Schwann cell overproliferation during nerve regeneration and after tumorigenic challenge. Brain, 136(7), 2262–2278. https://doi.org/10.1093/brain/awt130
Gomez-Sanchez, J. a, Lopez de Armentia, M., Lujan, R., Kessaris, N., Richardson, W. D., & Cabedo, H. (2009). Sustained axon-glial signaling induces Schwann cell hyperproliferation, Remak bundle myelination, and tumorigenesis. The Journal of Neuroscience : The Official Journal of the Society for Neuroscience, 29(36), 11304–11315. https://doi.org/10.1523/JNEUROSCI.1753-09.2009
Gonzalez-Perez, F., Udina, E., & Navarro, X. (2013). Extracellular matrix components in peripheral nerve regeneration. International Review of Neurobiology (1st ed., Vol. 108). Elsevier Inc. https://doi.org/10.1016/B978-0-12-410499-0.00010-1
Griffin, J. W., & Thompson, W. J. (2008). Biology and pathology of nonmyelinating schwann cells. Glia, 56(14), 1518–1531. https://doi.org/10.1002/glia.20778
Grinspan, J. B., Marchionni, M. a, Reeves, M., Coulaloglou, M., & Scherer, S. S. (1996). Axonal interactions regulate Schwann cell apoptosis in developing peripheral nerve: neuregulin receptors and the role of neuregulins. The Journal of Neuroscience : The Official Journal of the Society for Neuroscience, 16(19), 6107–6118.
Gutmann, E. & Holubar, J. (1950). The degeneration of peripheral nerve fibres. Journal of Neurology, Neurosurgery, and Psychiatry, 13, 89-105
Haas, C. A., Hofmann, H. D., & Kirsch, M. (1999). Expression of CNTF/LIF-receptor components and activation of STAT3 signaling in axotomized facial motoneurons: Evidence for a sequential postlesional function of the cytokines. Journal of Neurobiology, 41(4), 559–571. https://doi.org/10.1002/(SICI)1097-4695(199912)41:4<559::AID-NEU11>3.0.CO;2-A
Hantke, J., Carty, L., Wagstaff, L. J., Turmaine, M., Wilton, D. K., Quintes, S., … Jessen, K. R. (2014). c-Jun activation in Schwann cells protects against loss of sensory axons in inherited neuropathy. Brain, 137(11), 2922–2937.

https://doi.org/10.1093/brain/awu257
Harrisingh, M. C., Perez-Nadales, E., Parkinson, D. B., Malcolm, D. S., Mudge, A. W., & Lloyd, A. C. (2004). The Ras/Raf/ERK signalling pathway drives Schwann cell dedifferentiation. The EMBO Journal, 23(15), 3061–3071. https://doi.org/10.1038/sj.emboj.7600309
Herdegen, T., Skene, P., & Bähr, M. (1997). The c-Jun transcription factor - Bipotential mediator of neuronal death, survival and regeneration. Trends in Neurosciences, 20(5), 227–231. https://doi.org/10.1016/S0166-2236(96)01000-4
Hirata, K., & Kawabuchi, M. (2002). Myelin phagocytosis by macrophages and nonmacrophages during Wallerian degeneration. Microscopy Research and Technique, 57(6), 541–547. https://doi.org/10.1002/jemt.10108
Hirose T, Sano T, Hizawa K. (1986). Ultrastructural localization of S-100 protein in neurofibroma. Acta Neuropathol. 69:103–110.
Hoffman, P. N. (2010). A conditioning lesion induces changes in gene expression and axonal transport that enhance regeneration by increasing the intrinsic growth state of axons. Experimental Neurology, 223(1), 11–18. https://doi.org/10.1016/j.expneurol.2009.09.006
Holmes, F. E., Mahoney, S., King, V. R., Bacon, A., Kerr, N. C., Pachnis, V., … Wynick, D. (2000). Targeted disruption of the galanin gene reduces the number of sensory neurons and their regenerative capacity. Proceedings of the National Academy of Sciences of the United States of America, 97(21), 11563–11568. https://doi.org/10.1073/pnas.210221897
Hoos, A., Stojadinovic, A., Mastorides, S., Urist, M. J., Polsky, D., Di Como, C. J., … Cordon-Cardo, C. (2001). High Ki-67 proliferative index predicts disease specific survival in patients with high-risk soft tissue sarcomas. Cancer, 92(4), 869–874. https://doi.org/10.1002/1097-0142(20010815)92:4<869::AID-CNCR1395>3.0.CO;2-U
Hsieh, S. T., Kidd, G. J., Crawford, T. O., Xu, Z., Lin, W. M., Trapp, B. D., … Griffin, J. W. (1994). Regional modulation of neurofilament organization by myelination in normal axons. J Neurosci, 14(11 Pt 1), 6392–6401. Retrieved from http://www.ncbi.nlm.nih.gov/entrez/query.fcgi?cmd=Retrieve&db=PubMed&dopt=Citation&list_uids=7965044
Huebner, E. a, & Strittmatter, S. M. (2009). Axon Regeneration in the Peripheral and Central Nervous Systems. Results and Problems in Cell Differentiation. Author Manuscript, 48, 339–351. https://doi.org/10.1007/400
Hunt, D., Raivich, G., & Anderson, P. N. (2012). Activating transcription factor 3 and the nervous system. Frontiers in Molecular Neuroscience, 5(February), 7. https://doi.org/10.3389/fnmol.2012.00007
Hutton, E. J., Carty, L., Laurá, M., Houlden, H., Lunn, M. P. T., Brandner, S., … Reilly, M. M. (2011). C-Jun expression in human neuropathies: A pilot study. Journal of the Peripheral Nervous System, 16(4), 295–303. https://doi.org/10.1111/j.1529-8027.2011.00360.x
Huxley, A. F., & Stämpfli, R. (1949). Evidence for saltatory conduction in peripheral myelinated nerve fibres. Journal of Physiology, 108(1946), 315–339. https://doi.org/10.1113/jphysiol.1949.sp004335
Inserra, M. M., Bloch, D. A., & Terris, D. J. (1998). Functional indices for sciatic, peroneal, and posterior tibial nerve lesions in the mouse. Microsurgery, 18(2), 119–124. https://doi.org/10.1002/(SICI)1098-2752(1998)18:2<119::AID-MICR10>3.0.CO;2-0

Jacob, C., Lo, P., Engler, S., Baggiolini, A., Tavares, S. V., John, N., … Suter, U. (2014). HDAC1 and HDAC2 Control the Specification of Neural Crest Cells into Peripheral Glia, 34(17), 6112–6122. https://doi.org/10.1523/JNEUROSCI.5212-13.2014

Jacobs, J. M., & Love, S. (1985). Qualitative and quantitative morphology of human sural nerve at different ages. Brain : A Journal of Neurology, 108 (Pt 4, 897–924. Retrieved from http://www.ncbi.nlm.nih.gov/pubmed/4075078

Jaegle, M., Ghazvini, M., Mandemakers, W., Piirsoo, M., Driegen, S., Levavasseur, F., … Meijer, D. (2003). The POU proteins Brn-2 and Oct-6 share important functions in Schwann cell development. Genes and Development, 17(11), 1380–1391. https://doi.org/10.1101/gad.258203

Jaegle, M., Mandemakers, W., Broos, L., Zwart, R., Karis, a, Visser, P., … Meijer, D. (1996). The POU factor Oct-6 and Schwann cell differentiation. Science (New York, N.Y.), 273(5274), 507–510. https://doi.org/10.1126/science.273.5274.507

Jaegle, M., & Meijer, D. (1998). Role of Oct-6 in Schwann cell differentiation. Microscopy Research and Technique, 41(5), 372–378. https://doi.org/10.1002/(SICI)1097-0029(19980601)41:5<372::AID-JEMT4>3.0.CO;2-S

Jagalur, N. B., Ghazvini, M., Mandemakers, W., Driegen, S., Maas, A., Jones, E. a, … Meijer, D. (2011). Functional dissection of the Oct6 Schwann cell enhancer reveals an essential role for dimeric Sox10 binding. The Journal of Neuroscience : The Official Journal of the Society for Neuroscience, 31(23), 8585–8594. https://doi.org/10.1523/JNEUROSCI.0659-11.2011

Jenkins, R., & Hunt, S. P. (1991). Long-term increase in the levels of c-jun mRNA and jun protein-like immunoreactivity in motor and sensory neurons following axon damage. Neuroscience Letters, 129(1), 107–110. https://doi.org/10.1016/0304-3940(91)90731-8

Jessen, K. R., Brennan, A., Morgan, L., Mirsky, R., Kent, A., Hashimoto, Y., & Gavrilovic, J. (1994). The Schwann cell precursor and its fate: A study of cell death and differentiation during gliogenesis in rat embryonic nerves. Neuron, 12(3), 509–527. https://doi.org/10.1016/0896-6273(94)90209-7

Jessen, K. R., & Mirsky, R. (1991). Schwann cell precursors and their development. Glia, 4(2), 185–194. https://doi.org/10.1002/glia.440040210

Jessen, K. R., & Mirsky, R. (1997). Embryonic Schwann cell development: the biology of Schwann cell precursors and early Schwann cells. Journal of Anatomy, 191 (Pt 4, 501–505. https://doi.org/10.1046/j.1469-7580.1997.19140501.x

Jessen, K. R., & Mirsky, R. (2002). Signals that determine Schwann cell identity. Journal of Anatomy, 200(4), 367–376. https://doi.org/10.1046/j.1469-7580.2002.00046.x

Jessen, K. R., & Mirsky, R. (2005). The origin and development of glial cells in peripheral nerves. Nat Rev Neurosci, 6(9), 671–682. https://doi.org/nrn1746 [pii]\n10.1038/nrn1746

Jessen, K. R., & Mirsky, R. (2008). Negative regulation of myelination: Relevance for development, injury, and demyelinating disease. Glia, 56(14), 1552–1565. https://doi.org/10.1002/glia.20761

Jessen, K. R., & Mirsky, R. (2016). The repair Schwann cell and its function in regenerating nerves. The Journal of Physiology, 0(July 2015), 1–11. https://doi.org/10.1113/JP270874

Jessen, K. R., Mirsky, R., & Arthur-Farraj, P. (2015). The Role of Cell Plasticity in Tissue Repair: Adaptive Cellular Reprogramming. Developmental Cell, 34(6), 613–620. https://doi.org/10.1016/j.devcel.2015.09.005

Jessen, K. R., Mirsky, R., & Morgan, L. (1987). Axonal signals regulate the differentiation of non-myelin-forming Schwann cells: an immunohistochemical study of galactocerebroside in transected and regenerating nerves. The Journal of Neuroscience, 7(10), 3362–3369. Retrieved from http://www.jneurosci.org/content/7/10/3362.abstract

Jessen, K. R., Mirsky, R., & Morgan, L. (1991). Role of Cyclic AMP and Proliferation Controls in Schwann Cell Differentiation. Annals of the New York Academy of Sciences, 633(1), 78–89. https://doi.org/10.1111/j.1749-6632.1991.tb15597.x

Jessen, K., R, M., & Lloyd, A. (2015). Schwann cells: Development and Role in Nerve Repair. Cold Spring Harbor Perspectives in Biology., 7(7), 1–16.

Joseph, N. M., Mukouyama, Y.-S., Mosher, J. T., Jaegle, M., Crone, S. a, Dormand, E.-L., … Morrison, S. J. (2004). Neural crest stem cells undergo multilineage differentiation in developing peripheral nerves to generate endoneurial fibroblasts in addition to Schwann cells. Development (Cambridge, England), 131(22), 5599–612. https://doi.org/10.1242/dev.01429

Jun, M., Zhang, L., Han, W., Shen, T., Ma, C., Liu, Y., … Zhu, D. (2012). Activation of JNK/c-Jun is required for the proliferation, survival, and angiogenesis induced by EET in pulmonary artery endothelial cells. J Lipid Res, 53(6), 1093–1105. https://doi.org/10.1017/CBO9781107415324.004

Jurecka W., Ammerer H.P., Lassmann H. (1975). Regeneration of a transected peripheral nerve. An autoradiographic and electron microscopic study. Acta Neuropathol. 32:299–312.

Kaplan, S., Odaci, E., Unal, B., Sahin, B., & Fornaro, M. (2009). Chapter 2 Development of the Peripheral Nerve. International Review of Neurobiology (1st ed., Vol. 87). Elsevier Inc. https://doi.org/10.1016/S0074-7742(09)87002-5

Fawcett, JW. & Keynes, RJ. (1990). Peripheral Nerve. Retrieved from https://classconnection.s3.amazonaws.com/636/flashcards/3536636/png/peripheral_nerve-142CBEAF7967FFF40A8.png

Kioussi, C., Gross, M. K., & Gruss, P. (1995). Pax3: A paired domain gene as a regulator in PNS myelination. Neuron, 15(3), 553–562. https://doi.org/10.1016/0896-6273(95)90144-2

Kiryu-Seo, S., Kato, R., Ogawa, T., Nakagomi, S., Nagata, K., & Kiyama, H. (2008). Neuronal injury-inducible gene is synergistically regulated by ATF3, c-Jun, and STAT3 through the interaction with Sp1 in damaged neurons. Journal of Biological Chemistry, 283(11), 6988–6996. https://doi.org/10.1074/jbc.M707514200

Klein, D., Groh, J., Wettmarshausen, J., & Martini, R. (2014). Nonuniform molecular features of myelinating Schwann cells in models for CMT1: Distinct disease patterns are associated with NCAM and c-Jun upregulation. Glia, 62(5), 736–750. https://doi.org/10.1002/glia.22638

Klein, E. A., & Assoian, R. K. (2008). Transcriptional regulation of the cyclin D1 gene at a glance. Journal of Cell Science, 121(Pt 23), 3853–7. https://doi.org/10.1242/jcs.039131

Kuhlbrodt, K., Herbarth, B., Sock, E., Hermans-Borgmeyer, I., & Wegner, M. (1998). Sox10, a novel transcriptional modulator in glial cells. The Journal of Neuroscience : The Official Journal of the Society for Neuroscience, 18(1), 237–

50. Retrieved from http://scholar.google.com/scholar?hl=en&btnG=Search&q=intitle:Sox10+,+a+Novel+Transcriptional+Modulator+in+Glial+Cells#0%5Cnhttp://scholar.google.com/scholar?hl=en&btnG=Search&q=intitle:Sox10,+a+novel+transcriptional+modulator+in+glial+cells#0%5Cnhttp://s

Kurek, J. B., Austin, L., Cheema, S. S., Bartlett, P. F., & Murphy, M. (1996). Up-regulation of leukaemia inhibitory factor and interleukin-6 in transected sciatic nerve and muscle following denervation. Neuromuscular Disorders, 6(2), 105–114. https://doi.org/10.1016/0960-8966(95)00029-1

Le, N., Nagarajan, R., Wang, J. Y. T., Araki, T., Schmidt, R. E., & Milbrandt, J. (2005). Analysis of congenital hypomyelinating Egr2Lo/Lo nerves identifies Sox2 as an inhibitor of Schwann cell differentiation and myelination. Proceedings of the National Academy of Sciences of the United States of America, 102(Track II), 2596–2601. https://doi.org/10.1073/pnas.0407836102

Leah, J. D., Herdegen, T., & Bravo, R. (1991). Selective expression of Jun proteins following axotomy and axonal transport block in peripheral nerves in the rat: evidence for a role in the regeneration process. Brain Research, 566(1–2), 198–207. https://doi.org/10.1016/0006-8993(91)91699-2

LeBlanc, S. E., Jang, S. W., Ward, R. M., Wrabetz, L., & Svaren, J. (2006). Direct regulation of myelin protein zero expression by the Egr2 transactivator. Journal of Biological Chemistry, 281(9), 5453–5460. https://doi.org/10.1074/jbc.M512159200

Lee, F. K. M., Wong, A. K. Y., Lee, Y. W., Wan, O. W., Edwin Chan, H. Y., & Chung, K. K. K. (2009). The role of ubiquitin linkages on ??-synuclein induced-toxicity in a Drosophila model of Parkinson's disease. Journal of Neurochemistry, 110(1), 208–219. https://doi.org/10.1111/j.1471-4159.2009.06124.x

Lee, H. K., Jung, J., Lee, S. H., Seo, S.-Y., Suh, D. J., & Park, H. T. (2009). Extracellular Signal-regulated Kinase Activation Is Required for Serine 727 Phosphorylation of STAT3 in Schwann Cells in vitro and in vivo. The Korean Journal of Physiology & Pharmacology : Official Journal of the Korean Physiological Society and the Korean Society of Pharmacology, 13(3), 161–168. https://doi.org/10.4196/kjpp.2009.13.3.161

Lee, N., Neitzel, K. L., Devlin, B. K., & MacLennan, A. J. (2004). STAT3 phosphorylation in injured axons before sensory and motor neuron nuclei: Potential role for STAT3 as a retrograde signaling transcription factor. Journal of Comparative Neurology, 474(4), 535–545. https://doi.org/10.1002/cne.20140

Leppä, S., & Bohmann, D. (1999). Diverse functions of JNK signaling and c-Jun in stress response and apoptosis. Oncogene, 18(45), 6158–6162. https://doi.org/10.1038/sj.onc.1203173

Levi, a D., Bunge, R. P., Lofgren, J. a, Meima, L., Hefti, F., Nikolics, K., & Sliwkowski, M. X. (1995). The influence of heregulins on human Schwann cell proliferation. The Journal of Neuroscience : The Official Journal of the Society for Neuroscience, 15(2), 1329–1340.

Li, X.-Q., Verge, V. M. K., Johnston, J. M., & Zochodne, D. W. (2004). CGRP peptide and regenerating sensory axons. Journal of Neuropathology and Experimental Neurology, 63(10), 1092–103. Retrieved from http://www.ncbi.nlm.nih.gov/pubmed/15535136

Lindå, H., Sköld, M. K., & Ochsmann, T. (2011). Activating transcription factor 3, a useful marker for regenerative response after nerve root injury. Frontiers in

Neurology, MAY(May), 1–6. https://doi.org/10.3389/fneur.2011.00030
Lindwall, C., Dahlin, L., Lundborg, G., & Kanje, M. (2004). Inhibition of c-Jun phosphorylation reduces axonal outgrowth of adult rat nodose ganglia and dorsal root ganglia sensory neurons. Molecular and Cellular Neuroscience, 27(3), 267–279. https://doi.org/10.1016/j.mcn.2004.07.001
Lobsiger, C. S., Taylor, V., & Suter, U. (2002). The Early Life of a Schwann Cell. Biological Chemistry, 383(2), 245–53. https://doi.org/10.1515/BC.2002.026
Lopez, F., Belloc, F., Lacombe, F., Dumain, P., Reiffers, J., Bernard, P., & Boisseau, M. R. (1991). Modalities of synthesis of Ki67 antigen during the stimulation of lymphocytes. Cytometry, 12(1), 42–49. https://doi.org/10.1002/cyto.990120107
Lubinska, L. (1977). Early course of Wallerian degeneration in myelinated fibres of the rat phrenic nerve. Brain research, 130 (1), pp.47-63
Ma, C. H. E., Omura, T., Cobos, E. J., Latremoliere, A., Ghasemlou, N., Brenner, G. J., … Woolf, C. J. (2011). Accelerating axonal growth promotes motor recovery after peripheral nerve injury in mice. The Journal of Clinical Investigation, 121(11), 4332–47. https://doi.org/10.1172/JCI58675DS1
Ma, T. C., & Willis, D. E. (2015). What makes a RAG regeneration associated? Frontiers in Molecular Neuroscience, 8(August), 43. https://doi.org/10.3389/fnmol.2015.00043
Makwana, M., Werner, A., Acosta-Saltos, A., Gonitel, R., Pararajasingham, A., Ruff, C., … Raivich, G. (2010). Peripheral facial nerve axotomy in mice causes sprouting of motor axons into perineuronal central white matter: Time course and molecular characterization. Journal of Comparative Neurology, 518(5), 699–721. https://doi.org/10.1002/cne.22240
Mandal, T., Bhowmik, A., Chatterjee, A., Chatterjee, U., Chatterjee, S., & Ghosh, M. K. (2014). Reduced phosphorylation of Stat3 at Ser-727 mediated by casein kinase 2 - Protein phosphatase 2A enhances Stat3 Tyr-705 induced tumorigenic potential of glioma cells. Cellular Signalling, 26(8), 1725–1734. https://doi.org/10.1016/j.cellsig.2014.04.003
Madolesi, G. Madeddu, F. Bozzi, Y. Maffei, L. & Ratto GM. (2004). Acute physiological response of mammalian central neurons to axotomy: ionic regulation and electrical activity. FASEB J 2004 Dec 27;18(15):1934-6. Epub 2004 Sep 27.
Martin-Villalba, A., Winter, C., Brecht, S., Buschmann, T., Zimmermann, M., & Herdegen, T. (1998). Rapid and long-lasting suppression of the ATF-2 transcription factor is a common response to neuronal injury. Molecular Brain Research, 62(2), 158–166. https://doi.org/10.1016/S0169-328X(98)00239-3
Martini, R., Klein, D., & Groh, J. (2013). Similarities between inherited demyelinating neuropathies and wallerian degeneration: An old repair program may cause myelin and axon perturbation under nonlesion conditions. American Journal of Pathology, 183(3), 655–660. https://doi.org/10.1016/j.ajpath.2013.06.002
May, G. H. W., Elizabeth Allen, K., Clark, W., Funk, M., & Gillespie, D. A. F. (1998). Analysis of the interaction between c-Jun and c-Jun N-terminal kinase in vivo. Journal of Biological Chemistry, 273(50), 33429–33435. https://doi.org/10.1074/jbc.273.50.33429
McKerracher, L., & Rosen, K. M. (2015). MAG, myelin and overcoming growth inhibition in the CNS. Frontiers in Molecular Neuroscience, 8(September), 51. https://doi.org/10.3389/fnmol.2015.00051
Mcquarrie, I. G. (1985). Effect of a Conditioning Lesion on Axonal Sprout Formation

at Nodes of Ranvier, 249.
McQuarrie, I. G., Grafstein, B., & Gershon, M. D. (1977). Axonal regeneration in the rat sciatic nerve: Effect of a conditioning lesion and of dbcAMP. Brain Research, 132(3), 443–453. https://doi.org/10.1016/0006-8993(77)90193-7
Mei, L., & Xiong, W.-C. (2008). Neuregulin 1 in neural development, synaptic plasticity and schizophrenia. Nature Reviews. Neuroscience, 9(6), 437–52. https://doi.org/10.1038/nrn2392
Meier, C., Parmantier, E., Brennan, a, Mirsky, R., & Jessen, K. R. (1999). Developing Schwann cells acquire the ability to survive without axons by establishing an autocrine circuit involving insulin-like growth factor, neurotrophin-3, and platelet-derived growth factor-BB. The Journal of Neuroscience : The Official Journal of the Society for Neuroscience, 19(10), 3847–3859.
Meyer, D., & Birchmeier, C. (1994). Distinct isoforms of neuregulin are expressed in mesenchymal and neuronal cells during mouse development. Proceedings of the National Academy of Sciences of the United States of America, 91(3), 1064–8. Retrieved from http://www.pubmedcentral.nih.gov/articlerender.fcgi?artid=521454&tool=pmcentrez&rendertype=abstract
Meyer, D., & Birchmeier, C. (1995). Multiple essential functions of neuregulin in development. Nature, 378(6555), 386–390. https://doi.org/10.1038/378753a0
Meyer, D., Yamaai, T., Garratt, A., Riethmacher-Sonnenberg, E., Kane, D., Theill, L. E., & Birchmeier, C. (1997). Isoform-specific expression and function of neuregulin. Development, 124(18), 3575–3586. Retrieved from http://www.ncbi.nlm.nih.gov/pubmed/9342050
Michailov, G. V. (2004). Axonal Neuregulin-1 Regulates Myelin Sheath Thickness. Science, 304(5671), 700–703. https://doi.org/10.1126/science.1095862
Mirsky, R., & Jessen, K. R. (1996). Schwann cell development, differentiation and myelination. Current Opinion in Neurobiology, 6(1), 89–96. https://doi.org/10.1016/S0959-4388(96)80013-4
Mirsky, R., Winter, J., Abney, E. R., Pruss, R. M., Gavrilovic, J., & Raff, M. C. (1980). Myelin-specific proteins and glycolipids in rat Schwann cells and oligodendrocytes in culture. Journal of Cell Biology, 84(3), 483–494. https://doi.org/10.1083/jcb.84.3.483
Mirsky, R., Woodhoo, A., Parkinson, D. B., Arthur-Farraj, P., Bhaskaran, A., & Jessen, K. R. (2008). Novel signals controlling embryonic Schwann cell development, myelination and dedifferentiation. Journal of the Peripheral Nervous System, 13(2), 122–135. https://doi.org/10.1111/j.1529-8027.2008.00168.x
Mokuno, K., Sobue, G., Reddy, U. R., Wurzer, J., Kreider, B., Hotta, H., … Pleasure, D. (1988). Regulation of Schwann cell nerve growth factor receptor by cyclic adenosine 3',5'-monophosphate. J Neurosci Res, 21(2–4), 465–472. https://doi.org/10.1002/jnr.490210237
Monje, P., Hernández-Losa, J., Lyons, R. J., Castellone, M. D., & Gutkind, J. S. (2005). Regulation of the transcriptional activity of c-Fos by ERK: A novel role for the prolyl isomerase Pin1. Journal of Biological Chemistry, 280(42), 35081–35084. https://doi.org/10.1074/jbc.C500353200
Monk, K. R., Feltri, M. L., & Taveggia, C. (2015). New insights on schwann cell development. Glia, 63(8), 1376–1393. https://doi.org/10.1002/glia.22852
Monuki, E. S., Kuhn, R., Weinmaster, G., Trapp, B. D., & Lemke, G. (1990).

Expression and activity of the POU transcription factor SCIP. Science (New York, N.Y.), 249(4974), 1300–1303. https://doi.org/10.1126/science.1975954

Monuki, E. S., Weinmaster, G., Kuhn, R., & Lemke, G. (1989). SCIP: A glial POU domain gene regulated by cyclic AMP. Neuron, 3(6), 783–793. https://doi.org/10.1016/0896-6273(89)90247-X

Morgan, L., Jessen, K. R., & Mirsky, R. (1991). The effects of cAMP on differentiation of cultured schwann cells: Progression from an early phenotype (04+) to a myelin phenotype (P○+, GFAP-, N-CAM-, NGF-receptor-) depends on growth inhibition. Journal of Cell Biology, 112(3), 457–467. https://doi.org/10.1083/jcb.112.3.457

Morris, J. K., Lin, W., Hauser, C., Marchuk, Y., Getman, D., & Lee, K.-F. (1999). Genetic rescue of cardiac defect in erbB2 null mutant mice reveals essential roles of erbB2 in development of the peripheral nervous system. Neuron, 23, 1–20.

Morrison, S. J., White, P. M., Zock, C., & Anderson, D. J. (1999). Prospective identification, isolation by flow cytometry, and in vivo self-renewal of multipotent mammalian neural crest stem cells. Cell, 96, 737–749. https://doi.org/10.1016/S0092-8674(00)80583-8

Morrissey, T. K., Levi, a D., Nuijens, a, Sliwkowski, M. X., & Bunge, R. P. (1995). Axon-induced mitogenesis of human Schwann cells involves heregulin and p185erbB2. Proceedings of the National Academy of Sciences of the United States of America, 92(5), 1431–1435. https://doi.org/10.1073/pnas.92.5.1431

Mueller M, Leonhard C, Wacker K, Ringelstein EB, Okabe M, Hickey WF, Kiefer R. (2003). Macrophage response to peripheral nerve injury: the quantitative contribution of resident and hematogenous macrophages. Lab Invest. 83:175–185.

Mukouyama, Y.-S., Gerber, H.-P., Ferrara, N., Gu, C., & Anderson, D. J. (2005). Peripheral nerve-derived VEGF promotes arterial differentiation via neuropilin 1-mediated positive feedback. Development (Cambridge, England), 132(5), 941–52. https://doi.org/10.1242/dev.01675

Murphy, P., Topilko, P., Schneider-Maunoury, S., Seitanidou, T., Baron-Van Evercooren, A., & Charnay, P. (1996). The regulation of Krox-20 expression reveals important steps in the control of peripheral glial cell development. Development (Cambridge, England), 122(9), 2847–57. Retrieved from http://www.ncbi.nlm.nih.gov/pubmed/8787758

Naba, I., Yoshikawa, H., Sakoda, S., Itabe, H., Suzuki, H., Kodama, T., & Yanagihara, T. (2000). Successful generation of peripheral neuropathy with onion-bulb formation in the macrophage scavenger receptor classA knockout mouse treated with isoniazid. Neuroscience Letters, 290(1), 5–8. https://doi.org/10.1016/S0304-3940(00)01309-4

Nadra, K., Charles, A. S. D. P., Médard, J. J., Hendriks, W. T., Han, G. S., Grès, S., … Chrast, R. (2008). Phosphatidic acid mediates demyelination in Lpin1 mutant mice. Genes and Development, 22(12), 1647–1661. https://doi.org/10.1101/gad.1638008

Nagarajan, R., Svaren, J., Le, N., Araki, T., Watson, M., & Milbrandt, J. (2001). EGR2 mutations in inherited neuropathies dominant-negatively inhibit myelin gene expression. Neuron, 30(2), 355–368. https://doi.org/10.1016/S0896-6273(01)00282-3

Nakagomi, S., Suzuki, Y., Namikawa, K., Kiryu-Seo, S., & Kiyama, H. (2003). Expression of the activating transcription factor 3 prevents c-Jun N-terminal kinase-induced neuronal death by promoting heat shock protein 27 expression

and Akt activation. The Journal of Neuroscience : The Official Journal of the Society for Neuroscience, 23(12), 5187–5196.

Nakao, J., Shinoda, J., Nakai, Y., Murase, S., & Uyemura, K. (1997). Apoptosis regulates the number of Schwann cells at the premyelinating stage. Journal of Neurochemistry, 68(5), 1853–1862. https://doi.org/10.1046/j.1471-4159.1997.68051853.x

Napoli, I., Noon, L. A., Ribeiro, S., Kerai, A. P., Parrinello, S., Rosenberg, L. H., … Lloyd, A. C. (2012). A Central Role for the ERK-Signaling Pathway in Controlling Schwann Cell Plasticity and Peripheral Nerve Regeneration In Vivo. Neuron, 73(4), 729–742. https://doi.org/10.1016/j.neuron.2011.11.031

Navarro, X., Vivó, M., & Valero-Cabré, A. (2007). Neural plasticity after peripheral nerve injury and regeneration. Progress in Neurobiology, 82(4), 163–201. https://doi.org/10.1016/j.pneurobio.2007.06.005

Neumann, S., Bradke, F., Tessier-Lavigne, M., & Basbaum, A. I. (2002). Regeneration of sensory axons within the injured spinal cord induced by intraganglionic cAMP elevation. Neuron, 34(6), 885–893. https://doi.org/10.1016/S0896-6273(02)00702-X

Neumann, S., & Woolf, C. J. (1999). Regeneration of dorsal column fibers into and beyond the lesion site following adult spinal cord injury. Neuron, 23(1), 83–91. https://doi.org/10.1016/S0896-6273(00)80755-2

Newbern, J., & Birchmeier, C. (2010). Nrg1/ErbB signaling networks in Schwann cell development and myelination. Seminars in Cell and Developmental Biology, 21(9), 922–928. https://doi.org/10.1016/j.semcdb.2010.08.008

Nguyen, P. M., Putoczki, T. L., & Ernst, M. (2015). STAT3-Activating Cytokines: A Therapeutic Opportunity for Inflammatory Bowel Disease? Journal of Interferon & Cytokine Research : The Official Journal of the International Society for Interferon and Cytokine Research, 35(5), 340–50. https://doi.org/10.1089/jir.2014.0225

Norton, W. T., & Poduslo, S. E. (1973). Myelination in Rat Brain: Method of Myelin Isolation. Journal of Neurochemistry, 21(4), 749–757. https://doi.org/10.1111/j.1471-4159.1973.tb07519.x

Painter, M. W., Brosius Lutz, A., Cheng, Y. C., Latremoliere, A., Duong, K., Miller, C. M., … Woolf, C. J. (2014). Diminished Schwann cell repair responses underlie age-associated impaired axonal regeneration. Neuron, 83(2). https://doi.org/10.1016/j.neuron.2014.06.016

Parkinson, D. B., Bhaskaran, A., Arthur-Farraj, P., Noon, L. A., Woodhoo, A., Lloyd, A. C., … Jessen, K. R. (2008). c-Jun is a negative regulator of myelination. Journal of Cell Biology, 181(4), 625–637. https://doi.org/10.1083/jcb.200803013

Parkinson, D. B., Bhaskaran, A., Droggiti, A., Dickinson, S., D'Antonio, M., Mirsky, R., & Jessen, K. R. (2004). Krox-20 inhibits Jun-NH2-terminal kinase/c-Jun to control Schwann cell proliferation and death. Journal of Cell Biology, 164(3), 385–394. https://doi.org/10.1083/jcb.200307132

Parkinson, D. B., Dong, Z., Bunting, H., Whitfield, J., Meier, C., Mirsky, R., & Jessen, K. R. (2001). Transforming Growth Factor NL (TGF NL) Mediates Schwann Cell Death In Vitro and In Vivo : Examination of c-Jun Activation , Interactions with Survival Signals , and the Relationship of TGF NL -Mediated Death to Schwann Cell Differentiation, 21(21), 8572–8585.

Parmantier, E., Lynn, B., Lawson, D., Turmaine, M., Namini, S. S., Chakrabarti, L., … Mirsky, R. (1999). Schwann Cell – Derived Desert Hedgehog Controls the

Development of Peripheral Nerve Sheaths. Neuron, 23(4), 713–724. https://doi.org/10.1016/S0896-6273(01)80030-1

Parrinello, S., Noon, L. A., Harrisingh, M. C., Digby, P. W., Rosenberg, L. H., Cremona, C. A., … Lloyd, A. C. (2008). NF1 loss disrupts Schwann cell-axonal interactions: A novel role for semaphorin 4F. Genes and Development, 22(23), 3335–3348. https://doi.org/10.1101/gad.490608

Pate Skene, J. H., & Virag, I. (1989). Posttranslational membrane attachment and dynamic fatty acylation of a neuronal growth cone protein, GAP-43. Journal of Cell Biology, 108(2), 613–624. https://doi.org/10.1083/jcb.108.2.613

Patodia, S., & Raivich, G. (2012). Role of transcription factors in peripheral nerve regeneration. Frontiers in Molecular Neuroscience, 5(February), 8. https://doi.org/10.3389/fnmol.2012.00008

Pereira, J. A., Lebrun-Julien, F., & Suter, U. (2012). Molecular mechanisms regulating myelination in the peripheral nervous system. Trends in Neurosciences, 35(2), 123–134. https://doi.org/10.1016/j.tins.2011.11.006

Perry, V. H., Brown, M. C., & Gordon, S. (1987). The macrophage response to central and peripheral nerve injury. A possible role for macrophages in regeneration. The Journal of Experimental Medicine, 165(4), 1218–1223. https://doi.org/10.1084/jem.165.4.1218

Perry, V. H., & Brown, M. C. (1992). Role of macrophages in peripheral nerve degeneration and repair. BioEssays, 14(6), 401–406. https://doi.org/10.1002/bies.950140610

Perry VH, Brown M.C, Andersson PB. (1993). Macrophage responses to central and peripheral nerve injury. Adv Neurol. 59:309–314.

Poliak, S., & Peles, E. (2003). The local differentiation of myelinated axons at nodes of Ranvier. Nature Reviews. Neuroscience, 4(12), 968–980. https://doi.org/10.1038/nrn1253

Porrello, E., Rivellini, C., Dina, G., Triolo, D., Del Carro, U., Ungaro, D., … Previtali, S. C. (2014). Jab1 regulates Schwann cell proliferation and axonal sorting through p27. The Journal of Experimental Medicine, 211(1), 29–43. https://doi.org/10.1084/jem.20130720

Qiu, J., Cafferty, W. B. J., McMahon, S. B., & Thompson, S. W. N. (2005). Conditioning Injury-Induced Spinal Axon Regeneration Requires Signal Transducer and Activator of Transcription 3 Activation. J. Neurosci., 25(7), 1645–1653. https://doi.org/10.1523/JNEUROSCI.3269-04.2005

Qiu, J., Cai, D., Dai, H., McAtee, M., Hoffman, P. N., Bregman, B. S., & Filbin, M. T. (2002). Spinal axon regeneration induced by elevation of cyclic AMP. Neuron, 34(6), 895–903. https://doi.org/10.1016/S0896-6273(02)00730-4

Quintes, S., Brinkmann, B. G., Ebert, M., Fröb, F., Kungl, T., Arlt, F. A., … Nave, K.-A. (2016). Zeb2 is essential for Schwann cell differentiation, myelination and nerve repair. Nature Neuroscience, 19(8), 1050–1061. https://doi.org/10.1038/nn.4321

Raivich, G., Bohatschek, M., Da Costa, C., Iwata, O., Galiano, M., Hristova, M., … Behrens, A. (2004). The AP-1 transcription factor c-Jun is required for efficient axonal regeneration. Neuron, 43(1), 57–67. https://doi.org/10.1016/j.neuron.2004.06.005

Ramaglia, V., Wolterman, R., de Kok, M., Vigar, M. A., Wagenaar-Bos, I., King, R. H. M., … Baas, F. (2008). Soluble complement receptor 1 protects the peripheral nerve from early axon loss after injury. The American Journal of Pathology, 172(4), 1043–52. https://doi.org/10.2353/ajpath.2008.070660

Ramer, M. S., Priestley, J. V, & McMahon, S. B. (2000). Functional regeneration of sensory axons into the adult spinal cord. Nature, 403(6767), 312–316. https://doi.org/10.1038/35002084

Ranvier, L. A. (1871). Contributions a l'histologie et i la physiologie des nerfs peripherique. C. r. hebd. Seanc. Acad. Sci., Paris 73, 1168-1171.

Raphael, A. R., & Talbot, W. S. (2011). New Insights into Signaling During Myelination in Zebrafish. Current Topics in Developmental Biology, 97, 1–19. https://doi.org/10.1016/B978-0-12-385975-4.00007-3

Rasminsky, M., Kearney, R. E., Aguayo, A. J., & Bray, G. M. (1978). Conduction of nervous impulses in spinal roots and peripheral nerves of dystrophic mice. Brain Research, 143(1), 71–85. https://doi.org/10.1016/0006-8993(78)90753-9

Richardson, P. M., McGuinness, U. M., & Aguayo, A. J. (1980). Axons from CNS neurons regenerate into PNS grafts. Nature. https://doi.org/10.1038/284264a0

Richardson, P. M., & Verge, V. M. K. (1986). The induction of a regenerative propensity in sensory neurons following peripheral axonal injury. Journal of Neurocytology, 15(5), 585–594. https://doi.org/10.1007/BF01611859

Rotshenker, S. (2011). Wallerian degeneration: the innate-immune response to traumatic nerve injury. Journal of Neuroinflammation, 8(1), 109. https://doi.org/10.1186/1742-2094-8-109

Salzer, J. L. (2012). Axonal regulation of Schwann cell ensheathment and myelination. Journal of the Peripheral Nervous System : JPNS, 17 Suppl 3, 14–19. https://doi.org/10.1111/j.1529-8027.2012.00425.x

Salzer, JL. (1995). Mechanisms of adhesion between axons and glial cells. In: Waxman S, Kocsis J, Stys P, editors. The Axon. Oxford University Press; New York: pp. 164–184.

Salzer, J. L., Brophy, P. J., & Peles, E. (2008). Molecular domains of myelinated axons in the peripheral nervous system. Glia, 56(14), 1532–1540. https://doi.org/10.1002/glia.20750

Salzer, J. L., & Bunge, R. P. (1980). STUDIES OF SCHWANN CELL PROLIFERATION I . An Analysis in Tissue Culture of Proliferation during Development , Wallerian Degeneration , and Direct Injury, 84(March).

Samatar, A. a., & Poulikakos, P. I. (2014). Targeting RAS–ERK signalling in cancer: promises and challenges. Nature Reviews Drug Discovery, 13(12), 928–942. https://doi.org/10.1038/nrd4281

Schmalbruch, H. (1986). Fiber composition of the rat sciatic nerve. The Anatomical Record, 215(1), 71–81. https://doi.org/10.1002/ar.1092150111

Scholzen, T., & Gerdes, J. (2000). The Ki-67 protein: From the known and the unknown. Journal of Cellular Physiology, 182(3), 311–322. https://doi.org/10.1002/(SICI)1097-4652(200003)182:3<311::AID-JCP1>3.0.CO;2-9

Schreiber, M., Kolbus, A., Piu, F., Szabowski, A., Mo, U., Tian, J., … Wagner, E. F. (1999). Control of cell cycle progression by c-Jun is p53 dependent Control of cell cycle progression by c-Jun is p53 dependent, (Weinberg 1995), 607–619.

Schreyer, D. J., & Skene, J. H. (1991). Fate of GAP-43 in ascending spinal axons of DRG neurons after peripheral nerve injury: delayed accumulation and correlation with regenerative potential. The Journal of Neuroscience : The Official Journal of the Society for Neuroscience, 11(12), 3738–51. Retrieved from http://www.ncbi.nlm.nih.gov/pubmed/1836017

Schreyer, D. J., & Skene, J. H. (1993). Injury-associated induction of GAP-43 expression displays axon branch specificity in rat dorsal root ganglion neurons.

J.Neurobiol., 24(0022–3034 (Print)), 959–970. https://doi.org/10.1002/neu.480240709

Schwaiger, F. W., Hager, G., Schmitt, A. B., Horvat, A., Hager, G., Streif, R., … Kreutzberg, G. W. (2000). Peripheral but not central axotomy induces changes in Janus kinases (JAK) and signal transducers and activators of transcription (STAT). European Journal of Neuroscience, 12(4), 1165–1176. https://doi.org/10.1046/j.1460-9568.2000.00005.x

Seijffers, R., Allchorne, A. J., & Woolf, C. J. (2006). The transcription factor ATF-3 promotes neurite outgrowth. Molecular and Cellular Neuroscience, 32(1–2), 143–154. https://doi.org/10.1016/j.mcn.2006.03.005

Seijffers, R., Mills, C. D., & Woolf, C. J. (2007). ATF3 increases the intrinsic growth state of DRG neurons to enhance peripheral nerve regeneration. Journal of Neuroscience, 27(30), 7911–7920. https://doi.org/10.1523/JNEUROSCI.5313-06.2007

Sereda, M., Griffiths, I., Pühlhofer, A., Stewart, H., Rossner, M. J., Zimmermann, F., … Nave, K. A. (1996). A transgenic rat model of Charcot-Marie-Tooth disease. Neuron, 16(5), 1049–1060. https://doi.org/10.1016/S0896-6273(00)80128-2

Shah, N. M., Marchionni, M. A., Isaacs, I., Stroobant, P., & Anderson, D. J. (1994). Glial growth factor restricts mammalian neural crest stem cells to a glial fate. Cell, 77(3), 349–360. https://doi.org/10.1016/0092-8674(94)90150-3

Shaulian, E., & Karin, M. (2001). AP-1 in cell proliferation and survival. Oncogene, 20(19), 2390–2400. https://doi.org/10.1038/sj.onc.1204383

Sheean, M. E., McShane, E., Cheret, C., Walcher, J., Müller, T., Wulf-Goldenberg, A., … Birchmeier, C. (2014). Activation of MAPK overrides the termination of myelin growth and replaces Nrg1/ErbB3 signals during Schwann cell development and myelination. Genes and Development, 28(3), 290–303. https://doi.org/10.1101/gad.230045.113

Shen, Y. J., DeBellard, M. E., Salzer, J. L., Roder, J., & Filbin, M. T. (1998). Myelin-associated glycoprotein in myelin and expressed by Schwann cells inhibits axonal regeneration and branching. Molecular and Cellular Neurosciences, 12, 79–91. https://doi.org/10.1006/mcne.1998.0700

Sherman, D. L., & Brophy, P. J. (2005). Mechanisms of Axon Ensheathment and Myelin Growth, 6(September), 683–690. https://doi.org/10.1038/nrn1743

Sheu, J. Y., Kulhanek, D. J., & Eckenstein, F. P. (2000). Differential patterns of ERK and STAT3 phosphorylation after sciatic nerve transection in the rat. Experimental Neurology, 166(2), 392–402. https://doi.org/10.1006/exnr.2000.7508

Shin, J. E., Cho, Y., Beirowski, B., Milbrandt, J., Cavalli, V., & DiAntonio, A. (2012). Dual Leucine Zipper Kinase Is Required for Retrograde Injury Signaling and Axonal Regeneration. Neuron, 74(6), 1015–1022. https://doi.org/10.1016/j.neuron.2012.04.028

Shy, M. E., Shi, Y., Wrabetz, L., Kamholz, J., & Scherer, S. S. (1996). Axon-Schwann cell interactions regulate the expression of c-jun in Schwann cells. J Neurosci Res, 43(5), 511–525. https://doi.org/10.1002/(SICI)1097-4547(19960301)43:5<511::AID-JNR1>3.0.CO;2-L

Siconolfi, L. B., & Seeds, N. W. (2001). Mice lacking tPA, uPA, or plasminogen genes showed delayed functional recovery after sciatic nerve crush. The Journal of Neuroscience : The Official Journal of the Society for Neuroscience, 21(12), 4348–4355. https://doi.org/21/12/4348 [pii]

Sobecki, M., Mrouj, K., Camasses, A., Parisis, N., Nicolas, E., Ll??res, D., … Fisher,

D. (2016). The cell proliferation antigen Ki-67 organises heterochromatin. eLife, 5(MARCH2016), 1–33. https://doi.org/10.7554/eLife.13722
Stacey, D. W. (2003). Cyclin D1 serves as a cell cycle regulatory switch in actively proliferating cells. Current Opinion in Cell Biology, 15(2), 158–163. https://doi.org/10.1016/S0955-0674(03)00008-5
Stewart, H. J., Morgan, L., Jessen, K. R., & Mirsky, R. (1993). Changes in DNA synthesis rate in the Schwann cell lineage in vivo are correlated with the precursor--Schwann cell transition and myelination. European Journal of Neuroscience, 5(9), 1136–44. Retrieved from http://www.ncbi.nlm.nih.gov/pubmed/7506619
Stewart, H. J. S. (1995). Expression of c???Jun, Jun B, Jun D and cAMP Response Element Binding Protein by Schwann Cells and their Precursors In Vivo and In Vitro. European Journal of Neuroscience, 7(6), 1366–1375. https://doi.org/10.1111/j.1460-9568.1995.tb01128.x
Stewart, H. J. S., Brennan, A., Rahman, M., Zoidl, G., Mitchell, P. J., Jessen, K. R., & Mirsky, R. (2001). Developmental regulation and overexpression of the transcription factor AP-2, a potential regulator of the timing of Schwann cell generation. European Journal of Neuroscience, 14(2), 363–372. https://doi.org/10.1046/j.0953-816X.2001.01650.x
Stoll, G. Griffin, JW. Li, CY & Trapp, BD (1989). Wallerian Degeneration in the Peripheral Nervous System: Participation of Both Schwann Cells and Macrophages in Myelin Degradation. . J Neurocytol 18 (5), 671-683. 10
Sunderland, S. (1951). A classification of peripheral nerve fnjuries producing loss of function. Brain, 74(4), 491–516.
Svaren, J., & Meijer, D. (2008). The molecular machinery of myelin gene transcription in schwann cells. Glia, 56(14), 1541–1551. https://doi.org/10.1002/glia.20767
Svennigsen, Å., & Dahlin, L. (2013). Repair of the Peripheral Nerve—Remyelination that Works. Brain Sciences, 3(3), 1182–1197. https://doi.org/10.3390/brainsci3031182
Syroid, D. E., Maycox, P. R., Burrola, P. G., Liu, N., Wen, D., Lee, K. F., … Kilpatrick, T. J. (1996). Cell death in the Schwann cell lineage and its regulation by neuregulin. Proceedings of the National Academy of Sciences of the United States of America, 93(17), 9229–9234. https://doi.org/10.1073/pnas.93.17.9229
Tanabe, K., Bonilla, I., Winkles, J. a, & Strittmatter, S. M. (2003). Fibroblast growth factor-inducible-14 is induced in axotomized neurons and promotes neurite outgrowth. The Journal of Neuroscience : The Official Journal of the Society for Neuroscience, 23(29), 9675–9686. https://doi.org/23/29/9675 [pii]
Tapinos, N., Ohnishi, M., & Rambukkana, A. (2006). ErbB2 receptor tyrosine kinase signaling mediates early demyelination induced by leprosy bacilli. Nature Medicine, 12(8), 961–966. https://doi.org/10.1038/nm1433
Taveggia, C., Zanazzi, G., Petrylak, A., Yano, H., Rosenbluth, J., Einheber, S., … Salzer, J. L. (2005). Neuregulin-1 type III determines the ensheathment fate of axons. Neuron, 47(5), 681–694. https://doi.org/10.1016/j.neuron.2005.08.017
Tedeschi, A. (2012). Tuning the orchestra: transcriptional pathways controlling axon regeneration. Frontiers in Molecular Neuroscience, 4(60), 1–12. https://doi.org/10.3389/fnmol.2011.00060
Tetzlaff, W. & Bisby, MA. (1989). Neurofilament elongation into regenerating facial nerve axons. Neuroscience. 1989;29(3):659-66.
Thomas, P. K. (1966). The cellular response to nerve injury. 1. The cellular outgrowth

from the distal stump of transected nerve. Journal of Anatomy, 100(Pt 2), 287–303.

Thomas, P. K., & Jones, D. G. (1967). The cellular response to nerve injury. II. Regeneration of the perineurium after nerve section. Journal of Anatomy, 101, 45–55. Retrieved from http://www.ncbi.nlm.nih.gov/pmc/articles/PMC1270857/

Tofaris, G. K., Patterson, P. H., Jessen, K. R., & Mirsky, R. (2002). Denervated Schwann cells attract macrophages by secretion of leukemia inhibitory factor (LIF) and monocyte chemoattractant protein-1 in a process regulated by interleukin-6 and LIF. The Journal of Neuroscience : The Official Journal of the Society for Neuroscience, 22(15), 6696–6703. https://doi.org/20026699

Topilko, P., Schneider-Maunoury, S., Levi, G., Baron-Van Evercooren, a, Chennoufi, a B., Seitanidou, T., … Charnay, P. (1994). Krox-20 controls myelination in the peripheral nervous system. Nature. https://doi.org/10.1038/371796a0

Topilko, P, & Meijer, D. (2001) Transcription factors that control Schwann cell development and myelination. In: Jessen KR, Richardson WD, editors. Glial Cell Development. Basic Principles and Clinical Relevance. 2. Oxford: Oxford University Press; 2001. pp. 223–244.

Tsujino, H., Kondo, E., Fukuoka, T., Dai, Y., Tokunaga, A., Miki, K., … Noguchi, K. (2000). Activating Transcription Factor 3 (ATF3) Induction by Axotomy in Sensory and Motoneurons: A Novel Neuronal Marker of Nerve Injury, 182, 170–182. https://doi.org/10.1006/mcne.1999.0814

Vargas, M. E., Watanabe, J., Singh, S. J., Robinson, W. H., & Barres, B. A. (2010). Endogenous antibodies promote rapid myelin clearance and effective axon regeneration after nerve injury. Proceedings of the National Academy of Sciences of the United States of America, 107(26), 11993–8. https://doi.org/10.1073/pnas.1001948107

Virchow, R. (1854). Ueber das ausgebreitete Vorkommeneinerdem Nervenmark analogen Substanz in den tierischen Geweben. Virchows Archivfarpathologische Anatomie 6, 562

Vleugel, M. M., Greijer, A. E., Bos, R., van der Wall, E., & van Diest, P. J. (2006). c-Jun activation is associated with proliferation and angiogenesis in invasive breast cancer. Human Pathology, 37(6), 668–674. https://doi.org/10.1016/j.humpath.2006.01.022

Waller, A. (1850). Experiments on the section of the glossopharyngeal and hypoglossal nerves of the frog and observations of the alterations produced thereby in the structure, Transactions of the Royal Society

Wanner, IB. Guerra, NK. Mahoney, J. Kumar, A. Wood, PM. Mirsky, R. & Jessen, KR
(2006). Role of N-cadherin in Schwann cell precursors of growing nerves. Glia, Oct; 54 (5): 439-459

Webster, H. deF, Martin, J. R., & O'Connell, M. F. (1973). The relationships between interphase Schwann cells and axons before myelination: A quantitative electron microscopic study. Developmental Biology, 32(2), 401–416. https://doi.org/10.1016/0012-1606(73)90250-9

Webster H, Favilla JT. (1984). Development of peripheral nerve fibers. In: Dyck PJ, Thomas PK, Lambert EH, Bunge R, editors. Peripheral Neuropathy. I. Philadelphia: W. B. Saunders Company; pp. 329–358.

Weinberg HJ, Spencer, PS. (1975) Studies on the control of myelinogenesis. I. Myelination of regenerating axons after entry into a foreign unmyelinated nerve. J Neurocytol **4**:395–418

Weinberg, H.J. & Spencer, P.S. (1978) The fate of Schwann cells isolated from axonal contact. J Neurocytol, 7: 555.doi:10.1007/BF01260889

Wolpowitz, D., Mason, T. B., Dietrich, P., Mendelsohn, M., Talmage, D. a, & Role, L. W. (2000). Cysteine-rich domain isoforms of the neuregulin-1 gene are required for maintenance of peripheral synapses. Neuron, 25(1), 79–91. https://doi.org/10.1016/S0896-6273(00)80873-9

Woodhoo, A., Alonso, M. B. D., Droggiti, A., Turmaine, M., D'Antonio, M., Parkinson, D. B., … Jessen, K. R. (2009). Notch controls embryonic Schwann cell differentiation, postnatal myelination and adult plasticity. Nat Neurosci, 12(7), 839–847. https://doi.org/10.1038/nn.2323

Woodhoo, A., & Sommer, L. (2008). Development of the schwann cell lineage: From the neural crest to the myelinated nerve. Glia, 56(14), 1481–1490. https://doi.org/10.1002/glia.20723

Woolf, C. J., Reynolds, M. L., Molander, C., O'Brien, C., Lindsay, R. M., & Benowitz, L. I. (1990). The growth-associated protein gap-43 appears in dorsal root ganglion cells and in the dorsal horn of the rat spinal cord following peripheral nerve injury. Neuroscience, 34(2), 465–478. https://doi.org/10.1016/0306-4522(90)90155-W

Wu, L. M. N., Wang, J., Conidi, A., Zhao, C., Wang, H., Ford, Z., … Lu, Q. R. (2016). Zeb2 recruits HDAC-NuRD to inhibit Notch and controls Schwann cell differentiation and remyelination. Nature Neuroscience, 19(8), 1060–72. https://doi.org/10.1038/nn.4322

Yang, D. P., Kim, J., Syed, N., Tung, Y.-J., Bhaskaran, A., Mindos, T., … Kim, H. A. (2012). p38 MAPK activation promotes denervated Schwann cell phenotype and functions as a negative regulator of Schwann cell differentiation and myelination. The Journal of Neuroscience : The Official Journal of the Society for Neuroscience, 32(21), 7158–68. https://doi.org/10.1523/JNEUROSCI.5812-11.2012

Yang, D. P., Zhang, D. P., Mak, K. S., Bonder, D. E., Pomeroy, S. L., & Kim, H. A. (2008). Schwann cell proliferation during Wallerian degeneration is not necessary for regeneration and remyelination of the peripheral nerves: Axon-dependent removal of newly generated Schwann cells by apoptosis. Molecular and Cellular Neuroscience, 38(1), 80–88. https://doi.org/10.1016/j.mcn.2008.01.017

Young, J. Z., Oxfd, M. A., Holmes, W., Oxfd, B. A., & Sanders, F. K. (1940). Nerve regeneration. Importance of the peripheral stump and the value of nerve grafts. The Lancet, 236, 128–130. https://doi.org/10.1016/S0140-6736(01)07979-X

Yu, W.-M. (2005). Schwann Cell-Specific Ablation of Laminin 1 Causes Apoptosis and Prevents Proliferation. Journal of Neuroscience, 25(18), 4463–4472. https://doi.org/10.1523/JNEUROSCI.5032-04.2005

Yu, W.-M., Chen, Z.-L., North, A. J., & Strickland, S. (2009). Laminin is required for Schwann cell morphogenesis. Journal of Cell Science, 122(Pt 7), 929–936. https://doi.org/10.1242/jcs.033928

Zochodne DW. (2003) Nerve regeneration and repair. Journal of the peripheral nervous system, JPNS, 8 (2),, pp. 59-60; author replies 61-2, 63-4

Zochodne DW. (2008) Neurobiology of Peripheral Nerve Regeneration Cambridge University Press 978-0-521-86717-7 - Neurobiology of Peripheral Nerve Regeneration Douglas

Zhang, Y., Bo, X., Schoepfer, R., Holtmaat, A. J. D. G., Verhaagen, J., Emson, P. C., … Anderson, P. N. (2005). Growth-associated protein GAP-43 and L1 act

synergistically to promote regenerative growth of Purkinje cell axons in vivo. Proceedings of the National Academy of Sciences of the United States of America, 102(41), 14883–8. https://doi.org/10.1073/pnas.0505164102

Zhou, L., & Too, H. P. (2013). GDNF family ligand dependent STAT3 activation is mediated by specific alternatively spliced isoforms of GFR??2 and RET. Biochimica et Biophysica Acta - Molecular Cell Research, 1833(12), 2789–2802. https://doi.org/10.1016/j.bbamcr.2013.07.004

Ziskind-Conhaim, L. (1988). Physiological and morphological changes in developing peripheral nerves of rat embryos. Brain Research, 470(1), 15–28. Retrieved from http://www.ncbi.nlm.nih.gov/pubmed/3409046

Zorick, T. S., Syroid, D. E., Brown, a, Gridley, T., & Lemke, G. (1999). Krox-20 controls SCIP expression, cell cycle exit and susceptibility to apoptosis in developing myelinating Schwann cells. Development (Cambridge, England), 126(7), 1397–1406.

Zou, H., Ho, C., Wong, K., & Tessier-Lavigne, M. (2009). Axotomy-Induced Smad1 Activation Promotes Axonal Growth in Adult Sensory Neurons. Journal of Neuroscience, 29(22), 7116–7123. https://doi.org/10.1523/JNEUROSCI.5397-08.2009